THE SEDIMENTOLOGY, STRATIGRAPHY AND DEPOSITIONAL HISTORY OF THE LOWER CRETACEOUS VIKING FORMATION AT HARMATTAN EAST AND CROSSFIELD, ALBERTA, CANADA

BY

SCOTT WILSON HADLEY, B.SC.

A Thesis

Submitted to the School of Graduate Studies

in Partial Fulfilment of the Requirements

for the Degree

Master of Science

McMaster University

1992

Master of Science (1992) McMaster University
(Geology) Hamilton, Ontario

TITLE: The Sedimentology, Stratigraphy and Depositional History of the Lower Cretaceous Viking Formation at Harmattan East and Crossfield, Alberta, Canada.

AUTHOR: Scott Wilson Hadley, B.Sc. (Hons.) (University of Western Ontario)

SUPERVISOR: Dr. R.G. Walker

NUMBER OF PAGES: xvi, 293

DEDICATION

To the memory of my mother whose spirit will guide me the remainder of my life.

ABSTRACT

The Lower Cretaceous (Albian) Viking Formation at Harmattan East and Crossfield, Alberta, contains two regionally extensive erosion surfaces, VE3 and VE4, separating three allomembers, A-B, D and E. These erosion surfaces can be mapped over large areas of the Alberta basin allowing for the creation of a Viking allostratigraphy.

The allostratigraphic base of the Viking alloformation in the study area is informally designated BV. The BV log marker is overlain by allomember A-B, which in turn is overlain by the regionally extensive ravinement surface VE3. The VE3 surface is sharply overlain by allomember D, a northeastward thinning clastic wedge composed of storm dominated facies and nonmarine deposits. Allomember D is in turn overlain by the regionally extensive ravinement surface VE4. Allomember E, which overlies this unconformity is a complex succession of coarse grained facies interbedded with dark mudstones. The upper part of allomember E is composed of dark mudstones bounded at the top by a regionally extensive condensed section (Base of Fish Scales) that informally marks the allostratigraphic top of the Viking alloformation in the study area.

Viking sedimentation began with the deposition of basinal and offshore transitional mudstones, siltstones and sandstones of allomember A-B. A major drop in sea level

allowed valleys to incise into these sediments. Nonmarine and upper shoreface deposits of allomember A-B were eroded at Harmattan East during the ensuing transgression that produced the VE3 ravinement surface. A second relative sea level lowering resulted in northeastward progradation of allomember D. Renewed transgression modified the older subaerial erosion surface on top of allomember D, forming the marine ravinement surface VE4 and the overlying deposits of allomember E. Multiple stillstands or slow rates of transgression produced the "steplike" southwestward climbing morphology on the VE4 surface. Fluvial systems supplied coarse sediment to each shoreface incision ("step"). During minor sea level falls, storm and tidal currents reworked sediment at these shorefaces and also transported sediment basinward over older "stepped" shorelines forming onlap markers E0 to E5. Continued transgression blanketed the coarse grained interbeds with offshore dark mudstones (Colorado Shale). A major pause in basin deposition led to the formation of a condensed section of fish skeletal remains (Base of Fish Scales). The base of this unit marks the end of Viking depostion in the study area.

The Harmattan East Viking oil field is producing from the coarse grained transgressive lag that overlies VE4. It is separated from Caroline field (along depositional strike) by a rise in the VE4 surface.

ACKNOWLEDGEMENTS

I am indebted to my supervisor, Dr. Roger Walker for his supervision, guidance and support during the course of this study. I am especially appreciative of his editorial skills which have improved this thesis considerably, and for providing funding for this study, through grants from the Natural Science and Engineering Research Council of Canada.

I am grateful to Amoco Canada Petroleum Company Ltd., Husky Oil Ltd., and Texaco Canada Resources Ltd. for providing base maps, geophysical logs and scout tikets needed for this study. My thanks extend to Steve Harding of Husky Oil Ltd. for his help in trace fossil indentification during the core logging phase of this study. I am especially grateful to Mark Hadley of PanCanadian for his late night editorial skills, and expertise in computer drafting of several tables found in this thesis.

Several people at McMaster University provided valuable support during the course of this study. My thanks extend to Sue Burbidge for aquiring hundreds of well logs and scout tickets; to Suzanne Nacha for typing in pages of data for the isopach maps; to Marg Rutka for her help in the mounting of photographic plates; and to Jennifer Wadsworth for her computer assistance with the surfer program. Special thanks are extented to Jack Whorwood for his masterful screens and colour slides; and to Len Zwicker for his expert preparation of thin sections.

I would like to thank past fellow graduate students for their friendship and memories during my stay at McMaster. In particular, Tom Boreen, Steve Davies, Jennifer Wadsworth, and Bruce Willmer. I would also like to thank my U of C roomates Simon Pattison, Bruce Power and Dr. Tony Reynolds for an interesting and eventful summer at the E.R.C.B.

A special thanks to my father Cy Hadley for his love and support. I am especially indebted to my wife Laura for her encouragement and for keeping me of sound mind throughout the duration.

TABLE OF CONTENTS

LIST OF FIGURES

LIST OF TABLES

Chapter 1 Formulation of the Research Problem

1.1 Introduction

Reservoirs in Cretaceous sandstones of western Canada are attractive targets for hydrocarbon exploration because they occur at shallow depths, are usually laterally extensive, and the hydrocarbons can be produced in a relatively short time interval. Exploitation or infill drilling of these Cretaceous oil and gas pools has provided an abundance of closely spaced subsurface information in the form of geophysical well logs, cores, and well cuttings. Because most of this data is closely spaced and readily accessible, it can be used to study stratigraphy in detail over large portions of a sedimentary basin.

This thesis is based on subsurface data from Alberta, and represents part of the ongoing research conducted at McMaster University on shallow marine shelf sediments that were deposited in the Cretaceous Western Interior Seaway. The following sections of this chapter are concerned with the formulation of a scientific problem which is to be addressed in this thesis.

1.2 Cretaceous Shelf Sandbodies: Ideas

A number of long, linear hydrocarbon reservoirs in

North America occur in sandstones which have been interpreted to have been deposited in shelf environments as shelf sand ridge deposits or offshore bars. They include the Cardium Formation (Walker, 1984), Viking Formation (Evans, 1970; Beaumont, 1984), Shannon Sandstone of Wyoming and Montana (Tillman and Martinsen, 1984), the Mosby Sandstone of Montana (Swift and Rice, 1984), and sandstones within the upper Mancos Shale of Colorado (Boyles and Scott, 1982). Often these sandstone bodies are described as being encased in marine shales. The sequences within the sandbodies seldom reveal evidence of subaerial exposure, nor do they show any connection with a time equivalent shoreline. Finally the sandstone reservoir geometries in map (plan) view are commonly long and linear.

Downing and Walker (1988) posed several questions that can be asked in relation to the shelf sand ridge or offshore bar interpretation.

1) What was the source of the coarse sediment?

2) What processes were responsible for transporting coarse sediment from the shoreline out into the basin?

3) How is the coarse sediment then focussed into long narrow sandbodies?

Coarse sediment can be transported from a shoreline into a basin by a number of processes, for example, storm waves, permanent currents, wind induced along shore currents, wave modified currents, tidal currents, and turbidity currents

(Walker 1985). If the sandstone bodies in the Western Interior Seaway (WIS) are to be interpreted as shelf sand ridges then a major question still remains, namely, how is the coarse sediment deposited and "molded" into long linear ridges?

An interpretation emphasizing fluctuations of relative sea level has been offered to explain both the coarse sediment supply problem, and the geometry of numerous WIS sandbodies in western Canada, (Cardium Formation, Bergman and Walker, 1987,1988; Plint et al., 1986; Viking Formation, Leckie, 1986a; Hein et al., 1986; Downing and Walker, 1988; Power, 1988; Reinson et al., 1988).

The work of Plint et al. (1986) and Bergman and Walker (1987, 1988) has shown that during the global sea level low of the Turonian, deposition of the Cardium was interrupted by short-lived relative sea-level falls. Seven sea level fluctuations were recognized in the subsurface by these workers. Each sea-level fall terminated shoreface progradation, and at the same time generated widespread hiatuses across the adjacent shelf. The long narrow sandbodies of the Cardium have been reinterpreted by these workers as incised shoreface deposits formed during subsequent transgressions. The coarse sandstones and conglomerates were shown <u>not</u> to be part of a simple coarsening upwards sequence but were invariably separated by erosion surfaces. An ensuing rise in sea level covered these shoreface deposits with marine mudstones and eroded any evidence of subaerial exposure.

The concepts of sea level fluctuations and deposition of coarse sediment at low-stand events has also been applied to the Viking Formation (Boreen and Walker, 1991). The long narrow sandbody trend of Gilby-Joffre has been reinterpreted to represent low-stand incised shoreface deposits (Downing and Walker, 1988; Raddysh, 1988). The coarse sediment body in these areas differs from previous interpretations of this same trend because of the documentation of internal sequences and erosional surfaces by these workers.

The reinterpretation of many Cardium and Viking sandstone bodies as incised shoreface deposits solves most of the problems of the offshore bar interpretation discussed earlier; namely, how coarse sediment can be transported across a shelf and focussed into linear ridges with internal coarsening upwards sequences. First, sediment was not transported across the shelf; instead, the shoreline moved basinward. Secondly, the linear aspect of the sandstone bodies is not related to the focussing of sediment into sand ridges but is due to deposition along a shoreline. Third, most of the coarse facies in these two formations lie upon erosion unconformities, and therefore, are not part of an internal coarsening-up sequence on the shelf (Downing and Walker, 1988).

1.3 Scientific Problem and Selection of Study Area

The detailed stratigraphy of the Cardium Formation proposed by Plint et al. (1986) is based on the correlation of erosion surfaces throughout the Alberta basin and the mapping of facies associations bounded by these surfaces. This mapping has allowed a more precise understanding of the depositional history of the Cardium to be attained by relating sediment packages and erosion surfaces to Cardium sea level fluctuation history.

The Viking Formation is similar to the Cardium in many respects. Both formations consist primarily of shallow marine sediments deposited within similar time spans (1-2 My). Many of the Viking fields are long and narrow (Fig 1.1). Sea level fluctuations and erosional surfaces in the Viking Formation have been discussed by Leckie (1986a), Hein et al. (1986), Downing and Walker (1988), Power (1988), Raddysh (1988) and Boreen and Walker (1991). These erosion surfaces appear to be similar to those in the Cardium, however, no detailed basin-wide stratigraphy has yet been proposed for the Viking. The depositional history of the Viking will only be understood once the erosion surfaces and all other Viking sandstone bodies are linked together stratigraphically.

Most of the Viking studies to date have dealt with fields in central Alberta with minimal attention on the most southerly Viking fields in Alberta. For this reason it was decided to undertake a study of the Harmattan East and

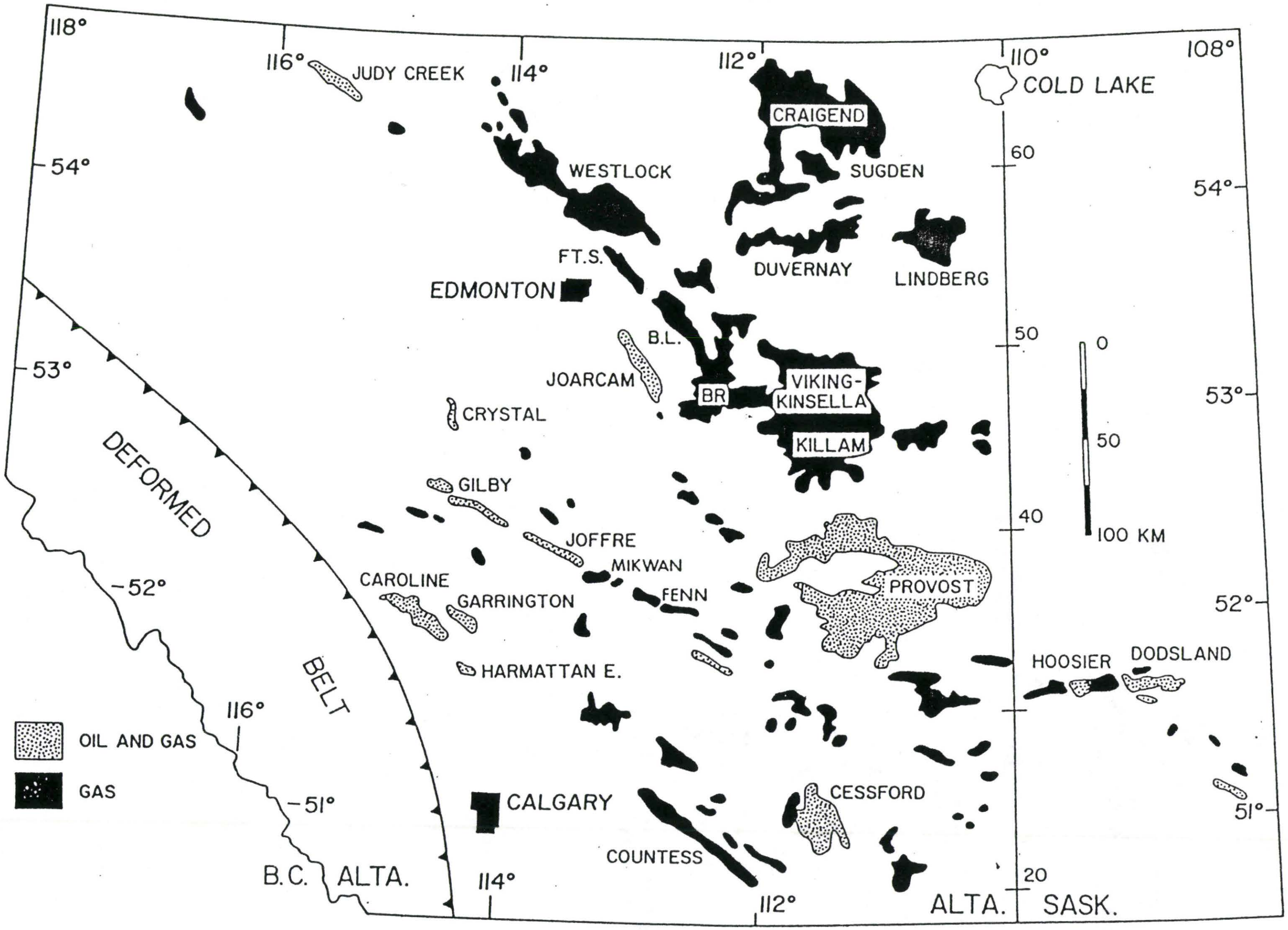

Fig. 1.1. Distribution of Viking sandbodies in Alberta and Saskatchewan. These sandbodies have been delineated from hydrocarbon production estimates provided by the Energy Resources Conservation Board. From Walker, in Downing (1986).

Crossfield area of western south-central Alberta. This area area of was chosen partly on the basis of previous McMaster research by Downing and Walker (1988) at Joffre, Power's (1988) work at Joarcam, and Raddysh's (1988) research at Gilby (Fig. 1.2). The erosional surfaces defined in these study areas are postulated to extend into southern areas of the Alberta Foreland basin where nonmarine and shoreface sediments of the Viking are known to exist (Hein et al., 1986; Leckie, 1986a) This hypothesis required a study of the Harmattan area where the Viking Formation is thought to have attained its maximum thickness. Documentation of facies associations and erosional surfaces at Harmattan East will hopefully contribute the most southern portion of a detailed stratigraphy presently being put together at McMaster (Boreen and Walker, 1991; Pattison, 1990).

This research was carried out in conjunction with Davies' (1990) investigation of Caroline-Garrington fields, Pattison's (1991) study of the Viking Crystal field, J.J. Bartlett's (pers. comm., 1991) research on Viking Formation sediments in the Joarcam - Beaverhill Lake area, and an investigation of the Willesden Green - Gilby Viking fields carried out by Boreen (1989) (Fig. 1.2).

The objectives of this thesis are:

1) to describe the vertical and lateral facies relationships of nonmarine, nearshore and shallow marine sedimentation preserved south of the Harmattan East field,

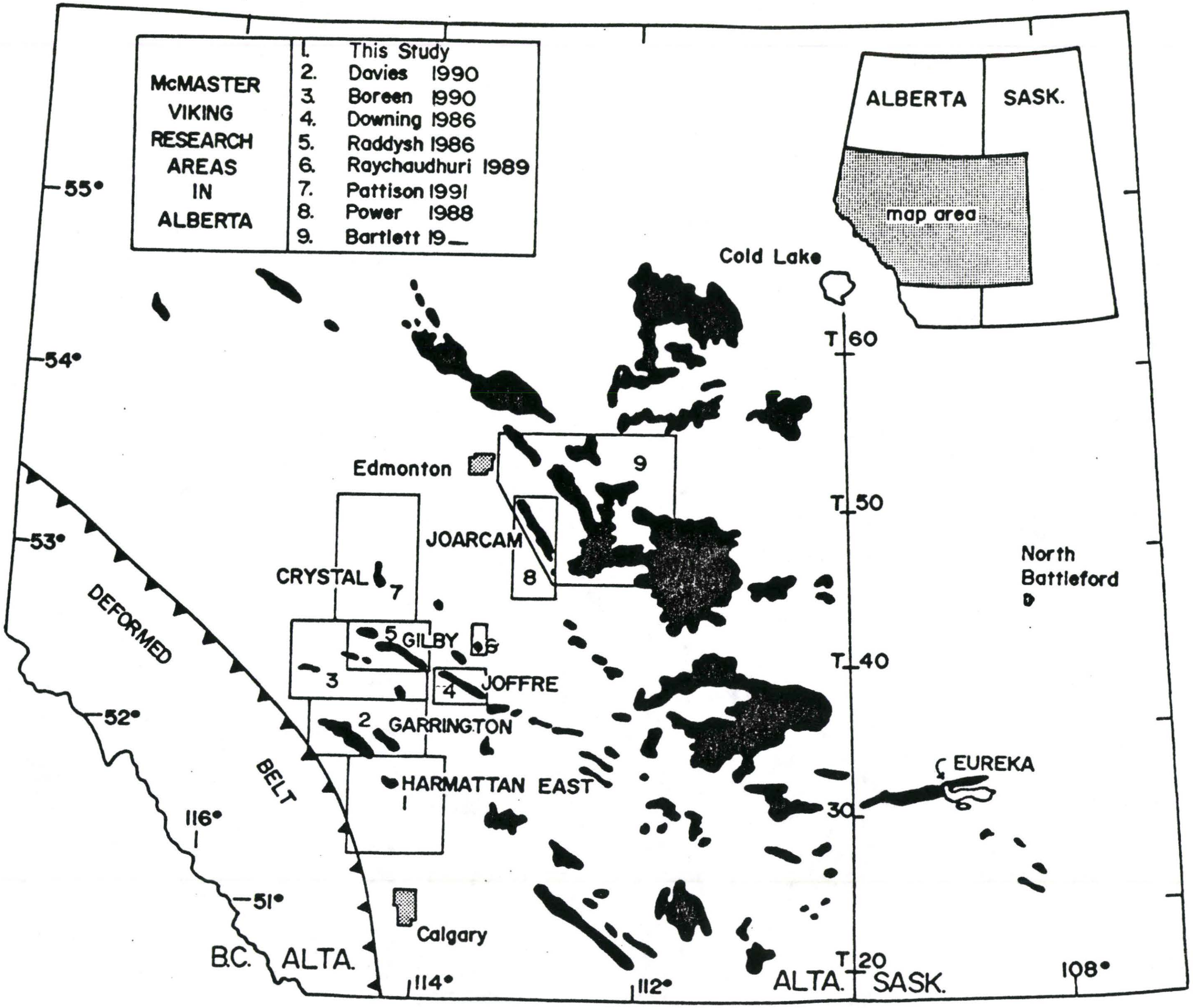

Fig. 1.2. Location of major oil and gas fields in the Viking Formation, Alberta and Saskatchewan. The numbered boxes represent previous areas of Viking research at McMaster University pertinent to this study. Nonmarine Viking facies are known in area of, and southwest of Harmattan East. Townships are numbered along the Alberta-Saskatchewan border; 10 townships cover 96.5 km (Modified after Downing and Walker, 1988).

2) to document erosional surfaces in Viking sediments at the Harmattan East and Crossfield area and to correlate sequences bounded by these surfaces to erosional surfaces defined by previous and present research on the Viking Formation,

3) to investigate the geometry of the oil producing reservoir at the Harmattan East field and interpret the relationship of this field to the proximal Caroline and Garrington fields. The abundance of drill core within the Harmattan East field and off field locations provides an excellent opportunity to investigate this correlation problem between fields.

1.4 Data Base

The data base in this study includes all available drill cores (122) penetrating the Viking Formation in an area encompassing townships 28 to 33, ranges 28W4M to 5W5M (Fig 1.3). Most cored intervals in this area are 16 to 18 m long and represent mostly the upper part (reservoir sandstones) of the Viking Formation (Appendix 1). Only one well (6-24-32-3W5M) in the study area had core representing the entire basal section of the Viking Formation. All cores described in this study are available for examination at the Core Research Centre operated by the Energy Resources Conservation Board in Calgary.

Approximately 600 gamma ray and resistivity well logs were used for isopach and correlation purposes. Resistivity logs are used primarily for correlation of markers within the study area as they are the most available log type. The gamma ray log is particularly useful for correlation of sandier units in this study area.

Sandstone samples were collected from various facies for petrographic analysis to assist in facies definition. Production records and core analyses for wells in the study area were obtained from Amoco Canada Petroleum Company Limited.

1.5 Location of Study

The study area is situated in western south-central Alberta. It encompasses townships 28 to 33, ranges 28W4M to 5W5M (Fig. 1.3). The southern boundary of the study is approximately 20 km north of the city of Calgary, and the northern boundary approximately 170 km south of the city of Edmonton. The northern part of the study overlaps with Davies' (1990) study of the Caroline and Garrington areas. One Viking oil field, Harmattan East, and the southern end of the Viking Caroline field are located in the area of study (Fig. 1.2).

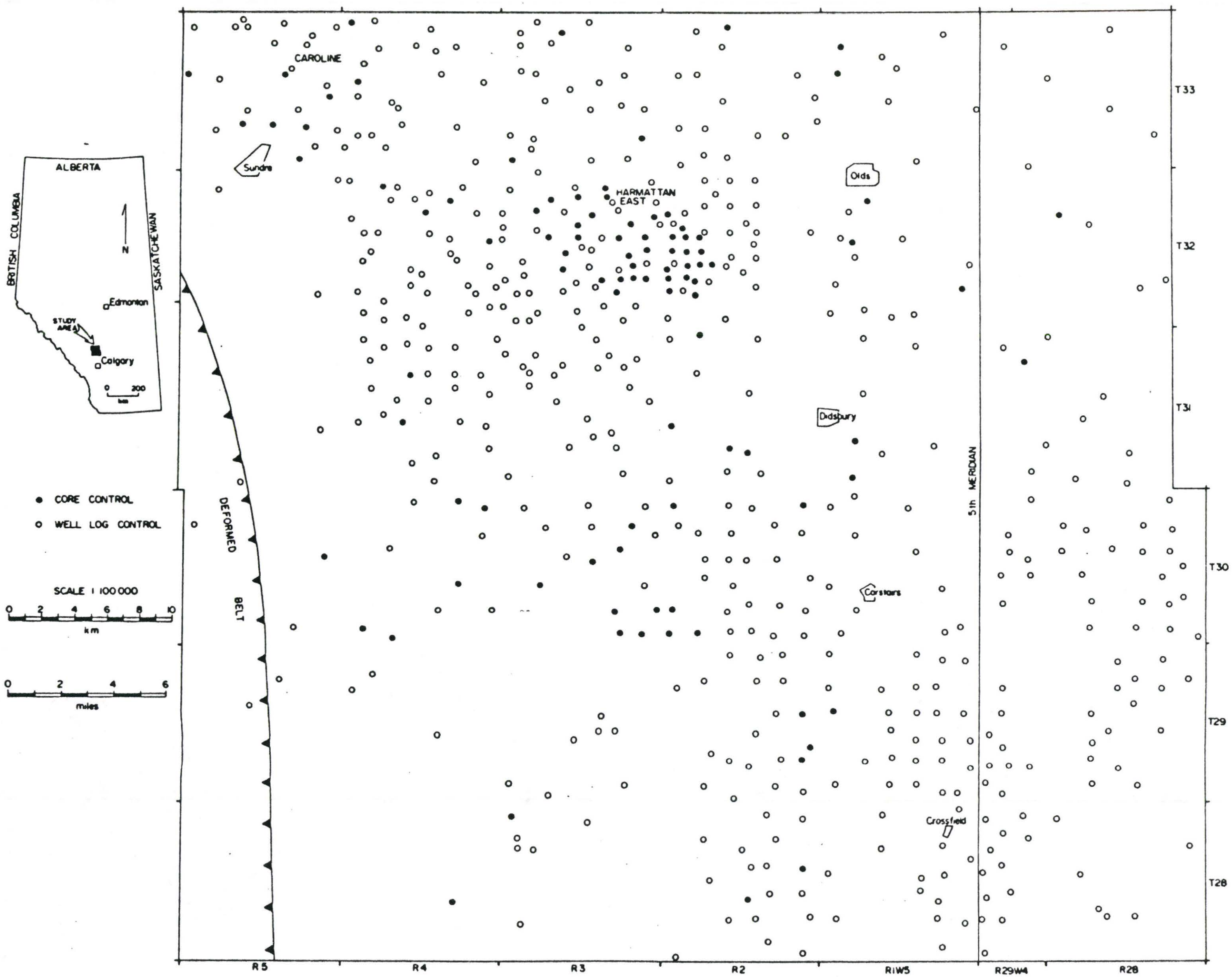

Fig. 1.3. Detailed study area, showing well log (open circles) and core (solid circles) control. One Viking oil field, Harmattan East, and the southern end of the Viking Caroline field are located in the area of study. Top left shows location within Alberta.

Chapter 2 Regional Stratigraphy and Setting

2.1 Introduction

The Lower Colorado Group in central Alberta includes in ascending order: the Joli Fou Formation, the Viking Formation, and an upper unnamed shale all considered to be primarily marine deposits (Fig. 2.1). In southern areas of Alberta the Lower Colorado includes the "Basal Colorado Sandstone (Banerjee, 1989), the Bow Island Formation, and the overlying shale interval. In the northwestern United States the Joli Fou is equivalent to Thermoplis and Skull Creek Shales (Gammell, 1953; Glaister, 1959; Tizzard and Lerbekmo, 1975; Leckie and Reinson, in press) (Fig. 2.2).

Viking Formation equivalents in Alberta include; the Paddy Member (Stelck and Koke, 1987); the Pelican Formation in the northeast, the Bow Island in the south (Boethling, 1977a) and the Mill Creek Formation in the southern Alberta foothills (Leckie, 1986a). Viking Formation equivalents in the northwestern United States include the Muddy, J and Newcastle sandstones (Simpson, 1975; Beaumont, 1984; Weimer, 1983) (Fig. 2.2).

The reader is referred to Appendix 2 for a detailed review of stratigraphy and biostratigraphy of the Lower Colorado Group. Most of the previous work on the Viking Formation has been based almost entirely on the recognition

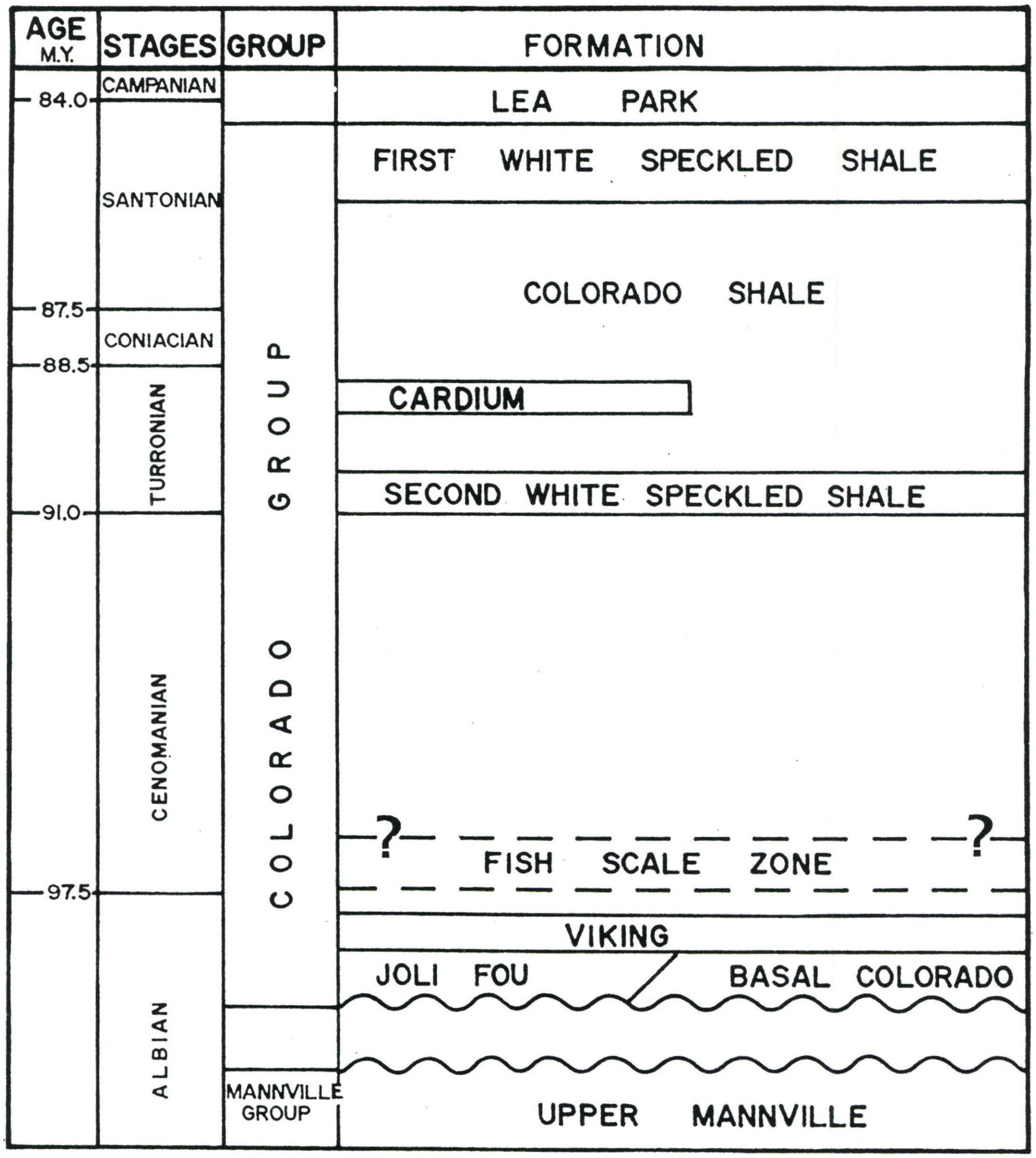

Fig. 2.1. Stratigraphic column of the Cretaceous Colorado Group in the central plains of Alberta. (Redrawn from stratigraphic correlation chart prepared by Core Laboratories Geological Sciences Department - Canada, 1988).

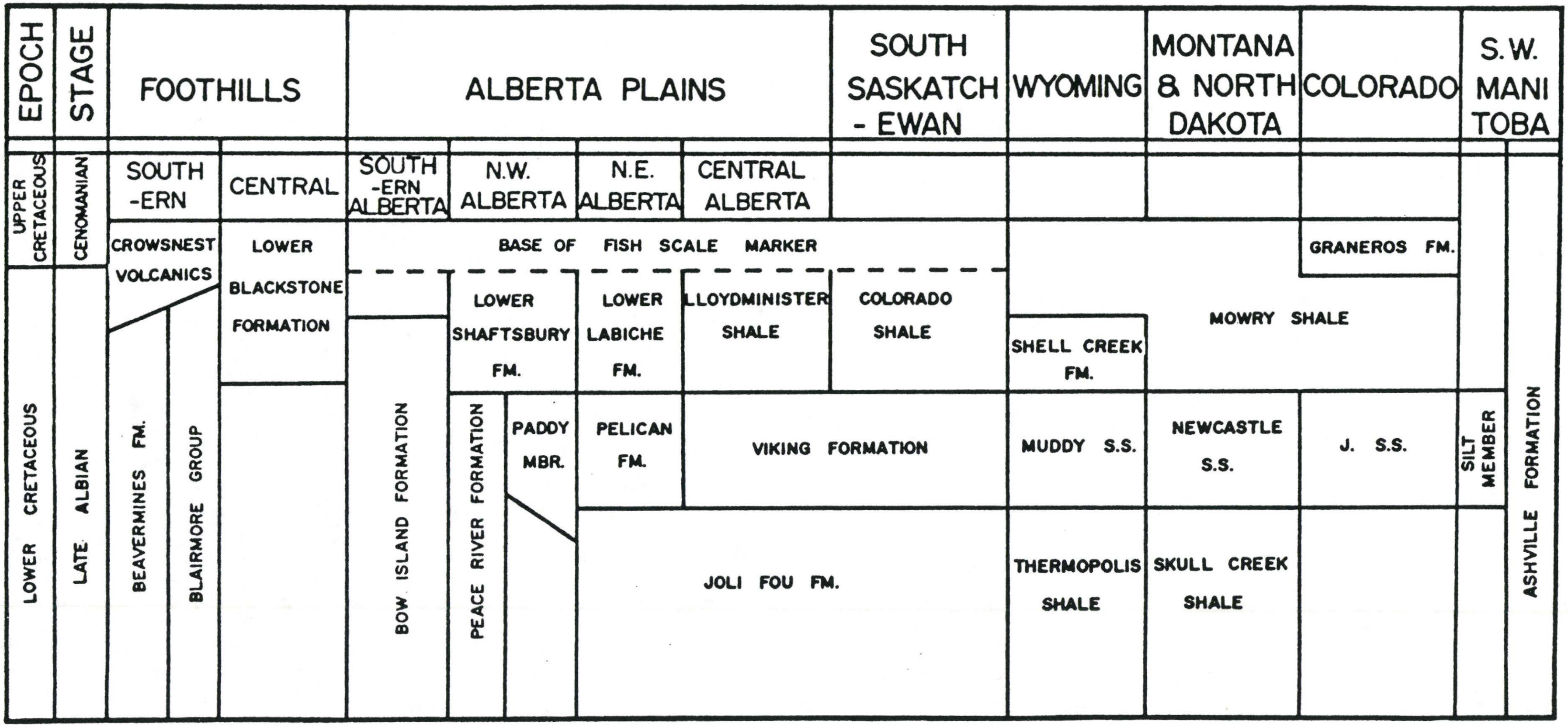

Fig. 2.2. Stratigraphic relationships of the Viking and Joli Fou Formations in western North America (from Robb, 1985).

of lithostratigraphic units. A more precise understanding of internal Viking Formation stratigraphy and depositional history can be achieved by application of allostratigraphic principles (NASCN, 1983) (Boreen and Walker, 1991).

2.2 Regional Viking Allostratigraphy

Recently, Boreen and Walker (1991) proposed an informal allostratigraphy for the Viking Formation in the area between Caroline and Willesden Green (Fig. 2.3). This stratigraphy is based on the recognition and correlation of three erosional bounding discontinuities designated VE2 through to VE4 (VE2 means Viking Erosion surface 2 etc.). The VE1 surface is designated B.V. (Base of Viking) in the work of Boreen and Walker (1991). The VE surfaces define five allomembers (A through E) within the Viking. The five from bottom to top include (A and B), regional parasequences of bioturbated silty to sandy mudstones, (C) valley fill deposits (eg. Crystal), (D) progradational shoreface to non-marine deposits (Harmattan - Caroline), and (E) transgressive mudstones, sandstones, and conglomerates (Fig. 2.3) (Pattison, 1990). The Viking allomembers are not exclusive to any one area although several are more pronounced in thickness. For example, in the Harmattan area, allomembers A-B and D constitute progradational shoreface sequences each approximately 20 metres thick in the southwest but these same members become thin (less than 5 metres) or are not preserved

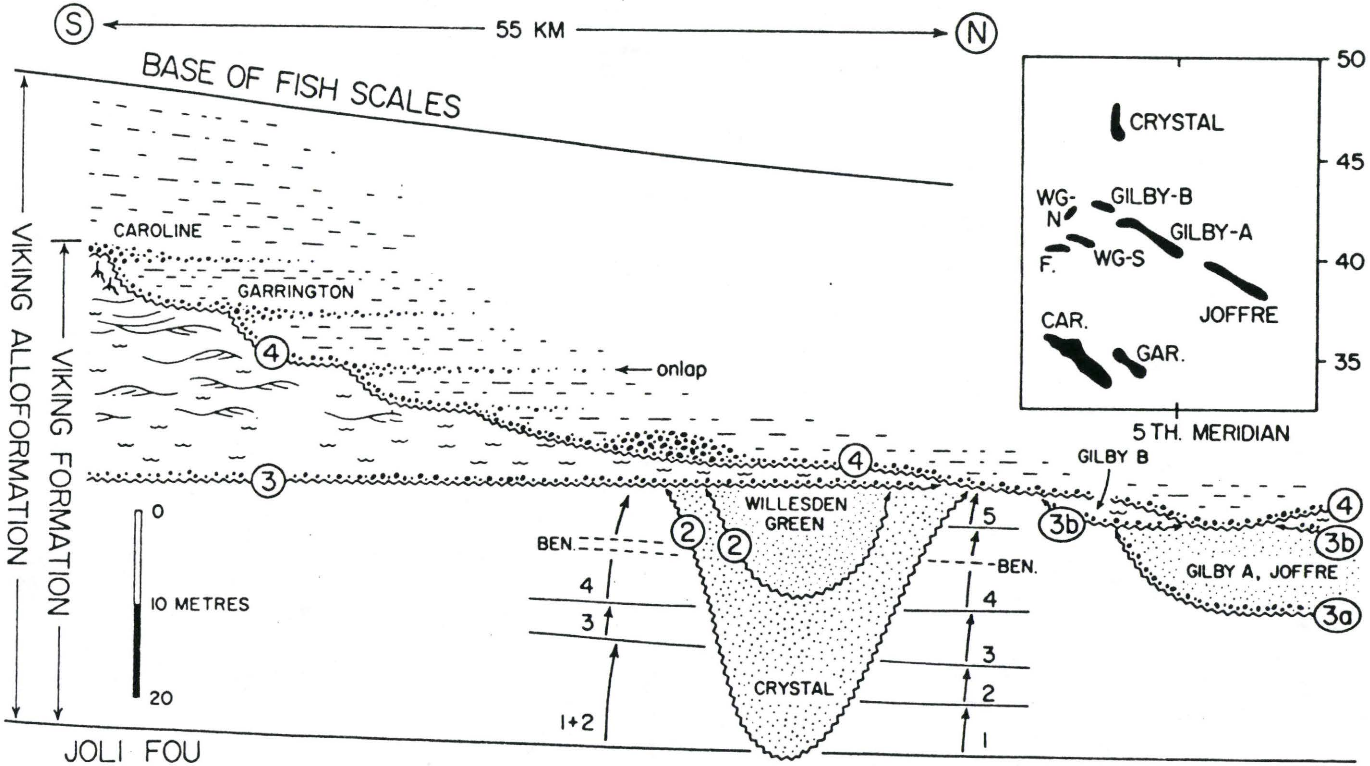

Fig. 2.3. Viking Formation allostratigraphy for the Caroline to Willesden Green area (Boreen and Walker, 1991) Basinwide erosion surfaces are labelled 2 to 4. Small arrows designate the five regional parasequences. Viking allostratigraphy is discussed in text.

in the northeast areas of Alberta.

2.3 Allostratigraphy at Harmattan East

The regional Viking allostratigraphic framework used in this study is shown in figure 2.4, and is an expanded and more detailed version of the southwestern portion of Boreen and Walker's allostratigraphy. Figure 2.4 encompasses the area south of Harmattan and extends northeast through Garrington towards Gilby field. The valley fill, channel estuarine deposits of the Crystal and Willesden Green fields are not incorporated on this schematic cross section.

The internal stratigraphy of the Viking Formation at Harmattan East field is shown in figure 2.5. The diagram is a well composite derived from log and core data from two wells in the oil producing Harmattan East field. The log curves in figure 2.5 are from 6-24-32-3W5 which in this thesis represents the "reference locality" or "reference area" for the southwest portion of the regional Viking allostratigraphy. Three cored wells from the "reference locality", 6-24-32-3W5, 6-20-32-2W5 and 14-32-31-2W5 have the longest continuous length cores in the thesis study area and taken together comprise a complete representation of the entire Viking Alloformation in the study area (Fig. 2.5). The three cores are useful for correlation purposes, and therefore, are designated the "type locality cores" for the "reference locality".

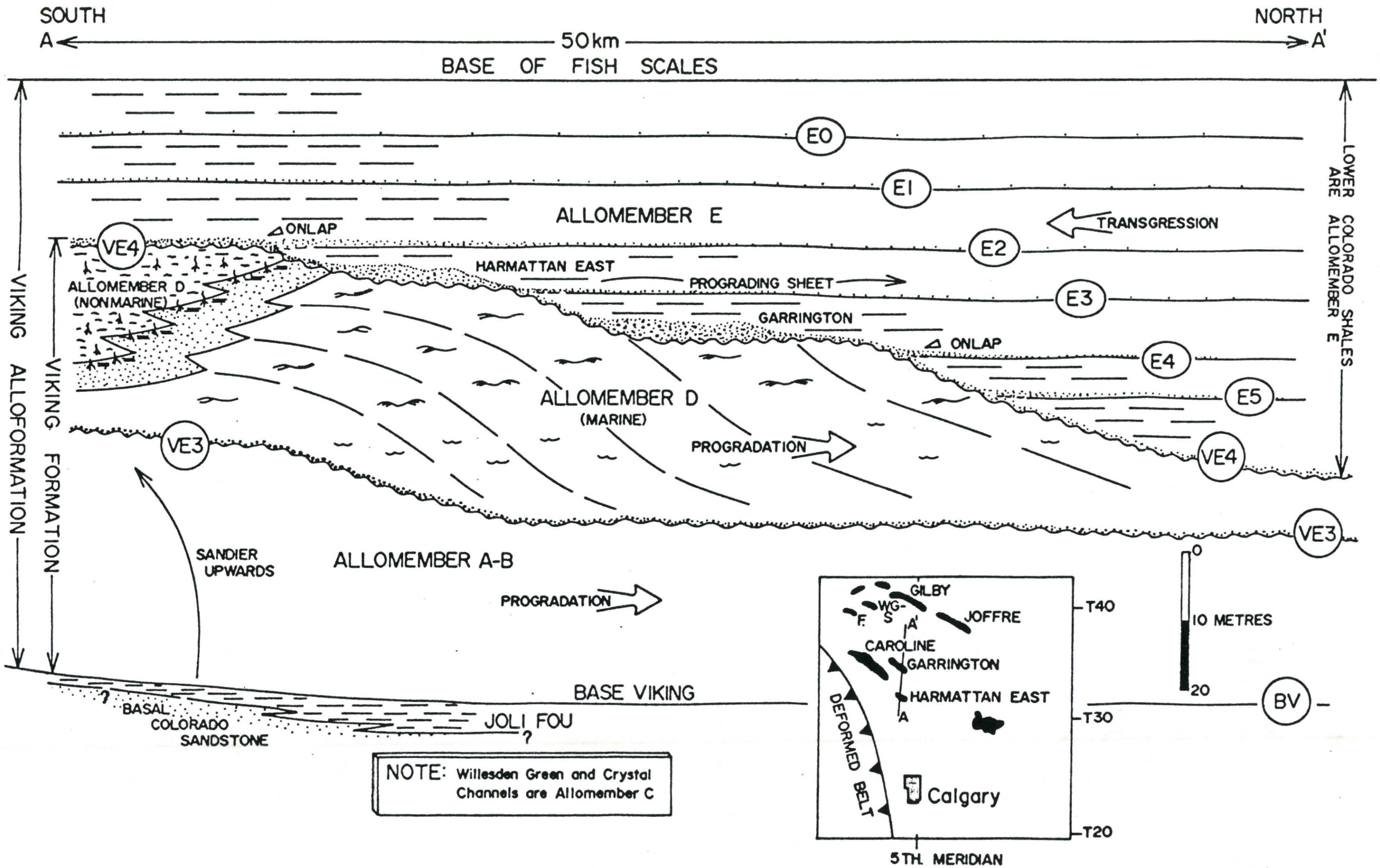

Fig. 2.4. Viking Formation allostratigraphy proposed in this thesis. The cross-section encompasses the area south of Harmattan East and extends north through Garrington towards Gilby. The channel-estuary Viking deposits of the Crystal, Willesden Green, Sundance, and Edson fields are not incorporated on the line. Viking allostratigraphy at Harmattan East is discussed in text.

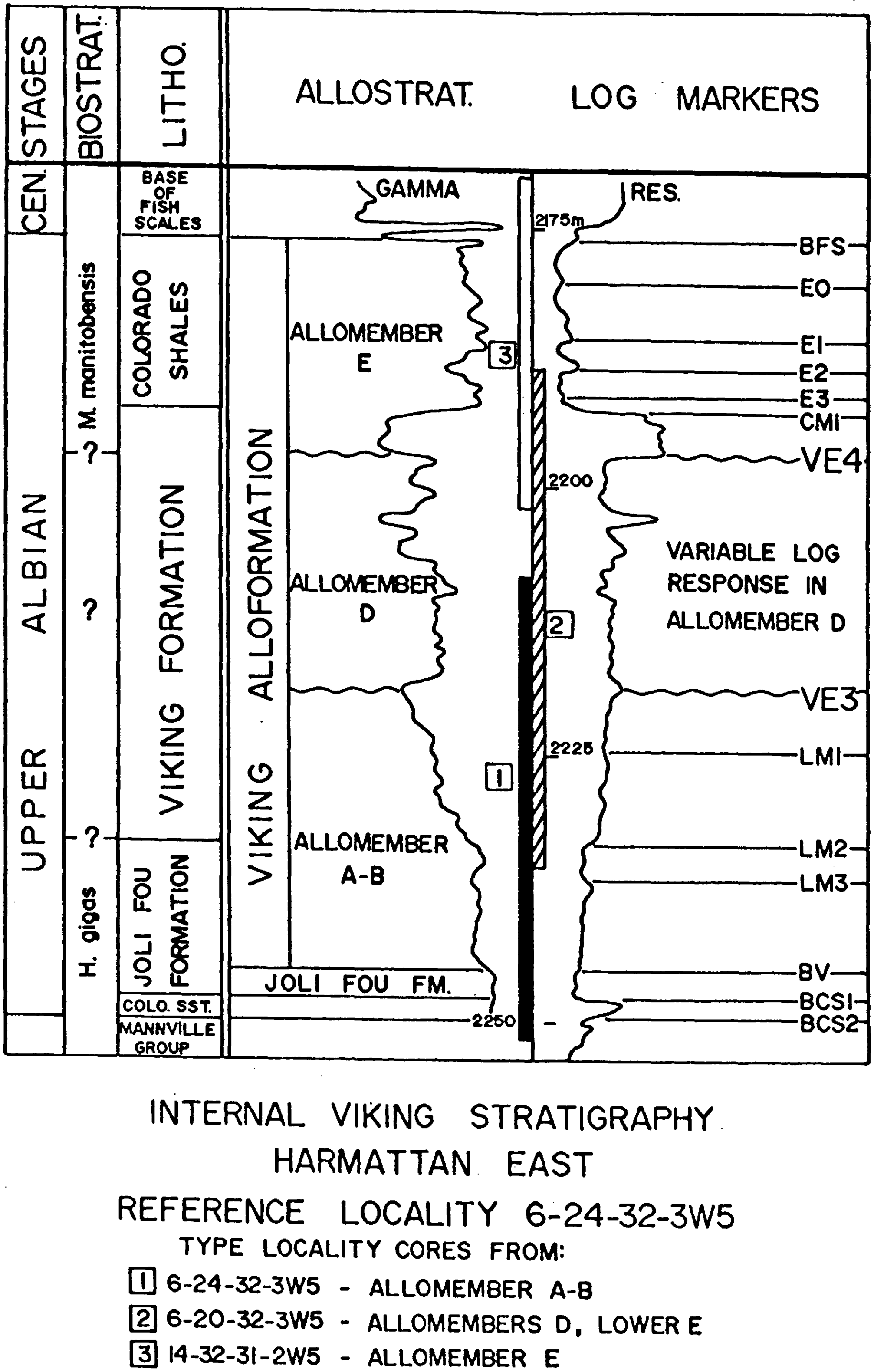

Fig. 2.5. Stratigraphy of Viking Formation, Harmattan East area. Log and core markers are discussed in text. Position of boundary between Haplophragmoides gigas and Milliammina manitobensis zones within Viking is unknown. Reference locality cores are discussed in chapter 5.

The lithostratigraphic base of the Viking Formation in the Harmattan area corresponds to log marker LM2, and the lithostratigraphic top corresponds with log marker CM1. The allostratigraphic base of the Viking alloformation corresponds to the BV log marker, while the allostratigraphic top is informally designated as the B.F.S. log marker.

Several markers and allomembers in the Harmattan area are based on the regional correlations suggested by Davies (1990); Boreen (1989); Bartlett (1991); Pattison (1991); and Boreen and Walker (1991). Other markers are derived by detailed log and facies correlation across the study area. These correlations are discussed more fully in Chapter 6.

The Base of Fish Scales is used as a datum for stratigraphic cross sections in this thesis. Markers E0 through E5 correlate as onlap markers onto VE4, and are the Viking "A grits" of Hein et al.,(1986). The E1 to E5 markers are the same as Davies' (1990), while E0 is an additional marker correlated in this study. The Viking "coarse sediment package" is defined throughout the study as the interval between CM1 and VE4. The VE3 pick is well defined on the gamma ray curve (Fig. 2.5) where it shows a prominent sandier upwards response overtop of allomember A-B. The interval between VE3 and VE4 (allomember D) represents the progradational "Cycle 2" of Leckie and Reinson (in press). Deflections exist on both gamma ray and resistivity logs between VE3 and VE4. Their reliability as log marker picks for isopach purposes is questionable because of the progradational character of the sequence (i.e. dominantly sandstone on sandstone packages that downlap toward VE3, thus creating a variable log character across the study area.

The LM1 marker between VE3 and LM2 is defined on the resistivity curve as a bump like deflection to the left. In core LM1 records the transition from muddy and pale siltstones to pale sandstones (refer to Chapter 4 for facies descriptions).

Finally, the markers below the Joli Fou Formation (BCS1 and BCS2) are the top and bottom of what is interpreted to be Basal Colorado Sandstone. Both markers correspond to prominent log deflections representing the first sandstones underlying the Joli Fou shales.

2.4 Depositional Setting

Deposition of Viking Formation sediments occurred on a broad shelf setting in the Alberta Foreland or Western Canada Basin. The shelf described as "sill like" by Boethling (1977a) separates the northern Alberta and Saskatchewan Williston basins. During part of the Cretaceous, vast embayments extending from the boreal region and Gulf of Mexico joined forming an elongate eperic seaway through the mid-continent of North America (Stelck, 1975).

Following the Mannville regression in mid Cretaceous the Colorado Sea advanced once again, first depositing shales of the Joli Fou Formation on reworked continental Upper Mannville sediments. Figure 2.6 shows the configuration of the interior seaway during Joli Fou (I. comancheanus) time. Sediments of the Upper Mannville, Basal Colorado and Cadotte Formations may represent the transgressive shorelines of this advancing Colorado sea and the Joli Fou shale the marine basin phase (Amajor and Lerbekmo, 1980).

Figure 2.7 shows the configuration of the interior seaway during Viking depositional time. Williams and Stelck (1975, p. 8) indicate the development of an endemic fauna (Neogastroplites) in the Mowry Sea indicates a partially landlocked seaway for the remainder of Albian time.
During Viking time a Colorado Sea shoreline is thought to have been in a position somewhere near the present edge of the disturbed belt (Amajor, 1980; Amajor, 1984).

Recent work on the Viking suggests that repeated regressions of the Colorado Sea or a decrease in the rate of subsidence combined with abundant sediment supply caused deposition of Viking sands (Tizzard and Lerbekmo, 1975; Hein et al., 1986; Leckie, 1986a; Downing and Walker, 1988; Reinson, 1988; Power, 1988; Raddysh, 1988; Leckie and Reinson, in press; Boreen and Walker, 1991). This work is discussed in chapter 3

Early Late Albian Seas

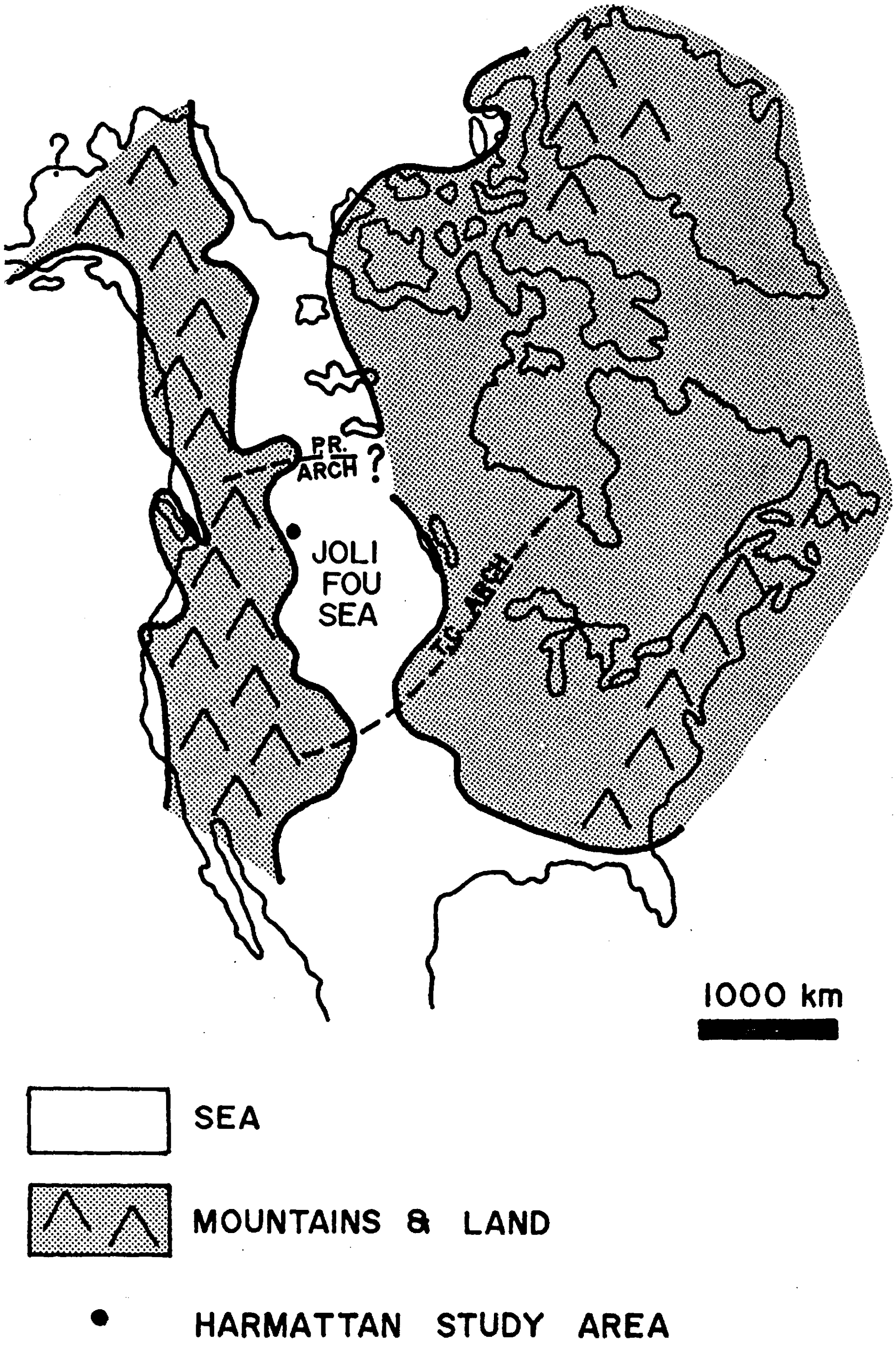

Fig. 2.6. Configuration of Cretaceous Western Interior Seaway during Joli Fou depositional time. Harmattan study area is shown as black circle. Base map is from Williams and Stelck (1975), and the extent of the Joli Fou seaway is from Koke and Stelck (1985).

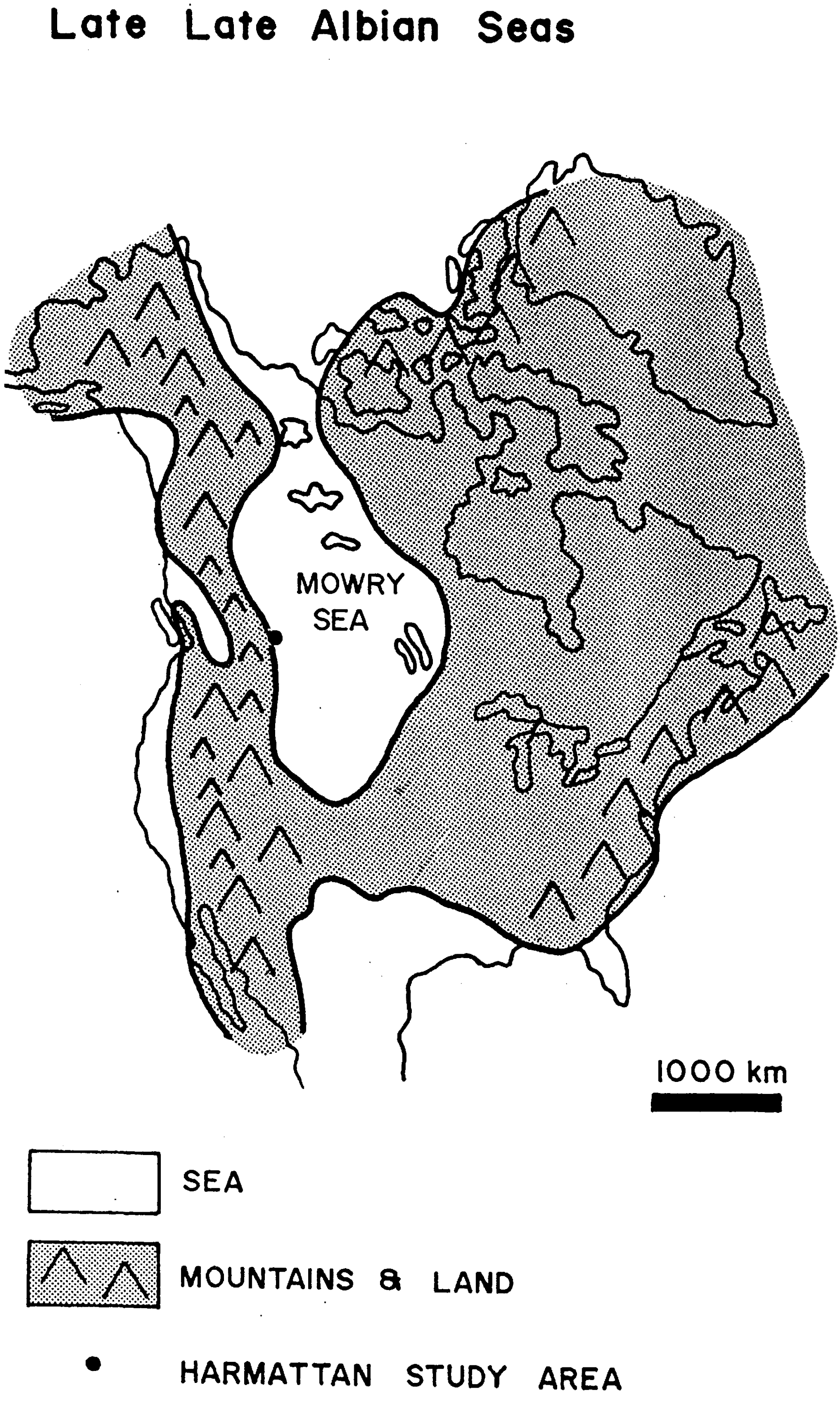

Fig. 2.7. Configuration of Cretaceous Western Interior Seaway during Viking depositional time. Harmattan study area is shown as black circle (redrawn from Williams and Stelck, 1975).

2.5 Regional Structure

The study area and its relation to some of the major structural elements of western North America are shown in Figure 2.8. The Peace River Arch is described by Cant and O'Connel (1988, p.537), as "...a major crustal anomaly in which granitic Precambrian rocks are uplifted about 1000m above their regional position in the basement." The outline of the arch on figure 2.8 represents the configuration in Middle Devonian. The West Alberta Basin is truncated to the west by the Rocky Mountains and West Alberta Arch.

The effect of structural control on the deposition of Viking Formation sediment is not discussed in the literature except for the depositional models proposed by Beaumont (1984) and Slatt (1985).

2.6 Local Structure: Thesis Area

A structure map created for the present study area suggests the Viking Formation dips southwest at a uniform rate of 11 m per kilometre (56' per mile). The study area lies just east of the Cordilleran deformed belt. Cores and well logs examined for this study did not show any evidence of major structural disturbance (e.g. fault repetition of the Viking interval). Several cores within the Harmattan East field contain microfaults and some sandstones are subvertically fractured. The timing of these fractures has not been worked out nor has their significance.

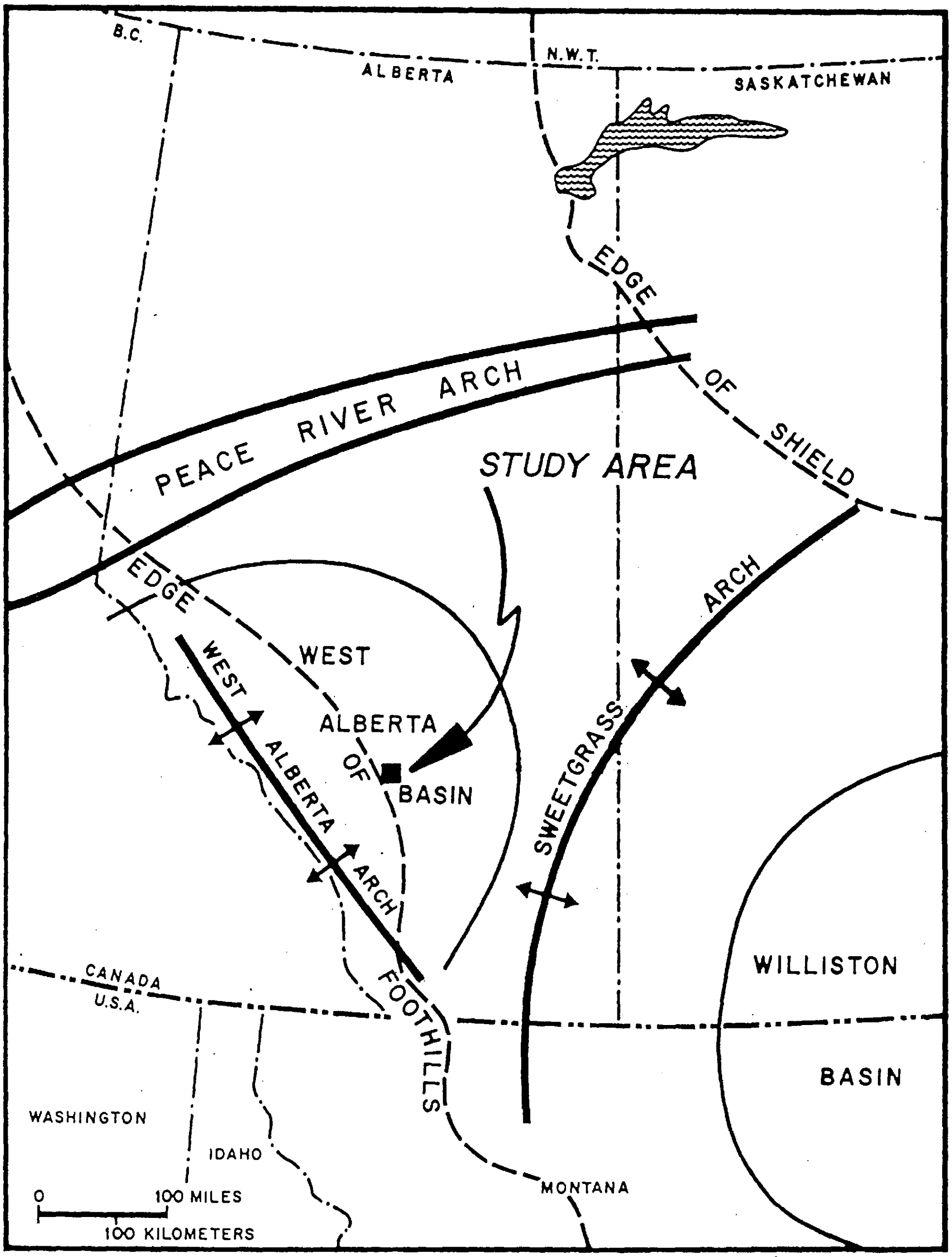

Fig. 2.8. Schematic diagram of Precambrian basin and arches Western Canada. The Harmattan East study area is shown as black box (after Putnam, 1982).

Chapter 3 Previous Work

3.1 Pre-1980 Work on the Viking Formation

Before 1980, published work on the Viking Formation in southern and central Alberta and southwestern Saskatchewan considered descriptive aspects of Viking deposits, and processes of deposition of Viking sediment. Mechanisms cited for deposition of these sediments are: 1) storm emplacement, 2) turbidity currents, 3) tidal currents, and 4) gravity flows.

Pre-1980 Viking literature is summarized in chronological order in Table 1. These studies considered facies sequences and depositional environments of the Viking in specific locations of Alberta and Saskatchewan. Interpretations of Viking sediments during this period included; 1) barrier bars, 2) offshore bars, 3) transgressive deposits, and 4) tidal reworked sand ridges (Citations in Table 1). In general, studies before 1980 conform to a viewpoint that Viking sediment was deposited in an offshore setting and subsequently reworked on the shelf.

3.2 Brief History of Post 1980 Viking Work

Post-1980 work on the Viking Formation is summarized in Table 2 according to deposit type, sediment supply (ie.

AUTHOR / DATE	STUDY AREA	PROCESS AND/OR DEPOSIT
Hunt (1954)	Joarcam Field	storm surge / shelf
Gammell (1955)	Central Alberta	regression / shoreface / bars
Beach (1956)	Southwest Alberta	turbidity currents
DeWeil (1956)	Alberta	longshore currents / bars
Stelck (1958)	Alberta	storm currents / shoreface / bars
Roessingh (1959)	South Alberta	turbidity currents
Jones (1961)	Southwest Saskatchewan	shallow sea / shoreface
1960's - Decline in number of studies on the Viking Formation		
Evans (1970)	Sask. Dodsland Hoosier	tidal currents / sand ridges
Shelton (1973)	Joffre Field	regression / barrier bar
Tizzard & Lerbekmo (1975)	Suffield Field	regression / barrier bar
Simpson (1975)	S.W. Saskatchewan	storm - tidal currents / beach - sand ridges
Lerand & Thompson (1976)	Provost Field	regression-transgression / sand ridges
Koldijk (1976)	Gilby B Pool	storm surge / shelf
Thomas (1977)	Provost Field	transgressive deposits
Boethling (1977b)	Alberta / Saskatchewan	transgression / bar and sheet sands

Table 1. Pre-1980 Viking literature summarized in chronological order. Refer to text for discussion.

TYPE OF DEPOSIT	AREA	SED IMENT SUPPLY	SEDIMENT DISPERSAL	REFERENCE
Offshore Ridges & Bars	Joffre	density currents	tidal currents	Reinson et al., 1983
	Joffre - Joarcam	transgression	?	Beaumont, 1984
	Joffre - Joarcam	reworked shoreline seds	hydrodynamic processes	Slatt, 1985
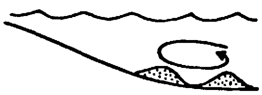	S. Alta. & S.W. Sask.	?	tidal currents	Amajor, 1986
	Caroline	reworked shoreface	tidal currents	Leckie, 1986a
	Eureka	sand plume distrib channel	storm currents	Pozzobon and Walker, 1990
	Garrington	storm surge currents	littoral currents	Hein et al., 1991
Deltas and Barrier Islands	Central Alta.	delta	regression	Amajor, 1980
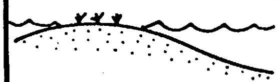	S.W. Sask.	delta	regression	Amajor, 1984, 1986
	Joffre - Gilby	?	transgression	Ryer, 1987
Gravity and Debris Flow Deposits	Harmattan	gravity flow	transgression	Hein et al., 1986
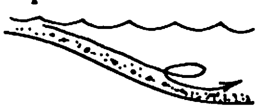	Caroline	subaqueous debris flow	bioturbation	Leckie, 1986a
Estuarine - Valley Fill	Crystal	fluvial-reworked shelf	transgression -tidal currents	Reinson et al., 1988; Leckie and Reinson, in press
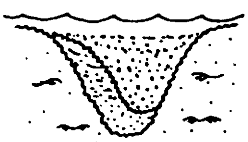	Crystal	fluvial-reworked shelf	fluvial -tidal currents	Pattison, 1990
	Willesden Green	fluvial-reworked shelf	transgression -tidal currents	Boreen and Walker, 1991
Incised Shorefaces	Joffre	fluvial	storm currents	Downing and Walker, 1988
	Gilby	fluvial	waves-longshore currents	Raddysh, 1988
	Joarcam	reworked shelf	storms	Power, 1988
	Caroline Garrington	fluvial - reworked shelf	storm - tidal currents	Davies, 1990
	Willesden Green	fluvial - reworked shelf	storm - tidal currents	Boreen and Walker, 1991

Table 2. Summary of post-1980 work on the Viking Formation according to deposit type, sediment supply, and mechanism of dispersal.

how the sediment was brought to the depositional sight), and sediment dispersal (ie. how the sediment was redistributed in the depositional environment). Most of this work (Citations in Table 2) seems to have been influenced by the principles and practice of sequence stratigraphy, namely, mapping of facies units, and the recognition and correlation of unconformity-bounded sedimentary packages over large study areas. Sea level change is usually identified as the mechanism which created the unconformities.

The earlier studies during this time period interpret the Viking Formation as: 1) offshore ridges and bars, 2) deltas and barrier islands, and 3) gravity and debris flow deposits (Citations in Table 2). The more recent studies interpret the Viking Formation as: 1) estuarine and valley fill deposits, and 2) incised shoreface deposits (Citations in Table 2). Deposition of Viking sediment is thought to have occurred during multiple transgressions and regressions as sea level fluctuated through Viking time. The interpretations vary as to number of transgressions and regressions, and the significance of one depositional process versus another.

Discussions of previous Viking Formation work can be found in: Robb (1985), Grant (1985), Downing (1986), Raddysh (1986), Power (1987), Boreen (1989), and Davies (1990). A review and discussion of previous work pertinent to this thesis area is presented in the following section (3.3).

3.3. Ideas in the Harmattan East Area

Non-marine sediments in the Viking Formation have been observed in the Harmattan East and Crossfield area of south-central Alberta (Hein et al., 1986; Leckie, 1986a). The internal stratigraphic relationship of this non-marine stratum to other Viking deposits to the north has received little attention. Amajor's (1980) subsurface study of the Viking in south-central Alberta and south-western Saskatchewan interpreted the Viking east of the present study area as shoreline (barrier island) deposits. The most recent work completed in the vicinity of the present study area is that of Grant (1985); Grant et al., (1985); Robb (1985); Hein et al. (1986); Leckie (1986a); and Hein et al., (1991).

Hein et al. (1986) suggest the Viking deposits at Caroline, Garrington, and Harmattan East fields record three "styles" of marine sedimentation created during various "phases" in Viking time (Fig 3.1). Phase 1 is thought to represent a regression with Viking deposits at Caroline field recording the initial progradation of a shoreline attached clastic wedge. The second stage is thought to represent a lowstand during a eustatic sea level drop. During this phase channels and valleys incised into the progradational shoreface deposits. The coarse sandstones and conglomerates at the Harmattan East field were deposited by storm induced gravity flows focussed within one of these incised channels

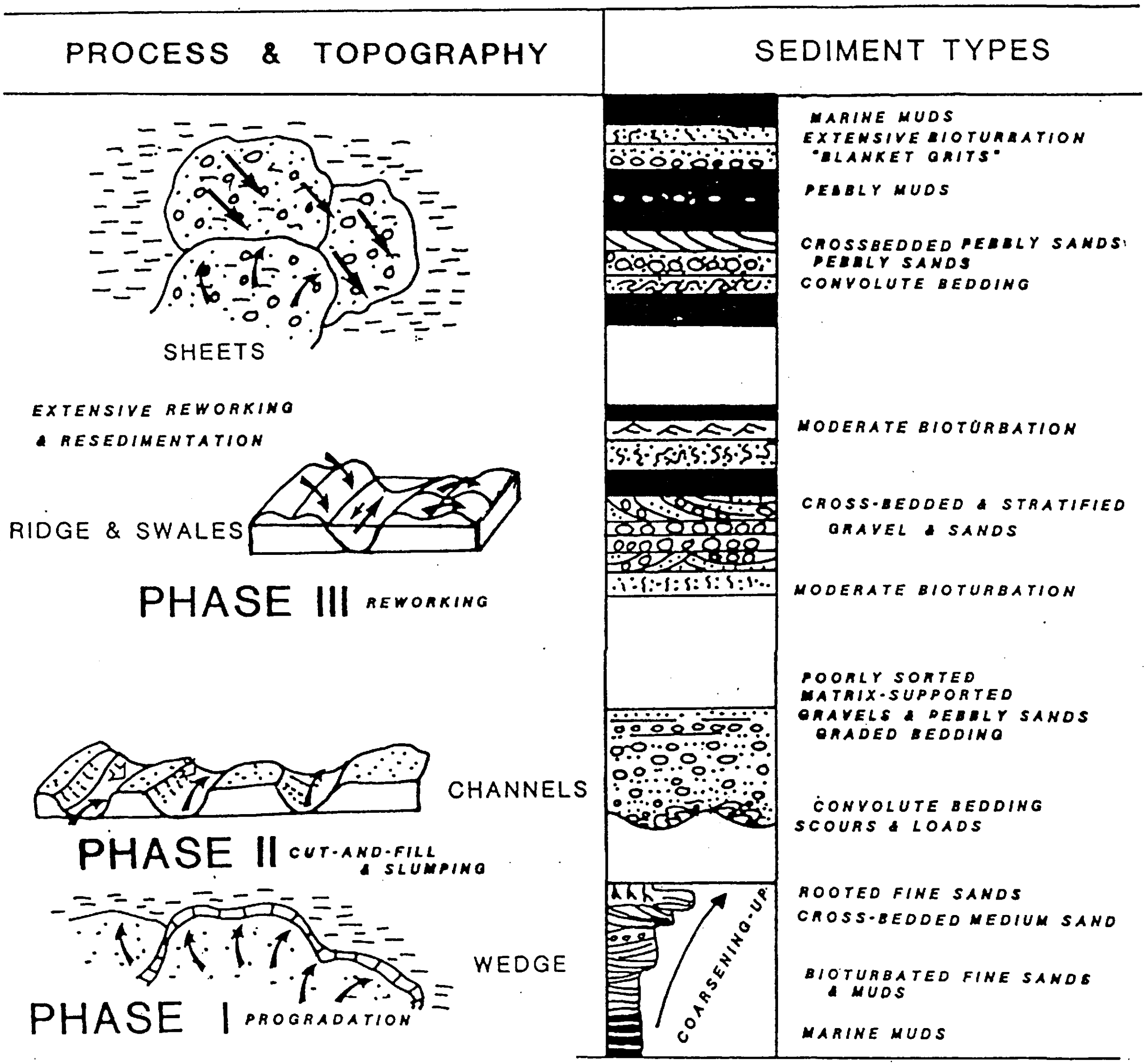

Fig. 3.1. Diagrammatic sketch illustrating the paleogeographic and sedimentation history of the Viking Formation in the Harmattan East, Caroline, and Garrington areas. Refer to text for discussion of phase's (from Hein et al., 1986).

(Grant, 1985) (Fig 3.1). Cant and Hein (1986, p. 310) describe a Viking channel at Harmattan East as exactly analogous to the style and type of fill of the Cardium Ricinus Channel (Walker, 1983a, b). The final stage invoked stillstand reworking and a rising sea level associated with a reduction in tectonic activity and depletion of sediment supply. The coarse sandstones and conglomerates at Caroline and Garrington fields are thought to represent ridge and swale deposits formed during this final transgressive reworking phase.

This interpretation is similar to that of Leckie (1986a) for a study of Viking sediments at Caroline. Leckie observed high angle and compound cross-bedding in sandstones and conglomerates in the north-west portion of the Caroline field and suggested they formed as tidal sand ridges during a major transgression.

The studies previously discussed were completed as 'field specific' studies. For example, the work of Grant (1985) and Robb (1985) dealt almost entirely with specific aspects of reservoir geology. Both studies concentrated on core within the fields and did not consider off field facies relationships except in a general sense. The regional synthesis of this work presented by Hein et al. (1986) does not attempt to relate the three fields in this area stratigraphically.

Recently, Hein et al., (1991) described the Viking

Formation at Garrington field as a shelf sand ridge complex. The ridge complex consisted of pods of coarse grained sediment (1-3 m of relief) superimposed on a paleotopographic high. The pods of sediment were interpreted by these workers as ancient equivalents to modern shelf sand or gravel waves.

Finally, Leckie (1986a) showed an interpretation of the relationship of Viking non-marine sediments in the Crossfield area to the coarse grained "tidal" sediments at the Caroline field. The correlation of facies between these areas is based on two wells separated by a distance of 140 km. The correlation is not shown with respect to the Harmattan East and Garrington fields.

In this thesis vertical and lateral facies relationships are used to show that the lower Viking Formation at Harmattan East was deposited as a series of multiple regressions and that the upper sandstones and conglomerates of the Viking in this area formed during a major transgression punctuated by multiple stillstands.

Chapter 4 Facies Descriptions, Interpretations, and Facies Petrographic Evaluation

4.1 Introduction

Fifteen facies were recognized while logging core (Appendix 1) at the Core Research Centre of the Alberta Energy Resources Conservation Board. Table 3 is a comparison of facies terminology with that of Davies' (1990) adjoining study of the Garrington and Caroline areas.

In this thesis facies are differentiated by their characteristic lithologies, grain sizes, sedimentary structures, contacts, and biological (trace fossil) features. All core was measured in metric units and grain size measurements were performed with a hand lens and Canstrat (Canadian Stratigraphic Service) grain size card (phi scale). Each facies description is followed by a preliminary interpretation.

Section 4.3 considers three of the facies from a petrographic viewpoint. A brief summary of the petrographic and S.E.M. investigation can be found at the end of this chapter (section 4.3.7).

THIS THESIS	DAVIES' (1990)
Facies 1: Dark Mudstone	Facies 9: Black Mudstone
Facies 2: Muddy Siltstone	Not recognized
Facies 3: Sandy Siltstone	Facies 1: Burrowed Muddy Siltstone
Facies 4: Pales Sandstone	Not Recognized
Facies 5a: Cross Bedded and Structureless Sandstone	Facies 7: Pebbly Cross Stratified Sandstone
Facies 6: Conglomerate	Facies 6: Conglomerate
Facies 7a: Fine Grained Burrowed Laminated Sandstone Mudstone	Facies 2: Burrowed and Laminated Sandy Mudstone
Facies 7b: Coarse Grained Burrowed Laminated Mudstone Sandstone	Not Recognized
Facies 8: Interbedded Sandstone Mudstone	Facies 3: Hummocky Cross Stratified Sandstone
Facies 9: Thick Bedded, Non-Bioturbated Sandstone	Facies 4: Swaley Cross Stratified Sandstone
Facies 10: Parallel Laminated and Cross Bedded Sandstone	Not Recognized
Facies 11: Rooted Brown Mudstone Siltstone	Facies 10: Paleosol
Facies 12: Convoluted and Laminated Mudstone-Sandstone	Not Recognized
Facies 13: Bioturbated Pebbly Sandstone Mudstone	Facies 8: Pebbly Burrowed Mudstone

Table 3. Comparison of facies terminology used in this thesis with that of Davies' (1990) adjoining study of the Caroline and Garrington areas.

4.2 Facies

4.2.1 Facies 1: DARK MUDSTONE

Facies 1 is divided into two subfacies 1a and 1b. Facies 1a varies from dark grey to black in colour and may contain rare millimetre scale silty laminations (Fig. 4.1). In the study area it is observed in only one well (6-24-32-3W5) where it is 15 m thick. No distinct burrow or trail forms were observed, but a hint of bioturbation can be seen in association with rare silty streaks. In core, mudstones of facies 1a are massive and show no fissility. In the 6-24-32-3W5 well, dark mudstones of the Joli Fou Formation are impossible to differentiate from dark mudstones of the basal Viking. In this same well two very thin (<2 mm thick) bentonite horizons occur within the dark mudstones.

Facies 1b is also a dark mudstone and is differentiated from facies 1a by fissility, silt and sand content, and the presence of sandstone dikes (described below). The mudstones of facies 1b range 1 to 10 m in thickness. These mudstones are fissile and may exhibit conchoidial fracture and often breaks into "poker chip" like pieces (Fig. 4.1). Parting planes often contain abundant fish scales. Siltstone and vfL to fL sandstone interbeds make up 5 to 10 percent of this facies by volume. The beds are sharp based, 0.2 to 2.0 cm thick, and are massive, parallel laminated, or ripple cross-laminated.

Sandstone dikes occur in the lower part of this facies

Figure 4.1: Facies 1 - Dark Mudstone

a) Massive dark black mudstone of subfacies 1a. Note blocky nature of core when compared to fissile black mudstone of subfacies 1b. Well 6-24-32-3W5; Depth 2229 m; Scale bar is 15 cm long.

b) Fissile dark black mudstone of subfacies 1b. The fissile nature of these mudstones create 'poker chip' like pieces. Well 6-19-32-3W5; Depth 2164 m; Scale bar is 15 cm long.

c) Close up view of subfacies 1a showing rare silty streaks in an otherwise massive dark mudstone. Well 6-24-32-3W5; Depth 2231.5 m; Scale bar is 3 cm long.

d) Folded sandstone dikes cross-cutting dark mudstones were only observed in subfacies 1b. Note the sharp contacts between the dikes and surrounding mudstone. Well 6-11-30-3W5; Depth 2238.4 m; Scale bar is 3 cm long.

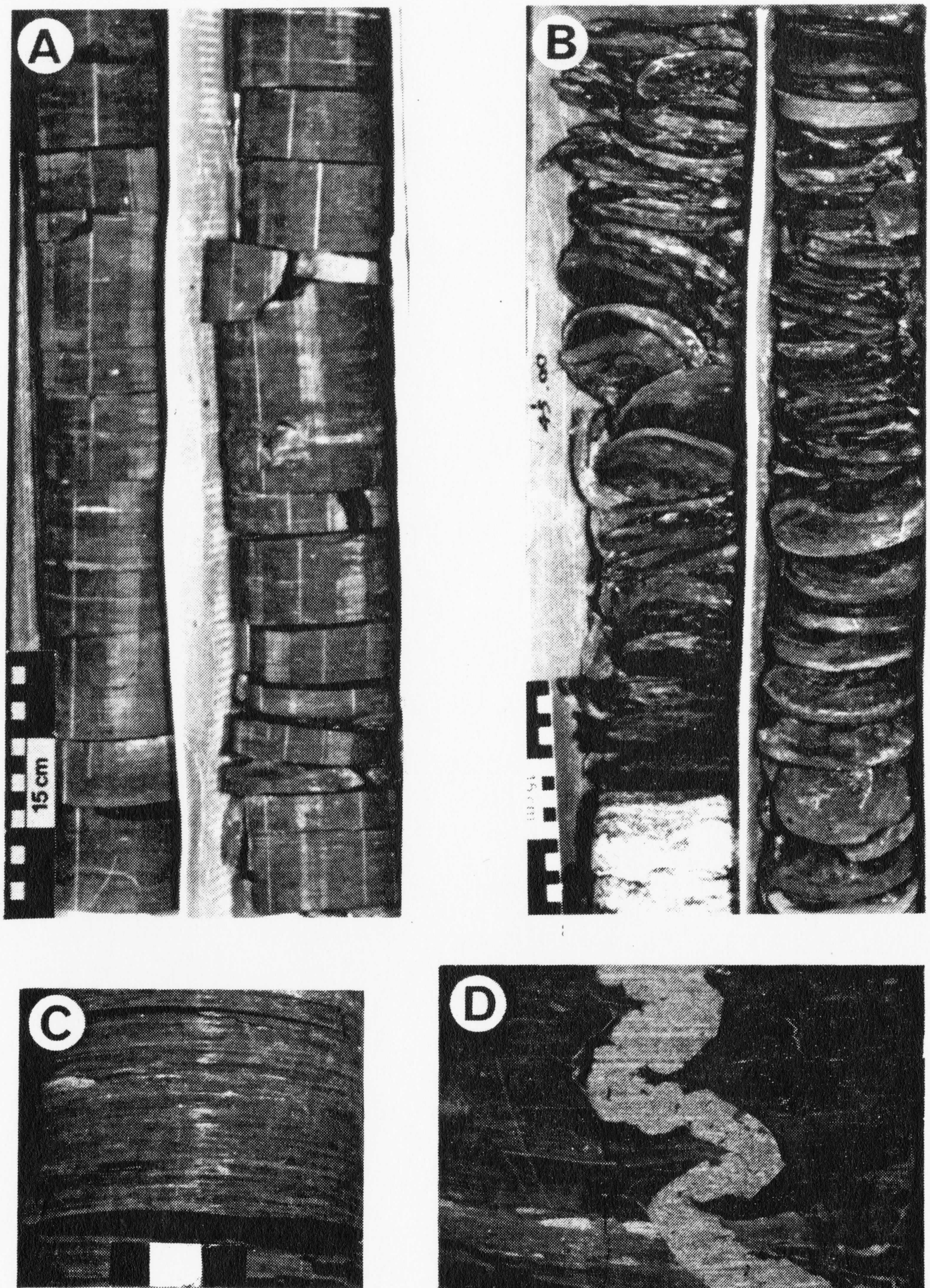
A
15 cm
B
C
D

and are seen in approximately 5 percent of the examined core (Fig. 4.1). The dikes are folded, subvertical, and internally contain a siltstone and vfL to vfU grained sandstone matrix. The dikes crosscut mudstone, siltstone, and sandstone beds. In cross section the dikes are 1 to 2 cm wide. The contacts between the dikes and surrounding mudstone are generally sharp. The dike walls often show slickensides (Leckie and Potocki, 1988). Finally, siderite beds, 10 to 15 cm thick commonly occur near the top of this facies.

Preliminary Interpretation

Facies 1a and 1b are interpreted to have been deposited in deep, quiet water in an offshore basinal environment that was well below storm wave base. The sandstone dikes in this facies are interpreted by Leckie and Potocki (1988, p. 325) to have formed by sand injection through mud during release of gas from overpressured sandstones in the lower Viking. The triggering mechanism for pressure release may have been an earthquake.

4.2.2 Facies 2: MUDDY SILTSTONE

Facies 2 is gradational from facies 1 (dark mudstones) into facies 3 (sandy siltstones). The muddy siltstone facies is 4 to 7 m thick, and is a homogeneous mixture of thoroughly bioturbated silt, clay, and mud with less than 5 percent vfL to vfU sand preserved in thin (1 - 8 mm) sandstone beds that are discontinuous due to bioturbation (Fig. 4.2). The rare sand beds are generally sharp based, normally graded, parallel to undulatory laminated, or massive, and have gradational tops. Recognizable trace fossils include Helminthoidea, Terebellina, Planolites, and Asterosoma.

Preliminary Interpretation

This facies was also deposited in deep, quiet water in an offshore setting well below storm wave base. The sandstone and siltstone interbeds are interpreted to be the deposits of distal storm-generated flows.

4.2.3 Facies 3: SANDY SILTSTONE

Facies 3 is gradational from facies 2 (muddy siltstone) into facies 4 (pale sandstone). The facies ranges 4 to 6 m thick and is seen in approximately 10 percent of the core examined. Facies 3 is a thoroughly bioturbated mixture of clay, silt and vfL to vfU sand, with higher proportions (10 to 35 %) of silt and fine sand than in facies 2 (Fig. 4.3). Facies 3 is generally lighter in colour than facies 2 as a result of its greater sand content. Rare 1 to 2 cm thick preserved sandstone beds occur, but are infrequently traced the width of the core because of the intensity of burrowing and bioturbation. The sandstone beds are sharp based, normally graded and have well developed undulatory laminae. Mottled siderite patches (2 cm thick) occur rarely and have diffuse boundaries.

Figure 4.2: Facies 2 - Muddy Siltstone

a) Extreme burrowing of organisms has resulted in a homogeneous mixture of mud, silt, and sand. Helminthopsis burrows are present. Well 6-24-32-3W5; Depth 2227.1 m; Scale bar is 3 cm long.

Figure 4.3: Facies 3 - Sandy Siltstone

b) This example shows a higher percentage of sand than the previous example. Rare Terebellina and Helminthopsis burrows are present. Well 6-24-32-3W5; Depth 2224.3 m; Scale bar is 3 cm long.

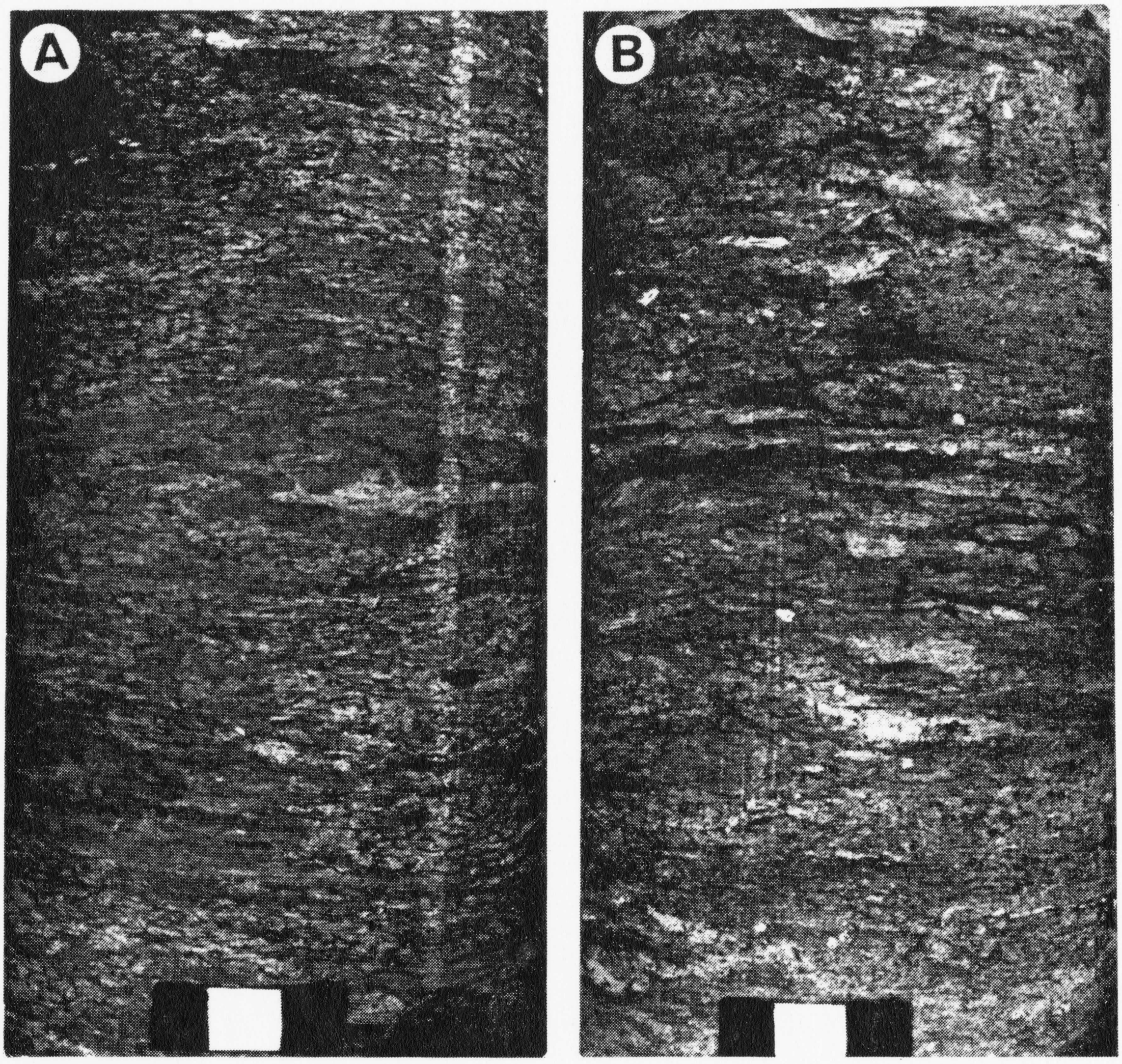
A
B

The dominant trace fossil in facies 3 is Helminthoidea which appears as dark, mud filled, 1 cm long by 1 mm thick like traces. Other recognized trace fossils include Terebellina, Planolites, and Asterosoma. Other less common trace fossils include Paleophycus, and Skolithos.

Preliminary Interpretation

This facies was deposited in a low energy environment below storm wave base. The low-diversity Cruziana ichnofacies assemblage (Planolites and Helminthoidea) suggest harsh ecological conditions produced by increased water turbidity and rapidly fluctuating rates of suspension of sediment.

4.2.4 Facies 4: PALE SANDSTONE

Facies 4 is 4 to 5 m thick and is gradational from facies 3 (sandy siltstone) (Fig. 4.4). It can be sharply overlain by facies 8 (interbedded sandstones - shale) or facies 6 (conglomerate). The pale sandstone facies is a thoroughly bioturbated mixture of sand (vfU-fU), silt and mud. The sand content ranges from 30 to 95 percent of the facies, giving it a lighter colour than facies 2 or 3. Facies 4 contains fewer muddy laminae and muddy siltstone streaks than facies 3.

Discrete sandstone beds of very fine to fine sand may occur near the top of the facies. These beds are 1 to 6 cm thick, sharp based, and have flat to low angle inclined

Figure 4.4: Facies 4 - Pale Sandstone

a) Gradational contact between facies 3 and facies 4. Note the increase in sand at top of photo. <u>Helminthopsis</u> burrows are present. Well 6-24-32-3W5; Depth 2221.3 m; Scale bar is 3 cm long.

b) Note that extreme burrowing has resulted in an almost complete destruction of sedimentary structures. Rare <u>Helminthopsis</u> and <u>Ophiomorpha</u> burrows are visible. Well 6-24-32-3W5; Depth 2219.9 m; Scale bar is 3 cm long.

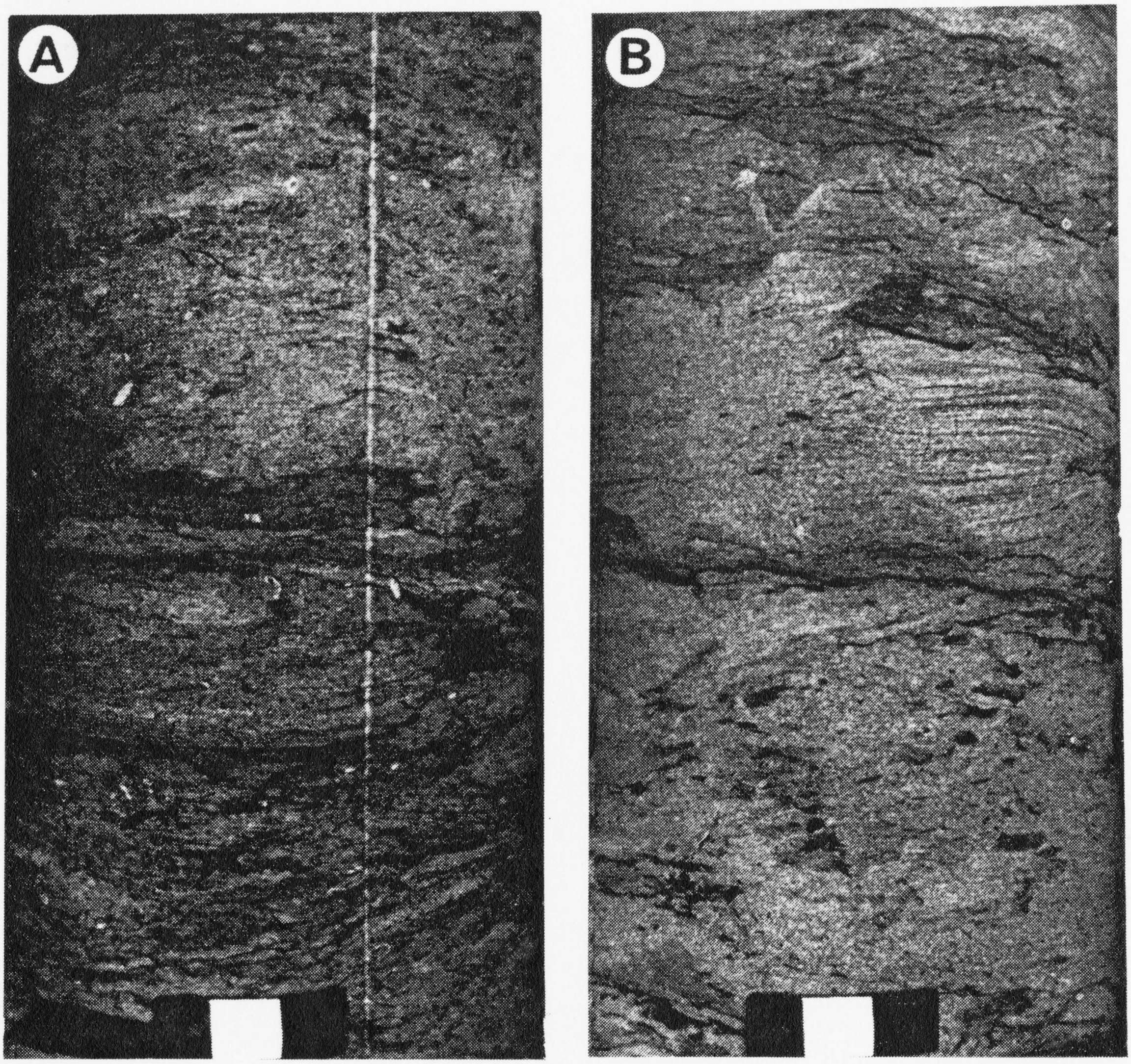
A
B

lamination.

In general, the facies exhibits an upwards decrease in bioturbation. Recognizable trace fossils include Ophiomorpha, Helmithoidea, Terebellina, Planolites, and rare Paleophycus, and Teichichnus. Ophiomorpha is the most abundant trace fossil in the facies. The burrow form occurs as both a light and dark textured infill with very thin (1 mm thick) mud linings surrounding the internal burrow walls. Some of the wall structures as seen in core cross section have irregular nodular like linings which resemble Ophiomorpha nodosa (Frey and Pemberton, 1985, p. 89).

Preliminary Interpretation

The high diversity of trace fauna in this facies is compatible with the Cruziana ichnofacies and implies relatively uniform rates of sedimentation, bottom water conditions, and minimal turbidity all characteristic of a lower shoreface environment of deposition (Moslow and Pemberton, 1988). The low angle inclined lamination in the upper part of the facies may be an expression of hummocky cross stratification.

4.2.5 Facies 5a: CROSS-BEDDED AND STRUCTURELESS PEBBLY SANDSTONE

This facies comprises the main reservoir rock of the Harmattan East oil pool. Facies 5a consists of mL to vcU grained and pebbly (5.0 to 7.0 mm in diameter) sandstones with occasional mudstone partings (< 2 cm thick) throughout (Fig. 4.5). The cross-bedding style in this facies is similar to that in facies 7b, but facies 5a has a greater percentage (95%) of sand, and minimal bioturbation and burrowing.

In this facies, individual sandstone beds may be a few centimetres to tens of centimetres thick. Three types of stratification observed within the sandstone are, 1) high angle cross bedding up to the angle of repose, 2) crude low angle cross bedding, and 3) compound cross bedding where two scales of cross bedding occur.

The first type of stratification mentioned above is the most common form of cross bedding in facies 5a. In core the toesets of the cross beds appear to flatten asymptotically, and within any cross bed set, the angle of cross bedding appears to increase upwards (Fig. 4.5). Sandstone bases are commonly planar. Cross laminae within a cross bed set are often accentuated by variation in grain size (Fig. 4.5). The cross bed sets range in size from 6.0 to 11.0 cm thick (average 8.0 cm). Individual sets commonly pass upwards gradationally into bioturbated and burrowed muddy sandstones of the same grain size. These muddy sandstones (10 to 20 cm thick) are often sharply truncated at the top by another bed of cross bedded sandstone.

Crude, low angle (<12 degree) bedding is also recognized in core of this facies. Dip angles of beds were difficult

Figure 4.5: Facies 5a - Cross-Bedded and Structureless Pebbly Sandstone

a) Low to high angle cross-bedding in a coarse grained sandstone. Well 9-26-30-3W5; Depth 7231 ft; Scale bar is 3 cm long.

b) Irregular black mudstone partings in a structureless granular sandstone. Note the mudstone rip up clast at top of photo. Well 16-13-32-3W5; Depth 2187 m; Scale bar is 3 cm long.

c) Low to high angle cross-bedding in a coarse grained sandstone with granules. Note the cross laminae accentuated by variations in grain size. Well 6-16-32-3W5; Depth 2205 m; Scale bar is 3 cm long.

d) Faintly laminated, low angle crossbedding in a pebbly sandstone. Well 8-28-32-3W5; Depth 2210.9m; Scale bar is 3 cm long.

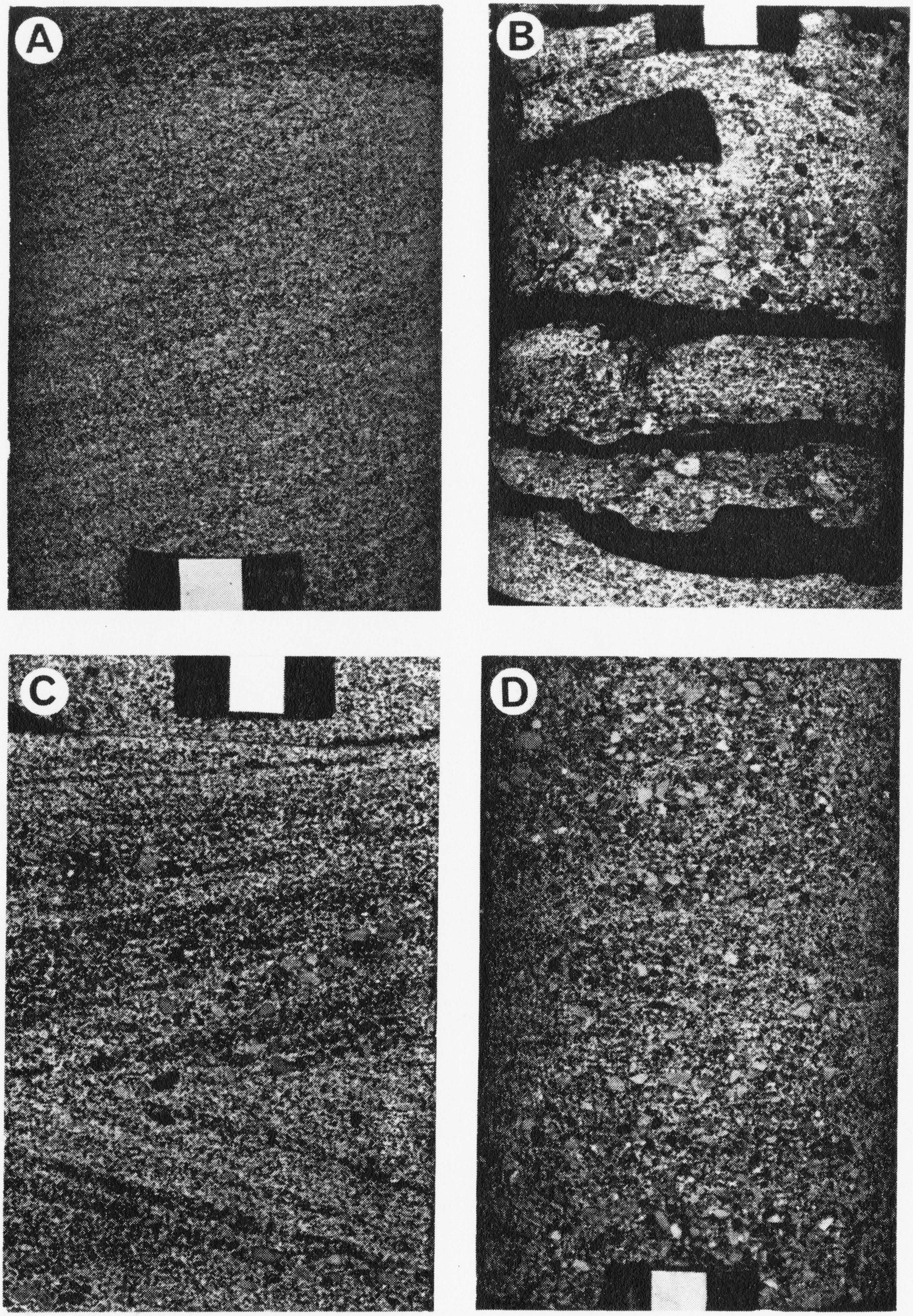
A
B
C
D

to measure because the core was usually sawn, and many plug samples had been removed. The sandstone more often appears as structureless 15 to 35 cm thick beds of mU grained to pebbly sandstone (Fig. 4.5). Occasionaly these beds fine upwards. These structureless beds commonly have 4.0 to 8.0 mm well rounded chert pebbles and 2.0 to 7.5 cm mudstone and siderite clasts dispersed throughout them.

Compound cross bedding was observed in several cores of this facies (Fig. 4.6). These cores are located in the north-west portion of the study area, and are in close proximity to the Viking Caroline field (Leckie, 1986a). This style of cross bedding was recognized in core as a coset of three or more sets of tangential cross beds whose set boundaries dip in the same direction as the internal cross beds (A.D. Reynolds, pers. comm., 1989). Internal cross beds have dip angles that range 18 to 28 degrees, while set boundaries have dip angles 10 to 12 degrees. Cosets range from 30 to 80 cm thick. Up to 2m thick cosets have been observed by A. D. Reynolds, pers. comm., 1989) in the Caroline field area. No mud drapes were observed in association with this style of cross bedded sandstone.

Bioturbation is minimal in sandstones of facies 5a. Rare Arenicolites and Skolithos are recognized in the muddier portions of this facies.

Preliminary Interpretation

The various styles of cross bedding in facies 5 indicate

Figure 4.6: Facies 5a - Cross-Bedded and Structureless Pebbly Sandstone

a) Granular sandstone with little if any development of cross stratification. Well 8-28-32-3W5; Depth 2211.4 m; Scale bar is 3 cm long.

b) This example show two styles of cross stratification at different dip angles. Note the sets of high angle cross beds (lighter coloured intervals) bounded by sets of lower angle master bedding surfaces (dark coloured intervals). Well 8-13-32-3W5; Depth 2188 m; Scale bar is 3 cm long.

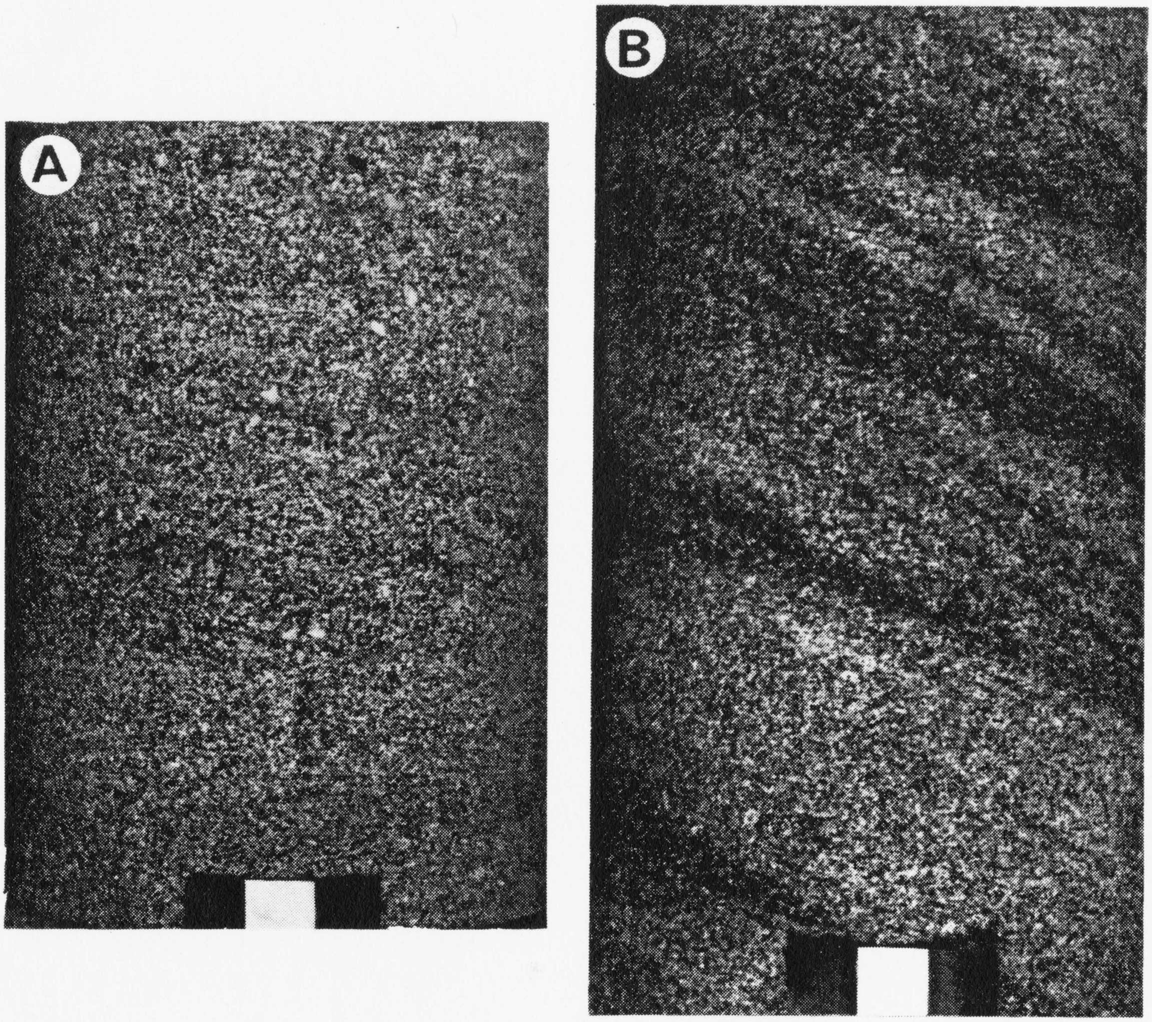
A
B

deposition in an environment where currents were strong enough to produce trough cross beds and compound cross beds. Waves and tides could have created these cross beds (Leckie, 1986a). The general absence of mud in this facies implies that continual reworking and winnowing of the sediment took place in the depositional environment. The rare trace fossils are indicative of the Skolithos ichnofacies, suggestive of a soft substrate in a high energy shallow marine setting.

4.2.6. Facies 5b: MUDSTONE-SILTSTONE RIP-UP, CROSS-BEDDED SANDSTONE

This facies consists of fU to vcU grained, fining upwards "salt and pepper" textured sandstone 1 to 4.5 m thick. The facies is observed in three of the study cores (7-28-31-4W5, 2-14-33-5W5, and 9-22-33-5W5). The sandstones contain low-angle planar to slightly trough shaped cross beds in sets 40 cm to 1 m thick. The angle of cross bedding generally increases upwards within each set (10 up to 26 degrees) (Fig. 4.7). Comminuted plant debris is common on foreset laminae. The base of the facies is sharp and erosive and overlies either facies 9 or 10. Pebble layers are common at bases and include chert (up to 2.0 mm in diameter), subangular siderite (up to 60 mm), and brown and green mudstone clasts (Fig. 4.7). The pebbles, siderite, and mudstone clasts form sharp based beds up to 10 cm thick.

Figure 4.7: Facies 5b - Mudstone-Siltstone Rip-Up, Cross-Bedded Sandstone

a) Low angle planar to slightly trough shaped cross beds in a coarse grained "salt and pepper" textured sandstone. Well 7-28-31-4W5; Depth 2395.3 m; Scale bar is 3 cm long.

b) This example is from the basal portion of the facies. It is characterized by pebbles, subangular siderite, and brown and green mudstone clasts. Well 2-14-33-5W5; Depth 2492.9 m; Scale bar is 3 cm long.

c) Mudstone-siltstone rip up clasts in a structureless medium grained sandstone. Note the delicate "wispy" nature of the smaller mudstone clasts. Well 7-28-31-4W5; Depth 2390 m; Scale bar is 3 cm long.

d) Massive and structureless "salt and pepper" textured, coarse grained sandstone. Waxy mudstone rip ups are present along parting planes. Well 7-28-31-4W5; Depth 2392.3 m; Scale bar is 3 cm long.

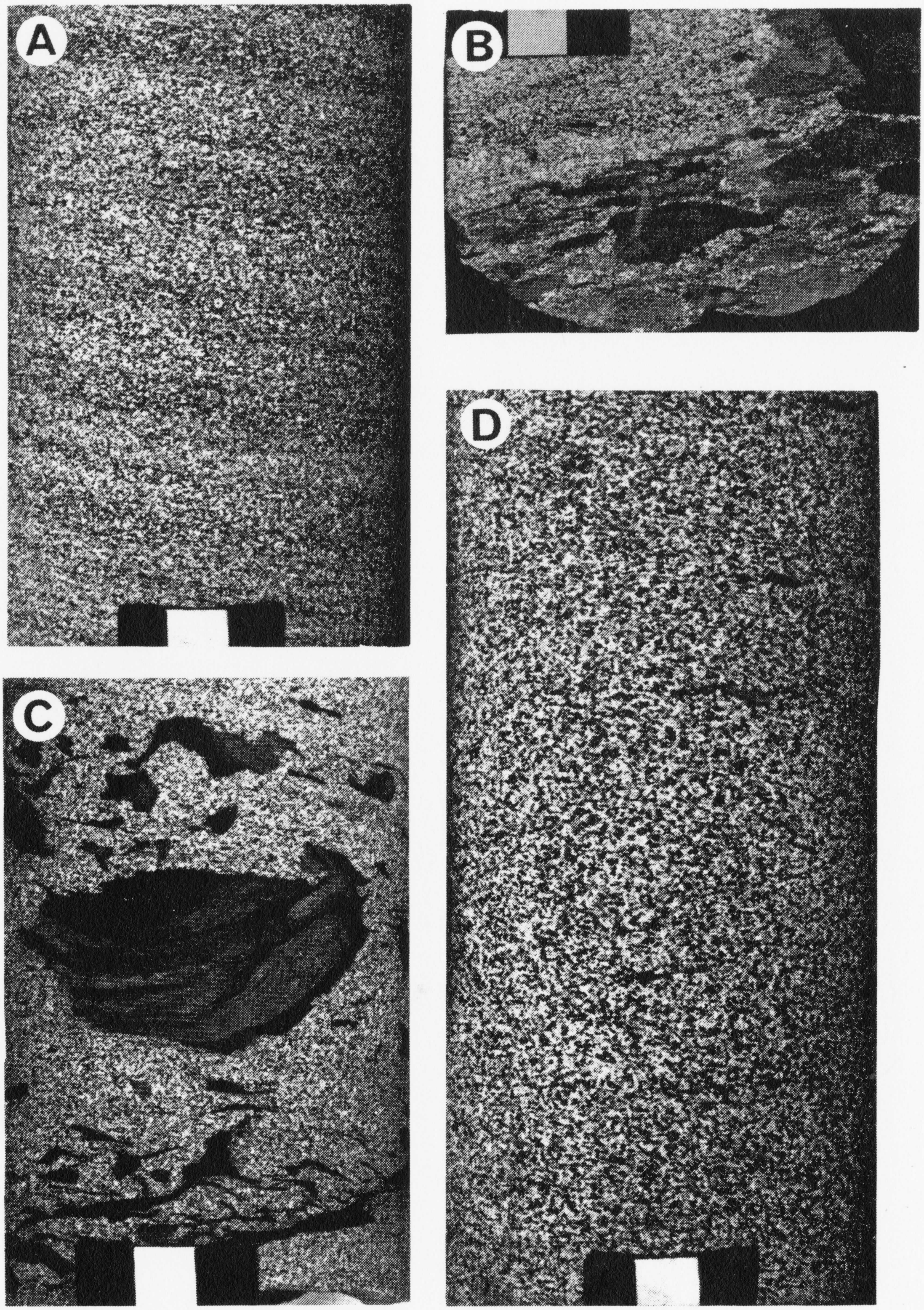
A
B
C
D

The sandstones of this facies are different from facies 5a in three ways. First, they are relatively poorly sorted and are highly feldspathic while sandstones of facies 5a are generally feldspar poor (refer to section 4.3 - Petrography). Secondly, facies 5b contains abundant mudstone and siltstone rip up clasts. These rip ups appear as two different types in cores of this facies. Black - grey angular mudstone siltstone rip ups (up to 60 mm in size) are observed in the 7-28-31-4W5 well and are associated with massive to structureless sandstones of this facies (Fig. 4.7). The second type of rip up clasts are brown to grey-green, waxy mudstone-siltstone (Fig. 4.7). These clasts are thin (< 2 mm thick) and resemble plate like discs (2 to 4 cm in diameter) when observed in plan view at broken core ends. Thirdly, no marine trace fossils were recognized, and the sandstones are not bioturbated. Marine trace fossils are always observed in facies 5a.

Preliminary Interpretation

The sandstones of facies 5b are interpreted to be deposits of unidirectional flows in fluvial-dominated channels. The cored sections of this facies are insufficient to distinguish the type of channel sequence this facies may represent. Several factors point to a fluvial as opposed to a tidal channel at the well locations mentioned above. These factors include lack of herringbone cross-stratification and tidal bundles, and lack of marine trace fossils or shell material. Section 4.3 discusses the petrographic differences between facies 5a and 5b.

4.2.7. Facies 6: CONGLOMERATE

Facies 6 primarily contains well rounded chert pebbles and cobbles that range in size from 0.6 mm to 15 cm (avg. 2.5 cm) in diameter. The conglomerate is clast supported and contains a matrix of either vfU to fU grained sand when it is seen in facies 9 (Fig. 4.8), or mL to vcU grained sand when it is interbedded in facies 5a (Fig. 4.8). The conglomerate is poorly sorted, rarely normally graded, occassionaly banded (Fig. 4.8), and ranges from one clast size thick to beds 90 cm thick (avg. 20 to 25 cm thick). Rare sandstone rip-ups and siderite clasts are found in the facies. Siderite rip ups are more common than sandstone rip ups, and usually comprise 5 percent of the clast population. The siderite clasts are generally well rounded and range in size from 0.8 cm to 4.2 cm in diameter. The bases of most conglomerate beds are erosive (Fig. 4.8). Tops of beds are usually gradational with the overlying facies. No trace fossils were observed in the conglomerates.

Preliminary Interpretation

Facies 6 may represent winnowed storm deposits. The pebbles and cobbles may have been transported out onto the shelf by geostrophic flows during extremely large storms. The hummocky and swaley cross-stratified sandstones which are

Figure 4.8: Facies 6 - Conglomerate

a) Poorly sorted, slightly banded conglomerate with a very fine grained sand and granule matrix. Well 6-18-32-3W5; Depth 2185.2m; Scale bar is 3 cm long.

b) Poorly sorted conglomerate. Well 14-7-32-3W5; Depth 2189.1 m; Scale bar is 3 cm long.

c) Poorly sorted conglomerate with a fine grained sand matrix sharply overlying facies 9 (Thick Bedded, Non Bioturbated Sandstone) below. Well 6-18-32-3W5; Depth 2189.7 m; Scale bar is 3 cm long.

d) Example of conglomerate facies with large cobble (approx. 15 cm in diameter) sharply overlying facies 9. Well 6-5-31-1W5; Depth 2052.5 m; Scale bar is 3 cm long.

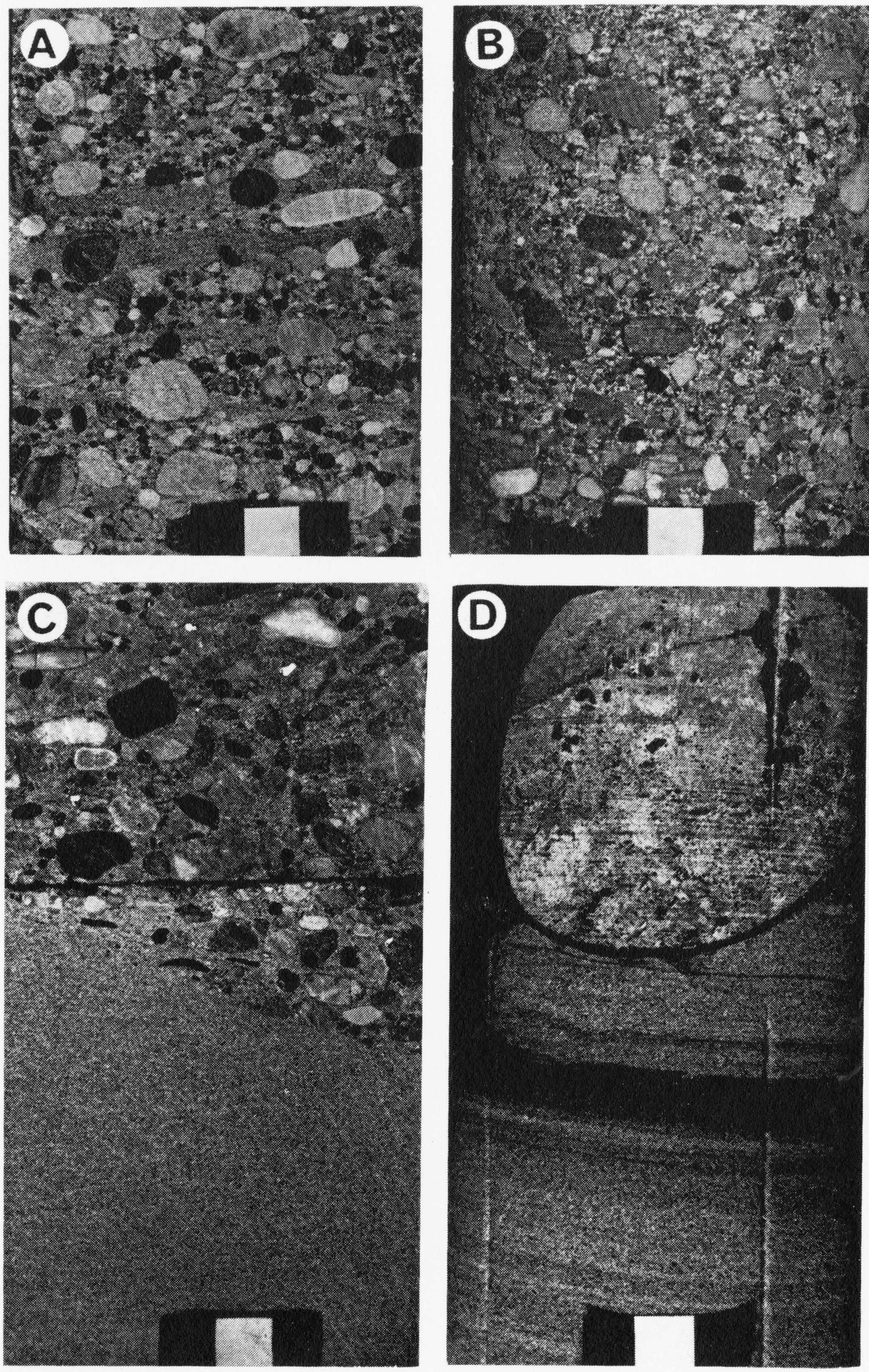
A
B
C
D

usually found above and below this facies may represent deposits from waning but still intense effects of large storm flows.

4.2.8. Facies 7a: FINE GRAINED BURROWED LAMINATED SANDSTONE -MUDSTONE

Facies 7a ranges 5 to 15 m thick and contains beds of vfL to fU sandstone alternating with beds of siltstone and mudstone. Sandstone beds are commonly 0.5 to 4 cm thick at the base of the facies (Fig. 4.9). The sandstones thicken towards the top where they are typically 4 to 10 cm thick. Sandstone makes up about 30 to 75 percent of the facies by thickness. Bases of sandstones beds are sharp and slightly erosive. Load structures occur at bases and are commonly ball-and-pillow or flame structures. The sand beds contain symmetrical (wave) ripple cross-lamination (de Raaf, Boersma and van Gelder, 1977). Thinner beds consist of parallel laminated sandstone which often exhibits excellent colour grading. The tops of most beds are undulatory and abruptly overlain by black mudstones (Fig. 4.9). Thin beds (0.5 to 3 cm) of conglomerate (facies 6) are interbedded in the lower part of the facies.

Bioturbation is moderate to absent and generally decreases upwards as the sand/mud ratio increases. Well defined trace fossils are generally absent from the thicker sandstones. The trace fossils Teichicnus, Planolites, Chondrites, Zoophycus, Paleophycus,(Fig. 4.9) and (rarely)

Figure 4.9: Facies 7a - Fine Grained Burrowed Laminated Sandstone-Mudstone

a) Thin, fine grained sand and silt beds in a muddy, burrowed background. Planolites, Terebellina, and Chondrites (arrow) trace fossils are present. Well 6-11-32-3W5; Depth 2248.9 m; Scale bar is 3 cm long.

b) Burrowed fine grained sandstone near top of this facies. Arenicolites trace fossil is present. Well 6-18-31-2W5; Depth 2208.9 m; Scale bar is 3 cm long.

c) Burrowed fine grained sandstone. Zoophycus trace fossil is present throughout most of the example. Well 6-12-32-1W5; Depth 1913.6 m; Scale bar is 3 cm long.

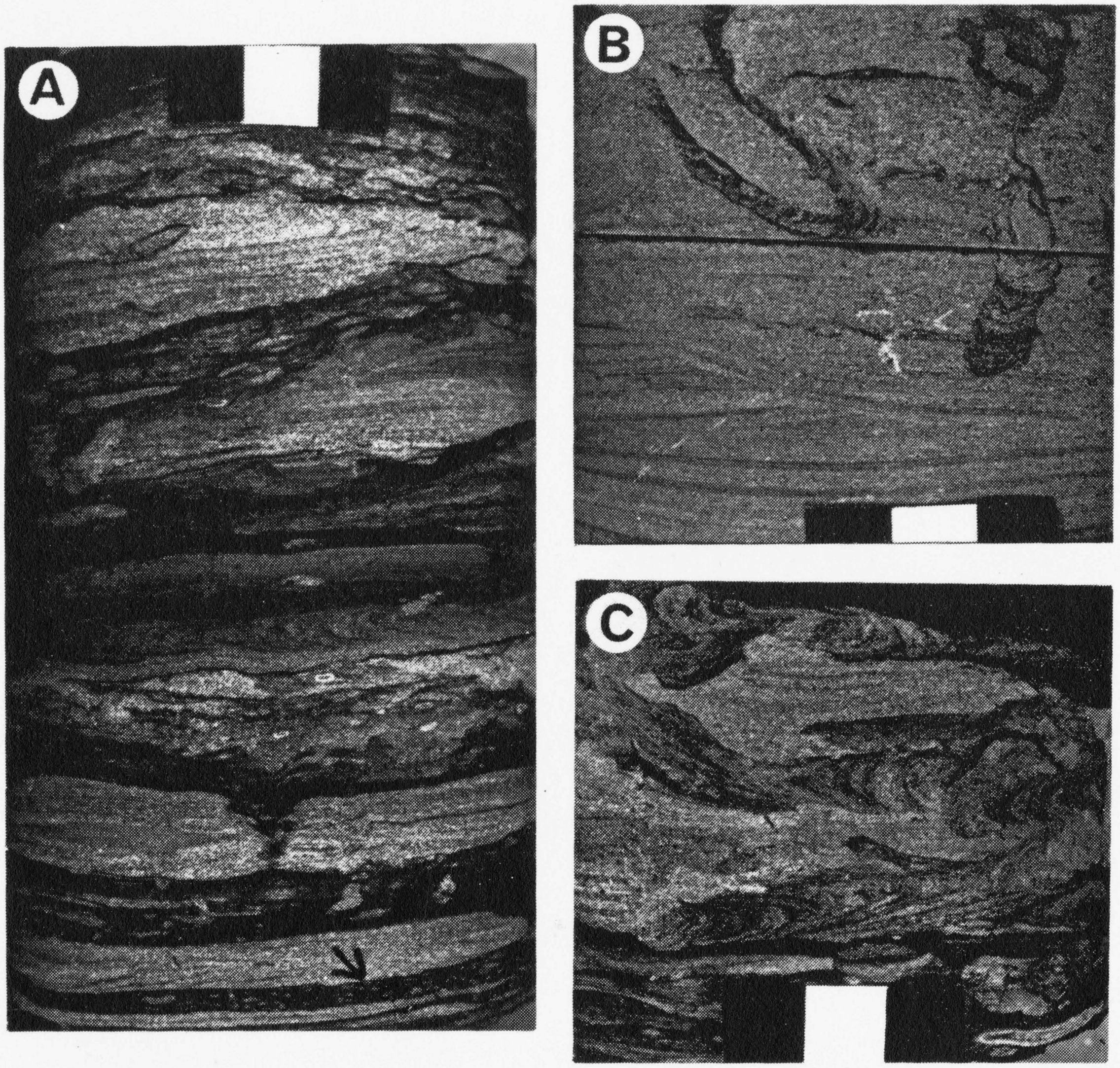
A
B
C

Skolithos, Arenicolite (pers. comm., G. Pemberton, 1988), and Rosselia are recognized in the thinner sandstones and siltstones (Fig. 4.9).

Facies 7a normally overlies facies 6 (massive conglomerate) which lies on the VE3 surface or alternatively sharply overlies facies 4 (pale sandstone). It is overlain by and interbedded with facies 8 (interbedded sandstone-mudstone).

Preliminary Interpretation

Wave ripple cross lamination in this facies may have been produced by waning storm events or small storms in a shallow wave agitated lower shoreface environment (Dott and Bourgeois, 1982; Swift and Rice, 1984; Plint and Walker, 1987). The thin mudstone beds were probably deposited in deeper quieter water of the lower shoreface.

The trace fossils in this facies belong to the Cruziana ichnofacies. Rare elements of the Skolithos ichnofacies (Skolithos and Arenicolites) indicate an assemblage comparable to a "storm related ichnofacies" (Frey and Howard, 1985).

4.2.9. Facies 7b: COARSE GRAINED BURROWED LAMINATED MUSTONE/SANDSTONE

This facies consists primarily of mL to vcU grained sandstones interbedded with mudstones and siltstones. The coarse grained sandstones comprise 20 to 35 percent of the facies by volume. The sandstone beds are 4 cm to 95 cm thick (avg. 15 cm), and generally decrease in frequency and thickness upward. Bases of individual sandstone beds are sharp and erosive, and may show loading structures (Fig. 4.10). The bed bases usually have scattered chert granules/pebbles (0.4 to 0.9 cm, avg. 0.5 cm) as well as subangular to rounded siderite clast rip ups (1 to 10 cm, avg. 6 cm). Armoured mud balls occur in this facies as an outer coating of pebbles (one pebble thick) "embedded" into and along the outer edges of mudstone clasts (Fig. 4.11).

Throughout facies 7b, much of the sand has a black and white "salt and pepper" appearance that is similar in texture to both facies 5a (cross bedded pebbly sandstone) and facies 10 (parallel laminated and cross bedded sandstone). Internally the sandstone beds may be cross bedded (dip angles up to 28 degrees), but more commonly appear massive or structureless (Fig. 4.10) Both trough and planar bedding have been observed. Individual consecutive foresets are often defined by subtle grain size variations.

Thinner (4 to 15 cm) sandstone beds of this facies are commonly underlain by 5 to 10 cm thick siderite beds. Recognized trace fossils in this part of the facies include _Arenicolites_ and _Skolithos_. The burrows of these two traces are commonly subvertical, sand filled, and terminate 1 to 3 cm into the mudstone or siderite bed below (Fig. 4.11). The _Arenicolites_ burrows appear on broken ends of cores as a

Figure 4.10: Facies 7b - Coarse Grained Burrowed Laminated Mudstone-Sandstone.

a) Laminated pebbly granular sandstone and mudstone. Note the sharp based erosive contact between the granular sandstone and pebbly mudstone at bottom. Well 6-34-33-5W5; Depth 2465.6 m; Scale bar is 3 cm long.

b) Pebbly granular sandstone exhibiting loading structure into underlying dark mudstone with scattered sand granules. Well 6-34-33-5W5; Depth 2465.7 m; Scale bar is 3 cm long.

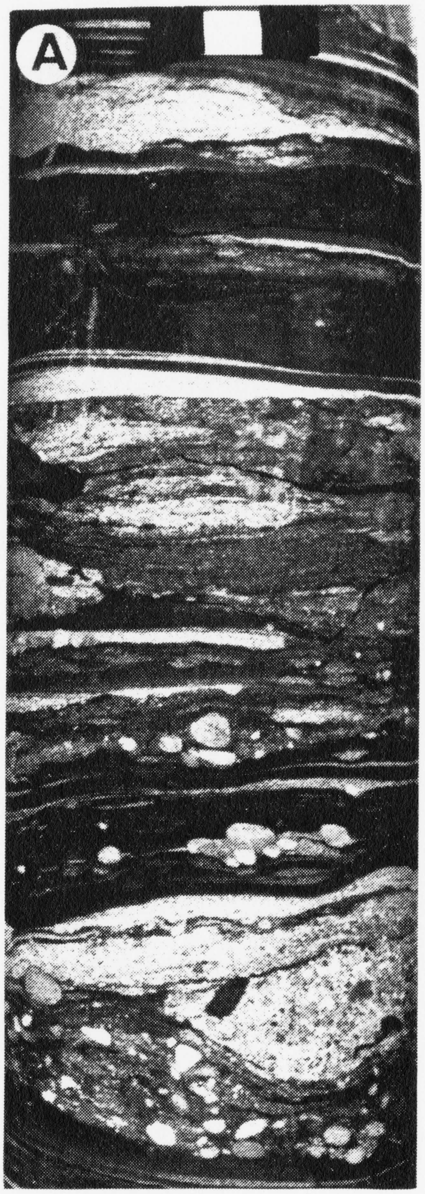
A

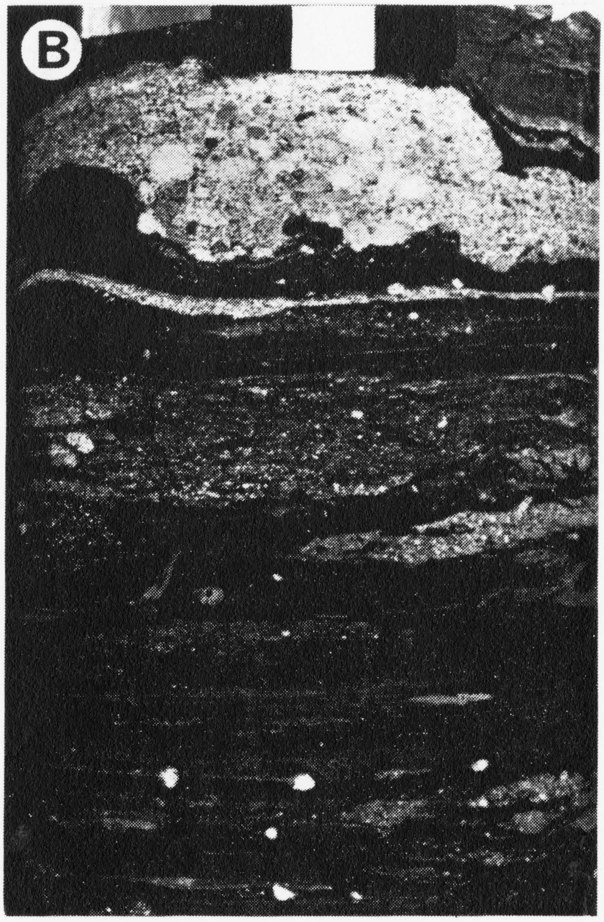
B

"dumb-bell" shaped sand filled burrows (Fig. 4.11).

Bed tops are commonly gradational (over a 5 cm vertical interval) with the background sediment of this facies (Fig. 4.11). Background sediment is predominantly dark mudstone with thin (< 3 cm) beds or lenses of siltstone or vfU grained sandstone. These lenses are commonly sharp based and colour graded. The structures in these lenses include parallel laminations, undulatory laminations, and current to combined flow laminations. Only a small amount of bioturbation occurs in this part of the facies. Recognized trace fossils include rare <u>Paleophycus</u>, <u>Planolites</u>, and <u>Teichicnus</u>? Fish scales are observed along mudstone bedding planes. Bentonites beds (< 2 cm) are occasionally observed in the mudstone beds.

Facies 7b is transitional with facies 5a (cross bedded pebbly sandstone) below and is gradational with subfacies 1b (Dark Mudstones) above.

<u>Preliminary Interpretation</u>

The presence of trough cross-bedded sandstone in facies 7b may indicate an offshore shallow shelf environment where unidirectional current processes were active. These currents had sufficient strength to erode the underlying substrate and transport chert pebbles and large mudstone rip ups. The dark mudstones were probably deposited well offshore in deep quiet water. The rare trace fossils associated with the sandstone beds of this facies are indicative of the <u>Skolithos</u> ichnofacies, suggestive of a soft substrate in a high energy

Figure 4.11: Facies 7b - Coarse Grained Burrowed Laminated Mudstone-Sandstone.

a) Burrowed granular sandstone. Burrowing in this example has resulted in a churned mixture of sand and mud. Note the gradational change upwards into sandy mudstones of this facies. Well 8-27-32-3W5; Depth 2195.5 m; Scale bar is 3 cm long.

b) Burrowed sandy mudstone showing a sand filled *Arenicolites* burrow which penetrates the underlying sideritized horizon. Well 8-13-32-3W5; Depth 2182.5 m; Scale bar is 3 cm long.

c) Armoured mud ball. Note the coating of chert pebbles along the outer edges of the clast. Well 14-27-32-3W5; Depth 2194 m; Scale bar is 3 cm long.

d) End on view of *Arenicolites* burrow appear as "dumb-bell" shaped sand filled burrows. Well 8-13-32-3W5; Depth 2182.5 m; Scale bar is 3 cm long.

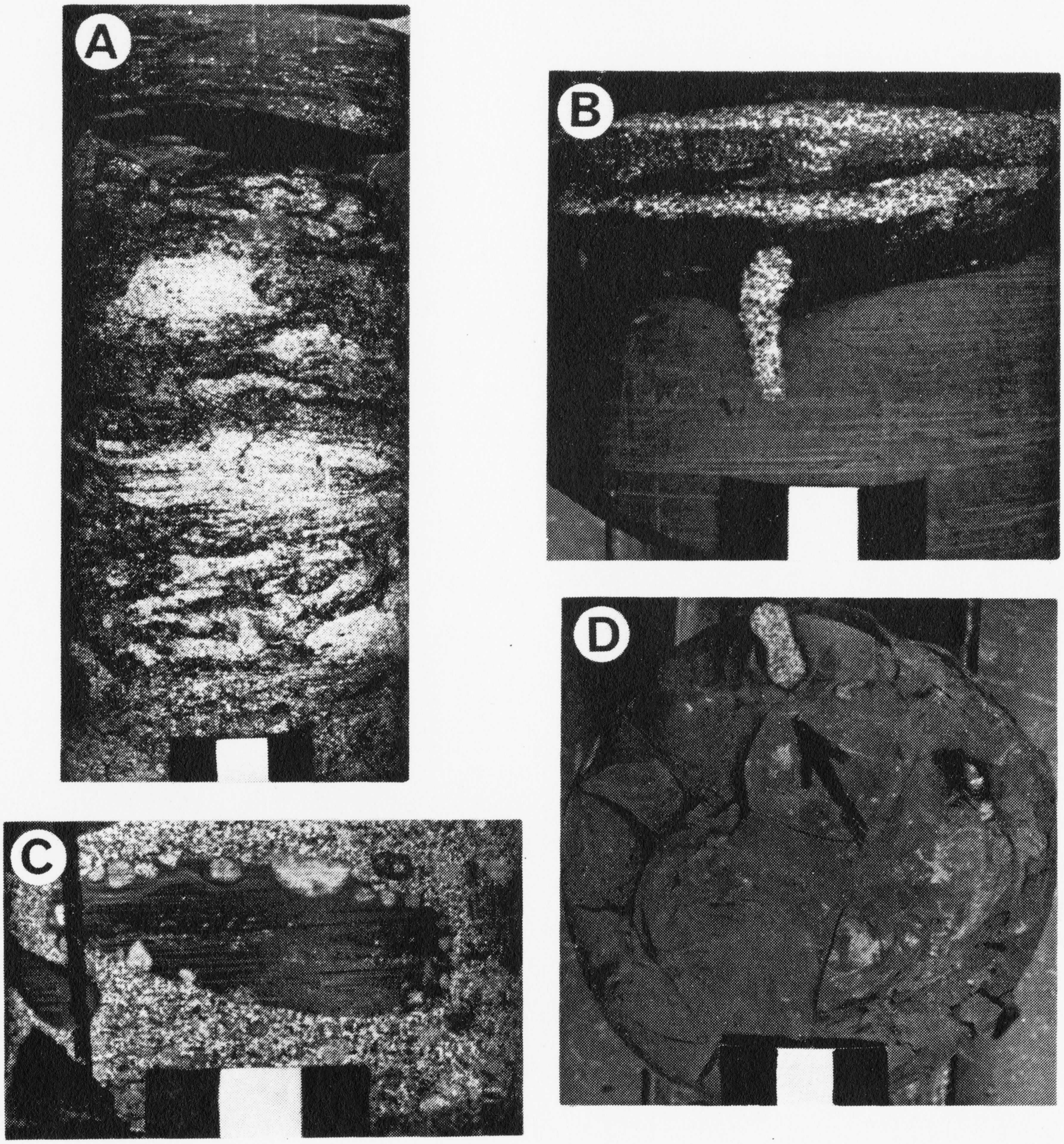
A
B
C
D

shallow marine environment.

4.2.10. Facies 8: INTERBEDDED SANDSTONE-MUDSTONE

This facies consists primarily of vfL to fU grained sandstones interbedded with lesser amounts of mudstones and siltstones than in facies 7a. The sandstone beds are .10 m to 1.5 m thick, and increase in frequency and thickness upwards. The base of beds are sharp and occasionally show sole marks and mudstone rip-up clasts. The internal stratification consists of horizontal to sub-horizontal parallel lamination, showing low angle (< 10 degree) inclined intersecting surfaces. The dips of the laminations may change slightly upwards through the bed, with or without distinct low-angle truncation surfaces. This stratification is interpreted to be hummocky cross-stratification. The laminae are often defined by finely comminuted plant debris ("coffee grounds") or subtle grain size variation. Bed tops are commonly colour graded, bioturbated and rarely contain wave ripple cross-lamination (Fig. 4.12).

Shales and siltstones interbedded with these sandstones are up to 15 cm thick and are infrequently bioturbated. Conglomerates (facies 6a) are occasionally interbedded in this facies, and occur as 2 to 30 cm thick beds. Deformed and convoluted bedding of vfL to fL sandstone and mudstone occurs rarely over 2 to 8 cm intervals (maximum 60 cm) in this facies 9 (Fig. 4.12).

Figure 4.12: Facies 8 - Interbedded Sandstone-Mudstone

a) Fine grained hummocky cross stratified sandstone. Low angle parallel laminations and wave rippled cross laminations are present at the top of this example. Well 6-18-32-3W5; Depth 2181.3 m; Scale bar is 3 cm long.

b) This example shows a convoluted, fine grained sandstone sharply overlain by a thin bed of conglomerate. Well 8-34-32-3W5; Depth 1913.4 m; Scale bar is 3 cm long.

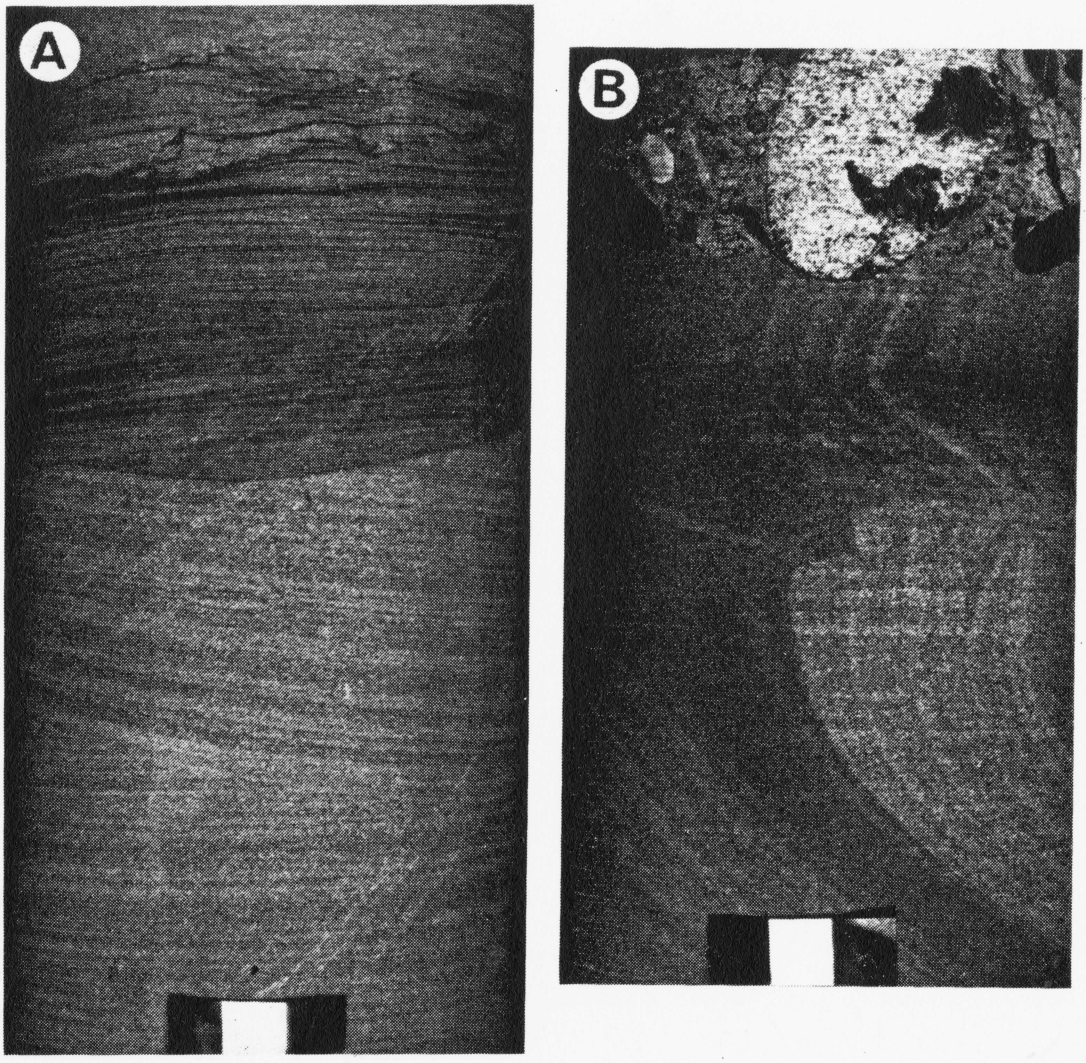
A
B

Recognizable trace fossils include <u>Planolites</u>, <u>Zoophycus</u>, <u>Chondrites</u>, and (rarely) <u>Paleophycus</u> and <u>Teichicnus</u>. The facies is transitional with facies 7a (fine grained burrowed laminated sandstone-mudstone) below and facies 9 (thick bedded, non-bioturbated sandstone) above.

<u>Preliminary Interpretation</u>

Facies 8 is interpreted to represent deposition in an offshore transition zone to lower shoreface setting of a wave dominated shoreline. The abundant low-angle lamination in the sandstone is interpreted as hummocky cross-stratification (HCS) (Leckie, 1986a). Wave ripples in this facies may represent reworking of HCS beds as storms waned or by later smaller storm reworking.

The trace fossil assemblage of facies 8 suggests a upward transition from the Cruziana ichnofacies into a Skolithos ichnofacies. <u>Skolithos</u> ichnofauna in the upper part of this facies suggest a soft-bottomed high energy marine environment while the Cruziana ichnofauna are comparable to that observed in facies 7a.

4.2.11. Facies 9 <u>THICK BEDDED, NON-BIOTURBATED SANDSTONE</u>

Facies 9 always overlies facies 8 (interbedded sandstone - mudstone) and is in turn overlain by facies 10 (cross-bedded and parallel laminated sandstone). Facies 9 is 2 to 10 metres thick in the study area and has an average thickness of 8 metres. This facies consists of low angle (<

15 degrees) parallel to slightly divergent stratification forming a nearly continuous sequence of sandstone (Fig. 4.13). The grain size commonly coarsens upwards from vfU to fU sand. Amalgamation surfaces are infrequently observed near the base of this facies.

Mudstone interbeds are rare in this facies and occur as thin mm scale partings. Steep sided scours interpreted as gutter casts occur rarely at the bases of some sandstone beds. The scours are up to 20 cm deep, and are filled as current rippled fL sand (Fig. 4.8). Facies 6 (conglomerate) is commonly interbedded in this facies. The conglomerates occur as either scattered chert pebbles over intervals of tens of centimetres, or as discrete beds 2 to 90 centimetres thick. The conglomerate beds are either sharp based or are gradational with the underlying fine grained sandstones (Fig. 4.8). The conglomerates are often clast supported and contain a matrix of vfL to fU grained sand that is macroscopically similar to sand of facies 9. Clasts range in size from .05 cm to as large as 15 cm (2 to 3 cm average). Deformed and convoluted bedding is common below these conglomerate beds. Large scale convolutions (up to 2 m thick) are often truncated by low angle inclined stratification or a conglomerate bed.

Other common aspects of facies 9 are 1) finely comminuted plant debris ("coffee grounds") which occur as 1 to 10 cm thick beds; 2) localized sideritic patches 1 to 3

Figure 4.13: Facies 9 - Thick Bedded, Non Bioturbated Sandstone

a) Fine grained sandstone showing low angle parallel to slightly divergent stratification. Low angle truncation of stratification near the top of this example is characteristic of swaley cross stratification. Well 6-5-31-1W5; Depth 2063.4; Scale bar is 3 cm long.

b) This example shows swaley cross stratified sandstone with a gutter cast filled as current rippled fine grained sandstone. Well 6-12-312-3W5; Depth 2188 m; Scale bar is 3 cm long.

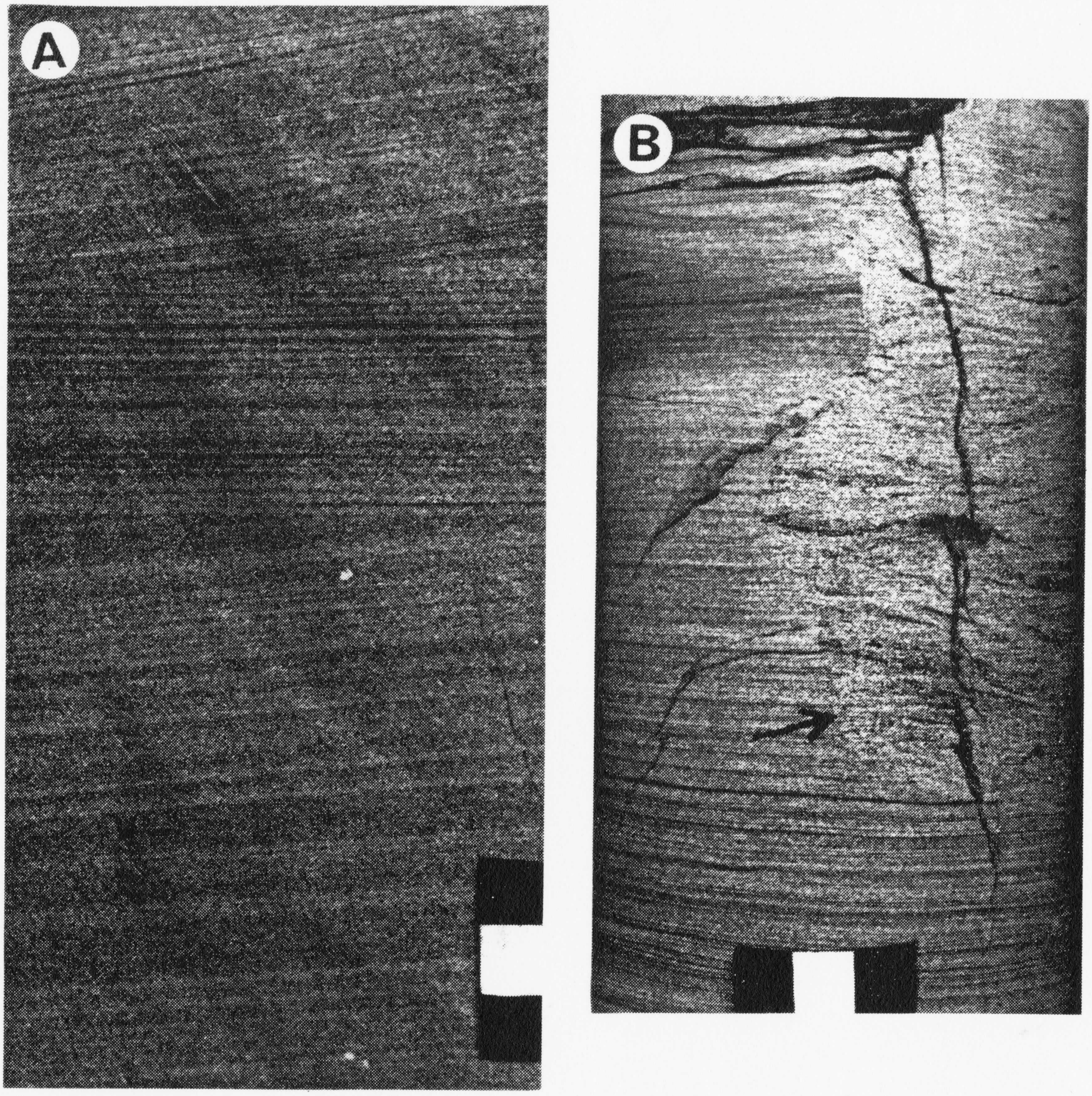
A
B

cm thick; and 3) mudstone clasts and shards which occur near the base of this facies as intraformational conglomerates.

There is minimal disruption of the sandstone by organisms. Recognized trace fossils are rare Skolithos and Ophiomorpha. Several escape burrows are also recognized in this facies (Fig. 4.14).

Preliminary Interpretation

The low angle inclined stratification is interpreted as amalgamated hummocky cross -stratification and/or swaley cross-stratification (Leckie and Walker, 1982; McCrory and Walker, 1986; and Plint and Walker, 1987). The overall absence of mudstone in this facies suggests a shallower shoreface environment than is proposed for facies 8.

4.2.12 Facies 10: PARALLEL LAMINATED AND CROSS-BEDDED SANDSTONE

Facies 10 always overlies facies 9 (thick bedded - non-bioturbated sandstone) and is 1 to 8 metres thick. The facies commonly has an abrupt base delineated by a grain size change from vfU - fU grained sandstone to mL - mU grained sandstone (Fig. 4.14). The sandstones of facies 10 have a "salt and pepper" texture that commonly resembles sandstones of facies 5b and facies 13. Occasionally, siderite grains occur along laminations in these "salt and pepper" textured sandstones but their distribution is localized and patchy (refer to section 4.3 - petrography).

Figure 4.14: Facies 9 - Thick Bedded, Non Bioturbated Sandstone.

a) Fine grained sandstone showing a conical shaped escape burrow. Well 8-5-30-4W5; Depth 2596.2 m; Scale bar is 3 cm long.

b) Fine grained S.C.S. sandstone sharply truncated at the top by medium grained sandstone of facies 10 (parallel laminated and cross-bedded sandstone). Well 6-36-30-4W5; Depth 2454.9 m; Scale bar is 3 cm long.

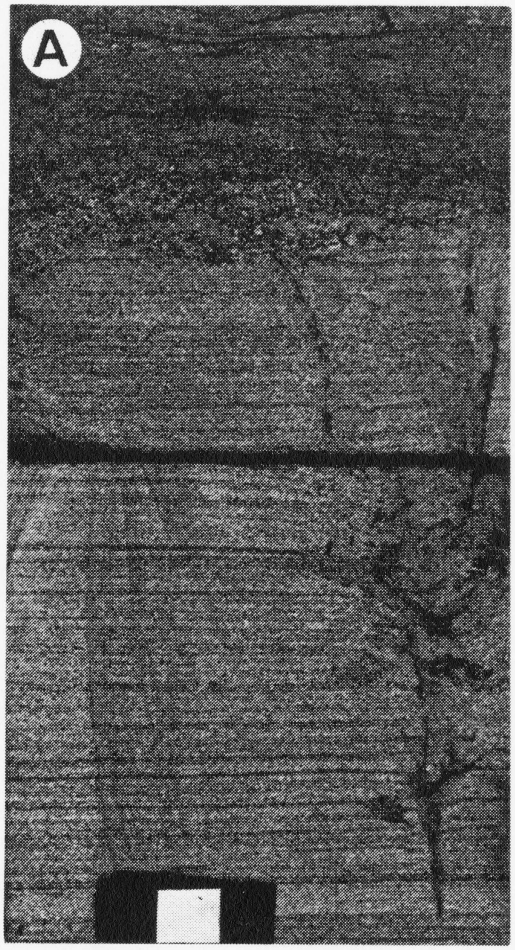
A

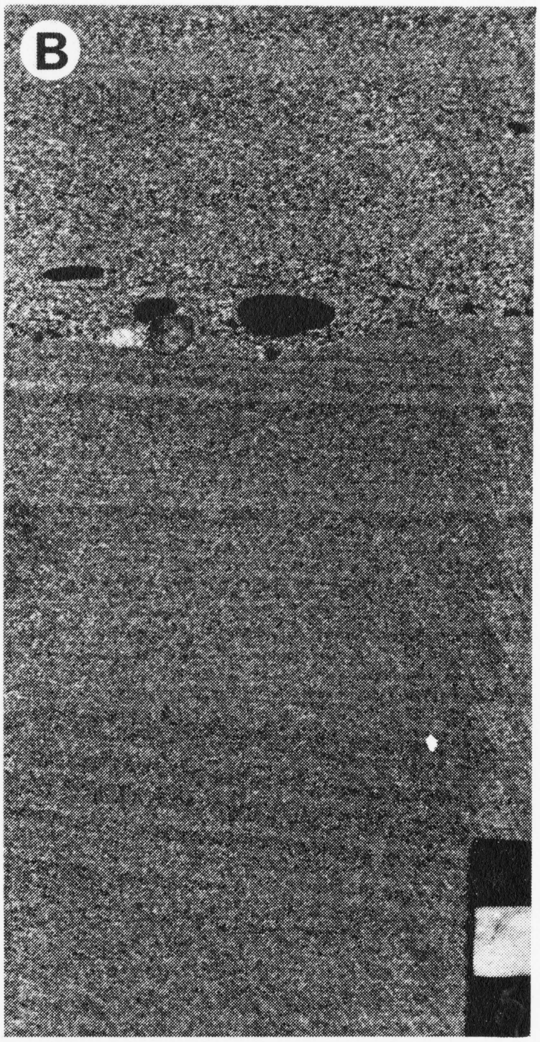
B

In the lower part of the facies the main sedimentary structures are trough cross bedding (measured dip angles of beds increase upwards to 28 degrees) in sets up to 40 cm thick which are interbedded with low angle (< 15 degrees) inclined stratified sandstones (swaley cross -stratification) (Fig. 4.15). Thin (< 10 cm thick) beds of clast supported , structureless conglomerate occur infrequently at or near the base of this facies.

In the middle to upper part of the facies, sandstones become more massive. These sandstones frequently have a 20 cm to 1.5 m zone of _Macaronichnus_ burrow traces, distinguished in core as small (1mm by 3mm) white, quartz sand, infilled burrows (Clifton and Thompson, 1978) (Fig. 4.15). Directly above the "_Macaronichnus_ zone" are parallel laminated sandstones. The laminations are often accentuated by concentrations of heavy minerals. Rare unlined _Skolithos_ occur within this part of the facies (Fig. 4.15).

The upper 1 to 2 metres of facies 10 consist of fL to fU massive structureless sandstone which is a light tan- grey colour. _In situ_ root traces are common and occur as delicate mm scale bifurcating traces filled with carbonaceous material. Larger roots (2 cm by 15 cm in length) occur less frequently (Fig. 4.15). The roots have rendered this sandstone structureless. No recognizable trace fossils are observed in the rooted sandstones.

Figure 4.15: Facies 10 - Parallel Laminated and Cross-Bedded Sandstone.

a) The basal portion of this facies is characterized by medium grained trough cross bedded sandstone. Well 8-5-30-4W5; Depth 2587.1 m; Scale bar is 3 cm long.

b) The middle to upper part of this facies is extensively burrowed by Macaronichnus. Well 14-23-30-4W5; Depth 2238.4 m; Scale bar is 3 cm long.

c) Parallel laminated fine grained sandstone with a unlined Skolithos burrow near base. This part of the facies is thought to represent beach laminations. Well 14-5-30-2W5; Depth 2201.2 m; Scale bar is 3 cm long.

d) This example is from the top meter of the facies. It shows a large bifurcating root trace in a fine grained structureless sandstone. Well 6-11-30-3W5; Depth 2245.1 m; Scale bar is 3 cm long.

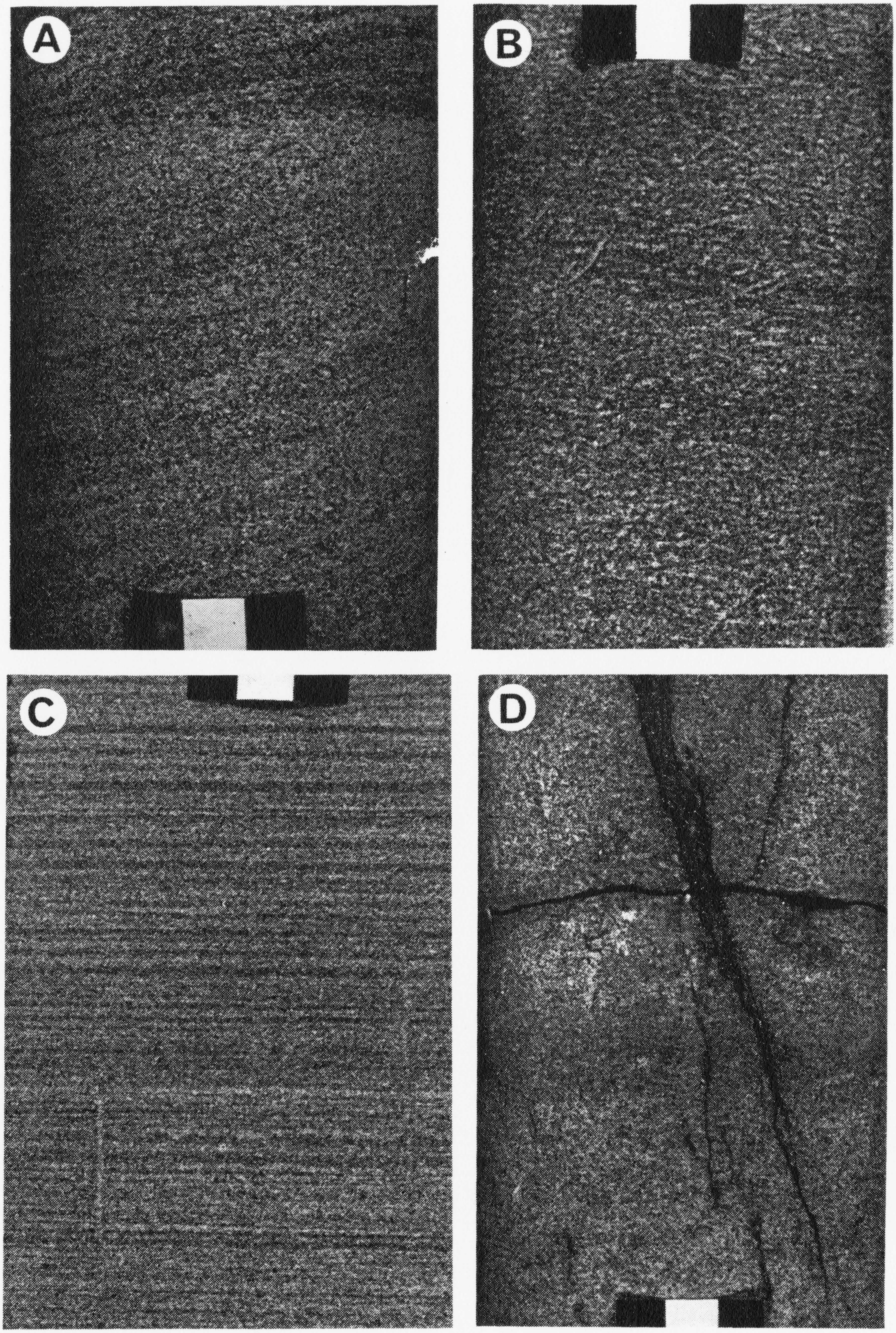
A
B
C
D

Preliminary Interpretation

Facies 10 is interpreted to represent deposition in an upper shoreface and beach environment. An extremely high energy upper shoreface to foreshore setting is suggested by the monospecific assemblage Macaronichnus. The scarcity of bioturbation textures in this facies is likely a result of high levels of physical energy creating harsh conditions for animal life (Moslow and Pemberton, 1988).

4.2.13 Facies 11 ROOTED BROWN MUDSTONE-SILTSTONE

Rooted brown mudstone siltstone gradationally ovelies facies 10 (parallel laminated and cross bedded sandstone) or is interbedded with non-marine facies 12 and 13 described below. Facies 11 is usually dark brown and is occasionally grey to pale grey-green in colour. It occurs as structureless friable beds 6 to 80 cm thick. The pale grey-green type is very friable often disaggregating into waxy irregular shaped structures (peds) when handled. Leckie (1986b, p.431) describes peds as "...naturally occurring aggregates of soil material separated from adjacent peds by cutans or natural voids". Peds were recognized in cores of this facies as subangular to blocky masses up to 4 cm in size which are often surrounded by waxy, oriented slickensided clay coatings (cutans?).

The brown type in facies 11 is more homogeneous and less friable than the grey-green type. It also contains a greater proportion of silt and vfU to fU grained sand (approximately 50 %) (Fig. 4.16). A tan-yellow, mottled siltstone unit (approximately 5 cm thick) with abundant root traces was observed in one core (well 8-26-29-2W5). This is located in the middle of the facies (Fig. 4.16). Very thin coals and coaly mudstones (1 to 5 cm thick) occur occasionally interbedded within the brown type (Fig. 4.16). The coals are vitreous and often contain variable proportions of dispersed silt and vfU sand. Several cores show fossils of unidentified plant remains, as well as coalified portions of small trees (Fig. 4.16). Fossilized plant material occur as carbonaceous imprints of leaves on parting planes in coaly mudstones of this facies. No body or trace fossils are recognized in facies 11.

Preliminary Interpretation

This facies may have been deposited in flood plain areas of a coastal plain far from any influence of fluvial channels. Facies 11 resembles paleosols described by Leckie and Foscolos (1986) and Plint and Walker (1987). The grey-green mudstone-siltstones may represent well drained soils where organic matter was destroyed by subaerial oxidation. Conversely the rooted brown mudstone-siltstones may represent poorly drained, and poorly aerated conditions of the coastal plain. The interbedded coals represent vegetated environments and may have been deposited in backshore marshes or at the margins of small lakes (Plint and Walker, 1987).

Figure 4.16: Facies 11 - Rooted Brown Mudstone-Siltstone.

a) The basal portion of this facies is a structureless mixture of fine grained sand is a dark brown mudstone. Thin root traces are common in this part of the facies. Well 6-36-30-4W5; Depth 2442.1 m; Scale bar is 3 cm long.

b) This example is dark brown in colour, with a tan-yellow, mottled siltstone horizon in the centre. There are abundant root traces throughout this example. Well 8-26-29-2W5; Depth 2174.7 m; Scale bar is 3 cm long.

c) Example of vitreous dark black coal bed. Well 6-17-30-3W5; Depth 2349.5m; Scale bar is 3 cm long.

d) Coalified portion of a small tree branch or root. Well 8-26-29-2W5; Depth 2175 m; Scale bar is 3 cm long.

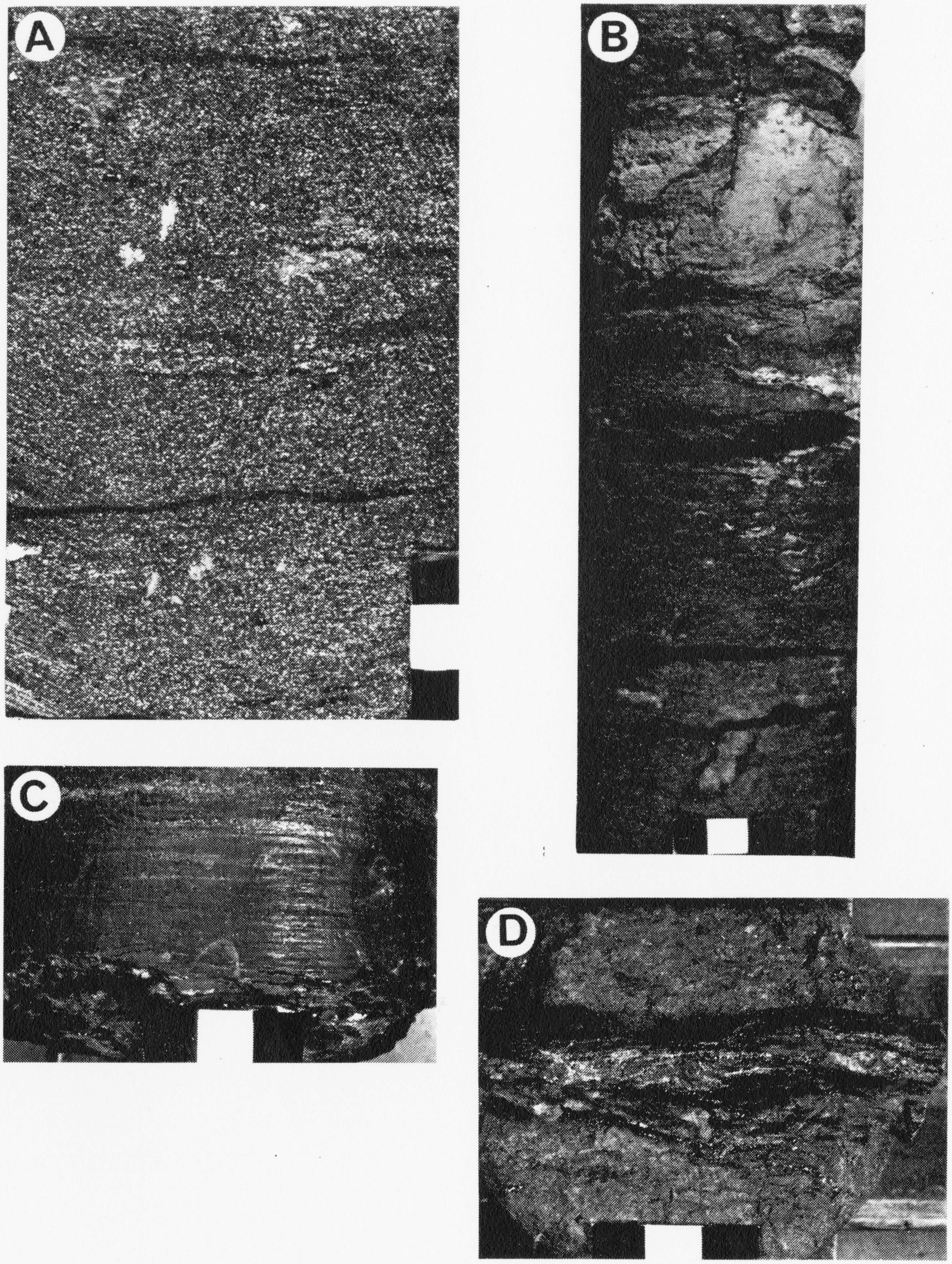
A
B
C
D

4.2.14 Facies 12: CONVOLUTED AND LAMINATED MUDSTONE-SANDSTONE

Convoluted and laminated mudstone-sandstone abruptly overlies facies 11 (Rooted brown mudstone-siltstone). Facies 12 is 1 to 4 metres thick and is overlain by either 1) mudstone clast cross bedded sandstone (facies 5e), or 2) rooted brown mudstone-siltstone (facies 11).

The mudstones in this facies are pale grey to dark black. Sideritic patches with diffuse boundaries are common in these mudstones. Light grey, vfL to fL grained sandstones are interbedded with the mudstones and comprise 25 to 75 percent of the facies. The sandstones are sharp based, have graded laminae and are 0.4 cm to 3.0 cm thick. The beds exhibit both crude low amplitude symmetrical (wave) ripple cross-lamination and asymmetrical (current) ripple cross-lamination (Fig. 4.17).

Post depositional sedimentary structures occur within this facies and include intense convolution, microfaults, and less commonly sand-filled syneresis cracks (Fig 4.17). Convolution structures commonly occur over the entire interval of this facies completely destroying the primary laminae. <u>In situ</u> roots are less common and are only recognized in the top 10 cm of this facies in a few cores (eg. 5-4-28-4W5). No body fossils are recognized. There is little disruption of the sediment by trace fossils, and the only form recognized was <u>Skolithos?</u> (Fig. 4.17).

Figure 4.17: Facies 12 - Convoluted and Laminated Mudstone-Sandstone.

a) Laminated mudstone and very fine grained sandstone exhibiting wave and current ripple cross laminations. Root traces or mud lined Skolithos burrows occur in the lower portion of this example. Well 6-15-28-2W5; Depth 2297.9m; Scale bar is 3 cm long.

b) This example shows a mixture of fine grained sandstone and mudstone. Intense convolution has destroyed most of the primary laminae. Well 6-31-28-3W5; Depth 2503.1 m; Scale bar is 3 cm long.

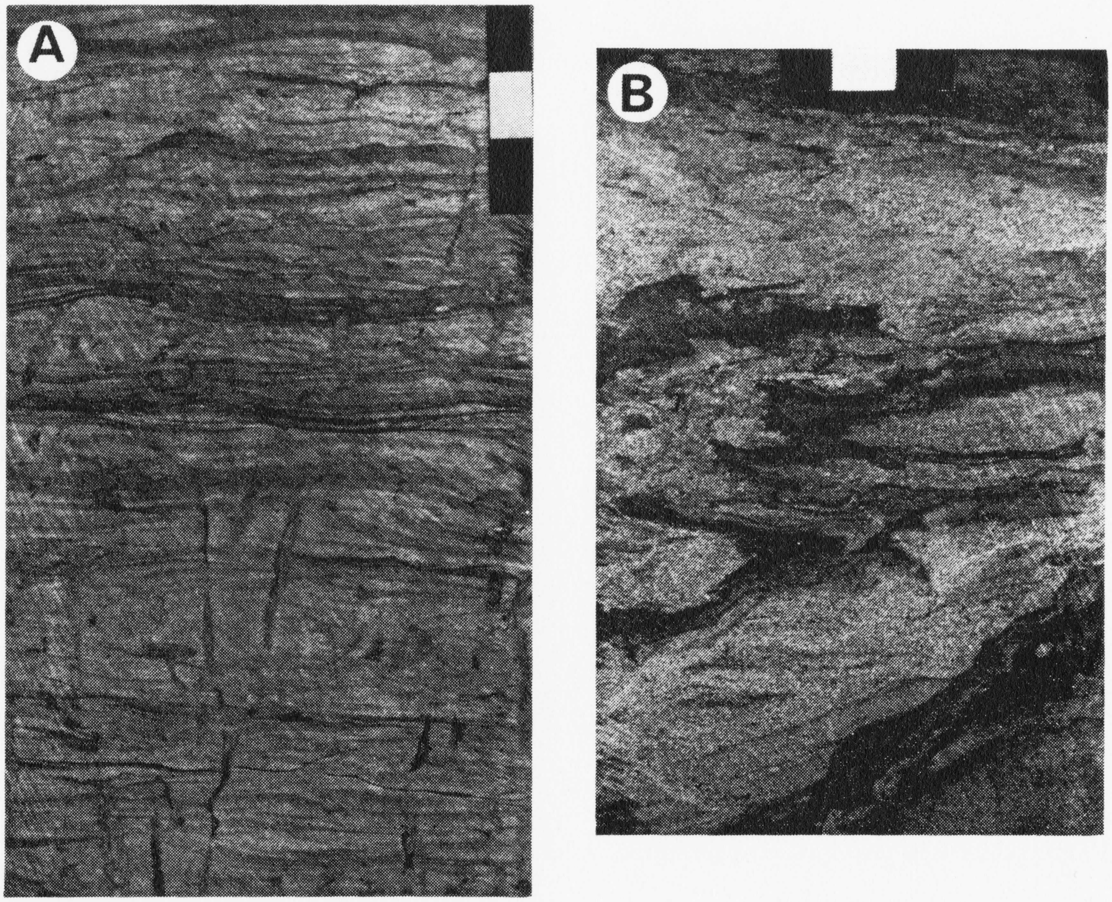
A
B

Preliminary Interpretation

The absence of body fossils (eg. bivalves, gastropods, and fish remains) in the mudstones of this facies indicate harsh ecological conditions in an environment that could not sustain animal life. The presence of roots at the top of this facies, as well as post depositional sedimentary structures (convolution and syneresis cracks) suggest deposition of sediment in brackish lagoons, large ponds or shallow small lakes.

Primary sedimentary structures in this facies suggest a marine influence. Sands may have been supplied to the previously mentioned environments by washoverfans, dunes and small rivers or creeks.

4.2.15 Facies 13: BIOTURBATED PEBBLY SANDSTONE-MUDSTONE

This facies consists of discontinuous beds (5 to 12 cm thick) of well rounded pebbles (up to 1.5 cm in diameter), dispersed in a sandy (mL - mU grained sand) mudstone matrix (Fig. 4.18). Clasts are generally matrix supported and have no apparent fabric. No imbricated clast were observed. Macroscopically, the facies resembles the thin muddier portions of facies 5a and 7B, but on the whole facies 13 is thicker (30 cm to 4.2 m thick), more massive, and is more thoroughly bioturbated.

Sandier portions of this facies give an impression of former multiple sand beds (Fig. 4.18). In the 14-8-31-1W5

Figure 4.18: Facies 13 - Bioturbated Pebbly Sandstone-Mudstone.

a) Bioturbated and burrowed granular sandstone and mud overlying a medium grained sandstone bed. Possible clay lined drapes occur near the bottom of this bed. Vertical Skolithos burrows are present. Well 14-8-31-1W5; Depth 2037 m; Scale bar is 3 cm long.

b) Bioturbated pebbly, granular sandstone and mud. A thin discontinuous bed of sand is present in the middle of this example. Well 6-34-33-5W5; Depth 2464.2 m; Scale bar is 3 cm long.

c) This example contains numerous pebbles scattered throughout a thoroughly bioturbated mixture of coarse sand and mud. Well 11-31-33-4W5; Depth 2392.2 m; Scale bar is 3 cm long.

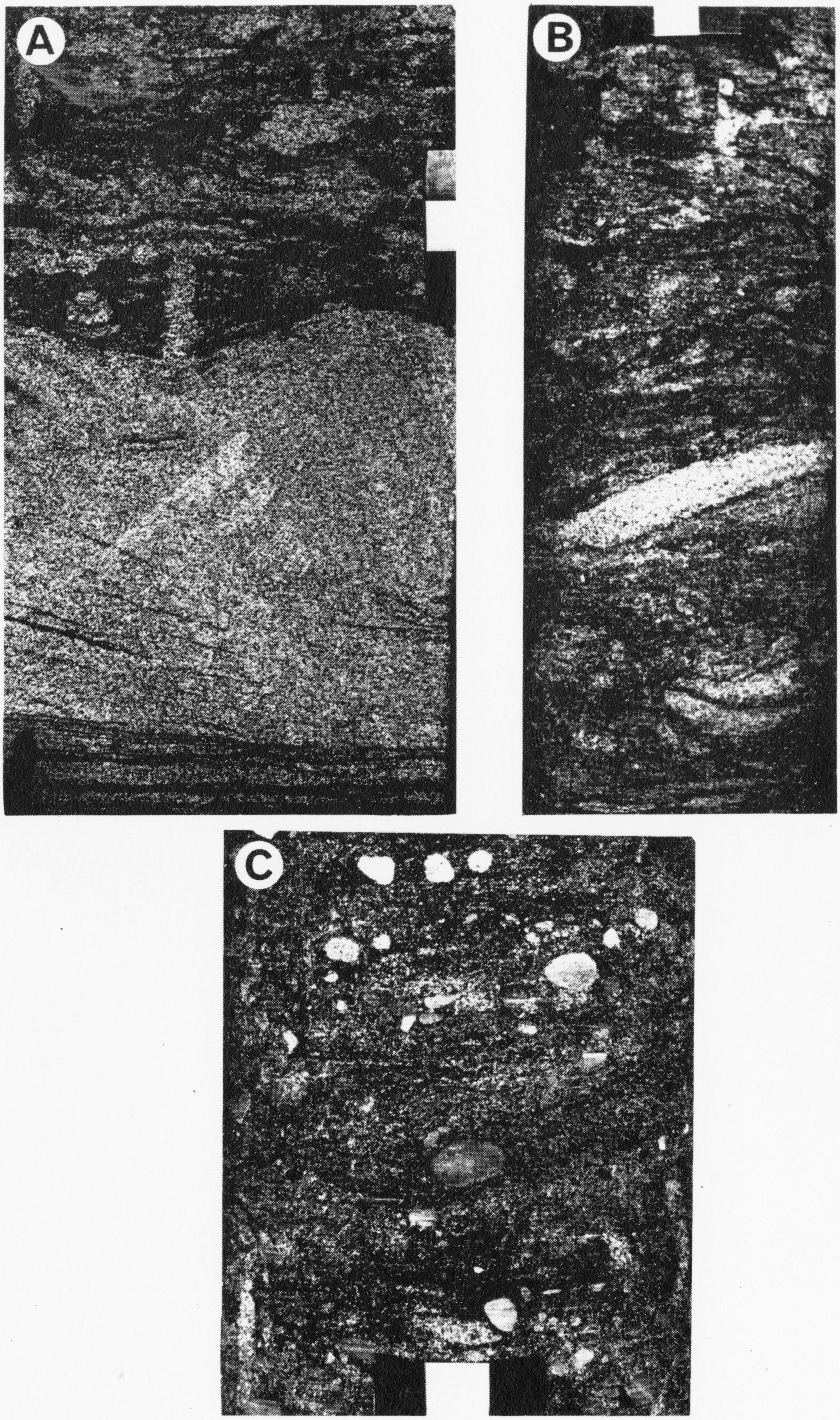
A
B
C

well, possible clay lined drapes occur in one of these sandier beds (Fig. 4.18). The trace fossils Skolithos and Arenicolites are observed in several cores, and occur as 6 to 8 cm vertical burrows filled with mU to mL grained sand. The burrows extend down from the bases of sandier beds.

Preliminary Interpretation

Similar pebbly mudstones in the Viking have been interpreted as evidence of subaqueous debris flow transport (Hein et al., 1986; Leckie 1986a). The sandier portions in facies 13 may represent partially preserved bedding. Facies 13 is thought to be the bioturbated equivalent of facies 5a and 7b (compare figure 4.10A and 4.18B). The possible clay lined drapes seen in one core of this facies suggests tidal currents were in this depositional environment. The pebbles and sands in this facies may have been transported by waves and tidal currents. The mud may have been introduced as matrix by the extensive bioturbation of the sediment by organisms (Leckie, 1986a). The rare presence of the marine trace fossils Skolithos, and Arenicolites indicates a soft substrate in a shallow marine setting.

4.3 Petrography and SEM Analysis - Facies 5a, 5b and 10

4.3.1 Introduction

This section provides a more detailed understanding of three facies (5a, 5b and 10) described earlier in this chapter. The primary purpose of this section was to determine the mineralogy of these three facies, and to ascertain petrographically if compositional and textural differences exist between the depositional settings previously proposed.

Section 4.3 does not consider the paragenetic sequence of diagenetic minerals for the samples examined. For a comprehensive review on sandstone diagenesis in the Viking Formation the reader is referred to the work of Grant (1985), Reinson and Foscolos (1986), and Longstaffe and Ayalon (1987). Figure 4.19 shows the location of wells in which various facies were sampled for petrographic and S.E.M. analysis.

4.3.2 Geological Problem Posed Prior to Petrographic Study

The VE4 contact is difficult to pick in core located in the southern and western part of the study area because the surface truncates medium to coarse grained sandstone of facies 10 (termed upper shoreface for the purpose of this section) and is overlain by macroscopically similar sandstones of facies 5a (termed transgressive lag for the purpose of this section). The separation between the upper shoreface and transgressive lag sandstone deposits can be picked from resistivity well logs (Fig. 4.20).

Another type of facies association is observed in several cored wells where medium to coarse grained sandstones (facies 5b) sharply overlie very-fine to fine grained hummocky and

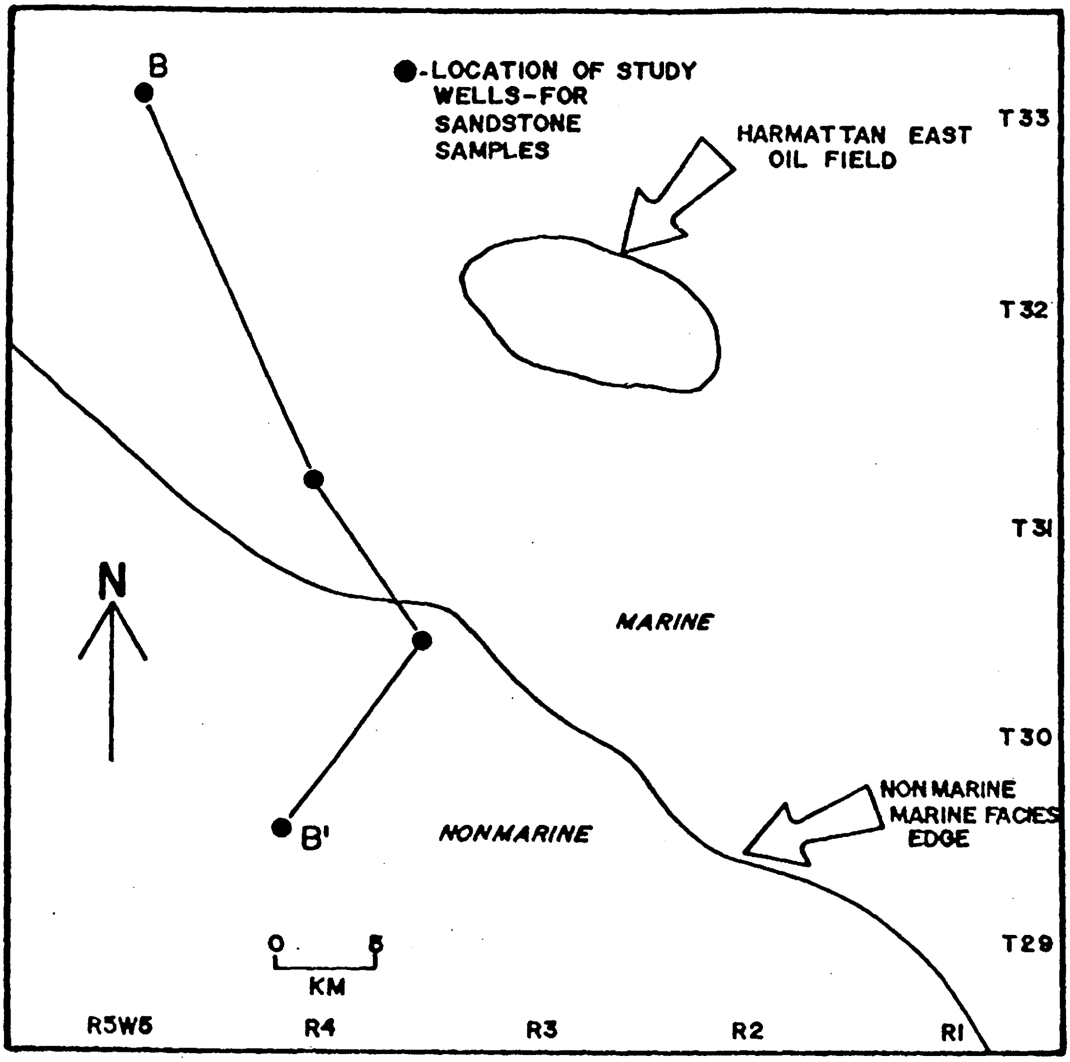

Figure 4.19. Location of four subsurface drill holes in which sandstone samples from the Viking Formation were obtained. The two locations in the southwest part of the map have Viking nonmarine facies. Cross section B-B′ is shown in figure 4.20.

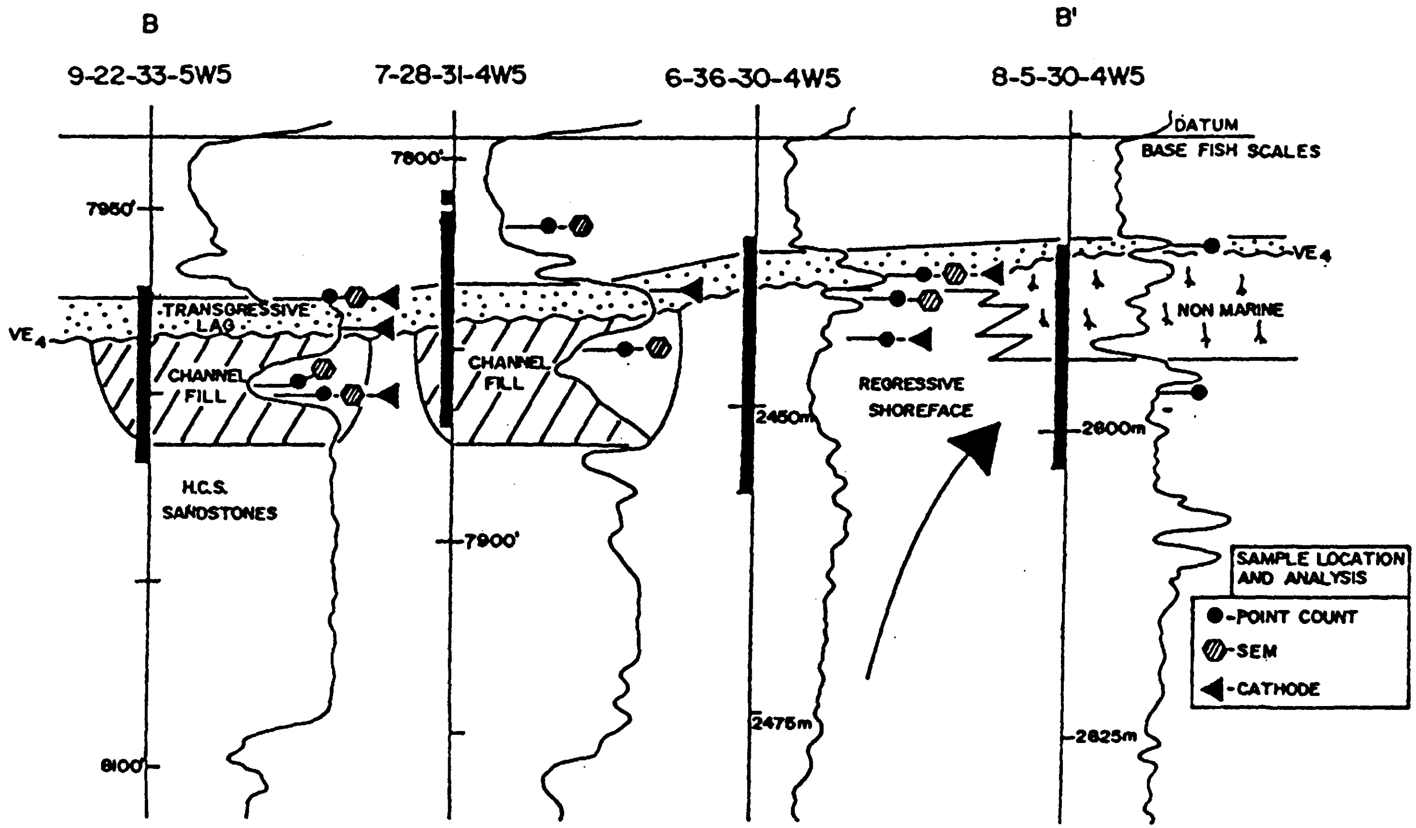

Figure 4.20. Stratigraphic cross section B-B′ of figure 4.19 showing four wells used for sampling of sandstones. Locations of samples and type of analysis performed on samples are shown on the right hand side of the resistivity log.

swaley cross-stratified sandstones. The sharply overlying sandstones (termed channel fill for the purpose of this section) are interpreted as either river or tidal channel deposits. The geological problem in this case is that the channel fill sands macroscopically resemble stratigraphic laterally equivalent sandstones of the upper shoreface in so far as overall colour, texture, and grain size.

4.3.3 Sample Distribution and Hypothesis

Twelve sandstone samples were chosen from three of the interpreted depositional settings (1. uppershoreface, 2. channel fill, and 3. transgressive lag.) Two hypothesis set up prior to the study of these samples were:

1) Channel fill (facies 5b) sandstones will contain a greater percentage of feldspar and clay than the other two facies.

2) Transgressive lag and upper shoreface sandstones deposited under high energy marine conditions should show less of a compositional imprint from its provenance (eg. greater percentage of quartz and chert and less detrital feldspar). Surface textures of grains may show evidence of mechanical abrasion (eg mechanical V's) thus allowing for possible environmental discrimination.

Samples of drill core obtained from four wells west and south-west of the Harmattan East oil field were considered (Fig. 4.19) The wells form a line roughly parallel to depositional strike of the area. A structure map of the Viking Formation in this area suggests Viking strata dip to the southwest at a uniform rate of 11m per kilometre (56′ per mile). The four study wells do not produce hydrocarbons from the Viking interval. Epoxy impregnation was not available at the time of thin section preparation therefore it was decided not to examine porous sandstones from the Viking Harmattan East oil field. The petrographic relationship of Viking reservoir sandstones in off field wells to those of the Harmattan East field was not considered in this thesis.

Figure 4.20 shows the location of samples examined as thin sections according to their position on a geophysical well log stratigraphic cross section. Location of samples observed with the scanning electron microscope and cathodoluminescence microscopy are also shown. Subsurface depths for these samples range from 2,300 m to 2,600 m.

4.3.4 Methods

Detrital grain assemblages of thirteen thin sections were studied using a combination of several techniques. Twelve thin sections were point-counted with a polarizing microscope, accumulating a minimum of 300 grain counts per sample. Feldspars were stained using the technique of Houghton (1980). In this staining procedure plagioclase feldspars stain red and alkali feldspars stain yellow. One thin section was damaged during staining and was not included in the point counting procedure. The polarizing microscope was also used to determine the texture, grain size and sorting of each sandstone.

Six samples were examined using cathodoluminescence (CL) with a Luminoscope. The Luminoscope permits recognition of details not normally visible by standard petrographic techniques (Smith and Stenstrom, 1965; Sippel, 1968; Zinkernagel, 1978). In this study CL is used to recognize quartz cements, thereby permitting recognition of recycled rounded grains, pressure solution features, and quartz overgrowths (Sibley and Blatt, 1976). The colour of luminescing quartz grains in sandstones is used to infer the type of source rocks (Matter and Ramseyer, 1985).

Seven samples were broken into smaller subsamples for observation under the scanning electron microscope (SEM). Each of the subsamples was first viewed under a binocular microscope in order to distinguish the best surface of the sample for viewing under SEM. The whole rock samples were glued to metal specimen plugs using a two part epoxy mixture. A thin layer of silver paint was placed around each sample for conduction purposes. The plugs were positioned in a vacuum evaporator and coated with a gold alloy while undergoing rotation. The samples were examined under the S.E.M. using various magnifications. Special attention was placed on recognition of surface textures on detrital grains, both mechanical and chemical (Krinsley and Doornkamp,1973;

Krinsley, 1978; Krinsley, 1985). Pore filling cements, clay minerals and grain coatings were also noted. Detrital grains and clays were analysed using energy-dispersive X-ray spectra. In most cases a spectrum was not obtained because of problems in obtaining an elevated count rate. This problem may be related to irregular topography of the whole rock sample which hindered the X-ray beam from focussing in on the desired location.

4.3.5 Petrology and Mineralogy

Data from the twelve point counts are summarized in table 4. Chert is included with rock fragments (Folk, 1974; Basu et. al, 1975) for classification purposes. The petrology and mineralogy of the sandstones from the three interpreted depositional settings are dealt with separately and incorporated into summary at the end of this section.

a) Upper Shoreface Sandstones

The average framework composition (in percent) of the shoreface sandstones is Q35 F8 R57. According to Folk's (1974) classification of sandstones, the shoreface sandstones are litharenites (Fig. 4.21). The major constituents of the shoreface sandstones are detrital quartz, chert and rock fragments. Overall the sandstones are well sorted and mature (Folk, 1974)

Quartz grains are subangular to rounded (Powers, 1953) consisting of 12 to 58 percent monocrystalline quartz and 26

	UPPERSHOREFACE			CHANNEL FILL			TRANSGRESSIVE LAG			
	8-5-30-4W5 (2591.9m)	6-36-30-4W5 (2444.1m)	6-36-30-4W5 (2441.1m)	7-28-31-4W5 (2393.1m)	9-22-33-5W5 (2438.8m)	9-22-33-5W5 (2437.9m)	6-36-30-4W5 (2439.2m)	7-28-31-4W5 (2383.2m)	8-5-30-4W5 (2584.8m)	9-22-33-5W5 (2431.0m)
	A	B	C	D	E	F	G	H	I	J
Monocrystalline Quartz	27.9	11.8	57.7	12.9	15.7	29.3	27.1	41.9	42.5	44.1
Poly Quartz (2-3 Crystals)	4.7	1.2	2.8	0.8	1.0	2.1	0.6	2.6	0.9	2.0
Poly Quartz (> 3 Crystals)	31.8	30.4	20.6	34.4	27.6	15.7	57.9	30.2	40.8	25.8
Stained Feldspar	1.8	7.1	10.0	19.5	27.6	8.5	3.2	3.5	7.5	13.6
Twinned Feldspar	1.6	0	0.6	5.8	1.3	1.2	0.6	0.6	0.3	0
Sedimentary Rock Fragments	12.1	22.0	2.2	5.0	1.0	2.5	1.8	5.0	3.4	9.4
Meta-Volc Rock Fragments	6.3	5.2	4.4	8.4	5.2	5.1	5.0	8.2	4.0	5.6
Matrix (Altered & Clay)	12.9	21.7	1.1	11.9	18.7	33.5	0.9	2.0	0.3	3.6
Cement	0	0	0	1.0	0	0.4	0.3	0	0.3	0
Pore Space	0.8	0.2	0.2	0	1.7	1.3	3.0	5.8	3.4	0.2
Q (Mono-Quartz)	32.4	15.2	58.6	14.8	19.8	45.5	28.2	45.6	42.8	41.3
F (Feldspar)	4.0	9.2	10.8	29.1	36.2	14.9	3.9	4.4	7.8	14.2
L (Rock Frags + Poly Qtz.)	63.7	75.6	30.6	55.9	43.8	39.6	67.7	50.0	49.4	44.5

Table 4. Petrographic major components from point count data recalculated for triangular plot QFL.

	SAMPLE	LOCATION
SHOREFACE	A	8-5-30-4W5
	B	6-36-30-4W5
	C	6-36-30-4W5
CHANNEL	D	7-28-31-4W5
	E	9-22-33-5W5
	F	9-22-33-5W5
TRANS. LAG	G	6-36-30-4W5
	H	7-28-31-4W5
	I	8-5-30-4W5
	J	9-22-33-5W5

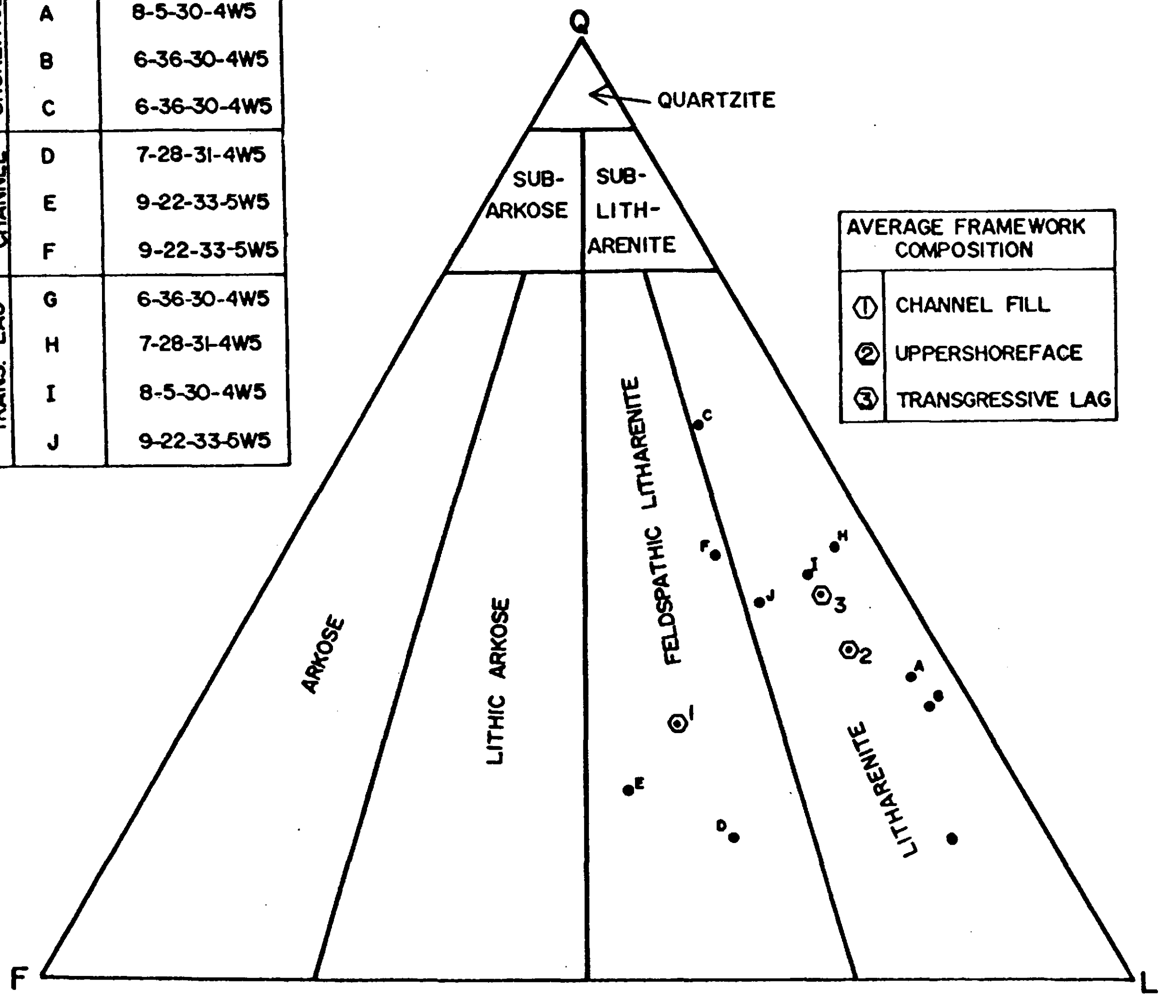

Figure 4.21. QFL plot (after Folk, 1974) for samples from facies 5a, 5b, and 10. Point count data are shown in Table 4.

to 36 percent polycrystalline quartz. Monocrystalline quartz is dominantly undulose (greater than 5 degrees of stage rotation) (Fig. 4.22). Under CL monocrystalline quartz is observed to luminesce light blue to blue violet (Fig. 4.22) and is suggestive of plutonic quartz. Brown luminescing quartz from regional metamorphic rocks is rarely observed (Marshall, 1988). Polycrystalline quartz having greater than three crystals per grain is more abundant than polycrystalline quartz having two to three crystals per grain. Polycrystalline quartz grains in some shoreface sandstones examined have elongate oriented crystals, often with strongly sutured contacts (Fig. 4.22), which are typical of schistose or gneissic source rocks (Folk, 1974).

Rock fragments are common and relatively abundant in all samples of the shoreface sandstones. Two types frequently observed are plutonic and sedimentary rock fragments. Sedimentary rock fragments are usually dark brown in colour under plane polarized light (Fig. 4.22). These same rock fragments are identified under CL by their overall dull luminescence and abundant bright luminescent inclusions of quartz (blue) and feldspars (luminesce bright lime green).

A peculiar aspect of sample B (Fig. 4.22) is siderite grains up to 0.3 mm which make up 12 percent of the modal composition of this sample. In cross polarized light (Fig. 4.22) the siderite is yellowish-brown and is made up of microcrystalline rhombic shaped crystals. Siderite appears

Figure 4.22: Petrography - Facies 10

a) Photomicrograph under cross-polarized light of monocrystalline quartz (M) and polycrystalline quartz (P) rich sandstone. The grain marked (P) is probably of high grade metamorphic origin. Well 8-5-30-4W5; Depth 2591.9 m; Scale as shown.

b) Photomicrograph under cross-polarized light of a possible siderite (S) fecal pellet made or microcrystalline rhombic shaped crystals. The siderite clasts were compacted during burial and flowed around adjacent quartz and chert grains. Well 6-36-30-4W5; Depth 2444.4 m; Scale as shown.

c) Photomicrograph under plane polarized light of deformed siderite clasts. Quartz and rock fragments are also observed. Red arrows point to possible pressure solution seams. Compare photo with figure 4.22d at right. Well 6-36-30-4W5; Depth 2444.4 m; Scale as shown.

d) Cathodoluminescence photomicrograph of figure 4.22c. Note dark patches of non-luminescent iron-rich siderite. The quartz in this example shows a brown-orange and mauve CL. Bright orange luminescent grain may be a carbonate. Well 6-36-30-4W5; Depth 2444.4 m; Scale as shown; Photographic conditions: 75 sec. ASA 400 Ektachrome.

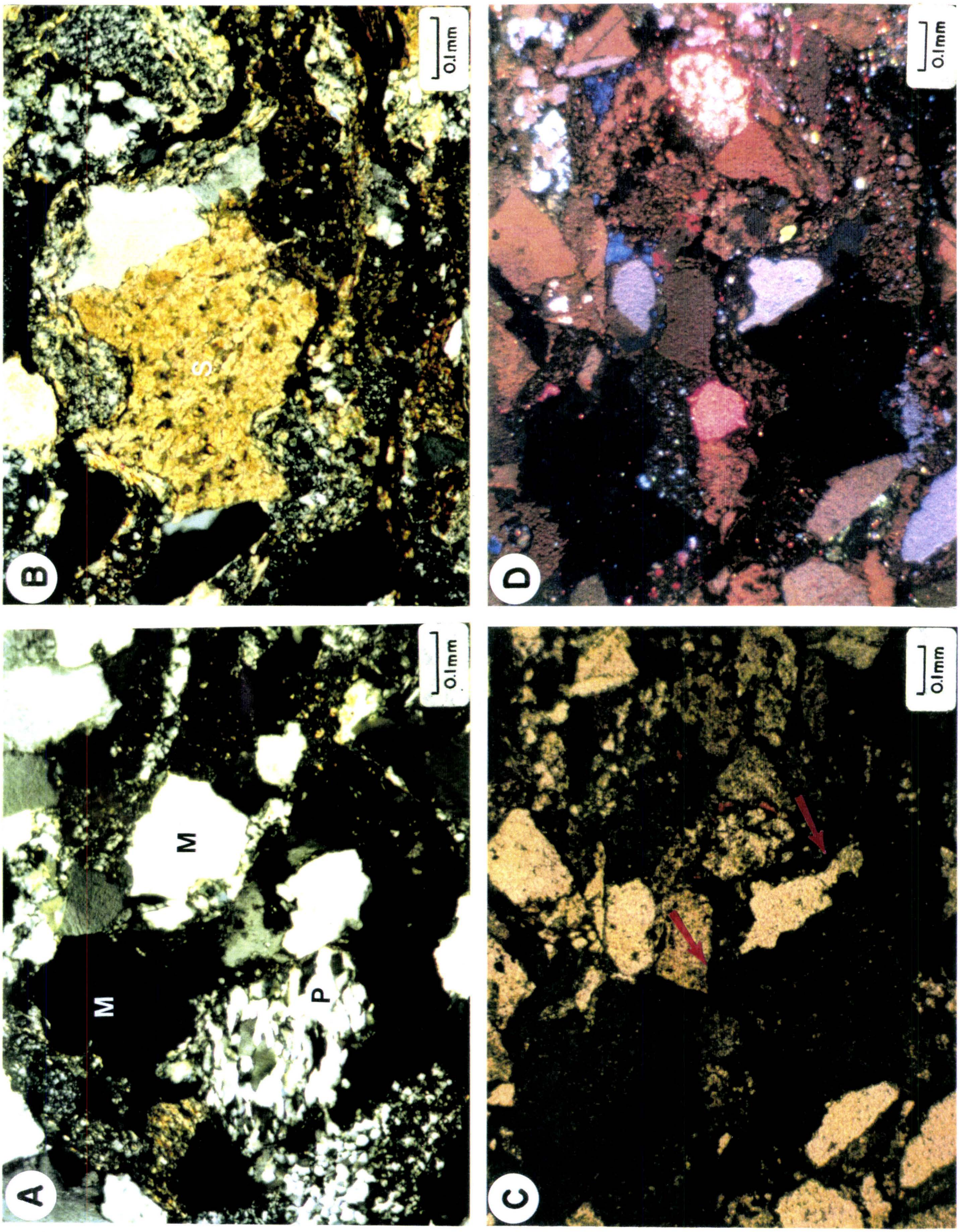
A
M
M
P
0.1mm
B
S
0.1mm
C
0.1mm
D
0.1mm

as dark grains under CL (Fig. 4.22). Iron rich siderites are non-luminescent (Amieux, 1982, cited in Marshall,1988). The siderite grains in sample B are deformed around more rigid detrital grains of quartz and chert implying they were not lithified at the time of deposition. The siderite grains may represent biogenic fecal pellets or alternatively may be detrital shale clasts. Carbonate rock fragments are observed rarely and occur as bright orange-red luminescent grains under CL (Fig. 4.22).

Feldspars observed in the shoreface sandstones comprise 4 to 11 percent of the framework composition. They are identified under CL as luminescent bright blue to lime-green grains (Fig 4.23). Most of the feldspars are altered to some extent ranging from a dusty-cloudy appearance to possible replacement by calcite or clay minerals (Fig 4.23).

Cement was not identified during the polarizing light microscope point counting procedure. Clay cement was grouped as matrix due to the difficulty in separating the two. Quartz cement in the form of overgrowths is observed under CL by its non-luminescence, but the amount of this particular cement was not quantified. Quartz is observed as a healing cement infilling fractured silicate grains (Fig. 4.23). Similar fractured quartz is described by Wilson and McBride (1988) for deeply buried Pliocene sandstones in the Ventura Basin, California.

Matrix in the form of clay and microcrystalline

Figure 4.23: Petrography - Facies 10 and Facies 5b

a) Photomicrograph under plane-polarized light showing subangular to subrounded quartz and rock fragments. Note fractured quartz grain (Q) in centre. Dull orange is pore space. Compare with figure 4.23b to right. Well 6-36-30-4W5; Depth 2444.4 m; Scale as shown.

b) Cathodoluminescence photomicrograph of figure 4.23a. Note general lack of quartz overgrowths. Fractured quartz grain (Q) is healed by quartz cement (red arrow). The luminescent lime green grain is feldspar (F). The red luminescent grain in the bottom left corner may be calcite replaced feldspar. Well 6-36-30-4W5; Depth 2444.4 m; Scale as shown. Photographic conditions 100 sec. ASA 400 Ektachrome.

c) Photomicrograph under plane polarized light. Note the difficulty in distinguishing quartz from feldspar and rock fragments. Orange is pore space. Compare with figure 4.23d to right. Well 9-22-33-5W5; Depth 2438.8 m; Scale as shown.

d) Cathodoluminescence photomicrograph of the same area as figure 4.23c. The mauve luminescent grains may be volcanic quartz, while the brown luminescent grains suggest quartz from regional metamorphic rocks. Note the abundance of bright blue luminescent feldspar. The small residual grain of feldspar (F) is almost completely altered to clay. Well 9-22-33-5W5; Depth 2438.8 m; Scale as shown.

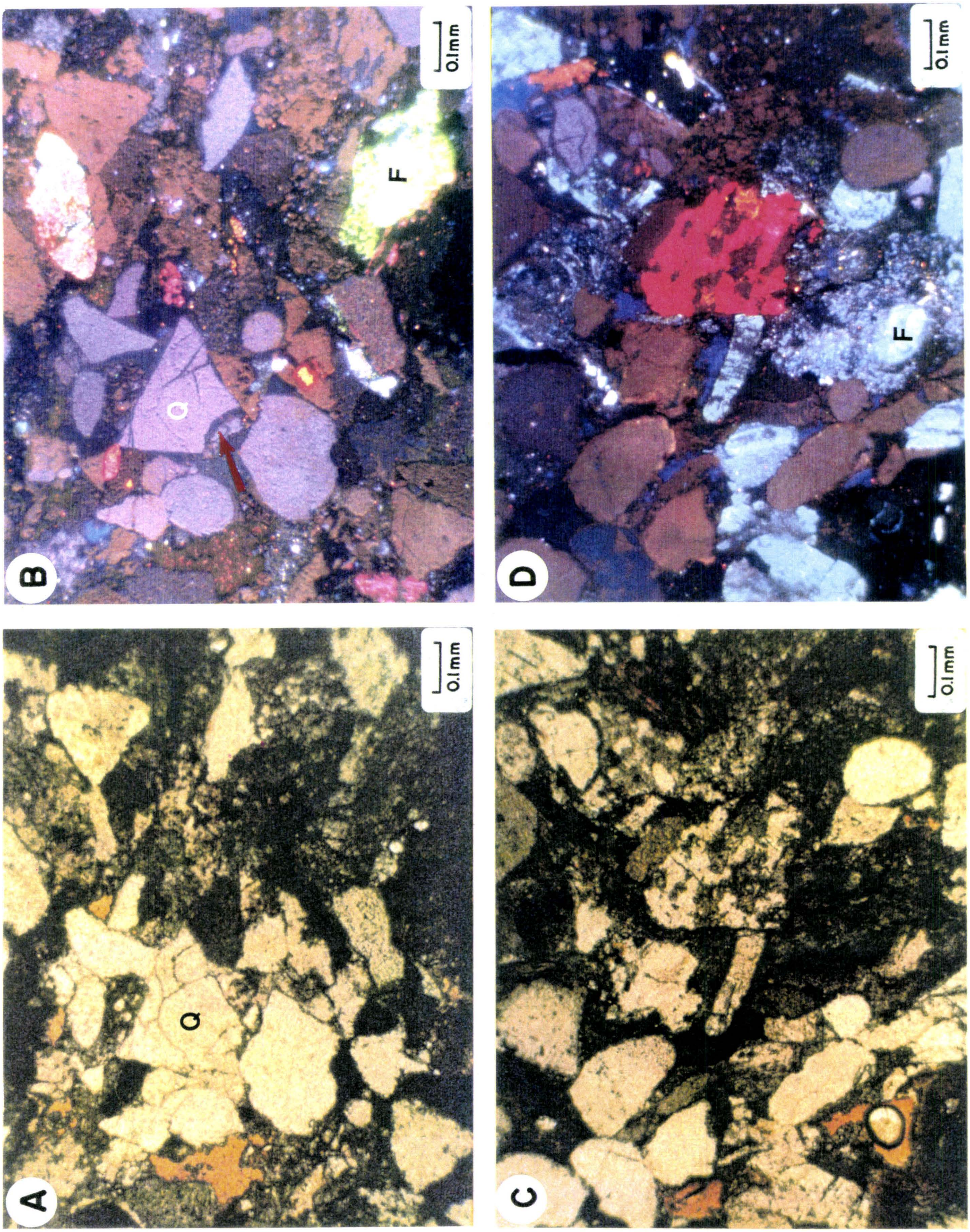
A
Q
0.1mm
B
Q
F
0.1mm
C
0.1mm
D
F
0.1mm

pseudomatrix around remnant altered grains ranges 2 to 22 percent of the modal composition of shoreface sandstones. The greater proportion of matrix (22%) in sample B may be related to operator error during the point counting procedure, in this case distinguishing between remnant grain boundaries of altered grains and authigenic clays.

Porosity of the shoreface sandstones is almost non existent (averages 1% thin section porosity). Some porosity may be secondary relating to dissolution and alteration of silicate grains.

b) <u>Channel Fill Sandstones</u>

The average framework composition in percent of the channel fill sandstones is Q27 F27 R46. According to Folk's (1974) classification of sandstones, the channel fill sandstones are feldspathic litharenites. The major constituents of the channel fill sandstones are similar to the shoreface sandstones. Both groups of sandstones have abundant detrital quartz, and rock fragments; however, the channel fill sandstones contain over three times the detrital feldspar Fig. 4.21).

The average grain size of the channel fill sandstones is 0.2 mm. The sandstones are moderately sorted to well sorted (Folk, 1974). Detrital quartz grains are subangular to rounded (Powers, 1953) consisting of 13 to 29 percent monocrystalline quartz and 18 to 35 percent polycrystalline quartz. The monocrystalline quartz of the channel fill sandstones luminesces brown to predominantly a mauve colour under CL (Fig. 4.23). The colours imply quartz from plutonic and regional metamorphic rocks (Matter and Ramsayer, 1985).

Feldspars comprise 15 to 36 percent fo the total detrital component of the channel fill sandstones. Plagioclase feldspars, primarily oligoclase are the most dominant feldspars. They are readily observed in thin section by their uptake of pink stain. Pink stained plagioclase feldspars comprise 18 to 35 percent of the total detrital component of channel fill sandstones. No alkali feldspars were observed. If they are present the staining procedure did not distinguish them as no yellow grains were observed. Twinned plagioclase comprise 1 to 6 percent of the total detrital component of channel fill sandstones. Plagioclase feldspars exhibit pericline, albite and carlsbad twinning (Fig. 4.24).

Under CL feldspar grains stand out vividly in contrast to quartz. Feldspars luminesce much more brightly than quartz for the same excitation conditions (Marshall, 1988). Figure 4.23 shows bright luminescing feldspars which may represent high temperature igneous and metamorphic feldspars (Kastner and Siever, 1979). Most feldspars like those observed in the shoreface sandstones exhibit partial to almost complete alteration and replacement (Fig. 4.24) Alteration of feldspars is primarily related to clay mineral replacement. In some cases feldspars exhibit a complex

Figure 4.24: Petrography - Facies 5b

a) Photomicrograph under cross polarized light. Mica fragment in centre exhibits plastic deformation around more resistant silicates. Warped twin planes on right side of feldspar may represent feldspar overgrowths. Clay-silt matrix may represent mechanical infiltration of clay. Darker rims around quartz grains (red arrows) may be clay cutans. Well 7-28-31-4W5; DEpth 2393.1 m; Scale as shown.

b) Photomicrograph under cross polarized light showing fractured and altered plagioclase feldspar (F). Well 9-22-33-5W5; Depth 2438.8 m; Scale as shown.

c) Photomicrograph under plane-polarized light of a deformed and altered plagioclase feldspar grain. Well 7-28-31-4W5; Depth 2393.1 m; Scale as shown.

d) Cross polarized photomicrograph of same area as figure 4.24c. The feldspar grain is being replaced by clay minerals. The round grain (red arrow) originally part of the feldspar has undergone slippage and rotation as indicated by the opposed twin plane. Well 7-28-31-4W5; Depth 2393.1 m; Scale as shown.

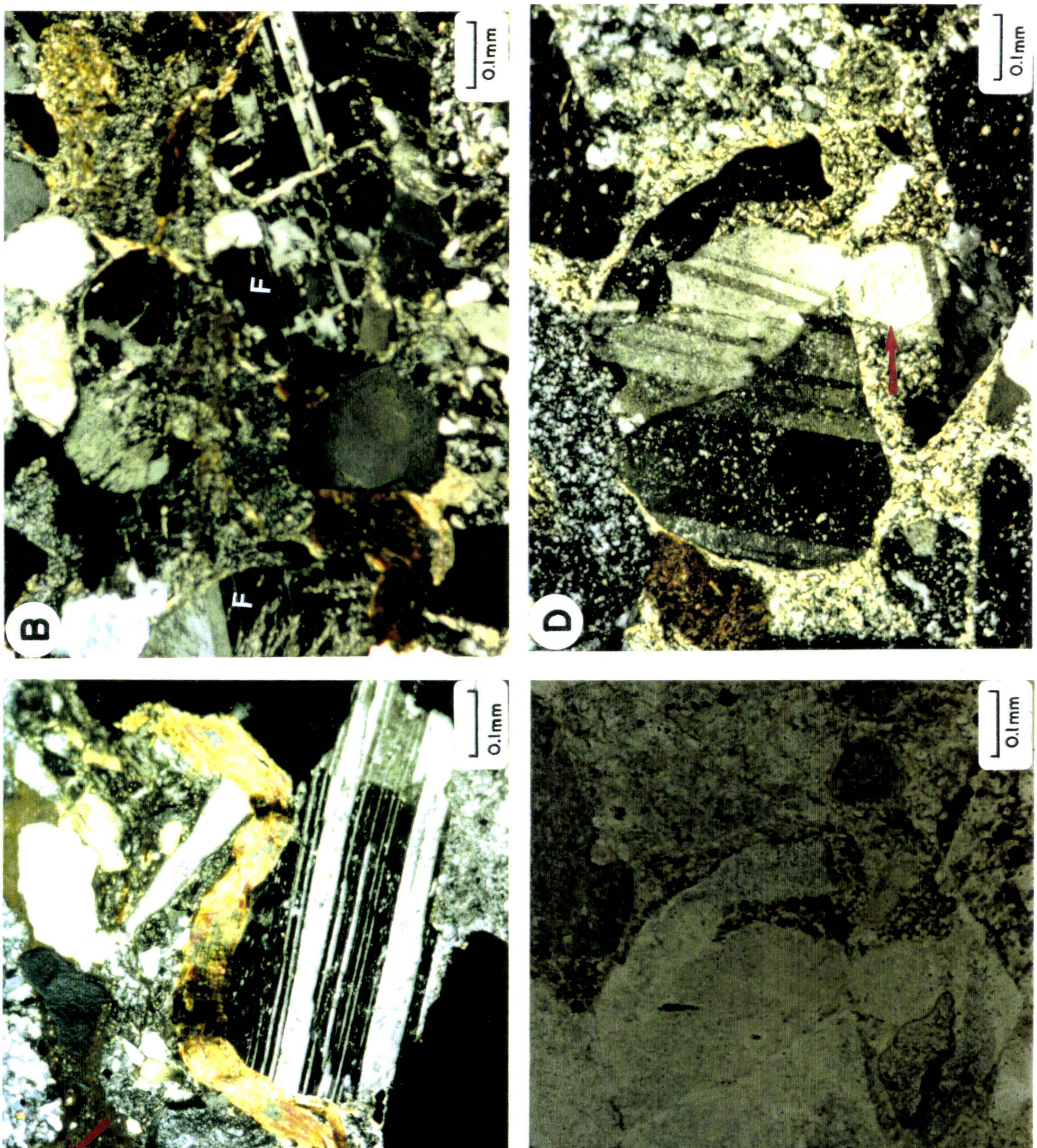
A
0.1mm
B
F
F
0.1mm
C
0.1mm
D
0.1mm

history of alteration and deformation (Fig 4.24).

Sedimentary and metamorphic rock fragments comprise 1 to 8 percent of the detrital component of channel fill sandstones. Sedimentary rock fragments observed in channel fill sandstones include siderite or clay clasts (Fig.4.25) and siltstone clasts. Figure 4.25 also shows a siltstone clast made up of silt sized monocrystalline chert and polycrystalline chert supported in a dark brown possibly phosphatic matrix. The presence of siltstone clasts in a sandstone is an indicator of sedimentary source rock. Siltstone fragments rarely survive extensive transport (Scholle, 1979). This may imply sample E was buried rapidly and not reworked extensively in its depositional environment. Siltstone clasts are not observed in sandstones of other depositional settings discussed earlier in this chapter. Mica fragments were observed in all channel fill sandstones and represent good indicators of the degree and nature of post depositional compaction (Fig. 4.24)

Matrix comprises 12 to 34 percent of the modal composition of channel fill sandstones and occurs as silicate grain replacement in the form of authigenic clays. In figure 4.24 clay and silt sized quartz grains occur as matrix between rigid silicate grains. The two quartz grains in the top left corner of the photomicrograph have a thin dark brown haloe or coating which may represent clay cutans formed as a result of mechanical infiltration of clay minerals (ie.

detrital pore filling clay). An alternative interpretation of this matrix is a shale clast which has squeezed between quartz grains forming a dispersed pseudo-matrix (Molenaar, 1986).

c) Transgressive Lag Sandstones

The average framework composition of the transgressive sandstones (in percent) is Q40 F8 R53. The sandstones are classified as litharenites according to Folk's (1974) classification. The major constituents of the transgressive sandstones are similar to those of the shoreface. Both suites of sandstones have the same percentage framework feldspar compositions on average (both 8%)(Fig. 4.21).

Quartz grains are subrounded to well rounded consisting of 27 to 40 percent monocrystalline quartz and 30 to 58 percent polycrystalline quartz. The quartz grains within these sandstones exhibit many forms of grain contact fabric some of which may be a result of pressure solution. Figure 4.25 reveals quartz grains having both concavo-convex and long contacts as well as quartz overgrowth cement contacts. Figure 4.25 also shows a detrital chert clast with sutured contacts. The chert grain also exhibits relict depositional texture. The grain contains abundant sponge spicules (monaxons) and unidentified foraminifera and may have derived from a limestone which had deposited in deep water. Monocrystalline quartz (Fig. 4.26) in transgressive sandstones luminesce light blue to blue violet suggestive of

Figure 4.25: Petrography - Facies 5a and 5b.

a) Photomicrograph under cross polarized light of a clay or siderite clast. This clast appears to have inhibited overgrowth cementation of surrounding quartz and feldspar grains. Well 7-28-31-4W5; Depth 2393.1 m; Scale as shown.

b) Photomicrograph under cross polarized light of a detrital siltstone clast. The red arrows point to the grain boundary of the clast. The clast is made up of angular quartz grains embedded in a possible phosphatic matrix. Well 9-22-33-5W5; Depth 2438.8 m; Scale as shown.

c) Photomicrograph under cross polarized light. Possible pressure solution quartz. The quartz grains exhibit concave-convex and long suture contacts (red arrows) with other grains. Well 6-36-30-4W5; Depth 2439.2 m; Scale as shown.

d) Photomicrograph under plane polarized light of a chert grain with relict depositional texture. The grain contains abundant sponge spicules (monaxons) and unidentifiable foraminifera. The red arrow points to a sutured contact between chert and adjacent quartz grains. Well 7-28-31-4W5; Depth 2388.1 m; Scale as shown.

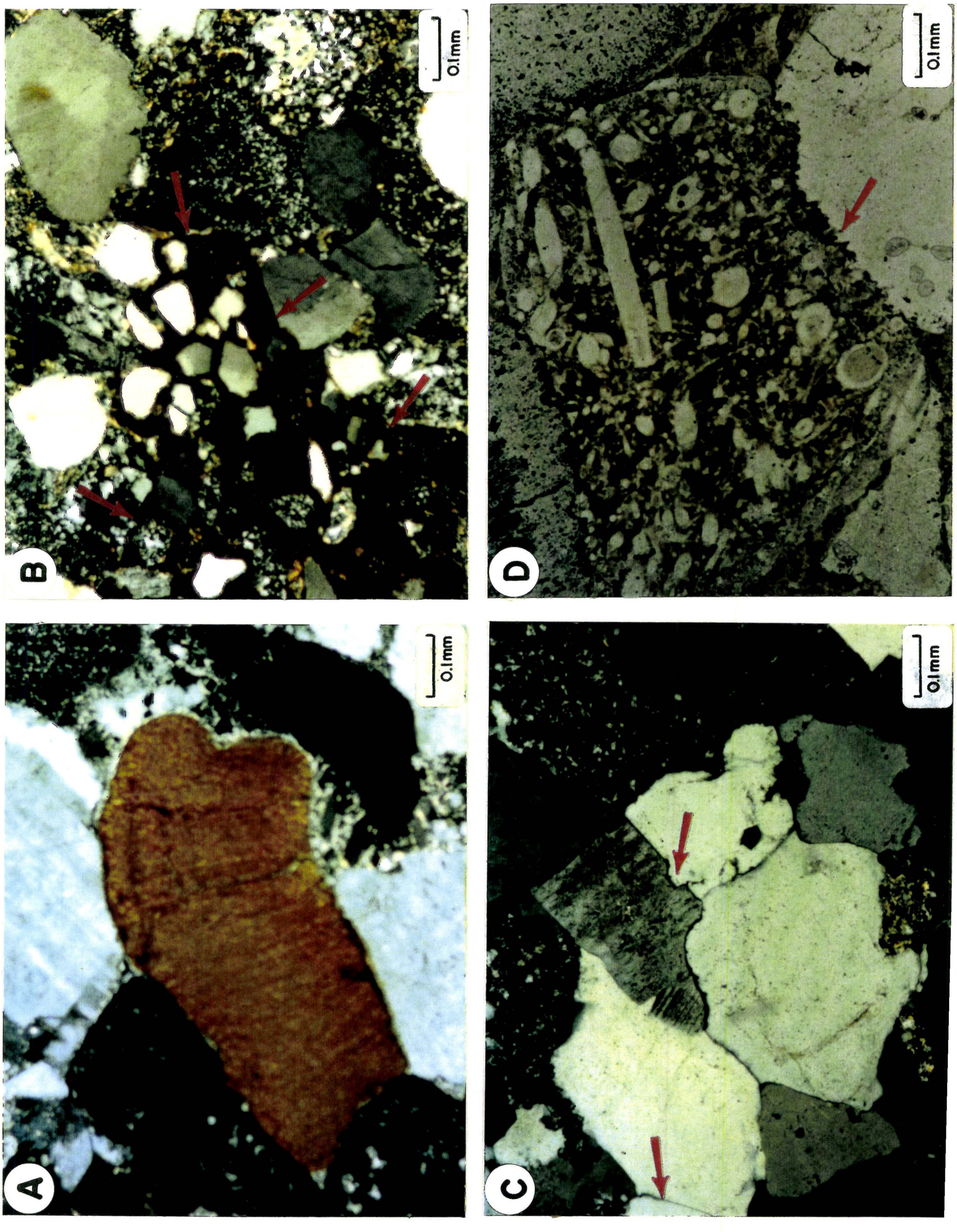
B
0.1mm
D
0.1mm
A
0.1mm
C
0.1mm

Figure 4.26: Petrography - Facies 5a

a) Photomicrograph under plane polarized light. Red arrow points to what appears to be a pressure solution contact between two grains, however the same point under CL shows the detrital grains separated by quartz overgrowth cement. Well 9-22-33-5W5; Depth 2431.0 m; Scale as shown.

b) Cathodoluminescence photomicrograph of figure 4.26a. Compare area above red arrow to same area in figure 4.26a. What appears as fractured quartz under plane polarized light is really several grains with quartz overgrowths as viewed under CL. Quartz overgrowths (O) are dark blue while volcanic quartz (V) are the light blue to mauve grains. Well 7-28-31-4W5; Depth 2388.1 m; Scale as shown.

c) Photomicrograph under plane polarized light showing tight compaction of quartz grains and rock fragments. Red arrow points to embayed contact between two grains. Well 7-28-31-4W5; Depth 2388.1 m; Scale as shown.

d) Cathodoluminescent photomicrograph of figure 4.26c. Quartz grains (Q) shows evidence of abraded overgrowths (red arrow). Quartz overgrowths (O) are dark blue and enclose some but not all grains. Authigenic clay (C) almost completely fills the pore space between grains. Well 9-22-33-5W5; Depth 2431 m; Scale as shown.

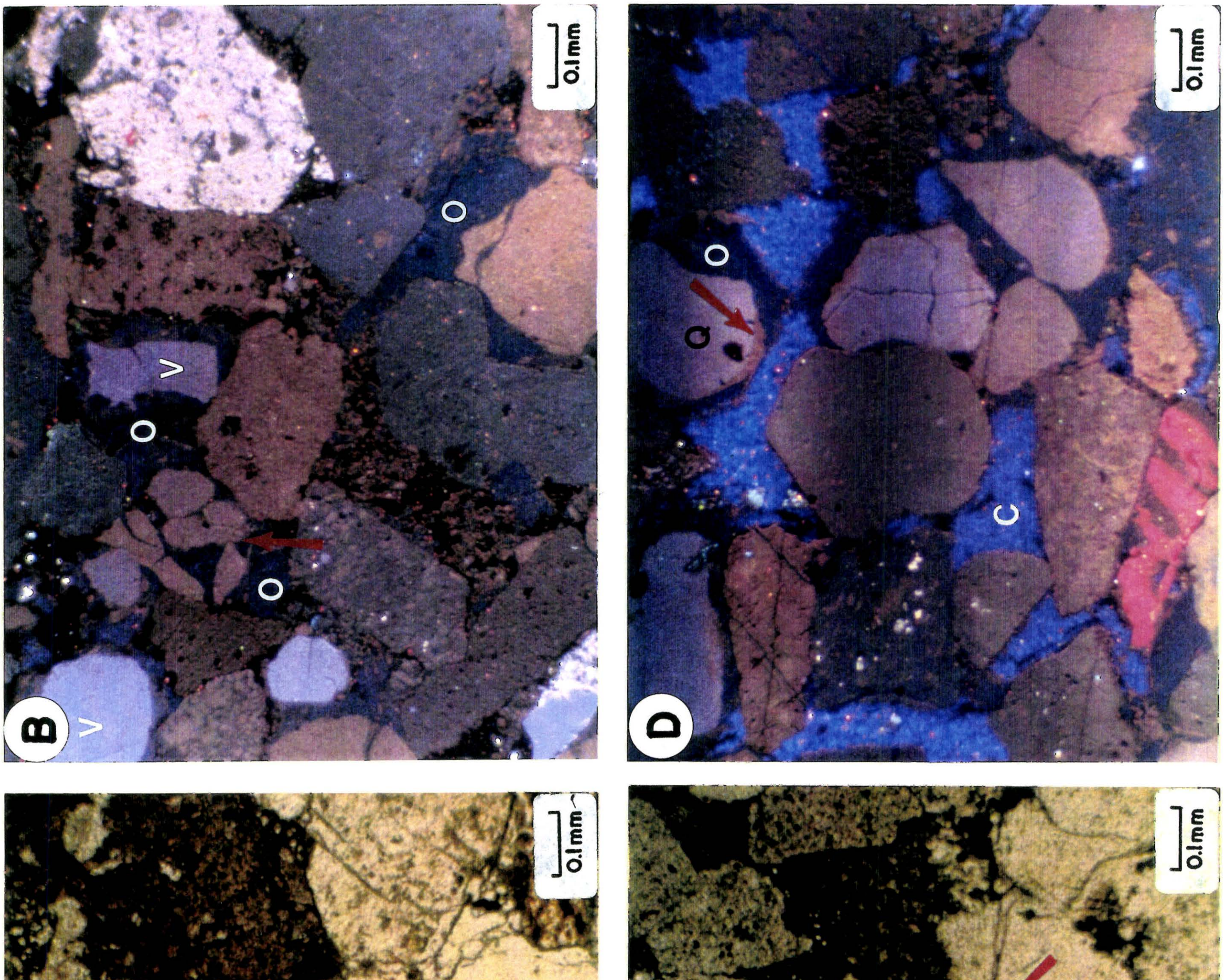
A
B
C
D
V
O
Q
C
0.1mm

plutonic quartz while polycrystalline quartz luminesces brown.

Other evidence for recycled clastic sediments in transgressive lag sandstones is noted under CL. As mentioned earlier, silica occurs as overgrowths on some but not all of the detrital grains within the transgressive lag sandstones. In plane polarized light the overgrowths are extensive enough to give the impression that the sandstone is composed of concavo-convex, sutured and long contacts (Fig. 4.26). However, CL (Fig. 4.26) shows these contacts are only apparent, and that the detrital grains remain relatively separate and are in fact cemented by quartz overgrowths.

Authigenic clay averages 2 percent of the modal composition of transgressive lag sandstones and is observed under CL by its dark blue luminescence (Fig. 4.26). It should be noted that figure 4.26D is the best example of authigenic clay observed under CL in the transgressive sandstones and does not represent the average relationship of clay to detrital grains observed.

Thin section porosity of transgressive lag sandstones averages 3 percent of the modal composition. The porosity may not be primary and is likely secondary porosity related to dissolution of rock fragments or feldspar grains.

d) <u>Sandstone Composition Summary</u>

The sandstone classification according to Folk (1974) is useful in distinguishing channel fill sandstones from sandstones of the uppershoreface and transgressive lag (Fig. 4.21). The three channel fill sandstones plot as feldspathic litharenites. Three of the transgressive lag sandstones (Samples H,I and J) cluster at the midpoint of the litharenite field. The uppershoreface sandstones are scattered throughout the litharenite field; however, the average composition of the three shoreface sandstones plots closely to the average framework composition of the transgressive lag sandstones. Matrix in the form of clay and altered grains is more abundant (up to 33 percent of the sandstone composition) in channel fill sandstones. The percentage of original feldspar may have been greater in channel fill sandstones. Helmold (1985, p. 149) indicates mechanical abrasion, replacement, dissolution and albitization are effective diagenetic processes which modify feldspar in sandstones. Replacement and dissolution of feldspars in channel fill sandstones was likely a dominant process. The authigenic clay in these sandstones may be a result of replaced feldspar.

The channel fill sandstones examined in this study suggest diagenetic replacement of plagioclase feldspar to clay. This process does not seem to have any affinity with respect to the sandstones of the three depositional settings examined. The decreased abundance of feldspar in the shoreface and transgressive sandstones may be attributed to mechanical abrasion of feldspar in the postulated high energy settings (ie. significant loss of feldspar occurred in the depositional environment prior to burial).

4.3.6 S.E.M. - Surface Texture Analysis

Sand grain textural analysis can be used to define modern and ancient environments where no cementation or lithification has occurred. The effect of diagenesis on the elimination of primary mechanical textures on quartz grains is poorly understood (Krinsley, 1978). This part of the chapter considered seven samples for grain surface textural analysis. The location of samples examined with S.E.M. is shown in figure 4.20. In summary, surface textures were only observed on grains from channel fill sandstones. Cement and clay minerals in the transgressive lag sandstones completely masked any primary surface textures that could have been present.

Three samples of channel fill sandstones were examined using SEM. Surface textures are partly obscured by the authigenic clay coatings. A typical view of a channel fill sandstone under SEM is given in figure 4.27 and 4.28. The detrital grains are plastered by silica cement and mixed layer clays (illite/smectite) the latter resembling corrugated particles of Krinsley and Doornkamp (1973). Former grain contacts are delineated by "bald areas" which have no clay minerals. Other grain surfaces suggest evidence

Figure 4.27: S.E.M. - Facies 5b.

a) Scanning electron micrograph of silica and smectite plastered grains. Possible corrugated particle (C) appears to drape underlying topography of grain. Quartz overgrowth (Q). Square is detail area of figure 4.27b below. Well 7-28-31-4W5; Depth 2393.1 m; Scale as shown.

b) Detailed scanning electron micrograph of area inside box of figure 4.27a above. Darker area on grain represents former grain contact positions. Illite/smectite filled pore space between grains are seen as clay ridges (arrows). Some of the clay in these ridges may be detrital. Well 7-28-31-4W5; Depth 2393.1 m; Scale as shown.

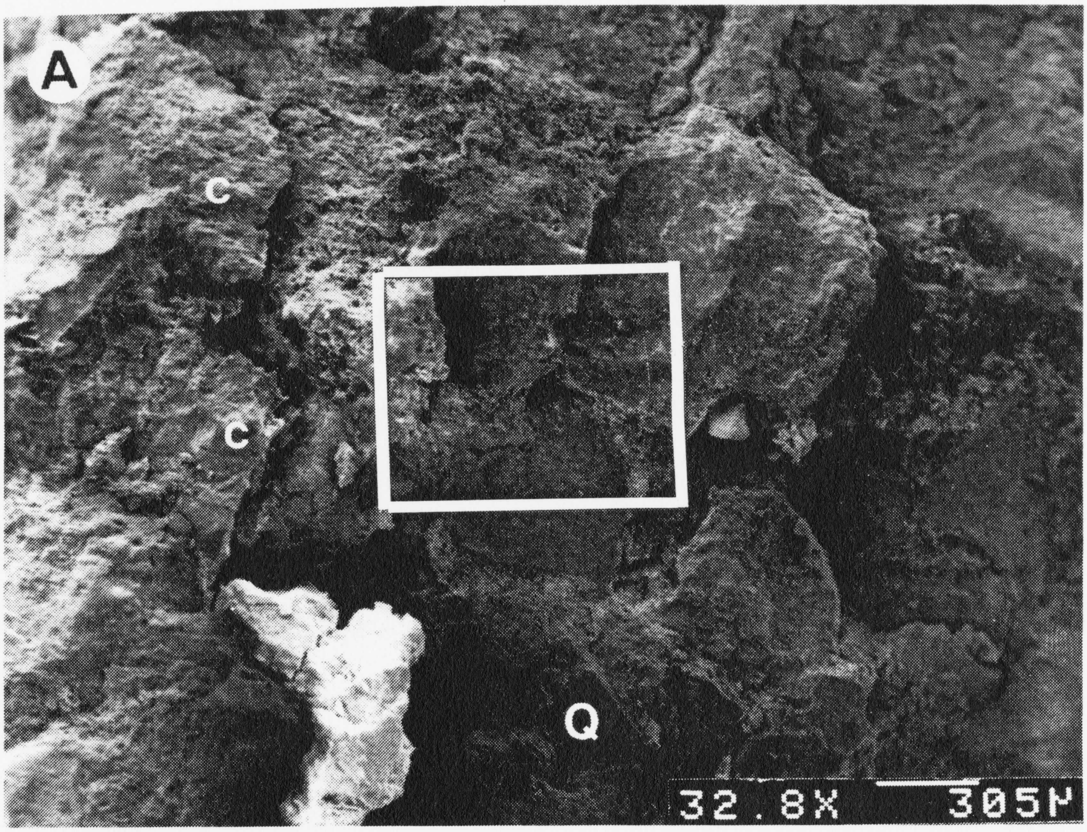
A
C
C
Q
32.8X 305μ

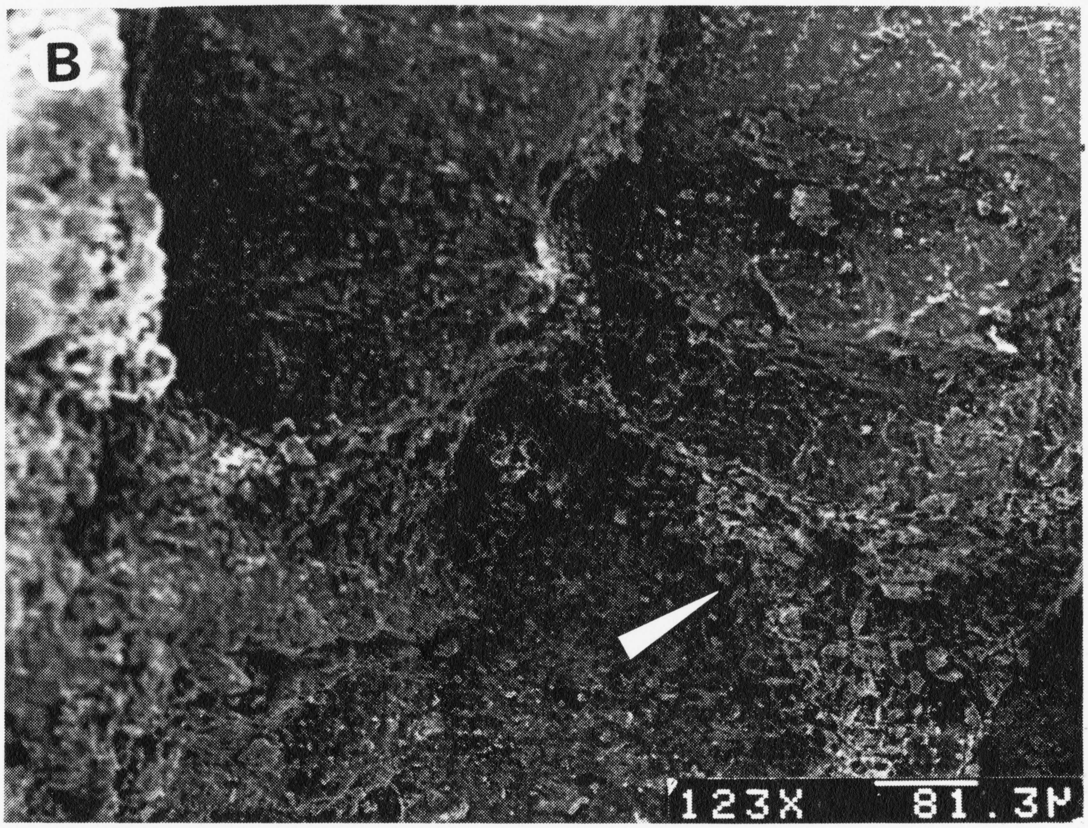
B
123X 81.3μ

Figure 4.28: S.E.M. - Facies 5b

a) Scanning electron micrograph of round quartz grains with pervasive coating of mixed layer illite and smectite. Well 9-22-33-5W5; Depth 2438.8 m; Scale as shown.

b) Detail scanning electron micrograph of area outlined by box in figure 4.28a. Pore filling authigenic , crenulated to filamentous illite/smectite mixed with blocky kaolinite books (arrows). Bald areas devoid of authigenic clays are areas of former grain contacts. Local saturation of silica (early pore fluids) may have lead to precipitation of globular silica (G). Well 9-22-33-5W5; Depth 2438.8 m; Scale as shown.

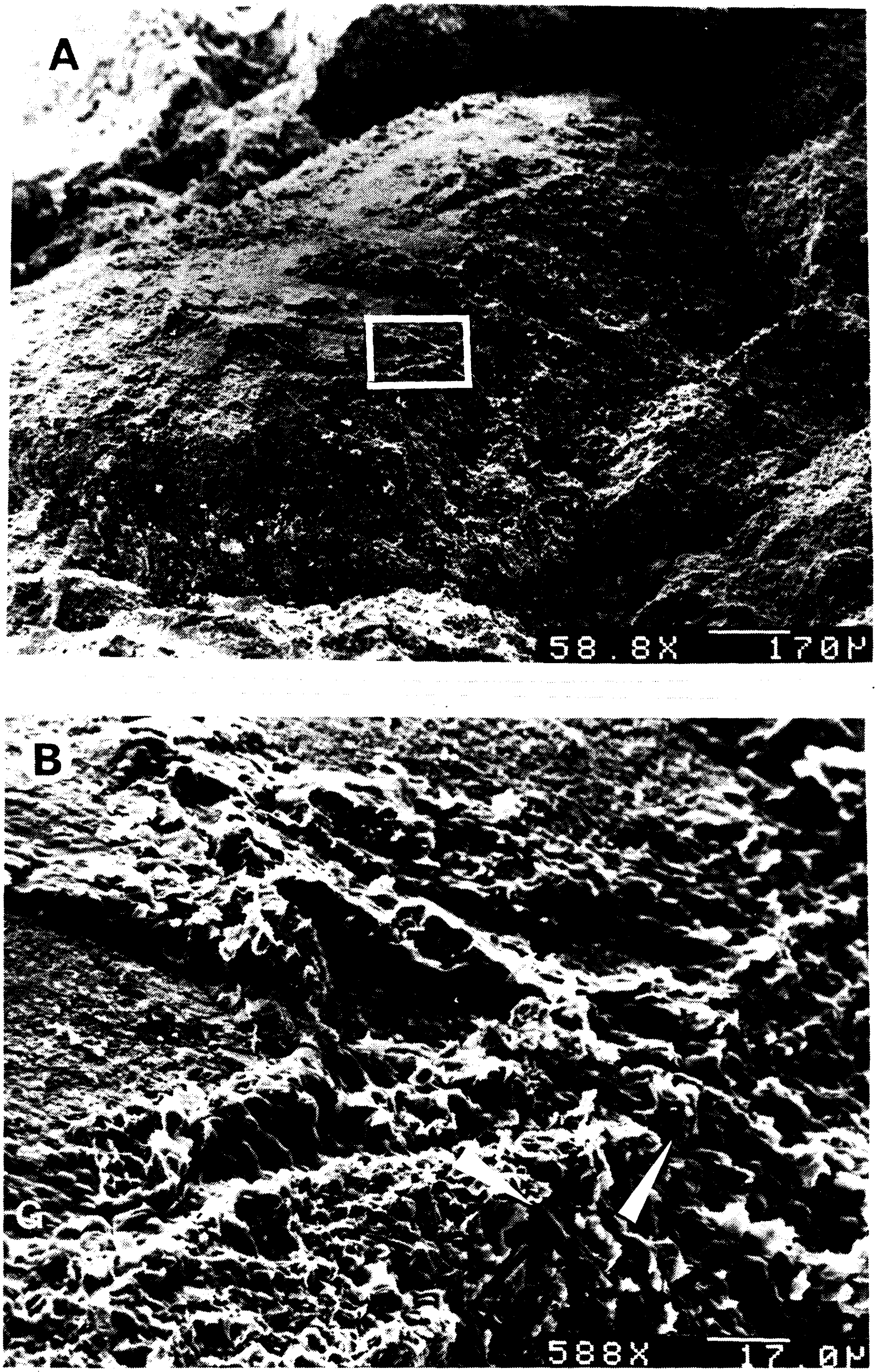
A
58.8X
170µ
B
G
588X
17.0µ

of mechanical and chemical processes. Figure 4.29 is similar to the two previous photos in that detrital grains are completely covered by authigenic clay. The surface of the grain within the outlined box shows sharp sided grooves which may have been produced by mechanical abrasion, possibly in an eolian environment. The relief on the grain surface produced by the grooves could have been sufficient to prevent further mechanical abrasion within the groove interior.

Early cementing pore fluids may have been important in the cementing of channel fill sandstones. This may expalin why these sandstones do not have reservoir quality porosity and permeability. Silicified fragmentary plant material (FPM) (Scott and Collinson, 1978) is interpreted to have been cemented to the side of a quartz grain (Fig. 4.30). The detailed view of this same image allows one to trace the FPM contact back to the grain surface boundary. The morphology of the "root like" fragment is plastered over by a coating of silica cement. According to Ribault (1978, p. 324) "...in fluvial environments with a medium energy level, mutual erosion of grains brings on solution of silica from quartz. Local saturation in dissolved silica leads to precipitation of globular silica deposits in the hollows of grains. In a lower energy fluvial system, early silica deposits may be expected to cover the entire surface." The FPM in figure 4.30 is thought to have been cemented to the edge of the detrital grain early in its depositional history.

Figure 4.29: S.E.M. - Facies 5b.

a) Scanning electron micrograph of tightly cemented quartz grains. Note former grain location (L) and curved overhang of clay which conformed to former outer grain wall boundary. Texture detail in box is described below under figure 4.29b. Well 7-28-31-4W5; Depth 2393.1 m; Scale as shown.

b) Detailed scanning electron micrograph of area within box in figure 4.29a. Note chemically altered surface (arrow) exhibiting a variable surface roughness. Possible mechanical grooves (G) show smooth walls. These walls could represent topographic low areas on the grain which were protected from any additional abrasion during deposition. Well 7-28-31-4W5; Depth 2393.1 m; Scale as shown.

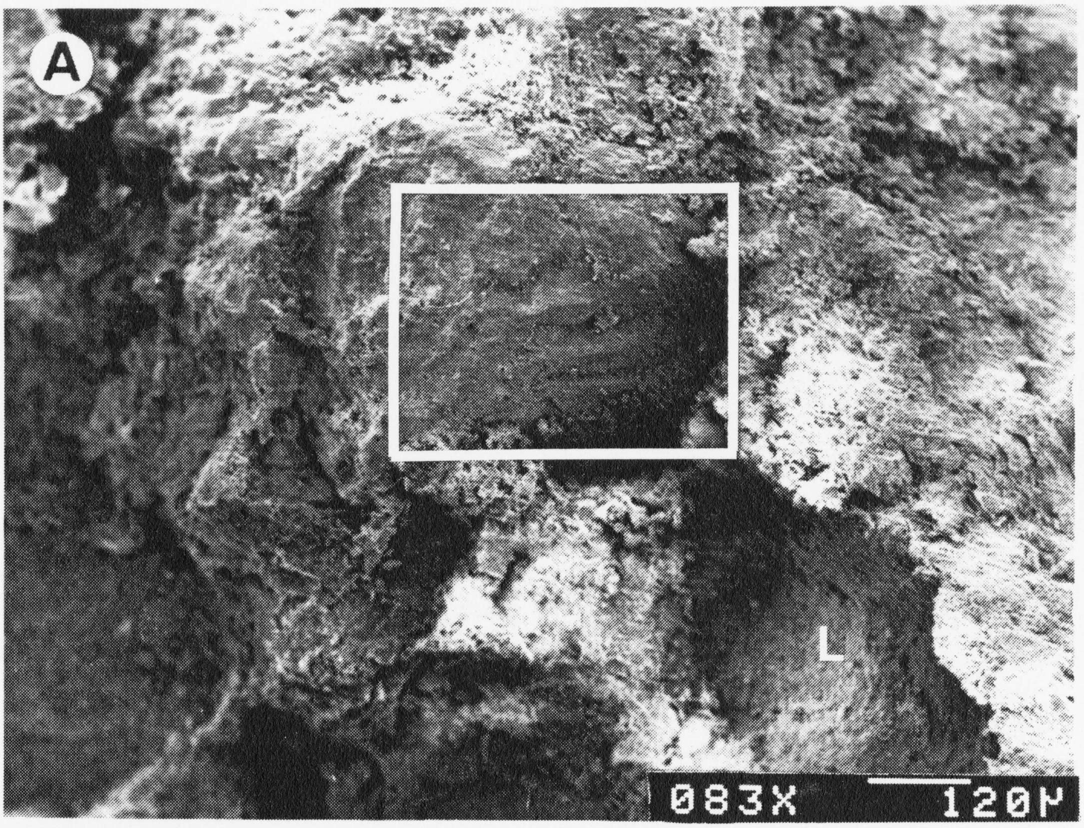
A
L
083X
120µ

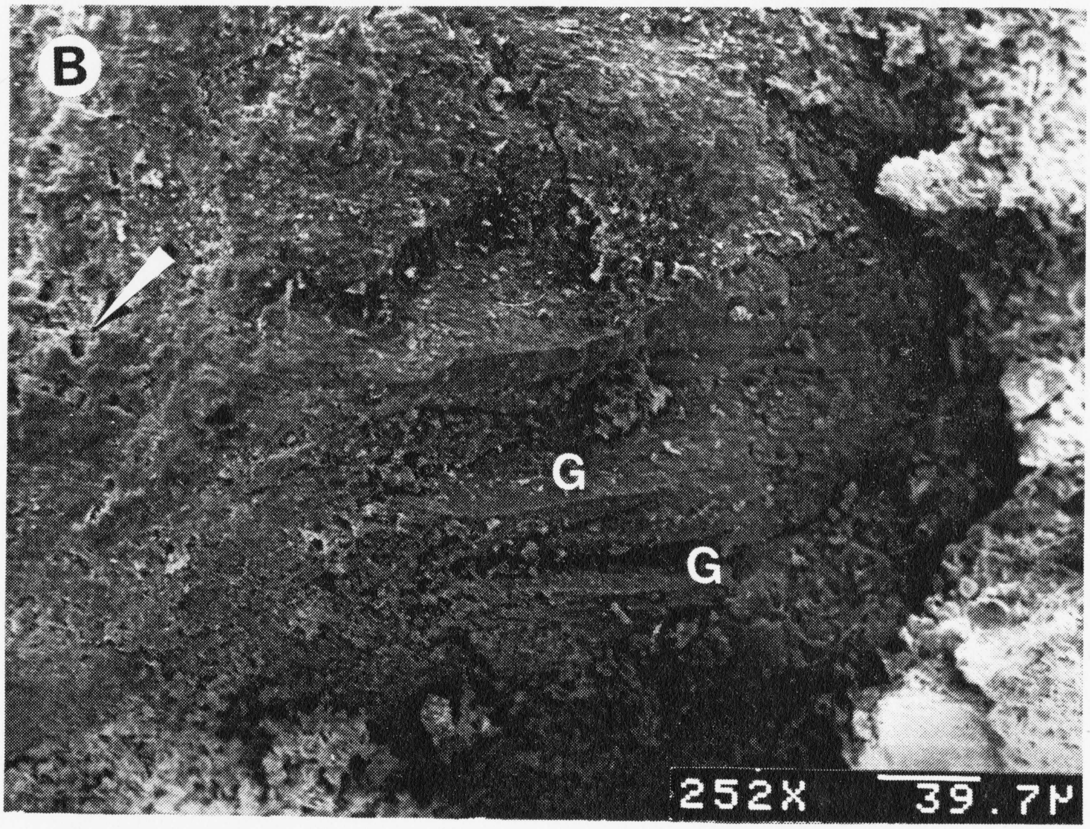
B
G
G
252X
39.7µ

Figure 4.30: S.E.M. - Facies 5b

a) Scanning electron micrograph of silicified fragmentary plant material (FPM) cemented to the side of a detrital grain. Area inside box is shown in figure 4.30b below. Well 9-22-33-5W5; Depth 2438.8 m; Scale as shown.

b) Detailed scanning electron micrograph of area within box in figure 4.30a. Arrow at top left points to raised edge of FPM covered by silica cement. Arrow at lower right points to structure which resembles peltate head of Scott and Collinson (1978, p. 145). Well 9-22-33-5W5; Depth 2438.8 m; Scale as shown.

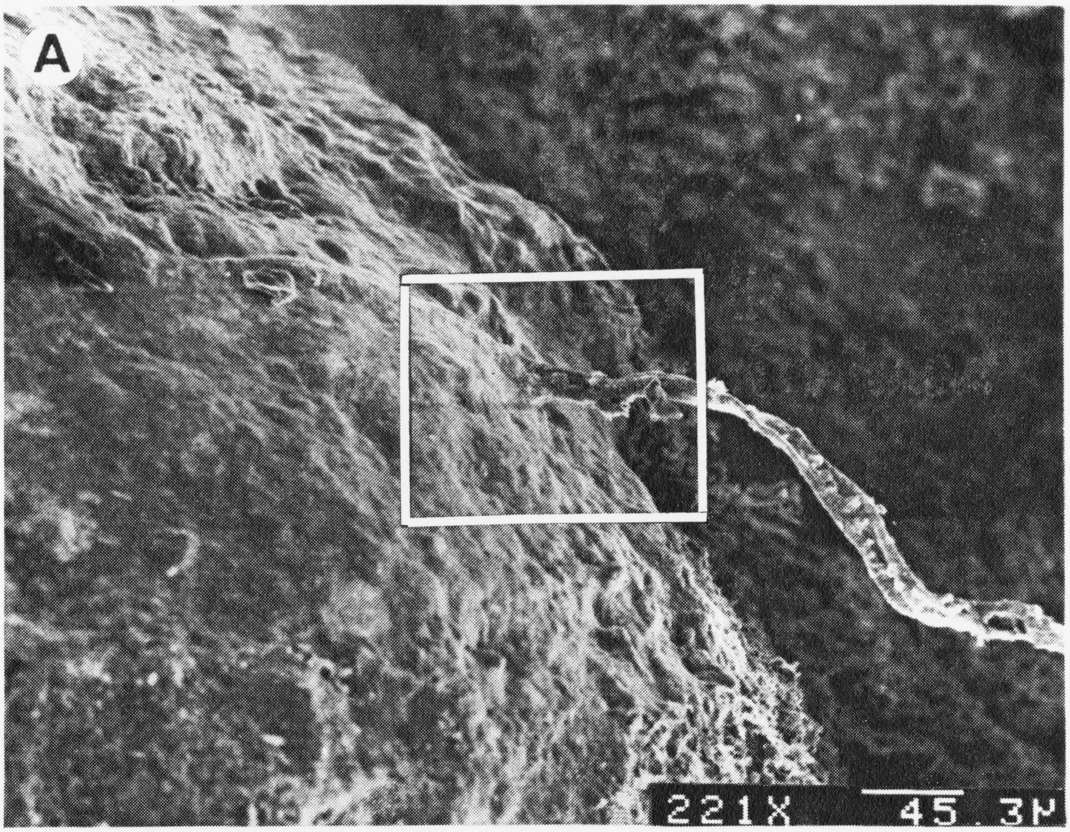
A
221X 45.3M


B
0.73KX 13.7M

The early silica cement could have protected the FPM from being destroyed at a later time.

As stated earlier, the transgressive lag sandstones did not have any recognizable surface textures. Lack of recognizable surface textures is attributed to pore filling illite, smectite and kaolinite clays, as well as quartz overgrowth cements. Kaolinite is observed as partial to complete pore filling clay in transgressive sandstones (Fig. 4.31). Energy dispersive X-Ray spectrum analysis (EDX) of the kaolinite (bottom of figure 4.31) yields nearly equal peak heights of Si and Al confirming the identification as kaolinite (Welton, 1984). The kaolinite occurs as face to face pseudohexagonal plates. Some of the plates appear to be embedded in the outer parts of the quartz overgrowths (Fig. 4.31) which indicates quartz and kaolinite coprecipitated in part (McBride, 1987) or alternatively quartz formed in part after kaolinite. The significance of this relationship as well as the relation to other diagenetic minerals in these sandstones was not established.

4.3.7 Summary of Petrographic and S.E.M. Investigation

1) Transgressive lag and uppershoreface sandstones are classified as litharenites. Sandstones of both depositional settings are similar with respect to average framework composition. Sandstones from interpreted channel fill deposits are classified as feldspathic arenites. The

Figure 4.31: Scanning electron micrograph of pseudohexagonal kaolinite (A) booklets surrounding quartz overgrowths (B). Lower photo is detailed view of area outlined in boxed area above. EDX analysis results of kaolinite (A) and quartz (B) are shown.

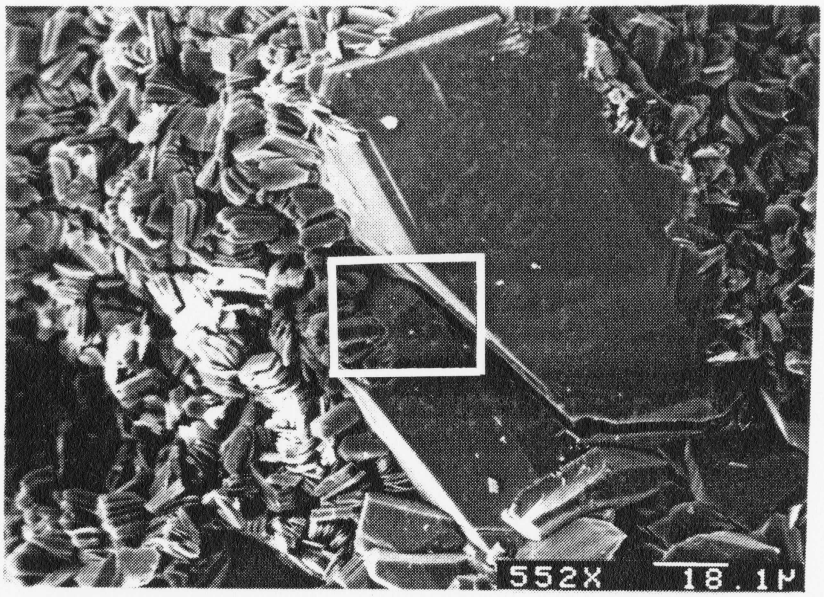
552X 18.1µ

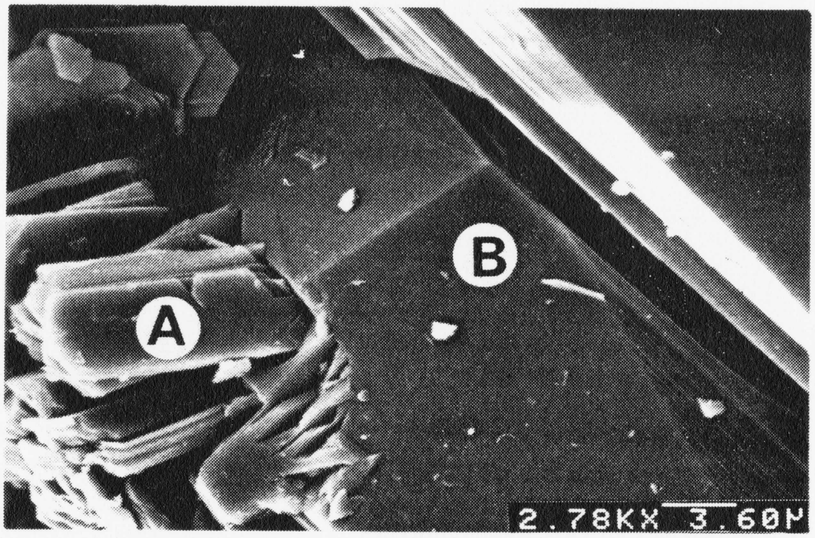
B
A
2.78KX 3.60µ

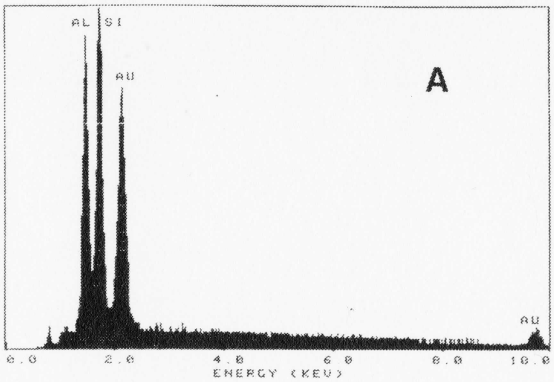
AL
SI
AU
A
AU
0.0
2.0
4.0
6.0
8.0
10.0
ENERGY (KEV)

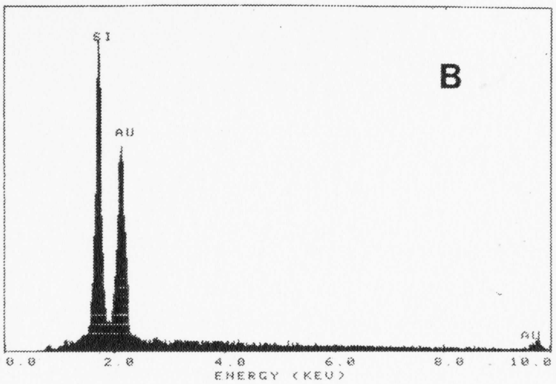
SI
AU
B
AU
0.0
2.0
4.0
6.0
8.0
10.0
ENERGY (KEV)

monocrystalline quartz to feldspar ratio in channel sandstones is approximately 1:1, while the transgressive lag and shoreface sandstone have a ratio of 4:1. Detrital feldspar is thought to have been preferentially destroyed within the latter two depositional environments as a result of marine reworking. The presence of altered and replaced feldspars suggests original framework compositions of sandstones may have been slightly different. Mechanical clay infiltration may have been an important process in the reduction of porosity in channel fill sandstones (possibly explaining why these sandstones are not reservoirs for oil) however, this is difficult to quantify because of diagenetic overprint.

2) Detrital quartz in all sandstones exhibits a range of colour under cathodoluminescence. Light blue to mauve violet varieties of quartz suggest high temperature plutonic quartz is more dominant than the brown variety produced from regional metamorphic rocks. This is a general observation and would require a CL point count study to accurately quantify this ratio.

Authigenic quartz under CL was nonluminescent which allowed several abraded quartz overgrowths to be distinguished from insitu ones. CL was useful for distinguishing feldspar grains from those which are significantly altered.

3) Surface texture analysis of sand grains was hampered by

the presence of authigenic minerals in the form of globular silica cement, clays, and quartz overgrowths. Minor evidence of fragmentary plant material was found in channel fill sandstones however, more analysis of the entire channel fill sequence is needed to confirm the presence of FPM's use as an indicator of depositional environment. No mechanical V's were observed on surfaces of grains in the transgressive lag sandstones. This may be attributed to lack of recognition and/or alteration and replacement of the grain surface.

Chapter 5 Bounding Surfaces, Allomembers and Facies Associations

5.1 Introduction

The purpose of this chapter is to describe the vertical facies relationships in terms of bounding surfaces, allomembers, and facies associations. Viking allomembers and erosion surfaces were introduced in chapter 2.2. The Viking allomembers are bounded by four regionally extensive bounding discontinuities termed VE1, VE2, VE3, and VE4. Bounding discontinuities are physically continuous surfaces that represent a hiatus or break in deposition, with or without accompanying erosion (NASCN, 1983, p.865). In this thesis VE3 and VE4 are interpreted as erosion surfaces. The VE1 and VE2 bounding discontinuities of Boreen and Walker (1991) are not found in the thesis study area. The Base Viking (BV) is interpreted as a correlative conformity.

Section 5.2 deals with the vertical facies relationships seen in core. Specific attention is placed on cores from the Harmattan East field because this is where most of the core control in the study is located. The vertical facies, of Viking nonmarine deposits southwest of the Harmattan East field is also discussed.

5.2 Vertical Facies Associations

The thickness of the Viking Formation within the study area ranges from 33 - 47 m (average 35 m in thickness). The Viking alloformation thickness ranges from 42 - 104 m, averaging 70 m in thickness across the study area. The Viking Alloformation at Harmattan East - Crossfield can be divided into three allomembers (A-B, D, and E) that are separated by correlative conformity BV, erosion surfaces VE3 and VE4 and at the top by BFS (datum). Figures 5.1 through to 5.4 show the reference wells for the different allomembers in the thesis study area. Graphic symbols relating to these figures are shown at the end of this chapter in figure 5.18.

Lateral facies changes within the allomembers necessitated more than one reference locality be chosen. Vertical facies associations at Harmattan East are shown in figures 5.1 and 5.2 while off field vertical facies associations of allomembers D and E are shown in figures 5.3 and 5.4.

The following discussion describes the bounding discontinuities and vertical facies associations in the three allomembers. Chapter 6 considers the lateral changes observed in the vertical sequence of facies within the study area.

5.2.1 Base Viking (BV)

In the thesis study area, the Base Viking is a

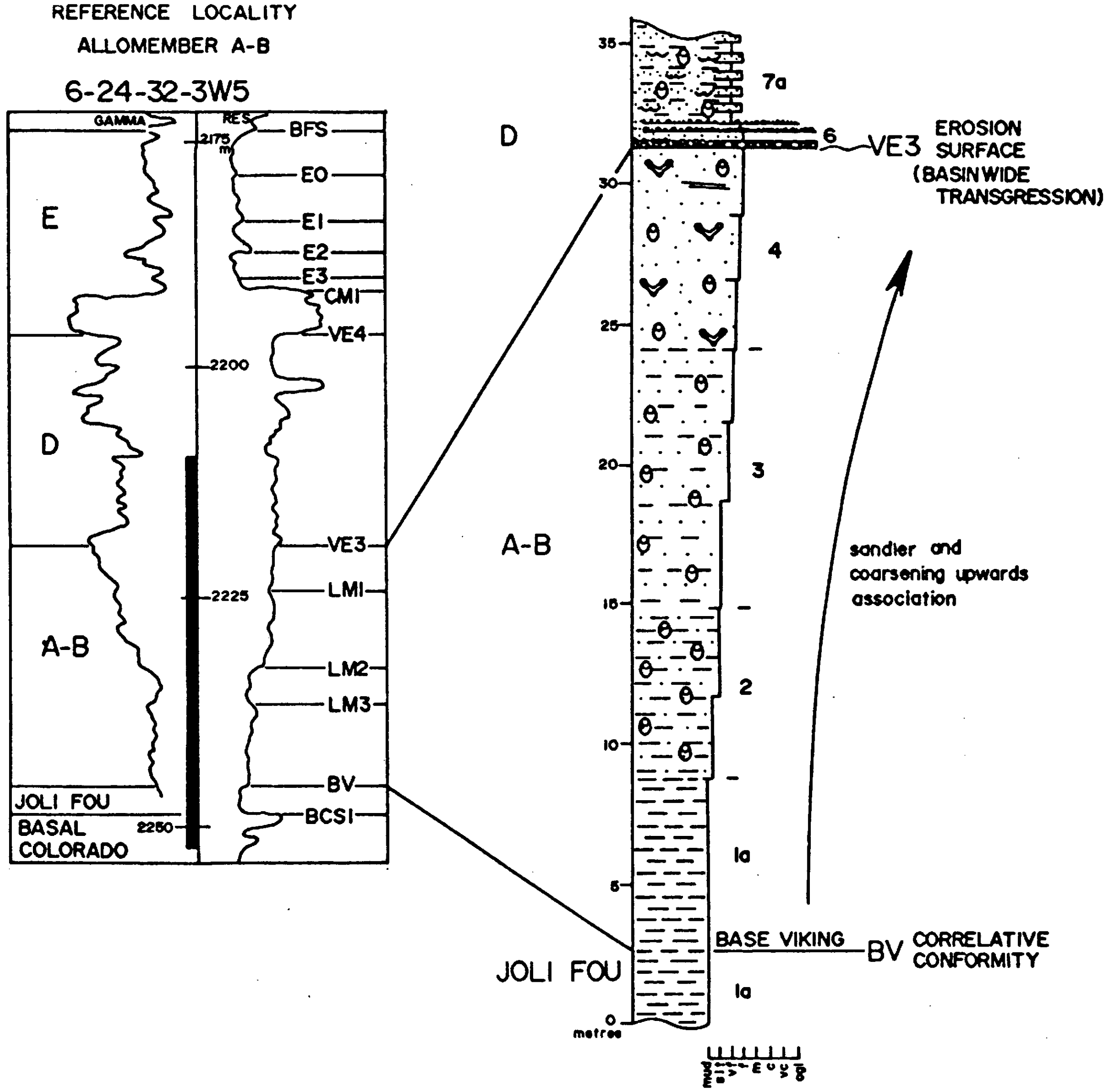

Figure 5.1. Reference locality core for allomember A-B at Harmattan East field. Logs and core from 6-24-32-3W5. Basal Colorado Sandstone and upper part of core (allomember D) are not shown. Core photos and discussion of allomember A-B can be found in following text.

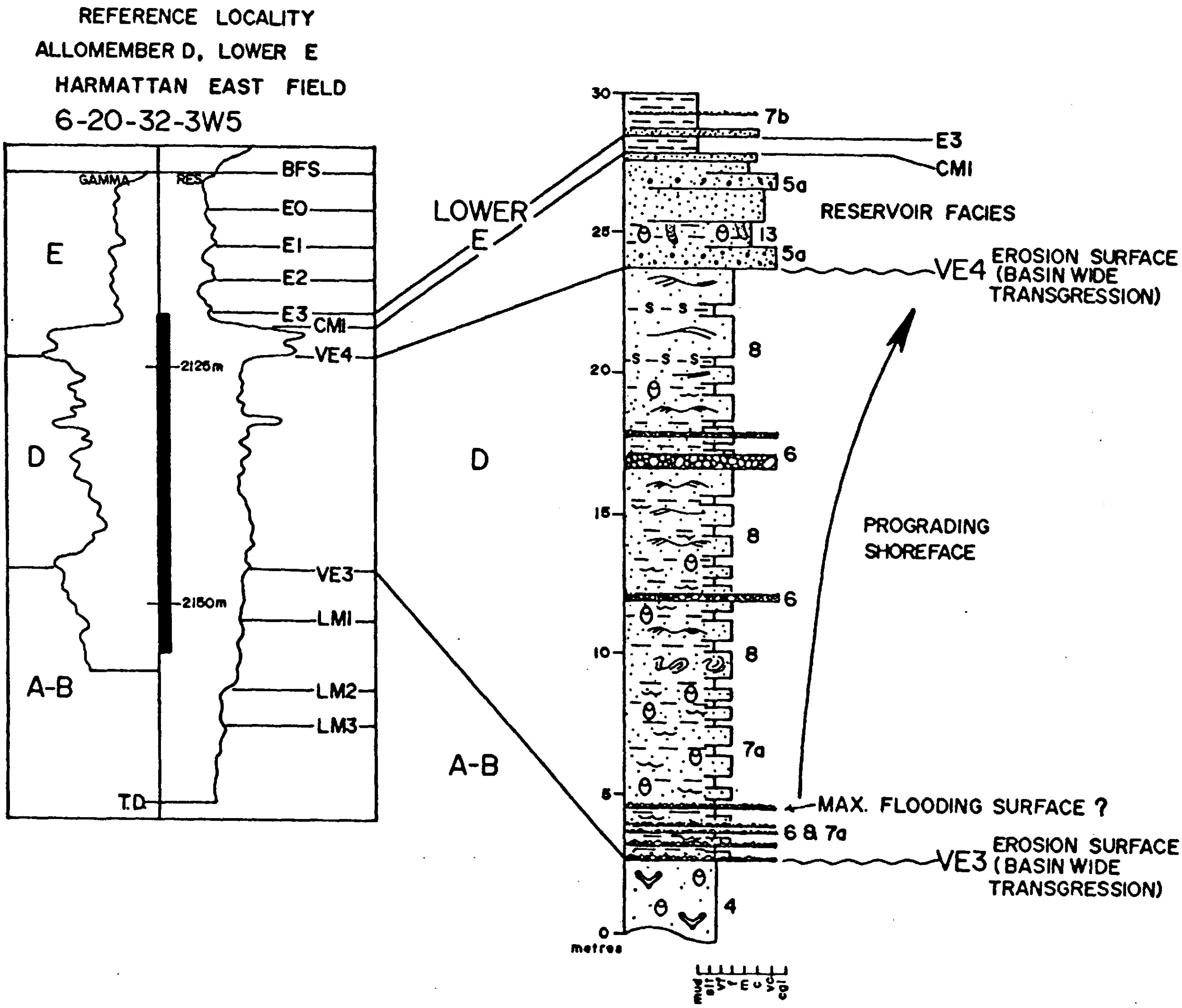

Figure 5.2. Reference locality core for allomember D and lower E (coarse sediment package) at Harmattan East field. Logs and core from 6-20-32-3W5. Lower part of core corresponding to allomember A-B is not shown. Core photos and discussion of allomembers in this well can be found in following text.

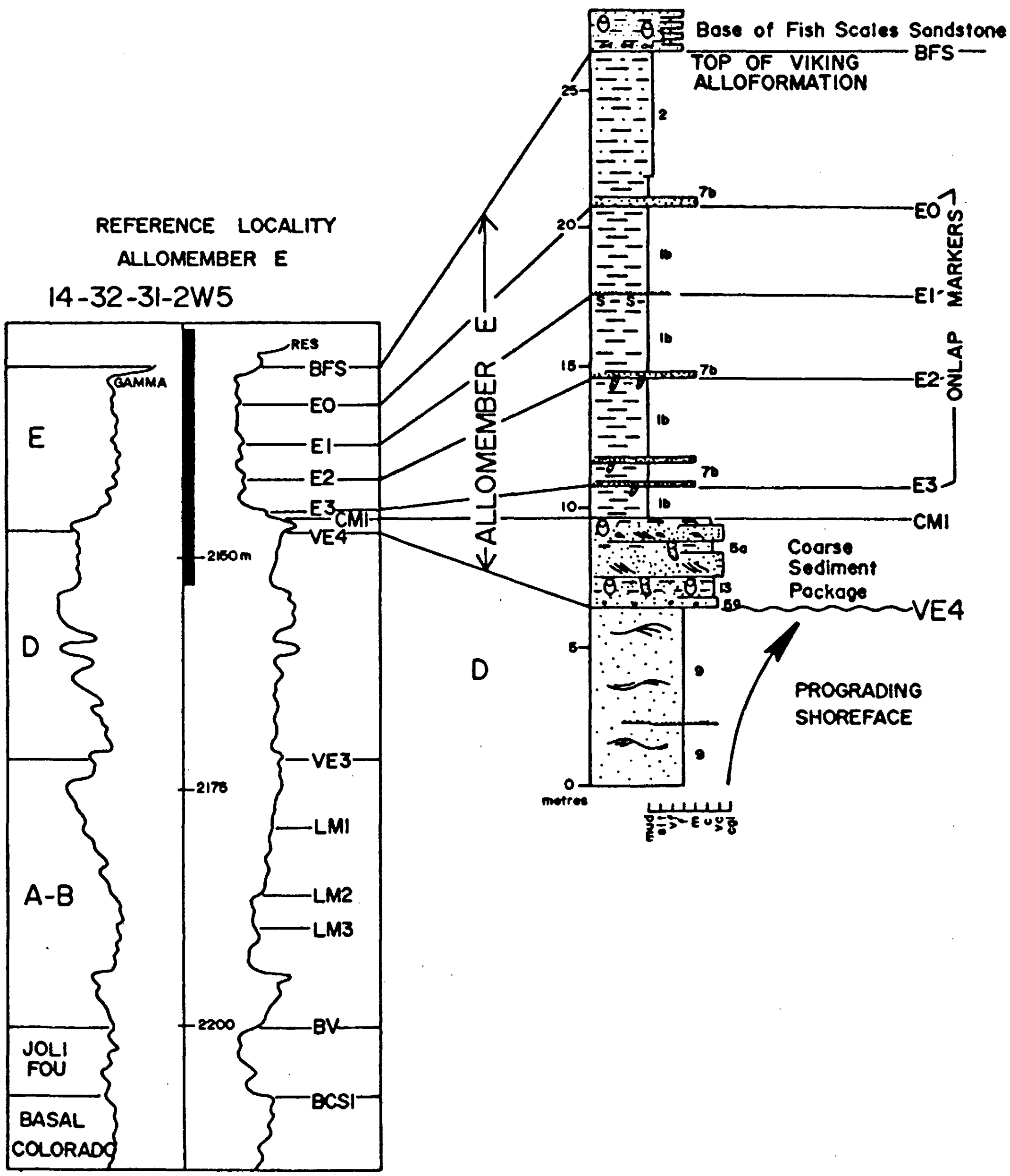

Figure 5.3. Reference locality for allomember E. Logs and core from 14-32-31-2W5. Upper part of core (Base of Fish Scales Sandstone) is not shown. Core photos and discussion of allomember E from this well is found in following text.

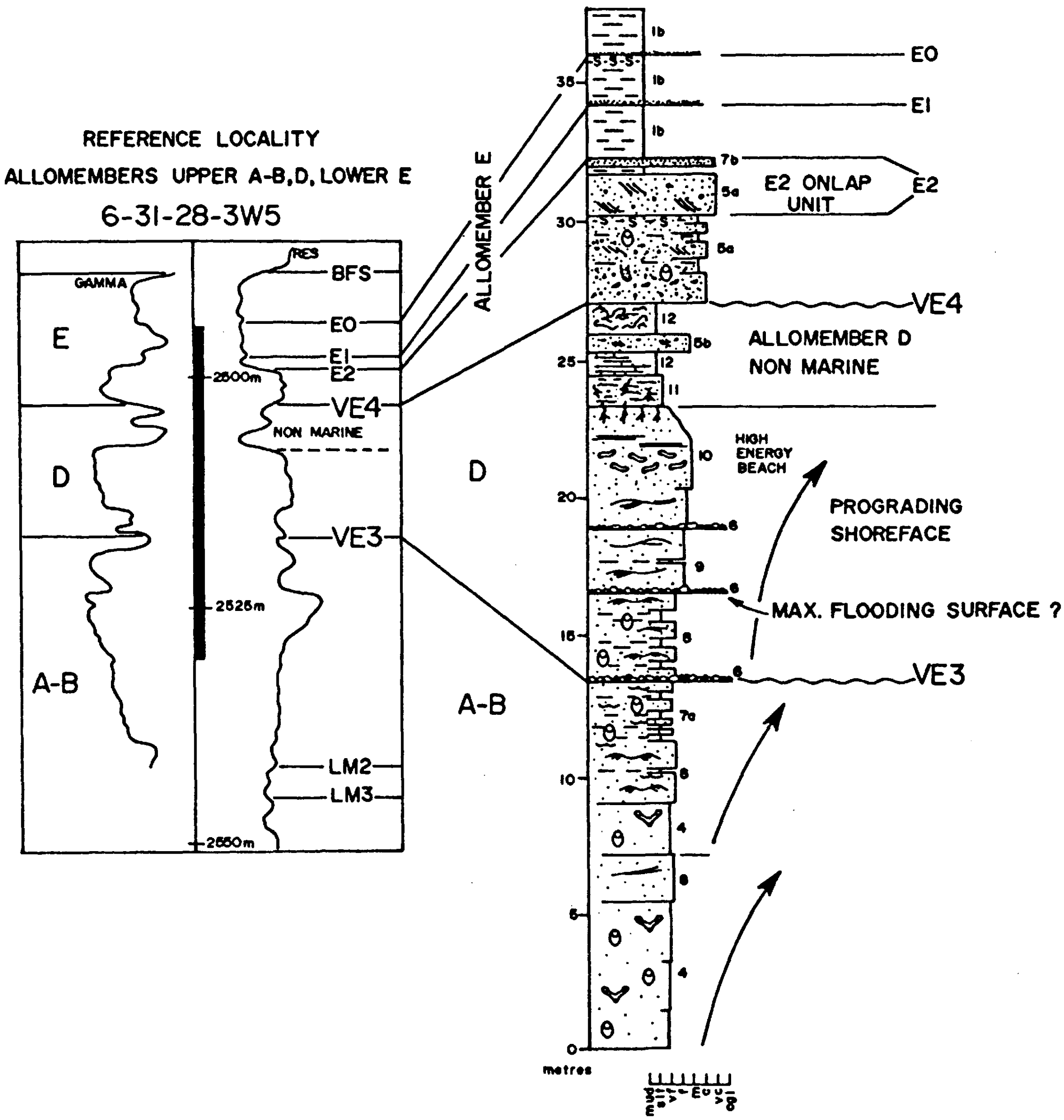

Figure 5.4. Reference locality for allomember A-B, D and lower E (off field, non-marine section). Logs and core from 6-31-28-3W5. Core photos of allomember D (upper shore face and non-marine facies) found in following text.

difficult pick to make both in core and on well logs. Only one core (6-24-32-3W5) penetrated the entire basal portion of the Viking Formation (Fig. 5.5). In the thesis area, BV is interpreted as a correlative conformity which marks the stratigraphic base of the Viking Alloformation.

In the 6-24-32-3W5 core, the BV log marker is underlain and overlain by facies 1a. Correlations within the study area suggest that allomember A-B either overlies the Joli Fou Formation and/or the Basal Colorado Sandstone.

5.2.2 Allomember A-B

A detailed study of allomember A-B is not possible within the study area, because only one core has penetrated the entire interval. Despite the lack of core control, a description of the vertical facies associations of this allomember is still possible. Allomember A-B directly overlies the BV correlative conformity and is sharply truncated at the top by the VE3 erosion surface (Fig. 5.5). Allomember A-B ranges from 19 - 49 m, averaging 30.5 m in thickness. The base of the allomember is picked using well logs (Fig 5.1). In core, the BV "pick" corresponds to a dark mudstone that is indistinguishable from the underlying dark shales of the Joli Fou Formation. In the southern area of the study, the allomember may overlie Basal Colorado Sandstones, or alternatively Joli Fou equivalent sands.

No discernable cycles are recognizable on well logs

Figure 5.5.

(next 8 pages) Basal Colorado Sandstone to VE3 contact. Well 6-24-32-3W5 (base at 2251.2m). Illustrates the sandier upwards sucession of allomember A-B in a continuous cored sequence. The following vertical succession can be seen. Basal Colorado sandstones sharply overlain by dark mudstones of the Joli Fou Formation, the BV contact gradationally overlain by facies 1a, 2, 3, and 4 of allomember A-B, and the sharp VE3 contact erosively overlain by conglomerate (facies 6) and burrowed laminated sandstone mudstone (facies 7a) of allomember D. Core is 10 cm in diameter. Scale bar is 15 cm long.

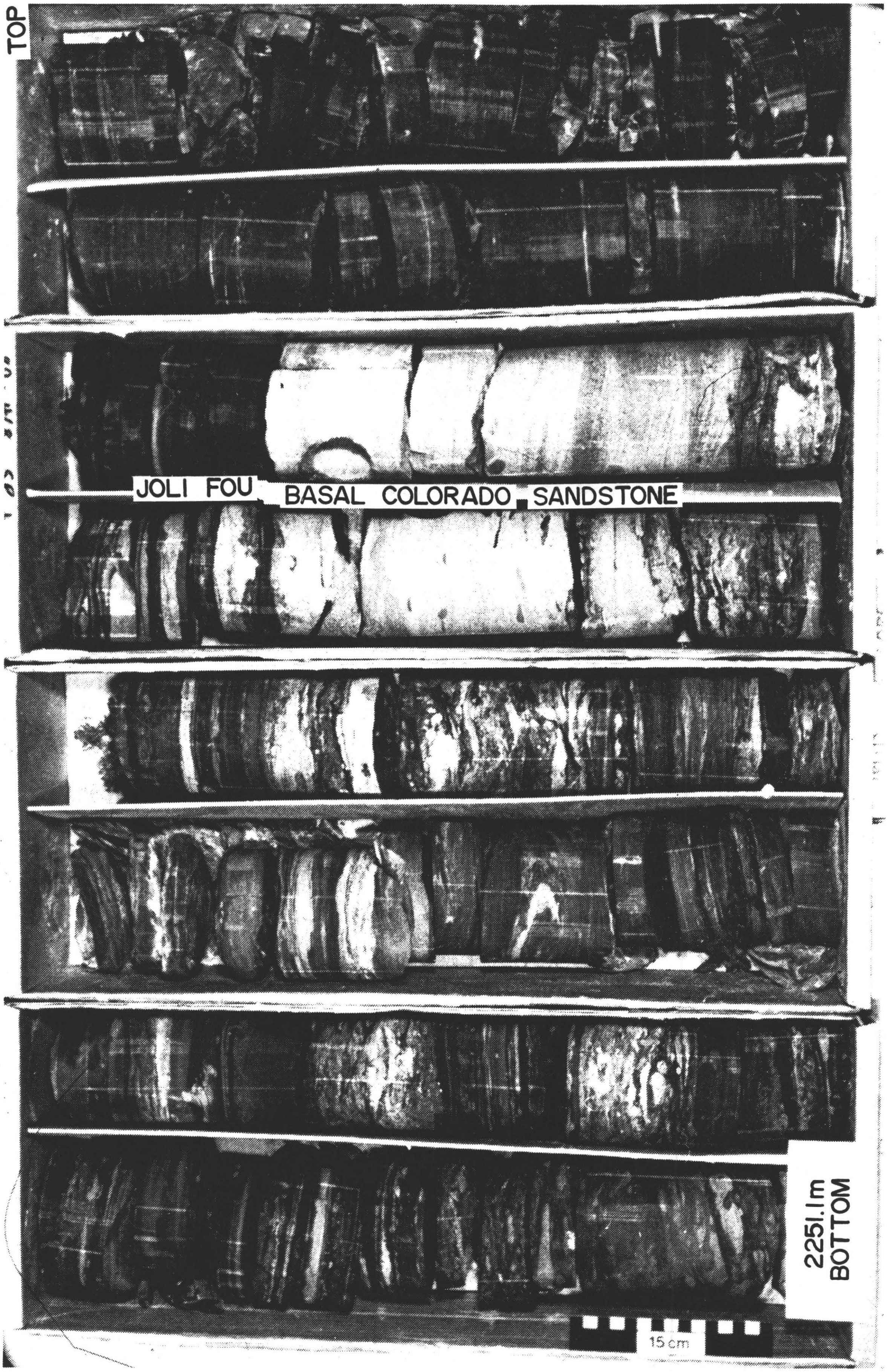
TOP
JOLI FOU
BASAL COLORADO SANDSTONE
2251.1m
BOTTOM
15 cm

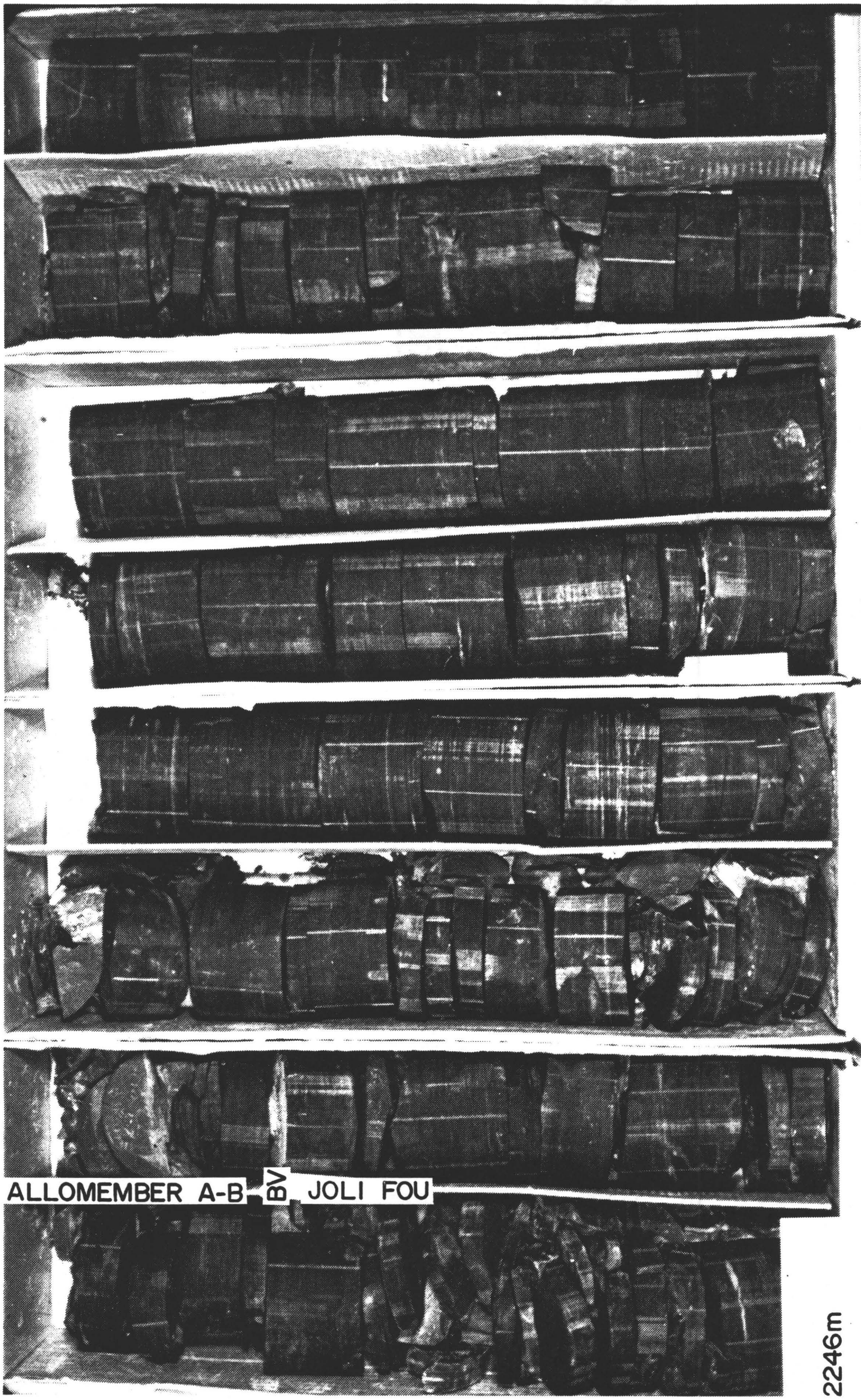
ALLOMEMBER A-B
BV
JOLI FOU
2246m

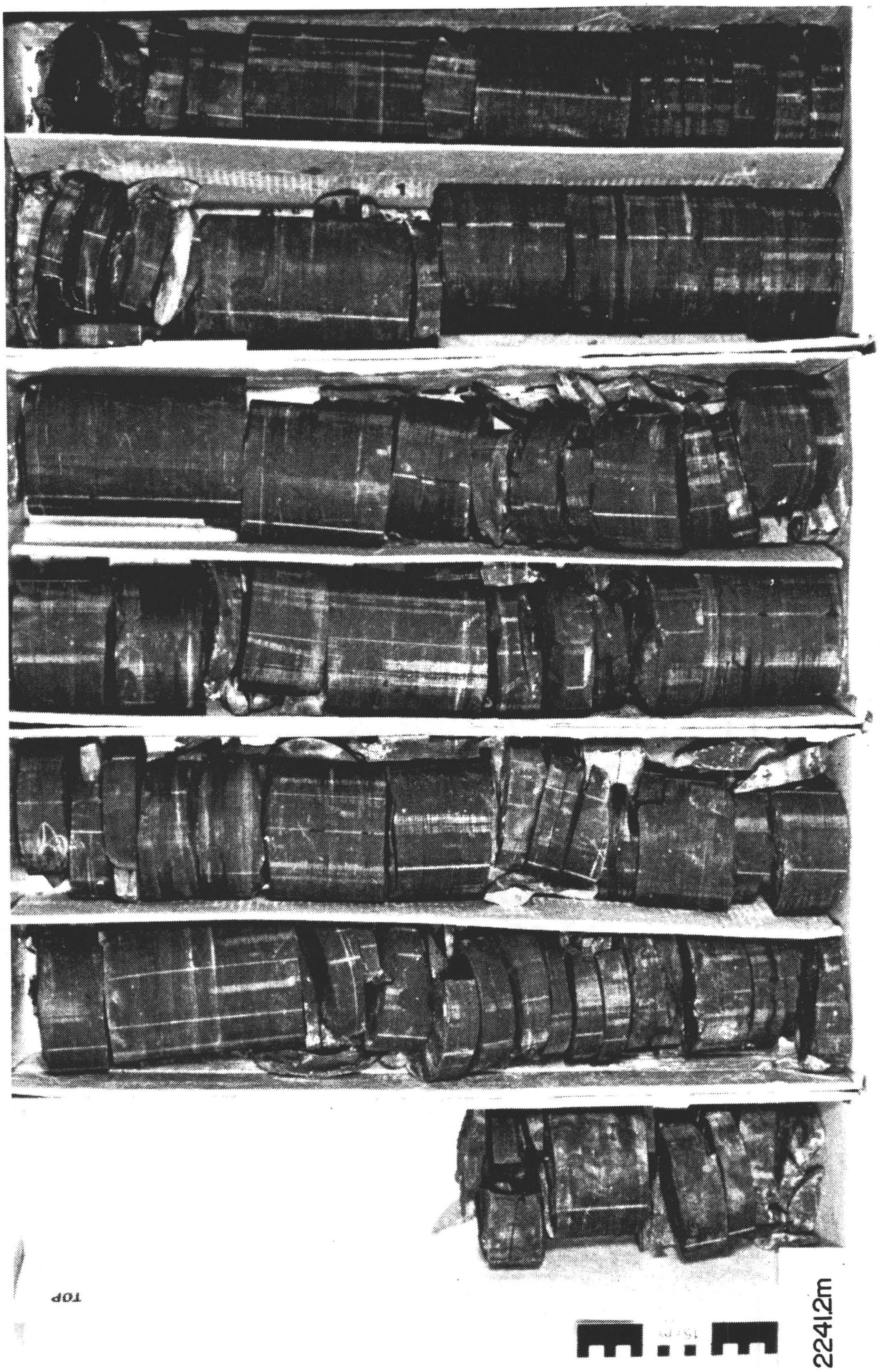
TOP
2241.2m

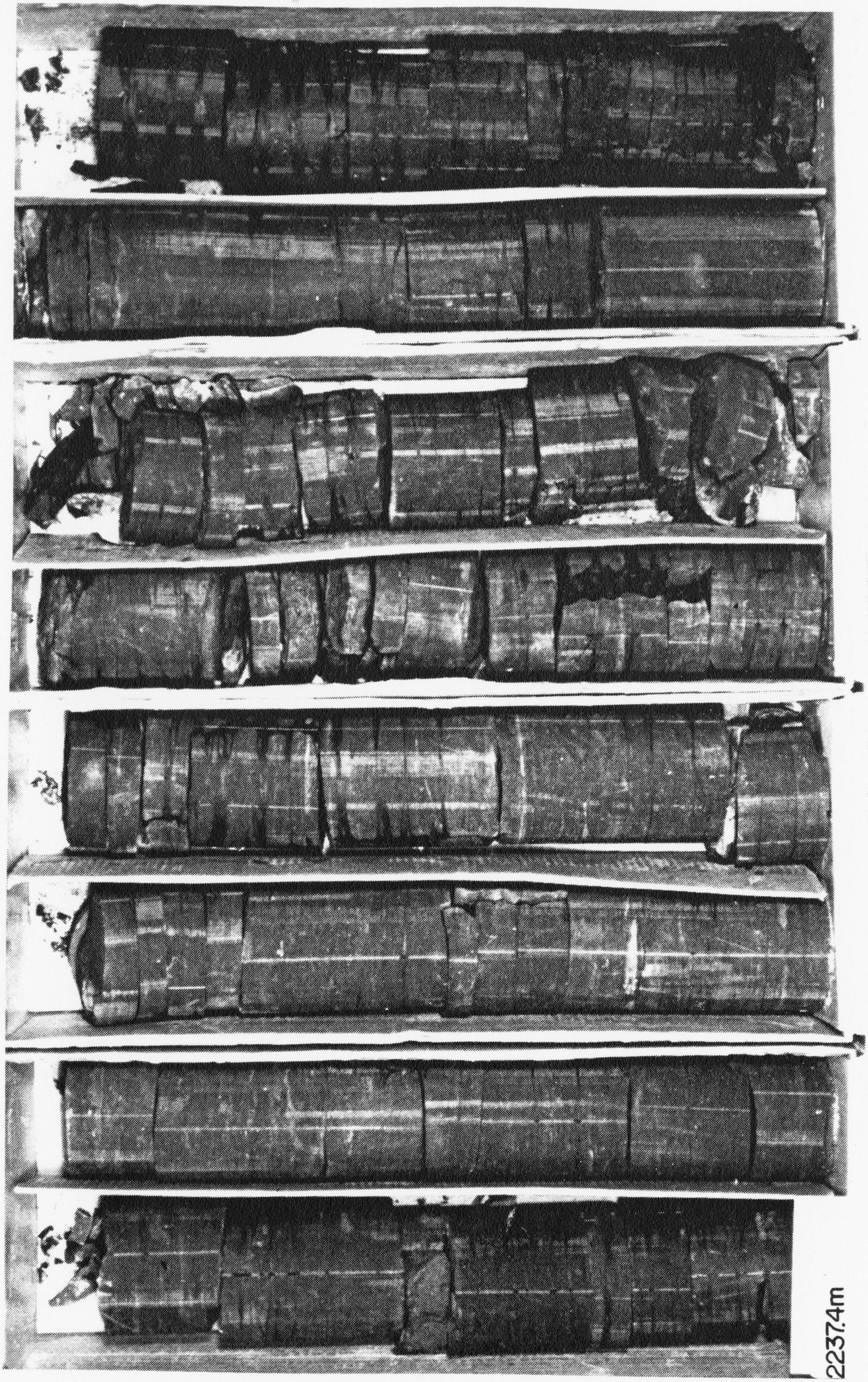
2237.4m

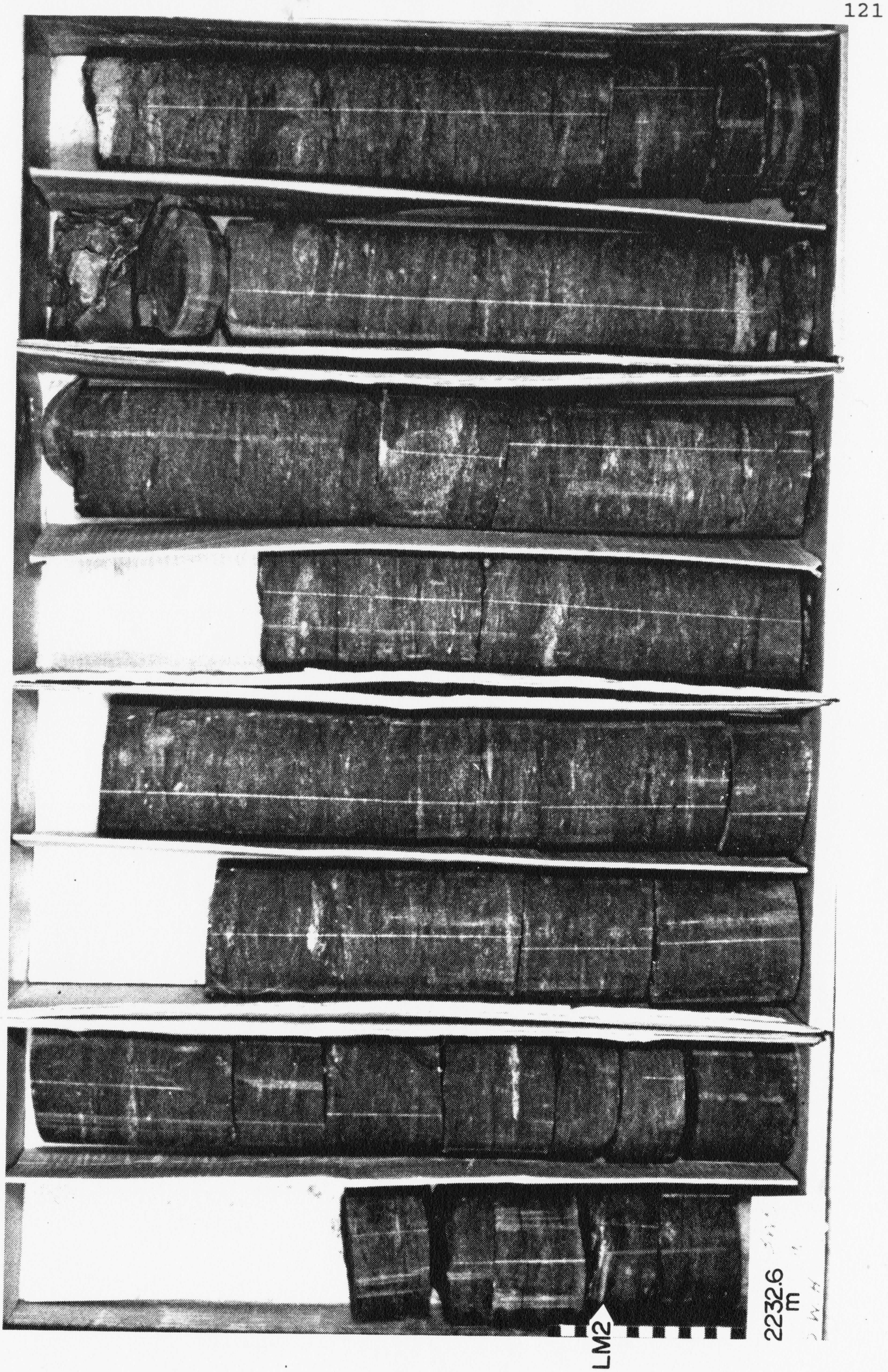
2232.6 m
LM2

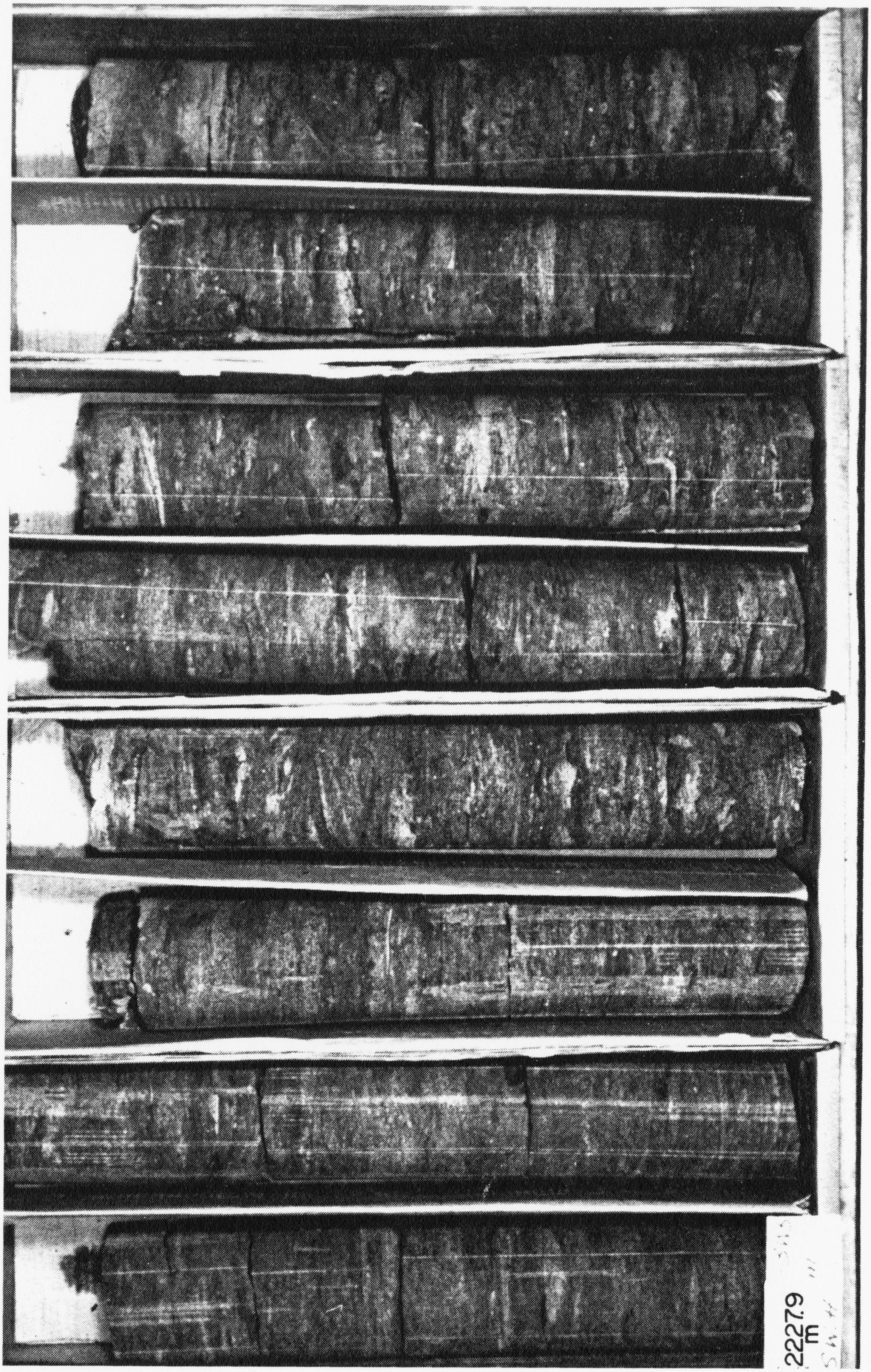
22279
m


2223.5 m


ALLOMEMBER A-B
VE3
ALLOMEMBER D
2218.8 m

through the lower portion of allomember A-B, however in the reference locality 6-24-32-3W5 core a very gradual siltier upwards trend occurs from facies 1a below into facies 2 above (Fig 5.5). Very thin bentonite beds (< 2mm thick) may correspond to the LM2 and LM3 log markers shown in figure 5.1. In core, these log markers occur at a gradational change between muddy siltstones (facies 2) below and sandy siltstones (facies 3) above.

Figure 5.5 shows that allomember A-B (above LM2) consists of a single sandier and coarsening-upwards sequence that is sharply truncated at the top by the VE3 surface. The vertical facies association above LM2 consists of facies 3 (sandy siltstones) passing gradationally upwards into facies 4 (pale sandstones). Well log marker LM1 in figure 5.1 corresponds to this change in facies.

The vertical facies associations in allomember A-B are more complicated southwest of Harmattan East (refer to reference locality core in figure 5.4). Several cores (5-14-28-4W5, 6-31-28-3W5), show facies 4 interbedded with facies 7a (fine grained burrowed laminated sandstone-mudstone) and facies 8 (interbedded sandstone - mudstone) (Fig. 5.6). The VE3 surface is harder to pick in cores located in the southwest part of the study. The thin conglomerate interval in figure 5.6 represents the VE3 "pick" established from well log correlations tied to the 6-24-32-3W5 core. An alternative interpretation for the VE3 surface

Figure 5.6.

(next 4 pages) Allomember A-B to allomember E. Well 6-31-28-3W5 (base at 2530m). Illustrates the sandier and more complex nature of facies in allomember A-B and D preserved in the southern part of the study area. The following vertical sucession can be seen. Interbedding of facies 4, 7a, and 8 of allomember A-B as two sandier upwards cycles truncated at the top by the VE3 contact (4 cm thick conglomerate bed), which in turn is overlain by facies 8,9, and 10 of allomember D. Core is 8.75 cm in diameter.

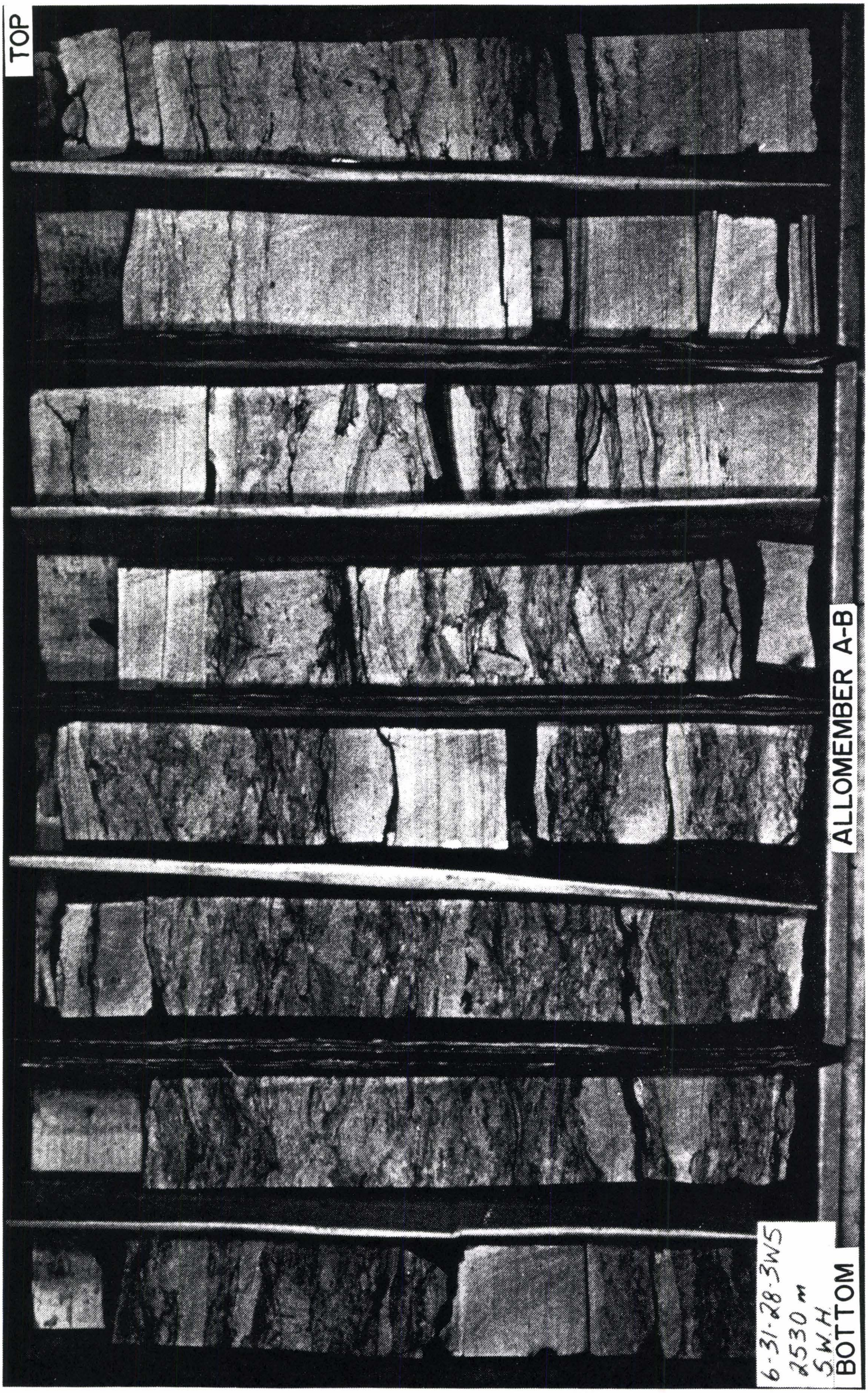
TOP
ALLOMEMBER A-B
BOTTOM
6-31-28-3W5
2530 m
S.W.H.


ALLOMEMBER A-B
31-28-3W5
525.6m
W.H


ALLOMEMBER A-B
31-28-3W5
521.0m

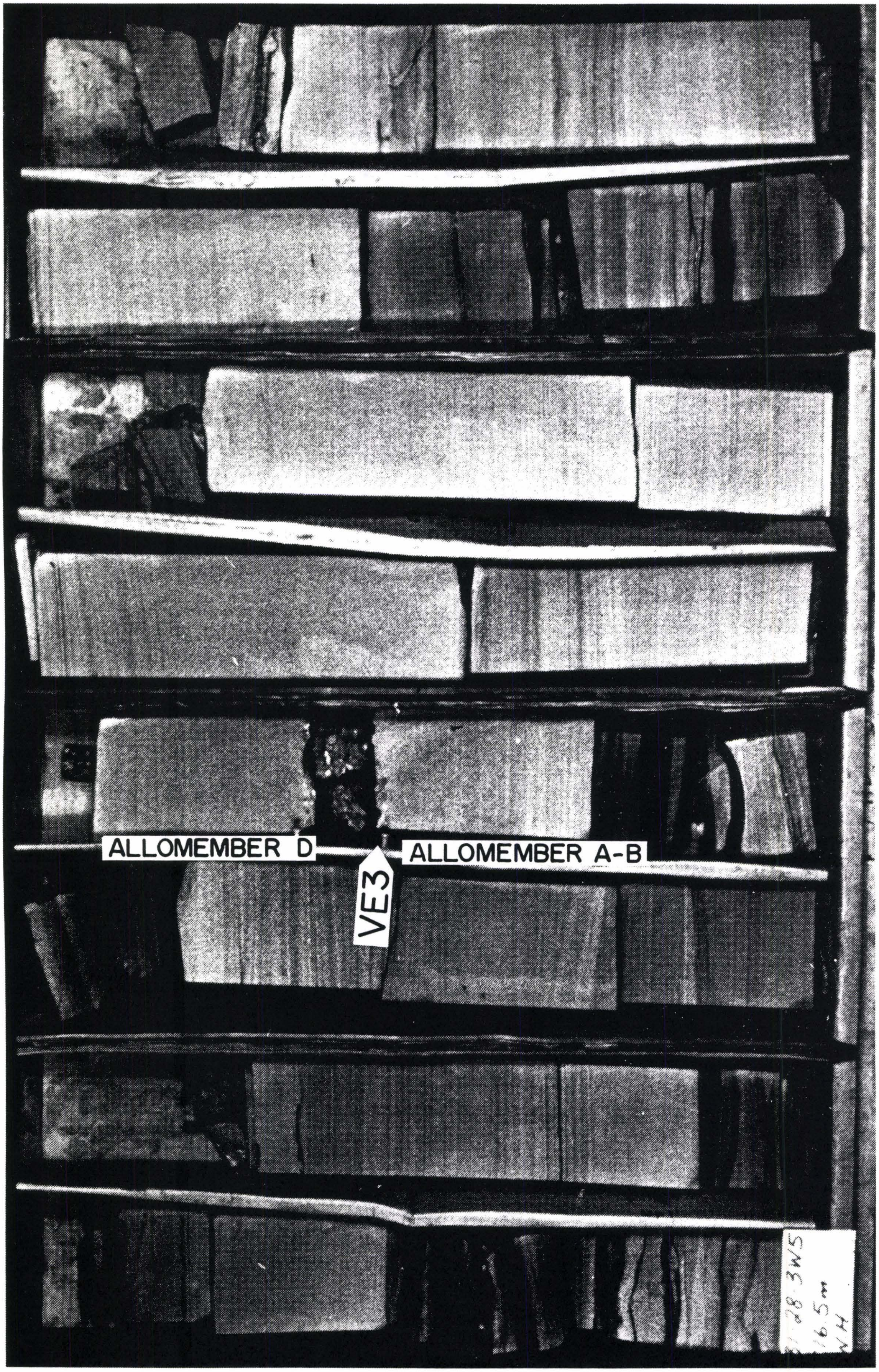
ALLOMEMBER D
ALLOMEMBER A-B
VE3

in figure 5.6 could be that it represents the base of a "storm event", and the VE3 erosion surface actually occurs somewhere below this "event". Regional well log correlations in Chapter 6 are used to show the relationship of the VE3 surface in the 6-24-32-3W5 well to the core shown in figure 5.6.

In general, allomember A-B appears to become sandier, coarser, and less bioturbated upwards. This overall trend is more pronounced in the vertical facies associations south and west of the Harmattan East field.

5.2.3 VE3 Erosion Surface

Allomember A-B is overlain by the VE3 erosion surface which in turn is overlain by allomember D (Fig. 5.2). The VE3 contact in the Harmattan East field is characterized in core by a sharp facies change from facies 4 below to either facies 7a (fine grained, burrowed laminated mudstone-sandstone), or facies 6 (conglomerate) above (Fig. 5.7). The conglomerates that rest on the VE3 surface normally occur as thin beds (approx. 5 cm thick) interbedded with facies 7a, and are usually found within the first metre above the VE3 contact. In one core (14-13-32-3W5) a 45 cm thick conglomerate was observed on the VE3 surface (Fig. 5.8). On the gamma ray well log, the VE3 contact is picked at the maximum deflection to the left that occurs above the LM1 marker (Fig. 5.2).

Figure 5.7.

VE3 contact

a) Gradational contact between facies 4 (allomember A-B) and facies 7a (allomember D) above. Note the granule at top right of photo which marks the VE3 contact. Well 6-20-32-3W5; Depth 2145m; Scale bar is 3 cm long.

b) Sharp contact between facies 4 (allomember A-B) and facies 6 (massive conglomerate) of allomember D. Well 14-13-32-3W5; Depth 2208.1m; Scale bar is 3 cm long.

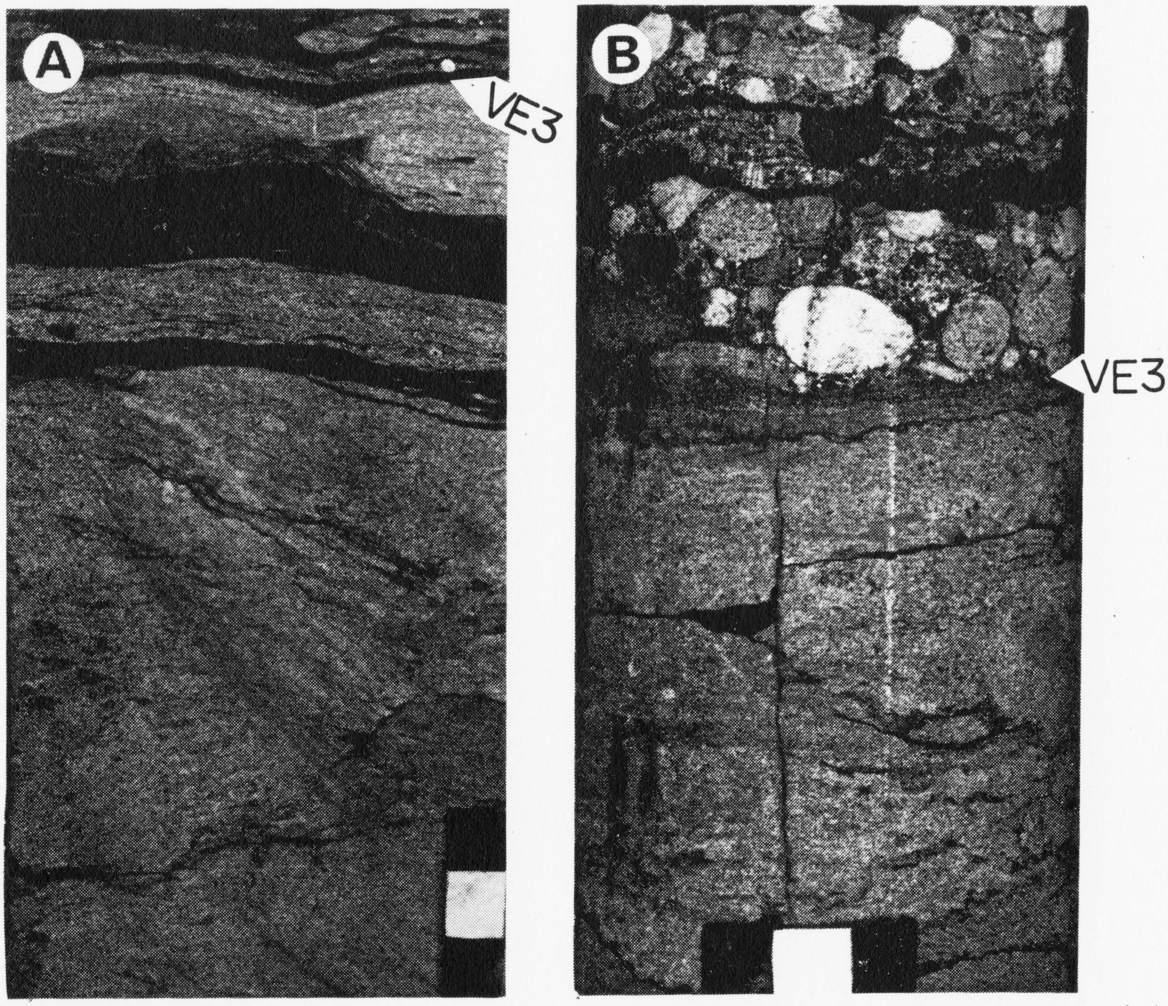
A
VE3
B
VE3

Figure 5.8.

Allomember A-B, VE3, and allomember D. Well 14-13-32-3W5 (base at 2210 m). Pale sandstones (facies 4) sharply overlain by VE3 contact. A 45 cm thick conglomerate and fine grained, burrowed laminated mudstone-sandstone (facies 7a) of allomember D rest on the VE3 surface. Core is 8.75 cm in diameter.

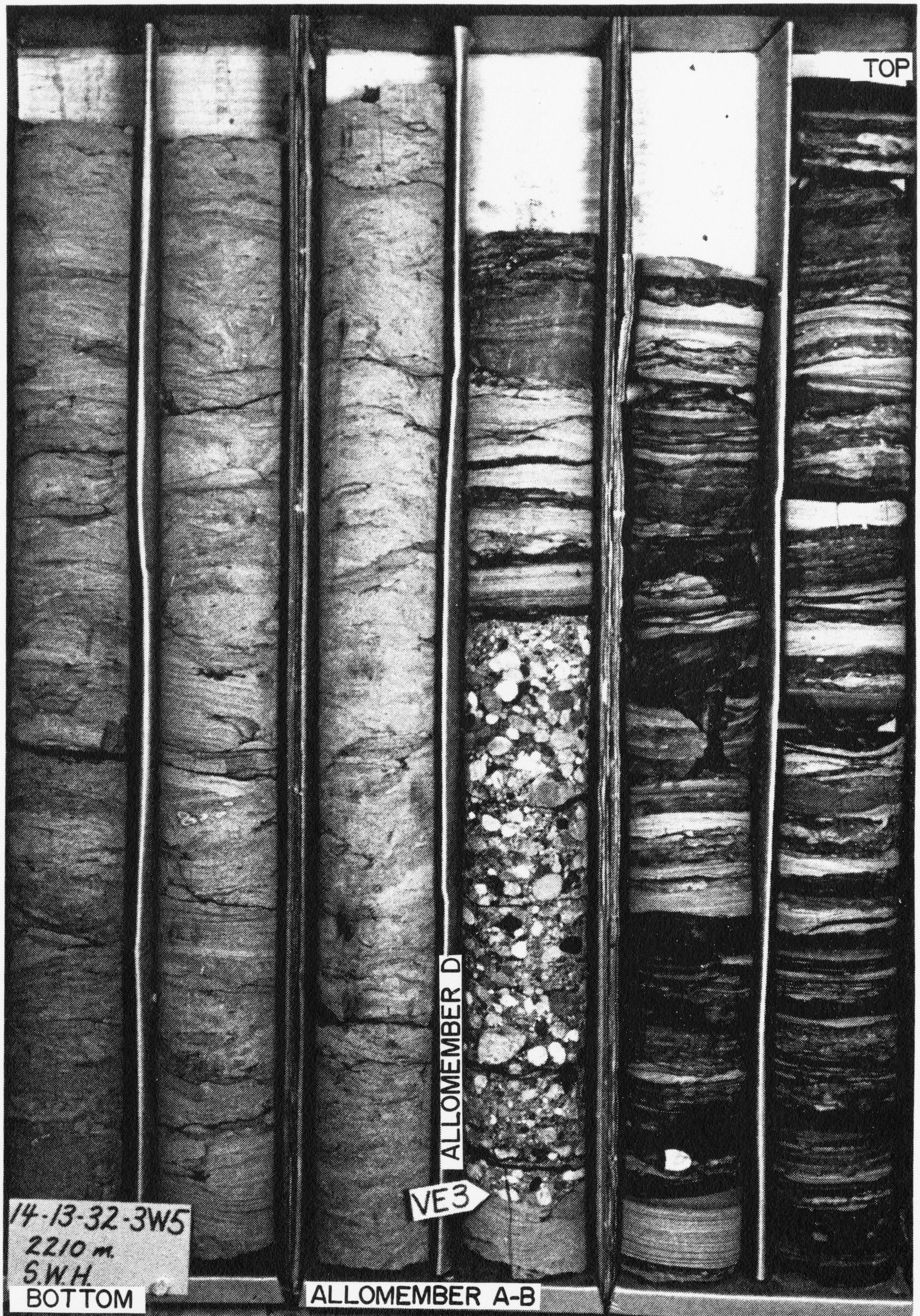
TOP
ALLOMEMBER D
VE3
14-13-32-3W5
2210 m.
S.W.H.
BOTTOM
ALLOMEMBER A-B

5.2.4 Allomember D

Allomember D lies directly on the VE3 surface and is sharply truncated at the top by VE4 (Fig. 5.2 and 5.4). This allomember is the main progradational shoreface package of the Viking Formation, and ranges from 14 - 29 m, averaging 26.5 m in thickness. Most cores in the study area include all, or the upper portion of the sediments of allomember D, and as a result the vertical facies changes within this allomember are better understood than those of allomember A-B below.

Figure 5.9 shows core photographs of a typical vertical sequence of four facies through allomember D at Harmattan East field. In most cases the facies occur in the ascending order 6, 7a, 8, and 9. Conglomerates of facies 6 usually directly overlie VE3 and may be up to 45 cm thick (Fig. 5.8).

Facies 7a gradationally overlies facies 6, and is generally confined to the lower part of allomember E. The sandstone beds in facies 7a usually become thicker and less bioturbated upwards. Occasionally facies 7a is seen in core truncated at the top by a thin (< 5 cm thick) chert pebble bed. This pebble bed may represent a maximum flooding surface associated with the conglomeratic lag that overlies VE3 (Fig. 5.8).

Upwards, facies 7a gradationally passes into facies 8 which in turn gradationally passes into facies 9. Facies

Figure 5.9.

(next 6 pages) (top of core is at upper left of each photo) Allomember A-B, VE3, allomember D, VE4, and allomember E. Well 6-20-32-3W5 (base at 2149.7m). Illustrates the sandier upwards sucession of allomember D in a continuous cored sequence. The following vertical sucession can be seen. Pale sandstone (allomember A-B) sharply truncated at the top by the VE3 surface which is then overlain by facies 6 and 7a, in turn gradationally passing into facies 8 and 9, all of allomember D. Note how the sandstone beds above the VE3 surface become thicker and less bioturbated as you move upwards in the section. Facies 6 commonly occurs as an interbedded facies in the upper part of allomember D. In this sequence of photos allomember D is truncated at the top by the VE4 surface and deposits of allomember E. Core is 8.75 cm in diameter. Scale bar is 15 cm long.


TOP
ALLOMEMBER D
VE3
ALLOMEMBER A-B
15 cm
6-20-32-2W5
2149.7m
S.W.H
BOTTOM

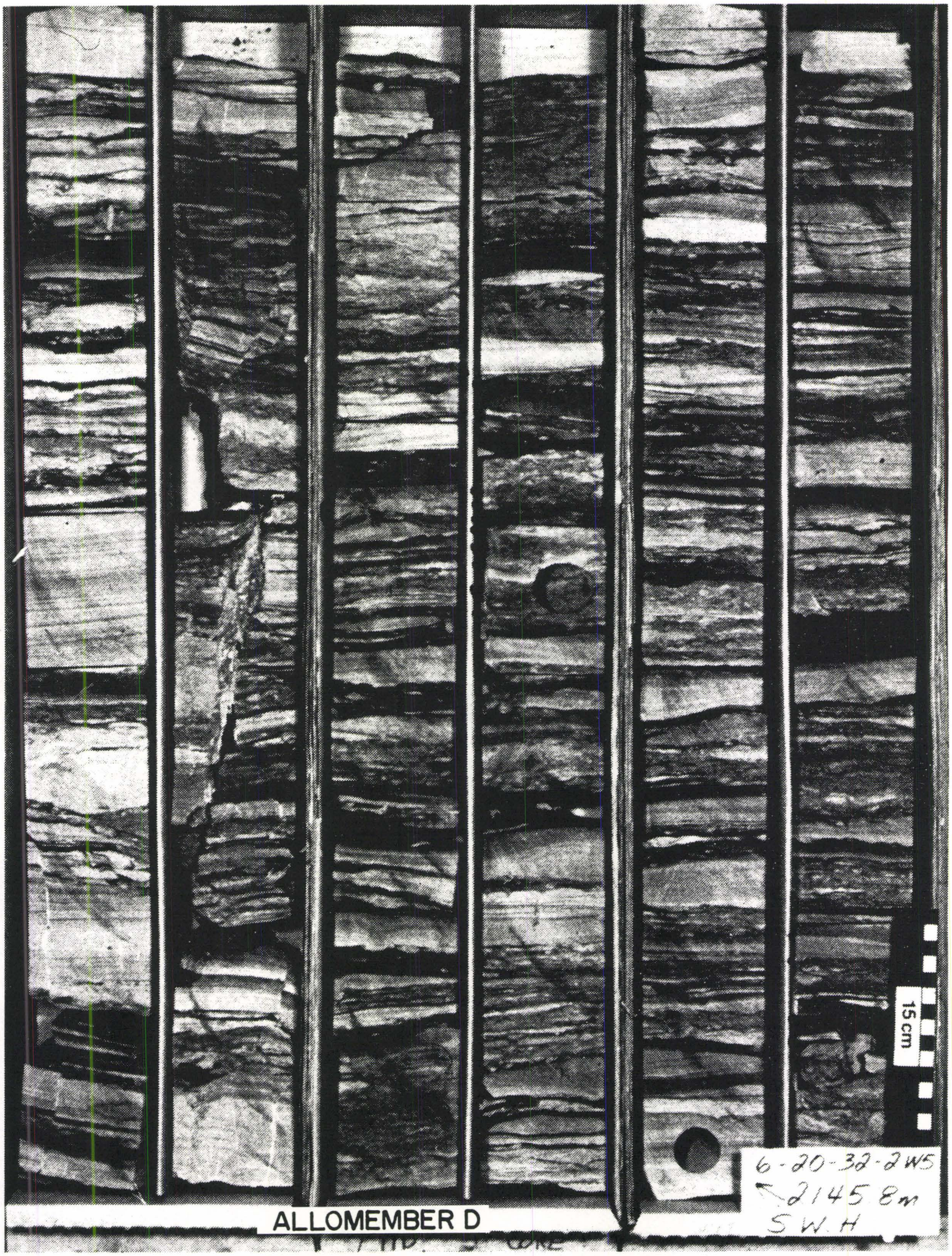
15cm
6-20-32-2W5
2145.8m
S.W.H
ALLOMEMBER D


15 cm
ALLOMEMBER D
6-20-32-2W5
← 2140.9 m
S.W.H.

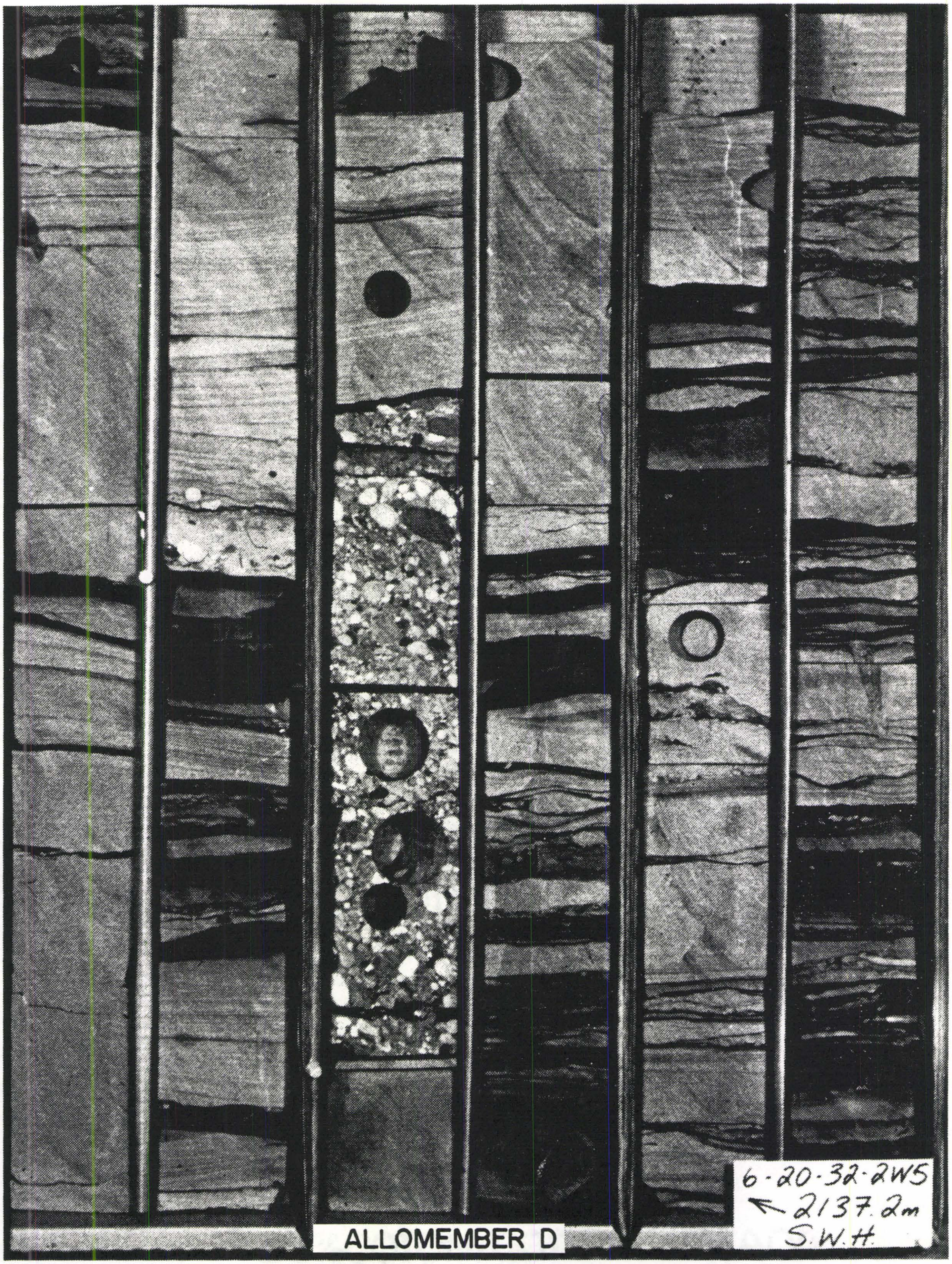
6-20-32-2W5
2137.2m
S.W.H.
ALLOMEMBER D

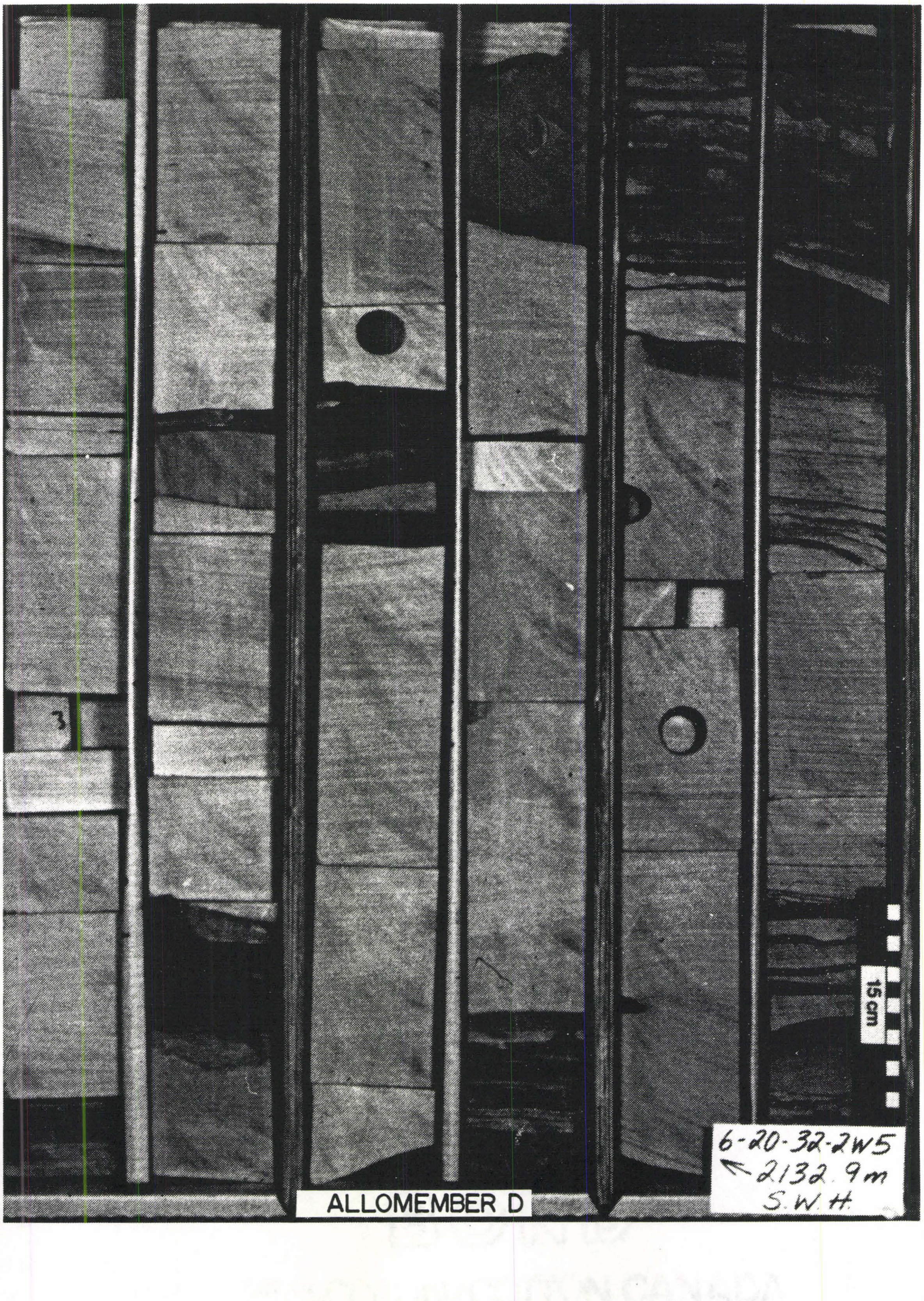
ALLOMEMBER D
15cm
6-20-32-2W5
2132.9m
S.W.H.


ALLOMEMBER E
VE4
ALLOMEMBER D
15cm
6-20-32-2W5
2128 6m
S.W.H.

6 commonly occurs as an interbedded facies in the upper part of allomember D. The gamma ray well log response in upper parts of allomember D often shows a marked change from facies 7a below into facies 8 above. This change is shown as a deflection to the left that records the first presence of thicker sandstone beds (ie. sandier upwards log response) (Fig. 5.2).

Figure 5.10 shows core photographs of a typical vertical facies sequence through the upper part of allomember D south of Harmattan East. In southern parts of the study area, the sediments form a coarsening upwards sequence that contains a similar vertical facies association to that previously discussed. Facies 9 is often overlain by facies 10 (parallel laminated and crossbedded sandstone) which in turn is sharply overlain by the nonmarine facies, 11 and 12. Sandstones of facies 9 and 10 are non-productive in the southern part of the study area and are not stratigraphically equivalent to the oil producing reservoir sands of the Viking Formation at Harmattan East. The non-marine facies become thicker to the south and west (towards the disturbed belt) and range from < 1 m to 8 m in thickness.

Facies 5b (mudstone-siltstone clast, crossbedded sandstone) was observed in three cores located south and west of the Harmattan East field (7-28-31-4W5, 2-14-33-5W5, and 9-22-33-5W5). In the 9-22-33-5W5 core, facies 5b sharply overlies facies 9 and is truncated abruptly at the top by the

Figure 5.10.

(next 4 pages) Upper part of allomember D. Well 8-5-30-4W5 (base at 2601.8 m). Illustrates the coarsening upwards sucession of the upper part of allomember D that is often preserved south and west of the Harmattan East field. The following vertical sucession can be seen. Facies 9 (thick bedded, nonbioturbated sandstone) is sharply overlain by facies 10 which is then sharply overlain by nonmarine facies 11 and 12. Allomember D nonmarine deposits are sharply truncated by the VE4 surface and deposits of allomember E. Core is 10 cm in diameter. Scale bar is 15 cm long.

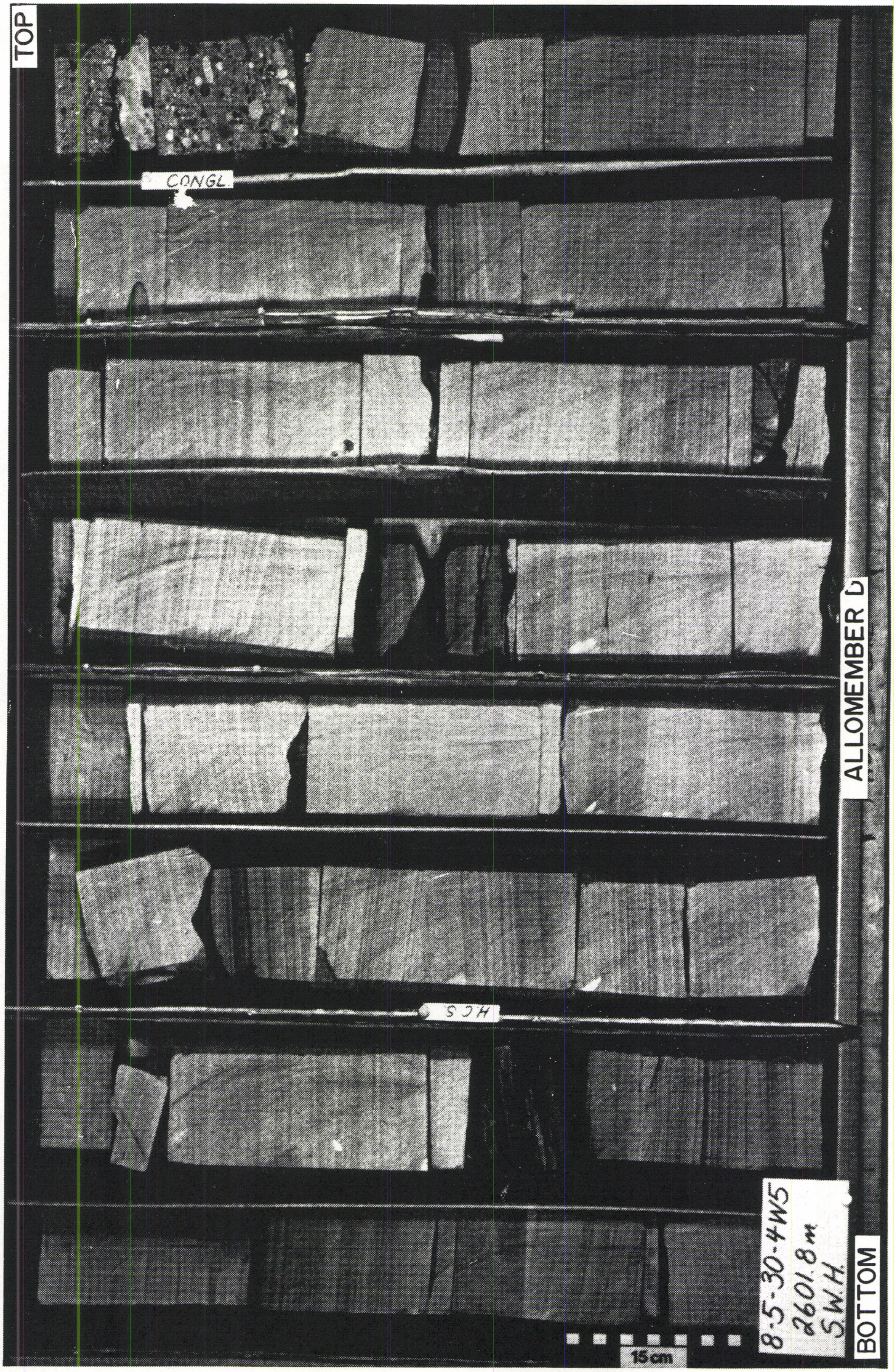
TOP
CONGL.
HCS
ALLOMEMBER D
8-5-30-4W5
2601.8m
S.W.H.
15cm
BOTTOM


MED SAND
FINE SAND
ALLOMEMBER D
8-5-30-4W5
2597.3 m
S.W.H.
15 cm

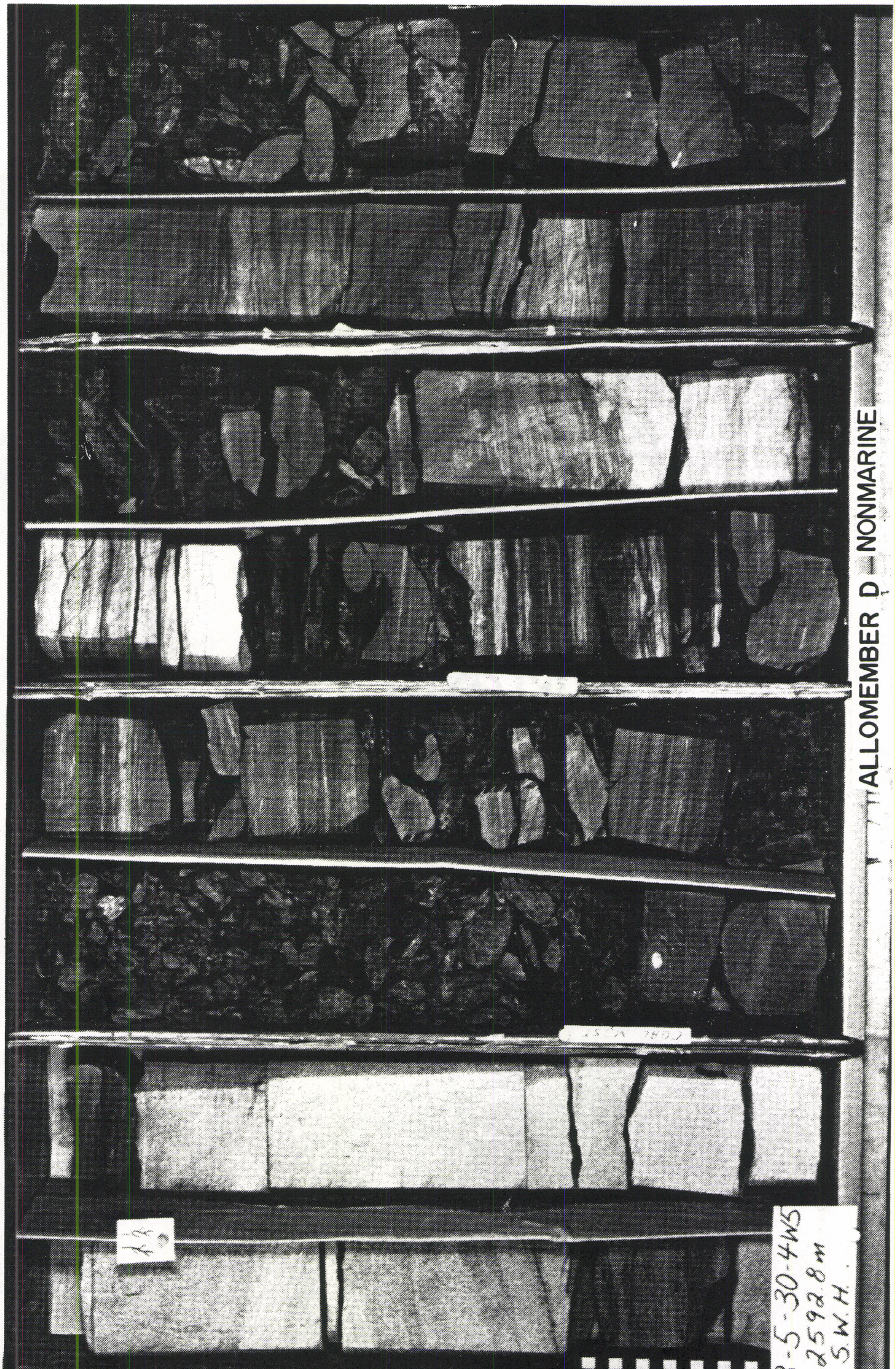
ALLOMEMBER D NONMARINE
8-5-30-4W5
2592.8m
S.W.H.
15 cm

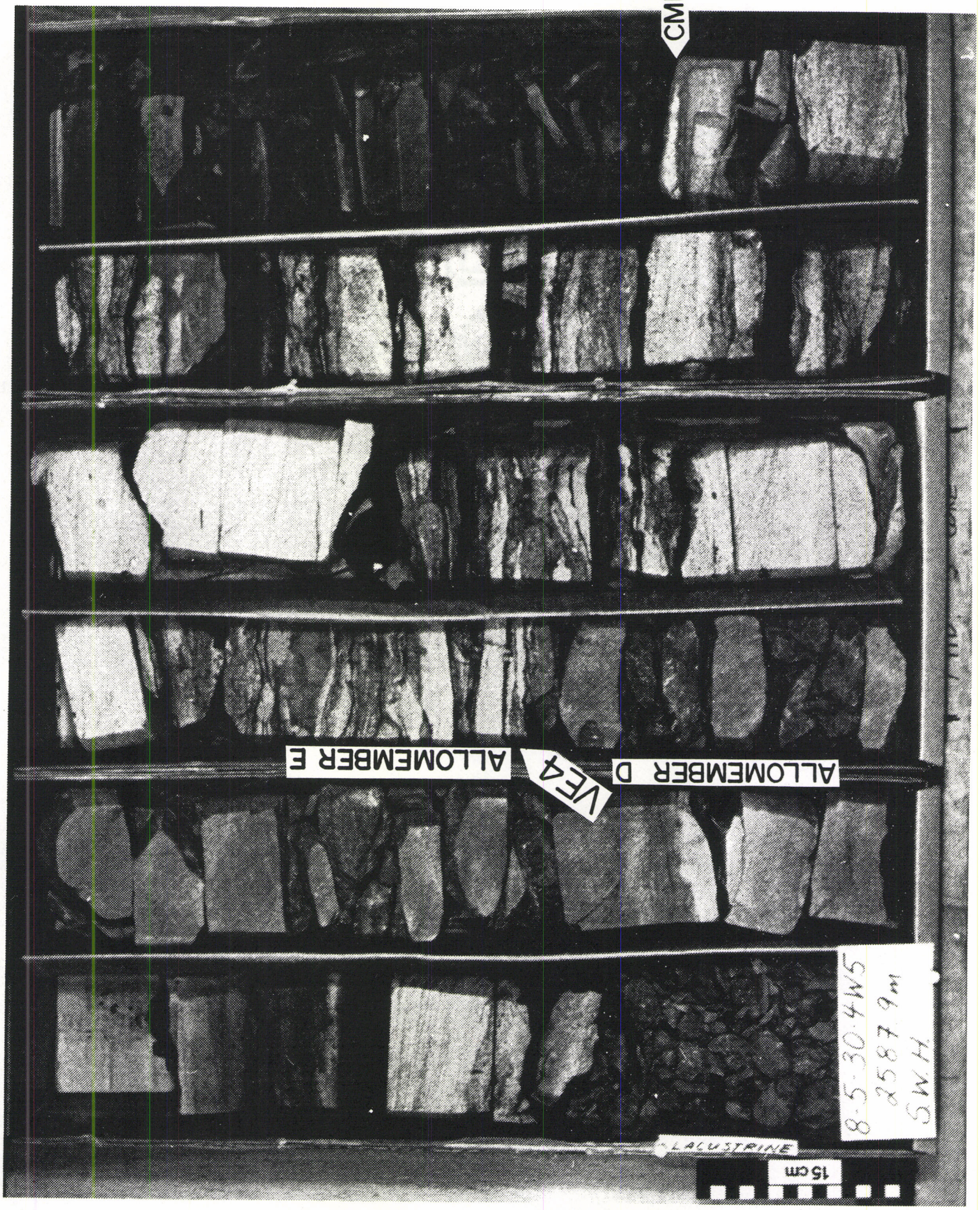
CMI
ALLOMEMBER E
VE4
ALLOMEMBER D
8-5-30-4W5
2587.9m
SWH
LACUSTRINE
15cm

VE4 erosion surface (Fig. 5.11). The basal portion of facies 5b in the 7-28-31-4W5 core displays the angular nature of mudstone clasts common to this facies while the upper part shows the sharp truncation of the overlying VE4 surface (Fig. 5.12). Petrographic criteria discussed in chapter 4.3 has shown that facies 5b sandstones in the 9-22 and 7-28 cores, although macroscopically similar to the overlying facies 5a sandstones were actually compositionally different. Throughout the study area allomember D is truncated sharply at the top by erosion surface VE4.

5.2.5 VE4 Erosion Surface

Allomember D is overlain by the VE4 erosion surface which in turn is overlain by allomember E (Fig. 5.2). The VE4 contact was observed in approximately 90 percent of the cores studied (Appendix B). The surface sharply truncates either facies 9, 10, 11, and 12. The lateral correlation of the VE4 surface, relationship to various facies, and amount of erosional relief on the surface are discussed more fully in chapter 6 and 7.

Four variations of the VE4 surface are shown in figure 5.13. The VE4 contact was the only (VE) surface that showed evidence of burrow structures. Several cores of VE4 displayed *Skolithos* burrows, and one core showed a *Teichicnus* burrow that extended 6 cm down into facies 11 (Fig. 5.13). Cross-bedded and structureless sandstones of facies 5a

Figure 5.11.

(next 2 pages) Allomember D, VE4, and allomember E. Well 9-22-33-5W5 (base at 2439.6 m) Illustrates the sharp contact between facies 8 and facies 5b of allomember D. The following sucession can be seen. Facies 8 is sharply truncated at the top by facies 5b which in turn is truncated at the top by the VE4 surface and deposits of allomember E. Core is 8.75 cm in diameter. Scale bar is 15 cm long.


TOP
CHANNEL LAG
HCS
FLU
MOST RIP UPS
15 cm
9-22-33-5W5
2439.6m
S.W.H.
BOTTOM
FACIES 8
FACIES 5b
ALLOMEMBER D

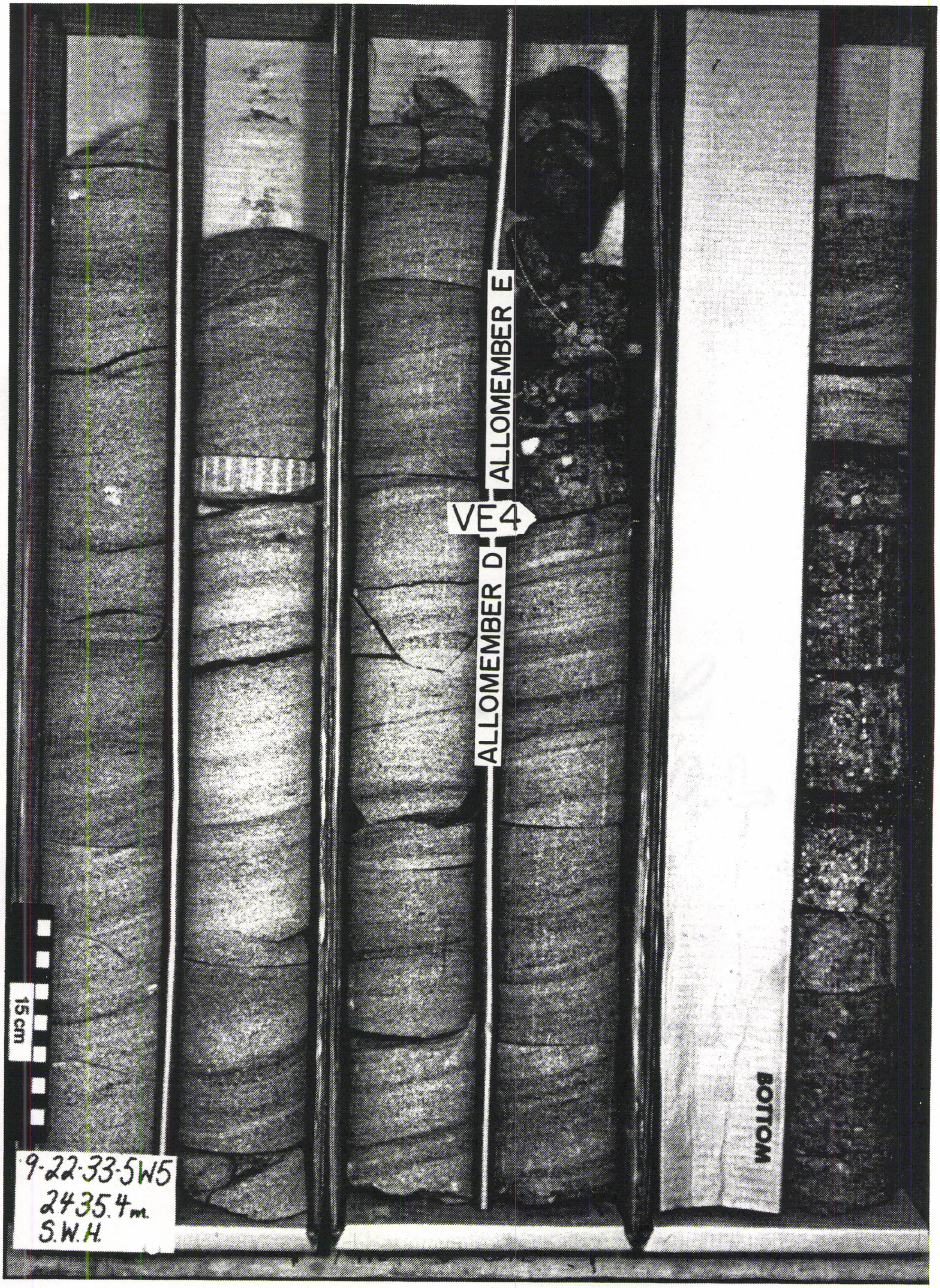
ALLOMEMBER E
VE4
ALLOMEMBER D
15cm
BOTTOM
9-22-33-5W5
2435.4m.
S.W.H.

Figure 5.12.

Allomember D, VE4, and allomember E. Well 7-28-31-4W5 (base at 2387.8 m). Facies 5b sandstones showing abundant angular, mudstone-siltstone ripups sharply overlain by pebbly sandstones (facies 5a) of allomember E. Core is 8.75 cm in diameter. Scale bar is 15 cm long.


15 cm
7-28-31-4W5
2387.8 m.
S.W.H.
ALLOMEMBER E
VE4
ALLOMEMBER D

Figure 5.13.

VE4 Contact

a) Sharp contact between nonmarine facies 11 (allomember D) below and facies 7b (allomember E) above. Note the vertical Teichicnus burrow extending down into facies 11. Well 8-12-30-3W5; Depth 2258.37m; Scale bar is 3 cm long.

b) Sharp contact between facies 8 (interbedded sandstone mudstone at Harmattan East field) overlain by facies 7b (allomember E) above. Note Skolithos burrows extending below VE4 contact. Well 16-11-32-3W5; Depth 2220.3 m; Scale bar is 3 cm long.

c) Sharp contact between nonmarine facies 11 below and facies 5a above. VE4 surface is indicated by arrow. No burrows were observed at this particular contact. Well 6-19-29-1W5; Depth 2123.8m; Scale bar is 3 cm long.

d) Sharp contact between facies 8 (allomember D) overlain by reservoir pebbly sandstones (facies 5a) of allomember E at Harmattan East field. Well 6-20-32-3W5; Depth 2124.2m; Scale bar is 15 cm long.

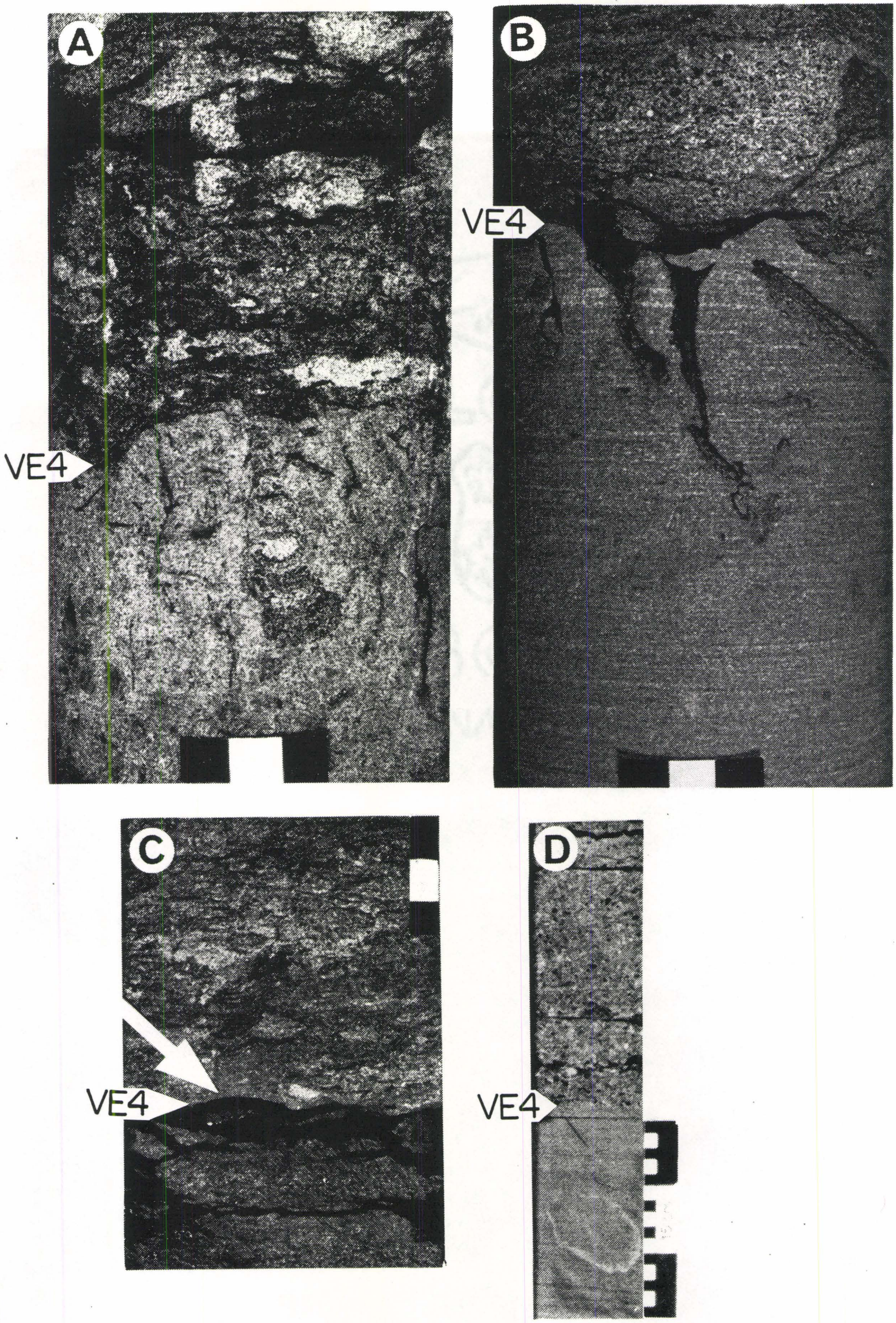
A
VE4
B
VE4
C
VE4
D
VE4

commonly overlie the VE4 contact at Harmattan East and areas to the northwest (Caroline field area). Facies 13 (bioturbated pebbly sandstone mudstone) usually overlies VE4 in off field areas to the south and south-east.

5.2.6 Allomember E

Allomember E lies directly upon the VE4 bounding surface. The coarse sandstones within this allomember are the main Viking Formation hydrocarbon reservoirs at the Harmattan East and Caroline fields. Most cores examined in this thesis have penetrated allomember E (Appendix B), therefore the sediments of this member are useful for a detailed study of this allomember at Harmattan East.

Allomember E ranges from 11-26 m in thickness, averaging 18.5 m. This allomember contains facies 5a, 7b, 13 and 1b. Figure 5.14 shows core photographs of a typical vertical sequence through the lower part of allomember E at Harmattan East. The vertical facies changes within this allomember are generally predictable within the Harmattan East field; however, in off field locations the changes are more variable and complicated.

The coarse sediment package at the base of allomember E at Harmattan East is mostly facies 5a with lesser amounts of facies 13. In general, facies 5a is thicker (up to 6 m) within the field boundary, and is primarily the reservoir facies of the Harmattan East oil field. Facies 5a is often

Figure 5.14.

(next 3 pages) (top of core is upper left of each photo) Allomember D, VE4, and allomember E. Well 6-16-32-3W5 (base at 2213.96m) illustrates the sharp contact between allomember E deposits above and allomember D deposits below. Facies 8 (allomember D) is sharply overlain by facies 5a and facies 13, which then passes upwards into alternating units of facies 7b and facies 1b. Core is 8.75 cm in diameter.

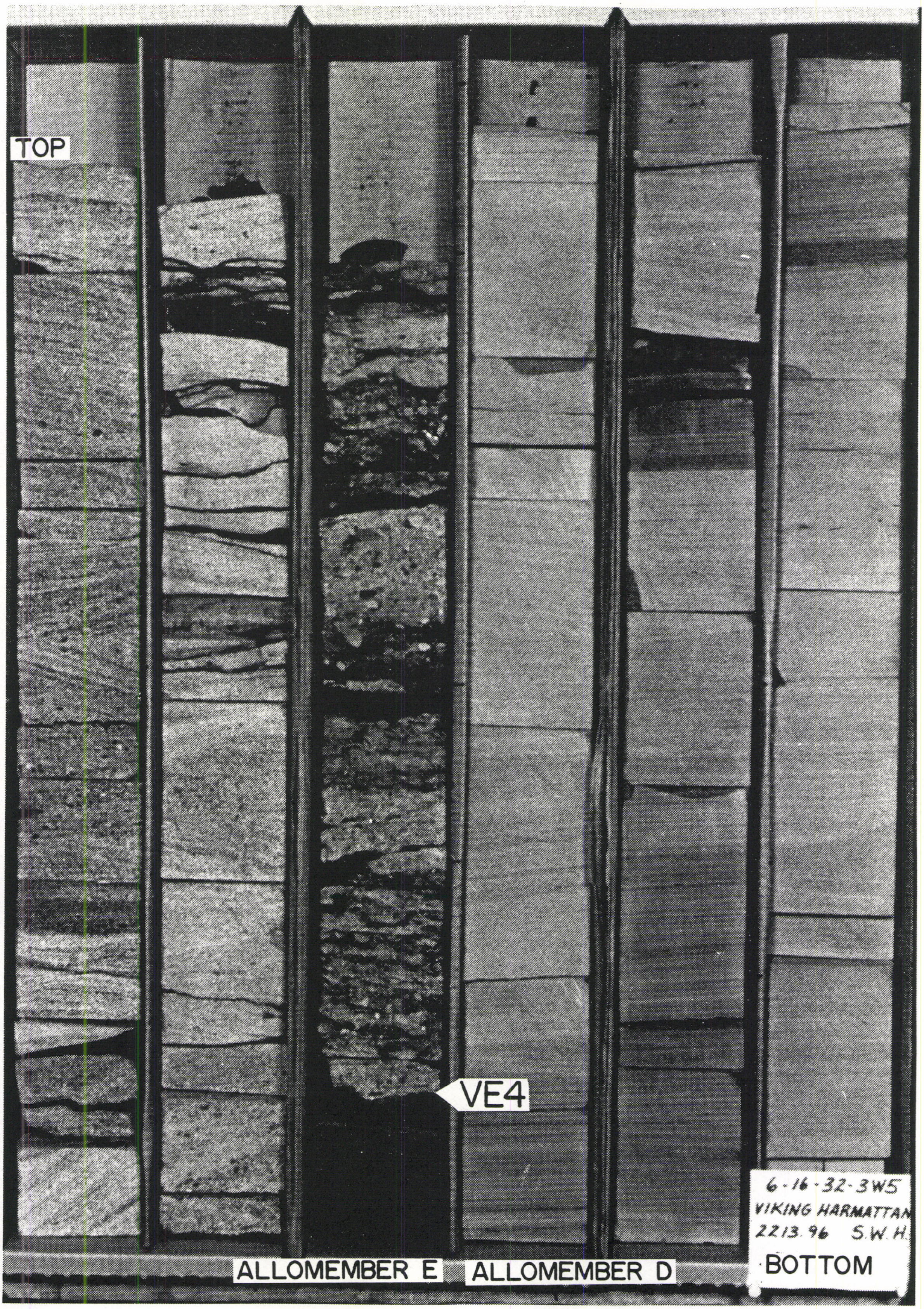
TOP
VE4
ALLOMEMBER E
ALLOMEMBER D
6-16-32-3W5
VIKING HARMATTAN
2213.96 S.W.H.
BOTTOM

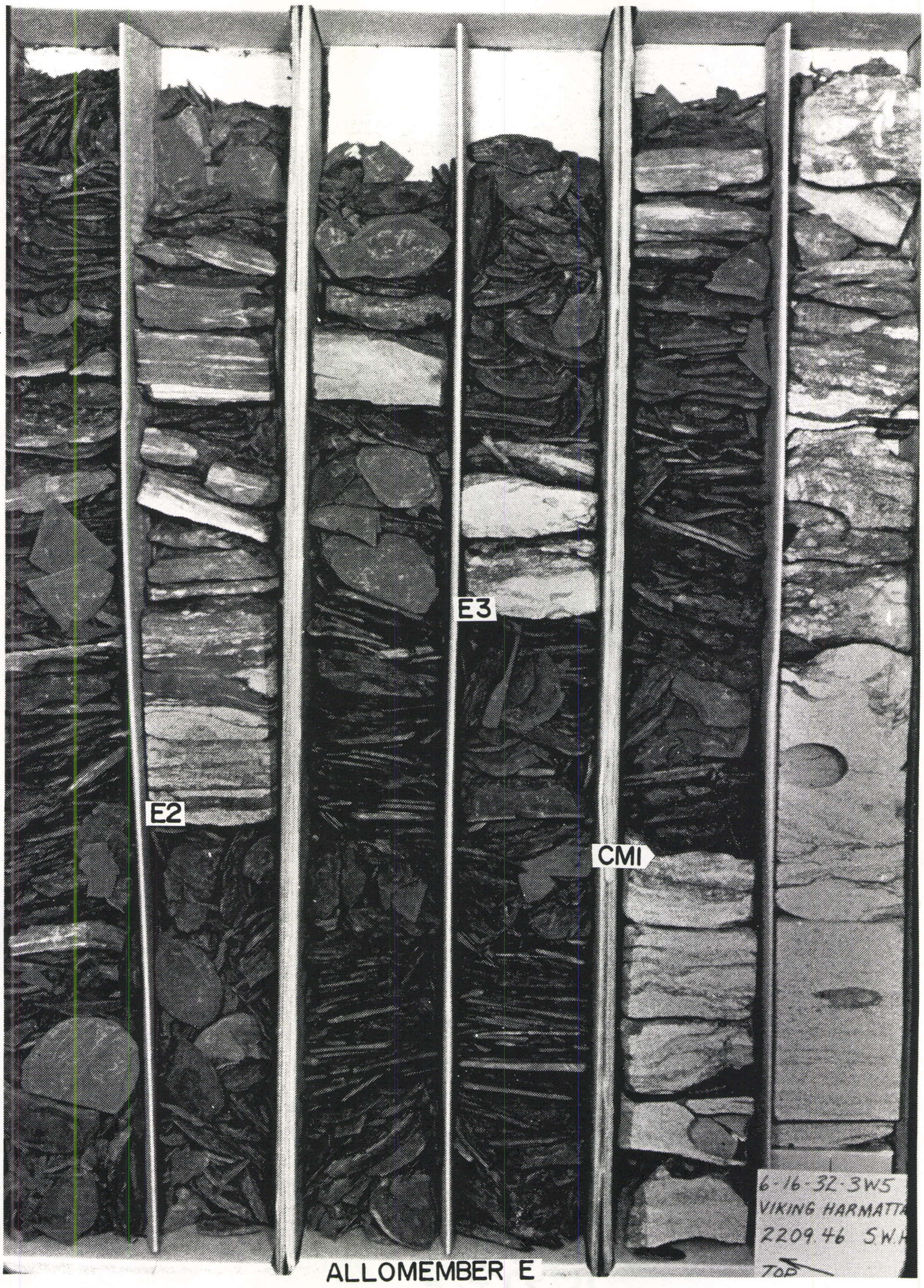
E2
E3
CMI
6-16-32-3W5
VIKING HARMATTA
2209.46 S.W.H
TOP
ALLOMEMBER E


EI
EO
ALLOMEMBER E

gradationally overlain by "muddier" rocks of facies 13. When this was observed in cores, facies 13 would often be truncated sharply by another unit of facies 5a. This is seen in core as alternating units of facies 5a and 13.

Upwards, the main coarse sediment package at Harmattan sharply passes into facies 7b which in turn passes into facies 1b. The coarse grained sandstone beds of facies 7b (Viking A 'grits' of Hein et al., 1986) usually become thinner, and less common upwards. These sandstone beds are usually underlain by thin (< 10 cm thick) sideritic mudstones that often display sand filled Skolithos and/or Arenicolites burrows. On well logs, these sandstones beds are recorded as bump like deflections to the left on the gamma ray, and to the right on the resistivity curves (Fig. 5.3). In most cases these deflections do not correspond to one particular bed, but instead record the presence of several closely spaced sandstone beds. Several sandstone beds of facies 7b have been correlated as onlap markers within allomember E . Five of these markers (E0 to E4) have been identified within the study area (Fig. 5.3). The lateral and areal distribution of these onlap markers is discussed in chapter 6 and 7.

Most cores of allomember E in off field areas have a similar vertical facies relationship to that seen in the Harmattan East field; however, the coarse sediment package that rests on VE4 is usually thinner, muddier, and more bioturbated. In several cases the coarse sediment package can be of similar thickness to that of on field wells. For example, in the 14-8-31-1W5 well, approximately 4 m of facies 13 lies upon the VE4 surface (Fig. 5.15).

Figure 5.16 illustrates a continuous cored sequence through all of allomember E. The well is located southeast of the Harmattan East Field and shows the relationship of the coarse grained deposits overlying the VE4 surface, as well as the relationship of the Base of Fish Scales sandstones to the dark mudstones of the upper part of allomember E. The contact between the sediments of allomember E and the Base of Fish Scales sandstone above is always sharp and is placed at the base of a condensed unit (Base of Fish Scales) that contains abundant fish skeletal remains (Fig. 5.17).

Figure 5.15.

Allomember D, VE4, and allomember E in off field position relative to Harmattan East. Well 14-8-31-1W5 (base at 2038.9m) illustrates sharp contact between facies 9 (allomember D) below and facies 13 (allomember E) above. This well is located southeast of the Harmattan East field along a similar line of depositional strike. A comparison of allomember E deposits above VE4 in this well to stratigraphically equivalent deposits in figure 5.14 shows the dramatic difference in lower allomember E sediments at on and off field locations. Core is 10 cm in diameter.


TOP
2037.01
2037.55
2038.09
ALLOMEMBER E
VE4
ALLOMEMBER D
2038.65
14-8-31-1W5
2038.9m
S.W.H
BOTTOM


TOP
VE4
ALLOMEMBER E
ALLOMEMBER D
15 cm
14-32-31-2W5
2149.3 m
SWH
BOTTOM

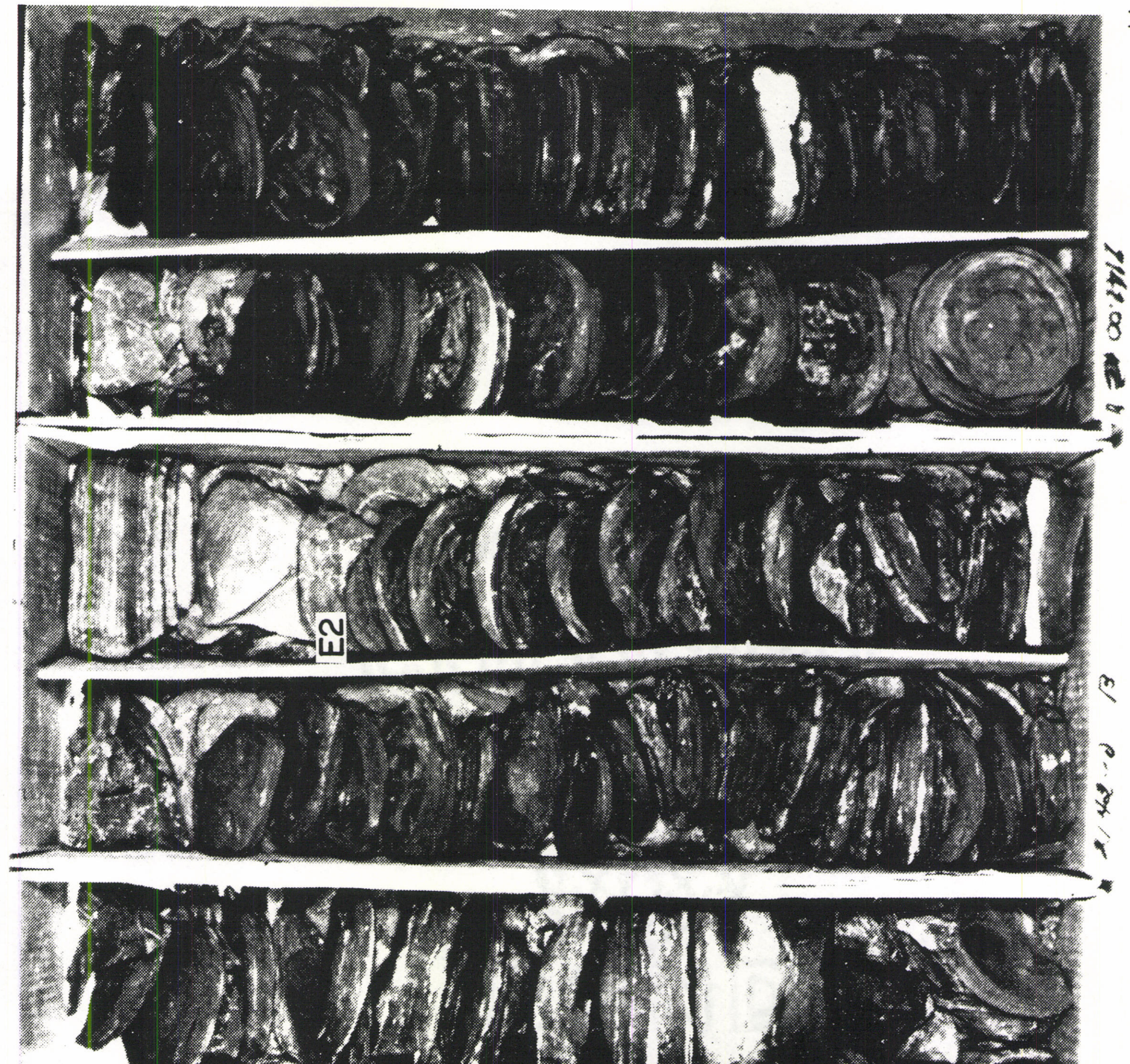
E2
E3
CMI


E1

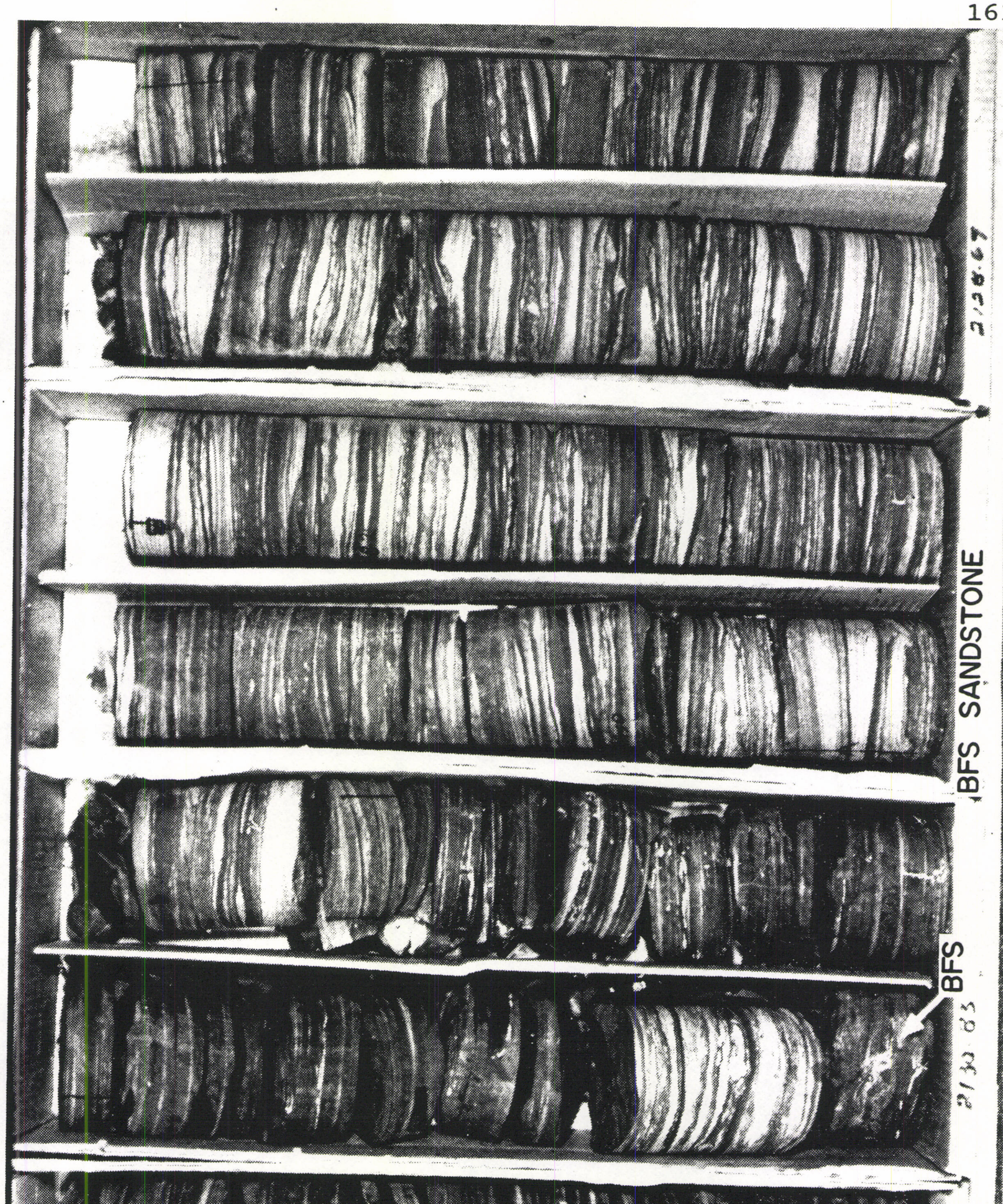
BFS SANDSTONE
BFS
ALLOMEMBER E
15 cm

Figure 5.17.

Base of Fish Scales

a) Base of Fish Scales Marker as seen in core. Arrow points to the top of a 2.5 cm thick unit of fish skeletal debris. This skeletal unit passes sharply upwards into mudstones and sandstones of the Fish Scales sandstone unit. The base of the skeletal unit marks both the top of the Viking Alloformation and the top of allomember E. Well 14-32-31-2W5; Depth 2130.3m; Scale bar is 3 cm long.

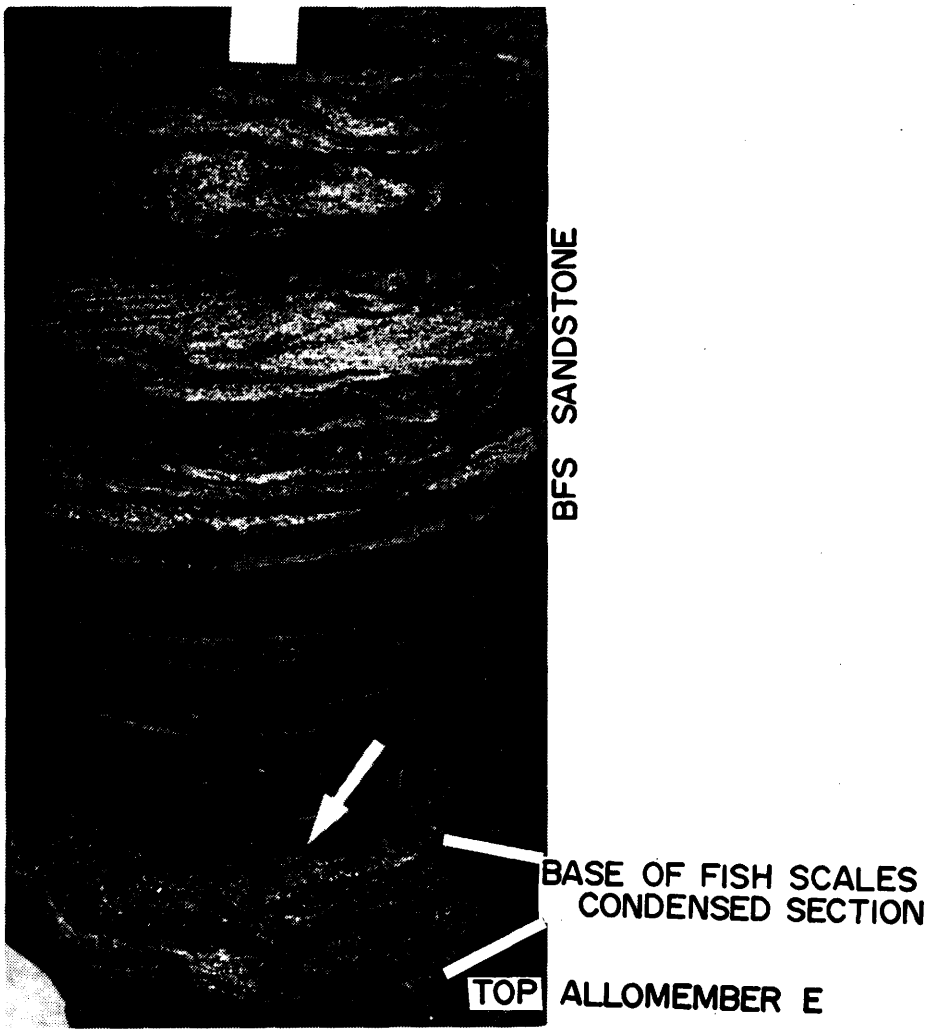
BFS SANDSTONE
BASE OF FISH SCALES
CONDENSED SECTION
TOP ALLOMEMBER E

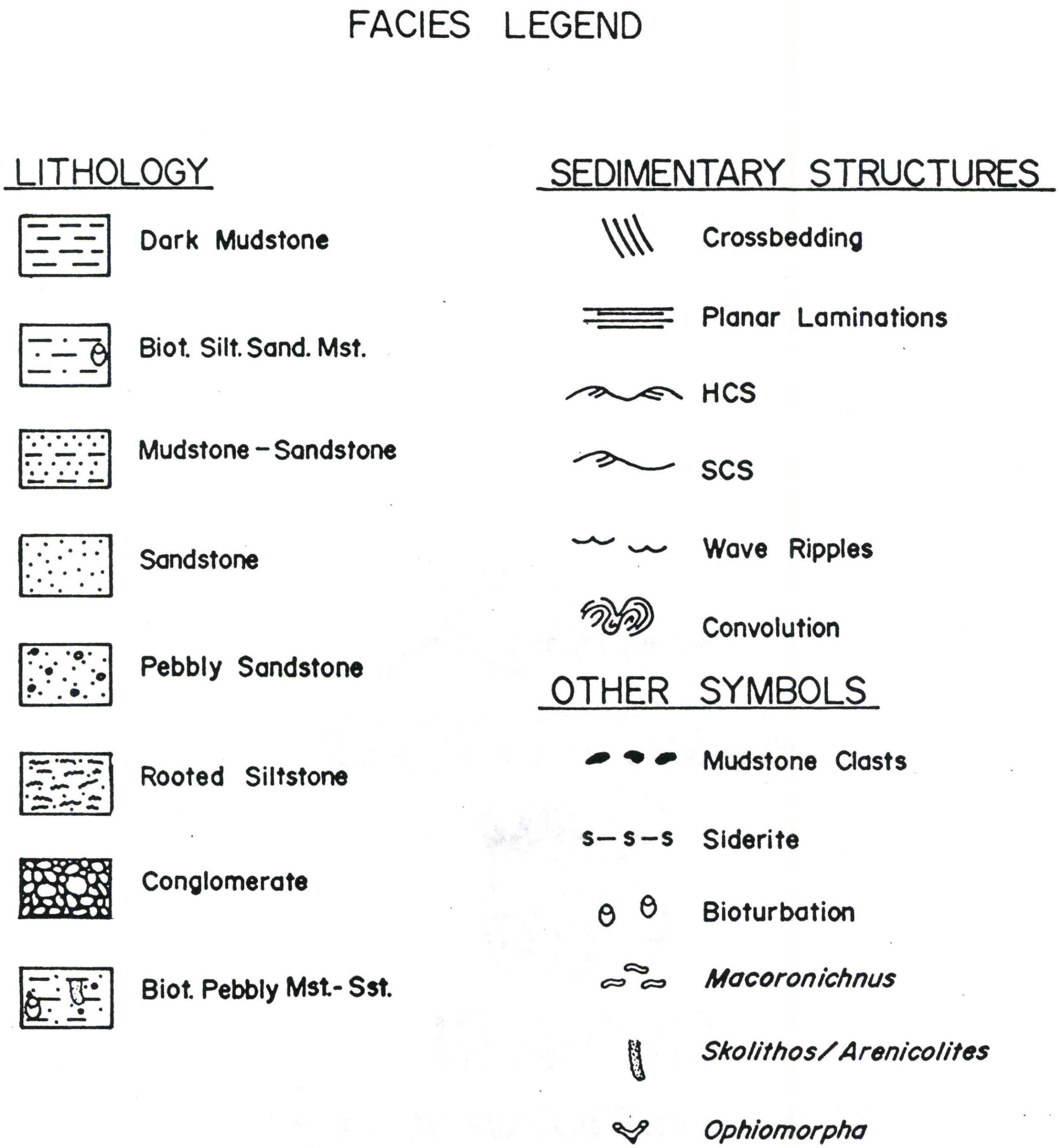

Figure 5.18. Symbols used for figures 5.1 through 5.4 and core cross sections in Chapter 6.

Chapter 6 Cross Sections: Lateral Facies Variations

6.1 Introduction

The purpose of this section is to examine the lateral distribution of the Viking allomembers and facies at Harmattan East - Crossfield. The distribution of the allomembers and facies was studied by constructing paired well log and core cross sections throughout the study area. The well log cross sections presented in this thesis have been adapted from larger (ie. greater number of well logs) reconnaissance cross sections constructed during the research phase of this study. These cross sections were used as a reference for gathering a data base of well log picks that were subsequently used for isopach mapping. The isopach maps were constructed to show changes in thickness between bounding surfaces and log markers in the study area, as well as to show topographic change on a particular surface. These maps are discussed in Chapter 7.

6.2 Log and Core Cross Sections

Five cross sections were constructed in order to examine the lateral facies relationships of the allomembers. Three of the cross sections are oriented northeast - southwest, perpendicular to depositional strike, and the other two sections are oriented northwest - southeast, parallel to depositional strike. The two strike oriented sections tie into the three dip sections completing a cross section tie link up of the study area.

The cross sections are labelled "A" through "E" and are located on maps attached to each well log cross section. The solid black bars on the log cross sections represent cored intervals used in the creation of the core cross sections. In all log cross sections, gamma ray (and rarely spontaneous potential) logs are shown to the left and resistivity are shown to the right.

Correlations of well logs were based mostly on markers established from core control. Gamma ray logs were used for the correlation of sandier units in the study area, however both the gamma ray and resistivity logs were used together for determining the exact location of bounding surfaces. The symbols used on the core cross sections are the same as those used in the reference locality diagrams previously shown in chapter 5 (Figures 5.1 - 5.4 and 5.18). Where erosion surfaces and core markers are correlated on core cross sections in the absence of core control, their positions have been interpreted from the corresponding well logs. These positions are marked as (L) on the core cross sections. All core cross sections are scaled in metres. All log and core cross sections are hung using the Base of Fish Scales as a datum. A summary of the important characteristics of the log and core cross sections is included at the end of this chapter (section 6.3) if the reader wishes to forego the following detailed descriptions.

6.2.1 <u>Log Cross Section A-A′ and Core Cross Section A</u>

Log cross section A-A′ is shown in figure 6.1 and the corresponding core cross section is shown in figure 6.2. Figure 6.1 is a dip oriented stratigraphic cross section that shows the lateral relationship of Viking allomembers at the Harmattan East field and areas to the southwest and northeast.

In this cross section, the correlation of the Joli Fou, Basal Colorado Sandstone, and BV are questionable because of the limited core control at these stratigraphic intervals. If these correlations are assumed to be correct, then the Joli Fou Formation appears to thin to the southwest where it becomes indistinguishable and is no longer correlatable. Also, it implies that the sandstone at the base of the core at 6-24-32-3W5 could be either the Basal Colorado Sandstone, or a sandstone which is laterally equivalent to the Joli Fou. The important point to be made here is that BV (base of the Viking alloformation) appears to rest on the Joli Fou Formation up to and in the vicinity of 16-14-32-3W5, and further to the southwest BV rests on Basal Colorado Sandstone.

Allomember A-B thickens to the southwest from about

Figure 6.1. Log cross section A-A'. Location of cross section is shown on accompanying map.

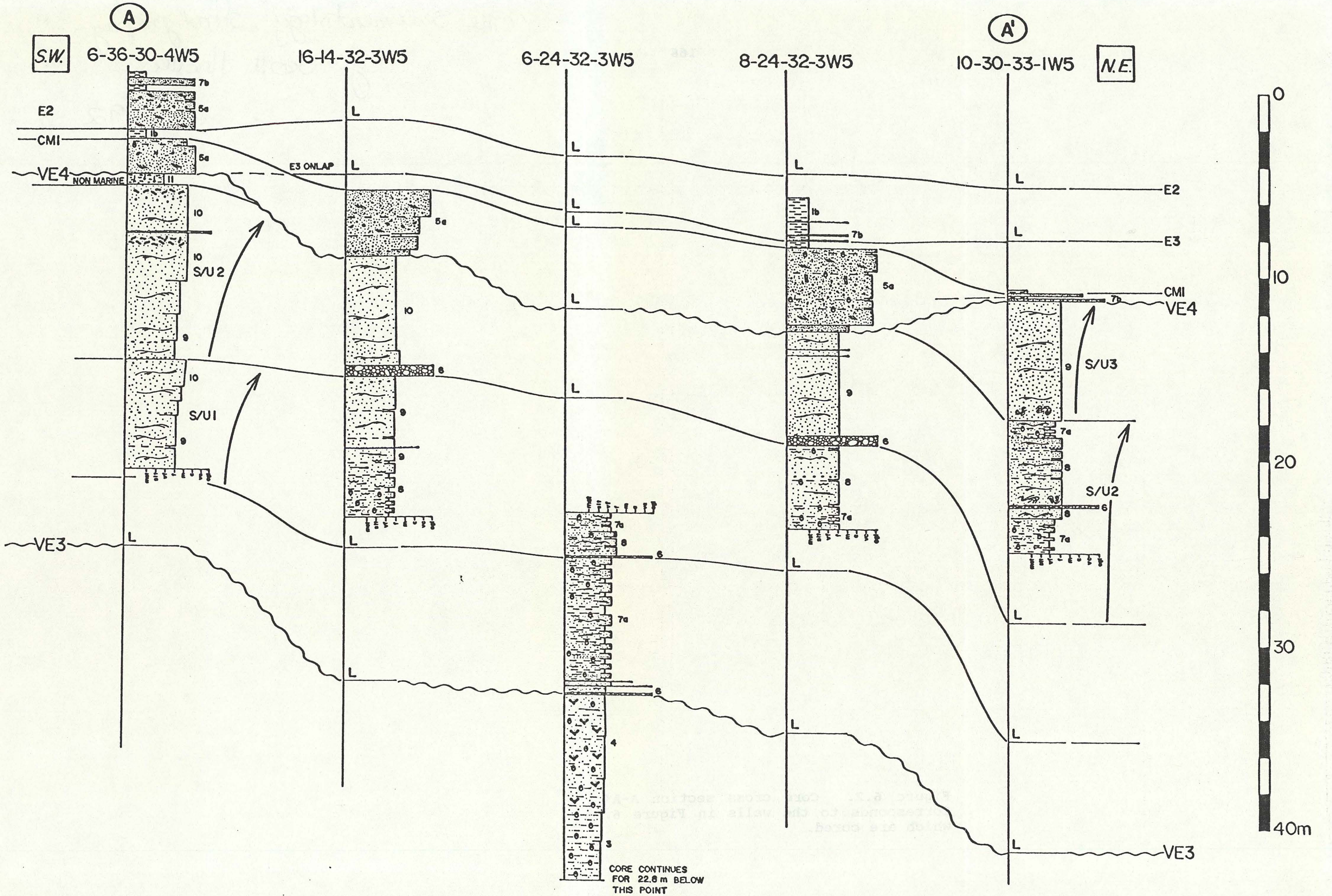

A
A'
S.W.
N.E.
6-36-30-4W5
16-14-32-3W5
6-24-32-3W5
8-24-32-3W5
10-30-33-1W5
E2
CM1
VE4
NON MARINE
E3 ONLAP
E3
VE3
S/U1
S/U2
S/U3
L
CORE CONTINUES FOR 22.8 m BELOW THIS POINT
0
10
20
30
40m

18 m at 10-30-33-1W5 (A') to about 28 m at 6-30-29-4W5 (A). Allomember A-B on well logs appears to represent a single sanding upwards sequence, and is shown by the upward curving arrow above LM2 and beside the gamma ray trace. In the 6-30-29-4W5 well, two cross section log markers are drawn below the VE3 surface to show that additional vertical sequence in allomember A-B is present in southern parts of the study area. The VE3 bounding surface truncates allomember A-B and displays an undulating topography that climbs to the southwest.

Allomember D is the main progradational shoreface sequence in the Viking Formation. Figure 6.1 shows that this allomember is quite variable in thickness throughout the study area. Its thickness at 10-30-33-1W5 (A') is about 29m, while at 6-30-29-4W5 (A) it is 17 m. The VE3 surface has two places with topographically steeper slopes, one between wells 10-30-33-1W5 and 10-8-33-2W5; where it steps up 7m, and the other between wells 6-30-29-4W5 and 6-36-30-4W5; where it steps up 7.5m. The term "step" will be used in the remainder of this thesis to describe a relatively steep topographical slope; the term "tread" will be used to describe a portion of the topography which is generally flat.

The first correlation line above the VE3 surface corresponds to the top of a "blocky" well log response on the gamma ray curve. This correlation may represent a maximum flooding surface associated with the transgressively produced

VE3 surface. Three sandier upwards units (S/U1 to S/U3) are labelled in the 10-30-33-1W5 well and rest on the "blocky" well log unit. The sandier upwards units are defined by the character of the gamma ray log and in most cases do not correspond to exact core markers. These units suggest two main things about the lateral relationship of the internal vertical sequence in allomember D. First, they show the progradational nature of the allomember in that the individual S/U units thin and downlap towards the northeast. Secondly, the upper units show the erosive nature of the VE4 surface. This can be seen by the truncation of S/U3 between 8-24-32-3W5 and 2-6-33-2W5, and the truncation of nonmarine deposits at 6-36-30-4W5 and 6-30-29-4W5.

The non marine facies (brown) in allomember D, as shown in figure 6.1 thicken toward the southwest reaching a maximum at 6-30-29-4W5 (A) of 6 m. The preserved thickness of the non marine strata appears to be related to the amount of erosion on the VE4 surface.

The VE4 bounding surface (Fig. 6.1) also shows an undulating topography that gently climbs to the southwest. The most pronounced "step" occurs immediately southwest of Harmattan between wells 16-14-32-3W5 and 7-2-32-3W5, where it "steps" up 3m. The coarse sediment package (yellow) lies upon the VE4 surface, and is thickest at the Harmattan East field (approx 4.5 m thick at 8-24-32-3W5), and thins off field to the northeast to < 1 m at 10-30-33-1W5 (A'). The coloured markers, labelled E0 to E3 in allomember E (Fig. 6.1) represent the correlation of sandstone beds and log markers above the VE4 surface. The lateral correlation of these markers suggests that they onlap onto CM1 in a southwest direction, with each marker closely paralleling the BFS datum. The E3 marker (red) onlaps southwest of the Harmattan East field between 7-2-32-3W5 and 16-14-32-3W5. The E2 marker (green) onlaps at 6-30-29-4W5. The E0 (purple) and E1 (orange) markers do not onlap on this cross section. Allomember E thins towards the southwest from 20 m at 10-30-33-1W5 (A) to 12 m at 6-30-29-4W5.

The corresponding core cross section to A-A', figure 6.2 shows the detailed lateral relationships of allomember A-B, D and E. The basal portion of the core (approx 22.8 m) at 6-24-32-3W5 is not shown because core cross section A considers the correlation of facies and allomembers stratigraphically higher. The remainder of the 6-24-32-3W5 core not shown in core cross section A can be seen in figure 5.1 of chapter 5.

The VE3 surface in figure 6.2 shows the stepped topography that was seen in the companion log cross section. Facies 7a overlies the VE3 surface at 6-24-32-3W5 and is truncated by a thin conglomerate bed (maximum flooding surface ?) that marks the top of the first unit above the VE3 surface. This same unit is the "blocky" well log unit above VE3 in figure 6.1. The sandier upwards units in allomember

D (Fig. 6.2) show a northeast lateral facies change. This change is shown in SU/2 where facies 10 (parallel laminated and cross bedded sandstone) well 6-36-30-4W5 in allomember D forms a coarsening upwards sequence capped by rooted sandstone that passes laterally to the northeast into facies 9 (thick bedded, non bioturbated sandstone) at 8-24-32-3W5 which in turn passes into facies 7a (fine grained burrowed laminated sandstone-mudstone) and facies 8 (interbedded sandstone-mudstone) at 10-30-33-1W5. Figure 6.2 also shows that the base of SU/2 corresponds to a thin bed of conglomerate (facies 6) at 16-14-32-3W5 and 8-24-32-3W5. These conglomerate beds within allomember D can sometimes be correlated over distances of several kilometers in the study area provided there is enough closely spaced core control. Their usefulness as a regional marker in the study area is therefore restricted to localized detailed cross sections.

The VE4 surface in figure 6.2 shows the truncation of SU/3 (mostly facies 9) between 8-24-32-3W5 and 10-30-33-1W5 (as in figure 6.1). Note that the coarse sediment package above VE4 (mainly facies 5a) is thickest at the Harmattan East field and the package thins substantially in a northeast direction at 10-30-33-1W5 where it becomes a < 50 cm thick unit of facies 5a. Also note that allomember E shows the lateral facies relationships of the E2 and E3 markers. In the 8-24-32-3W5 well, the E3 marker is characterized by thin coarse grained sandstone beds of facies

7b that onlap southwest of the Harmattan East field. The E2 marker is shown in core at 6-36-30-4W5 and corresponds to the base of a > 2 m thick unit of facies 5a that is separated from the main coarse sediment package by dark mudstones of facies 1b. The E2 marker as shown in figure 6.2 appears to thin towards the northeast from a maximum thickness of about 3 m to < 1 m.

6.2.2 Log Cross Section B-B′, C-C′ and Core Cross Section B and C

Log cross section B-B′ is shown in figure 6.3 and the corresponding core cross section is shown in figure 6.4. Log cross section C-C′ is shown in figure 6.5 and the corresponding core cross section in figure 6.6. These two dip oriented well log cross sections and corresponding core cross sections are discussed together in this section, and are used to show the lateral relationships of Viking allomembers and facies in locations adjacent to the Harmattan East field. Both well log cross sections show similar lateral relationships to those seen in well log cross section A-A′ (Fig. 6.1) therefore only the important points of cross sections B-B′ and C-C′ are discussed here.

The top of the Joli Fou or BV pick is problematic in both well log cross sections, because no cores were available and because a well log marker could not be calibrated lithologically.

Allomember A-B in both well log cross sections appears to thicken to the southwest. Cross section B-B′ shows three sanding upwards units that have been correlated on the basis of the shape of the gamma ray curve. The lowermost unit above LM2 is thickest (11 m) at 5-14-28-4W5 and thins to the northeast to <2 m at 14-32-31-2W5, where the unit appears to downlap towards LM2. The S/U units in allomember A-B display similar lateral relationships to that described previously in allomember D, where stacked sandier upwards units appeared to thin and downlap to the northeast. These units were truncated at the top by the VE4 surface. The upper unit in allomember A-B (Fig. 6.3) exhibits a variable lateral thickness that was probably produced by erosion on the VE3 surface. The VE3 surface in B-B′ rises to the southwest in a similar manner as seen in A-A′; however, the VE3 surface in C-C′ is relatively flat and the underlying unit (LM1 to VE3) is relatively consistent in thickness.

The internal lateral relationships of allomember D are essentially similar to those described in A-A′. The VE4 surface in cross sections B-B′ and C-C′ shows a gradual stepped topography that rises to the southwest. The coarse sediment package (yellow) which lies upon the VE4 surface thins towards the northeast to < 1 m.

The E4 marker (blue) is not present on well log cross section A-A′ because it does not occur in the area of the

Harmattan East field. In B-B′, the E4 marker onlaps between 6-20-33-28W4 and 16-29-32-1W5 and the onlap position corresponds with gradual rise in topography on the VE4 surface to the southwest. In C-C′, the E4 marker onlaps between 7-2-30-1W5 and 10-23-30-29W4, and amalgamates with the coarse sediment package (yellow). The E3 marker (red) also onlaps in both cross sections and is seen in C-C′ where it amalgamates with the coarse sediment package at 2-13-29-2W5. The most dramatic lateral relationship of onlap markers can be seen in cross section B-B′ where the E2 marker (green) amalgamates with the coarse sediment package at 6-31-28-3W5 and directly overlies the VE4 surface at 5-14-28-4W5. The E2 marker in B-B′ thins from 3m at 5-14-28-4W5 (B) to < 1 m at 7-34-33-28W4 (B′). Well log cross section B-B′ also shows a substantial thinning of allomember E in a southwest direction from 26 m at 7-34-33-28W4 (B′) to 12 m at 5-14-28-4W5 (B). This thinning trend of allomember E raises the problem of tracing the uppermost E markers (EO and E1), and the Base of Fish Scales datum further to the south and west. The simplest interpretation is that the VE4 surface maintains a steady gradual rise towards the southwest with the E0 and E1 markers eventually onlapping and amalgamating with the coarse sediment package immediately overlying VE4. The Base of Fish Scales (datum) would also eventually onlap onto the VE4 surface and the Base of Fish Scales Sandstone above would rest on allomember E.

Figure 6.3. Log cross section B-B'. Location of cross section is shown on accompanying map.

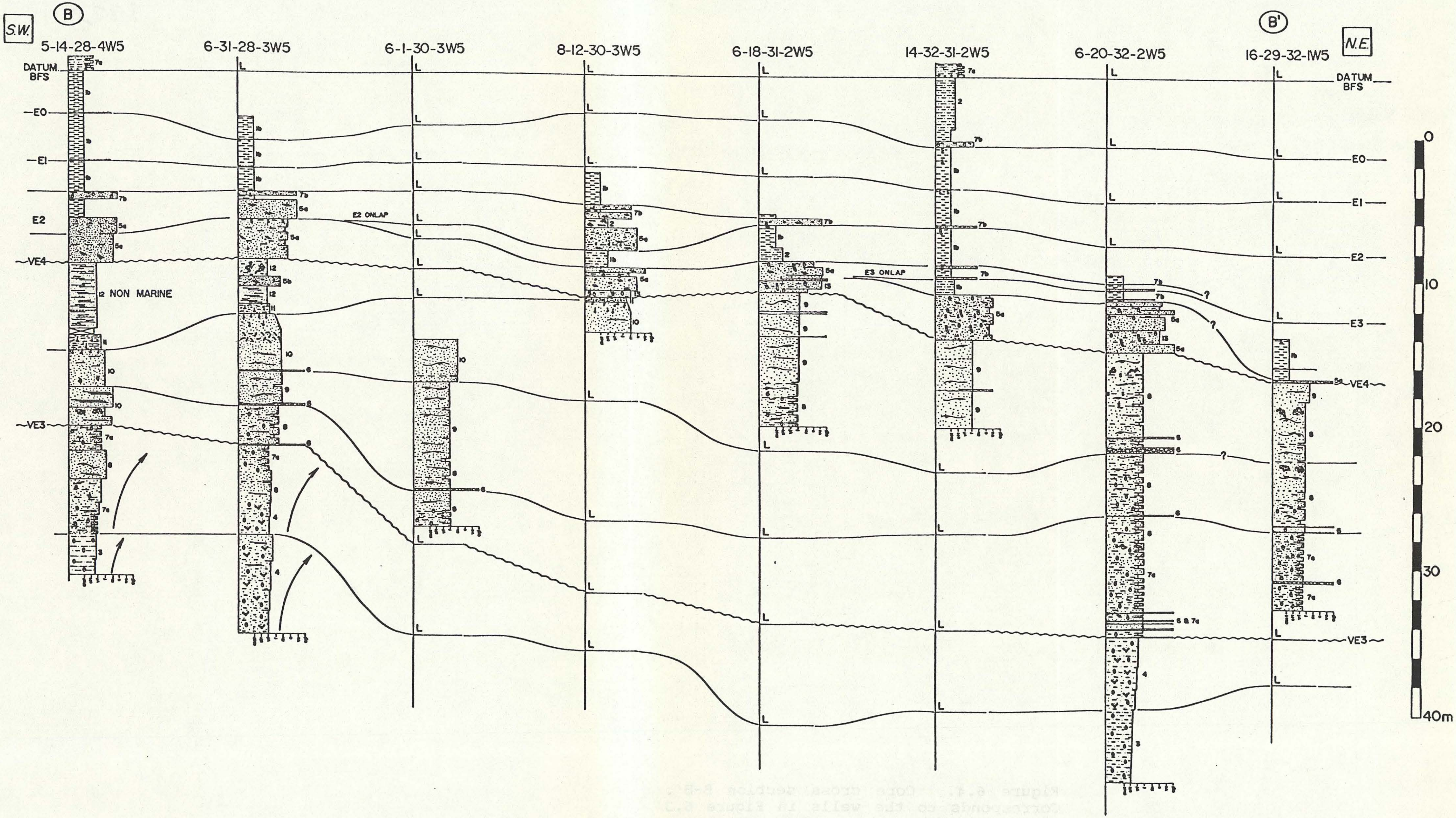

S.W.
B
5-14-28-4W5
6-31-28-3W5
6-1-30-3W5
8-12-30-3W5
6-18-31-2W5
14-32-31-2W5
6-20-32-2W5
16-29-32-1W5
B'
N.E.
DATUM BFS
E0
E1
E2
VE4
VE3
E3
12 NON MARINE
E2 ONLAP
E3 ONLAP
0
10
20
30
40m

The corresponding core cross sections illustrate the lateral facies described for the B-B′ well log cross section. Core cross section B (Fig. 6.4) shows that allomember A-B becomes sandier to the southwest with facies 4 (pale sandstones) at 6-20-32-2W5 passing laterally into facies 7a (fine grained burrowed laminated sandstone-mudstone) and facies 8 (interbedded sandstone-mudstone). This same relationship can be seen in core cross section C.

Allomember D (Fig. 6.4) shows a similar lateral facies change to that described in cross section A-A′. It consists mainly of facies 7a and 8 and appears to be truncated at the top by a thin chert pebble bed. The unit does not show any major lateral facies changes. Allomember D also shows a coarsening upwards sequence at 6-31-28-3W5 that changes laterally northeast into finer grained deposits of facies 8 and 9 (Fig. 6.4).

The lateral thinning of the coarse sediment package (allomember E) is also well displayed in core cross section B-B′. At 6-20-32-2W5 facies 13 is interbedded with facies 5a and forms a coarse sediment package approximately 5 m thick that laterally pinches out at 16-29-32-1W5 into a 20 cm thick facies 13.

A final point about core cross section B-B′ is concerned with the lateral facies changes of the onlap markers in allomember E. The E2 marker onlaps between 6-31-28-3W5 and 6-1-30-3W5. At 6-31-28-3W5, a crossbedded pebbly

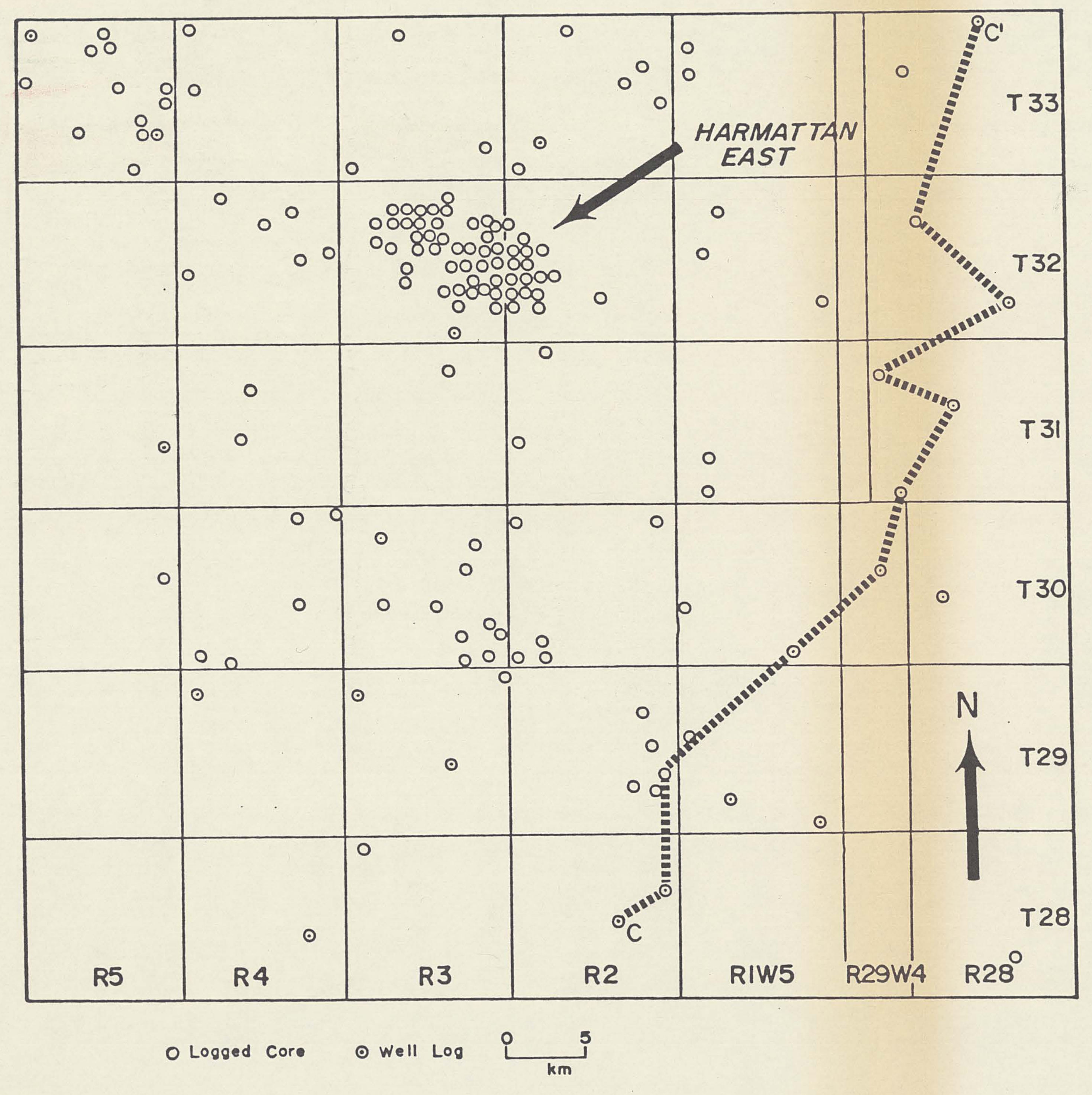

Figure 6.5. Log cross section C-C'. Location of cross section is shown on accompanying map.

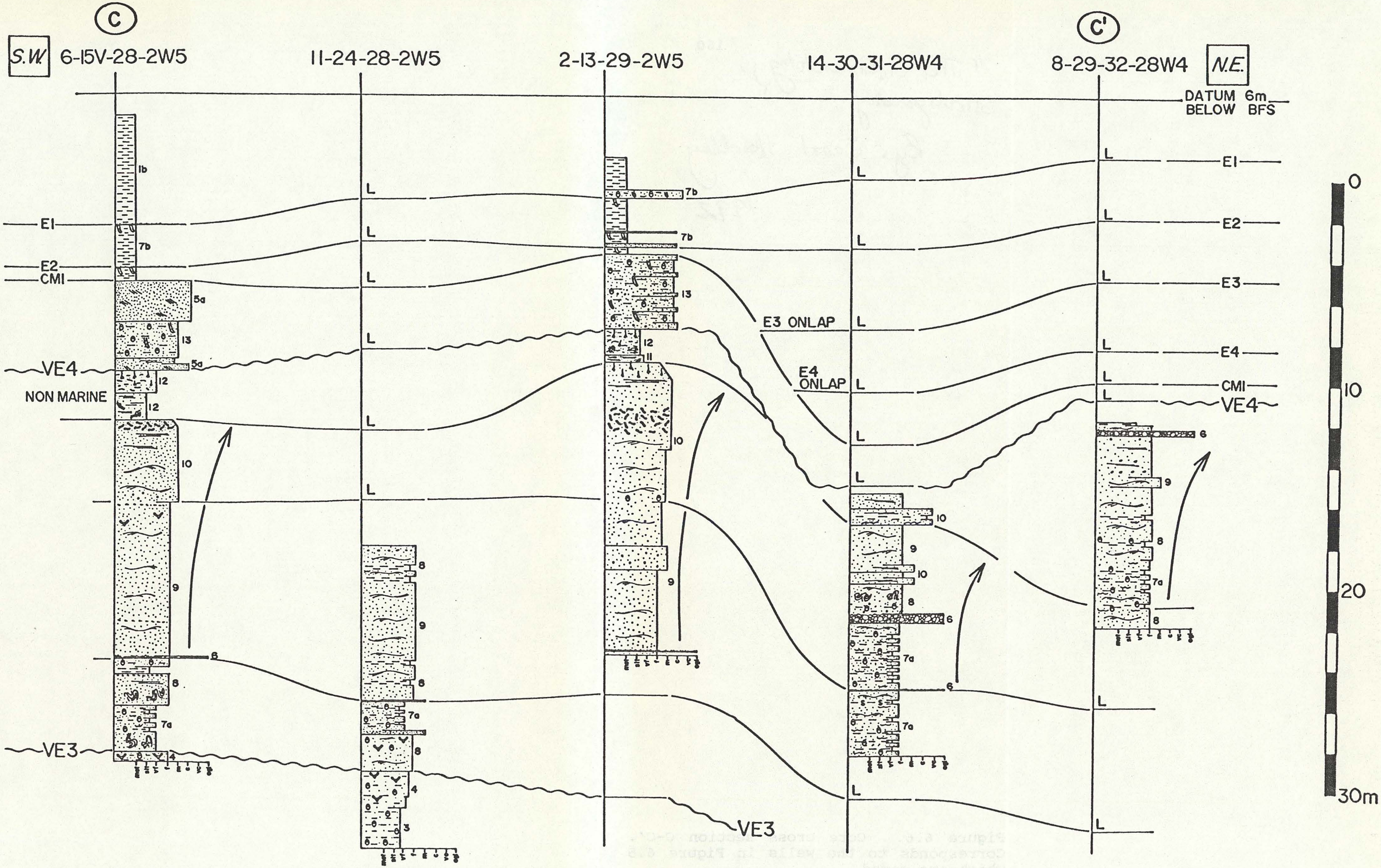

C
C'
S.W.
6-15V-28-2W5
11-24-28-2W5
2-13-29-2W5
14-30-31-28W4
8-29-32-28W4
N.E.
DATUM 6m BELOW BFS
E1
E2
CMI
VE4
NON MARINE
VE3
E3
E4
E3 ONLAP
E4 ONLAP
L
0
10
20
30m

sandstone (facies 5a) sharply truncates the main coarse sediment package, in this case a muddier facies 5a. To the northeast this crossbedded sandstone changes laterally into thinner crossbedded sandstone beds in 8-12-30-3W5 that contain mudstone rip up clasts. When traced still further to the northeast E2 becomes a thin coarse sandstone bed that is burrowed by Arenicolites at 14-32-31-2W5.

Core cross section C-C′ (Fig. 6.6) shows a different lateral facies relationship for the E3 onlap marker. The E3 marker onlaps at 2-13-29-2W5 and in core corresponds to the base of an approximately 3.5 m thick facies 13 (bioturbated pebbly mudstone). The correlation of E3 in a southwest direction to core at 6-15V-28-2W5 is questionable but the marker may correspond to the base of facies 5a that contains compound cross beds and sharply truncates facies 13.

6.2.3 Log Cross Section D-D′ and Core Cross Section D

Well log cross section D-D′ (Fig 6.7) and the corresponding core cross section (Fig. 6.8) are oriented parallel to depositional strike, and both show the stratigraphic relationship of Caroline to Harmattan East, as well as the lateral relationship of the allomembers and facies.

Allomember A-B thickens towards the southeast from a minimum of 26 m at 6-31-33-5W5 (D) to 40 m at 11-17-30-28W5 (D′). Allomember D is thicker (approx. 22 m) at Harmattan

East, and then thins to about 12 m towards the northwest at Caroline.

Log cross section D-D′ also shows the position of a possible channel in the upper part of allomember D at 9-22-33-5W5. The correlation is based on core from this well and is shown in core cross section D-D′. The channel appears to cut down into the sandier-upwards units of allomember D. Because it is truncated at the top by VE4, it is considered to be part of allomember D. The quality of well logs at 9-22-33-5W5 is rather poor (ie. old well logs from the 1950′s), hence they are not useful for contrasting log response shape to modern well log suites surrounding this location. Figure 6.8 shows the position of the channel in a core cross section. The channel (facies 5b) sharply overlies facies 9 (thick bedded, non bioturbated sandstones), and is truncated at the top by the VE4 surface and facies 5a. The closest core to the southeast of 9-22-33-5W5 shows a similar thickness of allomember D, but facies 9 is much thicker in this well and is truncated at the top by the VE4 surface.

In allomember E, (Fig. 6.7) the coarse sediment package (yellow) on top of VE4 does not show any major variations in thickness along strike. An important lateral facies transition within the coarse sediment package is shown on gamma ray and resistivity well log shapes in the 8-17-32-2W5 and 14-8-31-1W5 wells. The resistivity log response of the coarse sediment package at 8-17-32-2W5 (Harmattan East)

Figure 6.7. Log cross section D-D'. Location of cross section is shown on accompanying map.

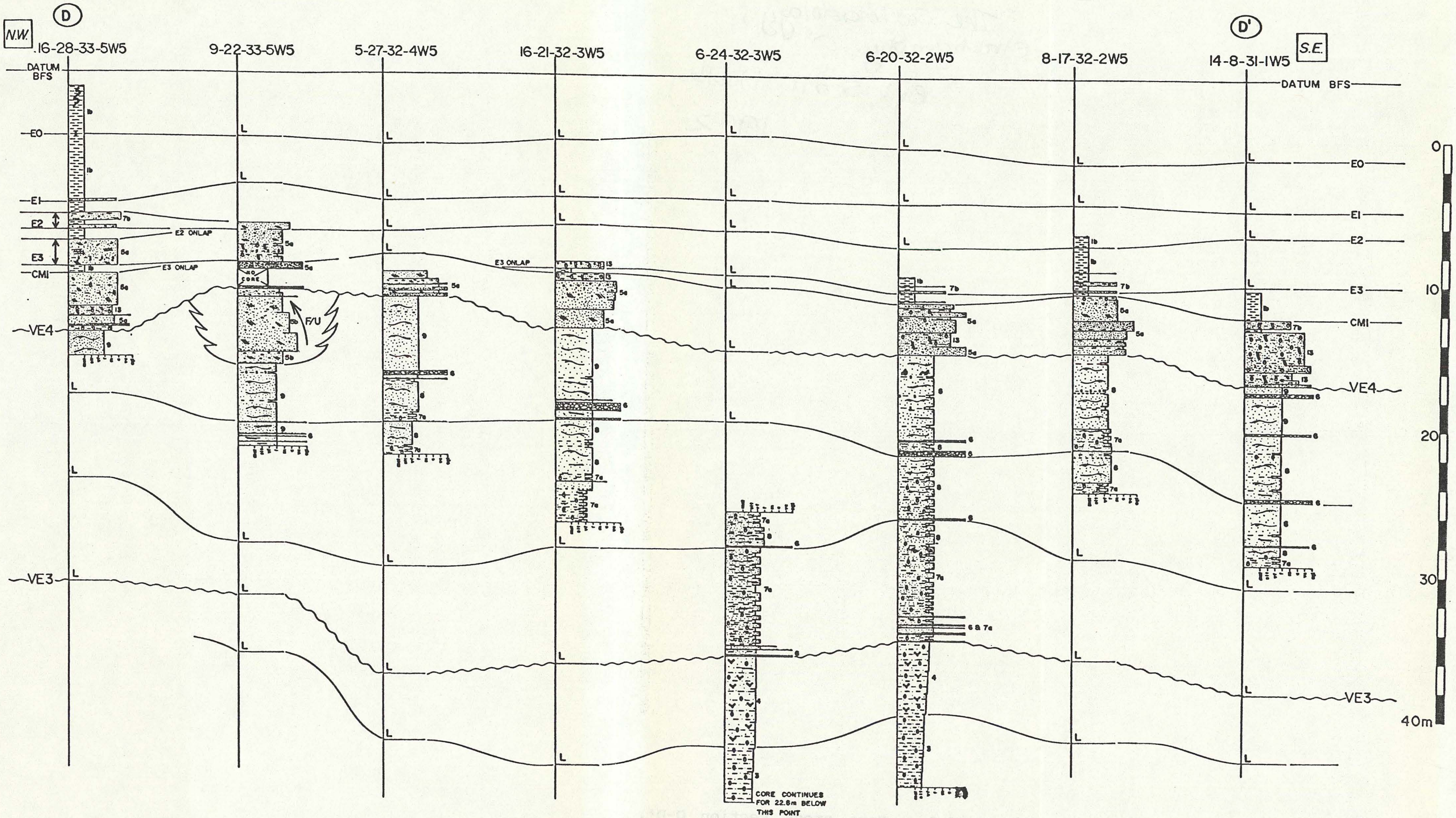
D
N.W.
16-28-33-5W5
9-22-33-5W5
5-27-32-4W5
16-21-32-3W5
6-24-32-3W5
6-20-32-2W5
8-17-32-2W5
14-8-31-1W5
D'
S.E.
DATUM BFS
E0
E1
E2
E3
CMI
VE4
VE3
E2 ONLAP
E3 ONLAP
F/U
CORE CONTINUES FOR 22.8m BELOW THIS POINT
6 & 7a
0
10
20
30
40m

shows a large deflection to the right and records the presence of oil filled reservoir sandstones within the field. At 14-8-31-1W5 (in an off field position) the resistivity well log response is essentially vertical (ie. no abrupt transitions). The VE4 contact and the top of the coarse sediment package (CM1) at 14-8-31-1W5 has been picked by correlating core to the log response. Both of these picks would have been very difficult to make without core control. Core cross section D-D′ (Fig. 6.8) shows that the difference in well log response in the coarse sediments on the VE4 surface at 8-17-32-2W5 and 14-8-31-1W5 can be explained by 1) a lateral facies change from "cleaner" sandstones of facies 5a at 8-17-32-2W5 into "muddier" rocks of facies 13 at 14-8-31-1W5 and 2, the change from oil filled reservoir sandstones at 8-17 towards non oil filled muddy sandstones at 14-8.

Log cross D-D′ also shows the onlap locations of the E4 and E3 markers. The E4 marker onlaps southeast of Harmattan East between 14-8-31-1W5 and 10-23-30-29W4. The onlap position of E4 corresponds with a gradual "step" in the VE4 surface between these two wells. The E3 marker onlaps in two areas of the cross section, one northwest of the Harmattan East field between 16-21-32-3W5 and 5-27-32-4W5, and the other southeast of the Caroline field between 16-28-33-5W5 and 9-22-33-5W5. The two E3 onlap positions shown in figure 6.7 appear to define a rise in the VE4 surface between the Harmattan East and Caroline fields. Log cross section D-D′ also shows that the E3 marker is thicker to the northwest at Caroline and becomes thinner to the southeast at Harmattan. This thickness relationship can also be seen in core cross section D-D′ (Fig. 6.8). The E3 marker at 16-21-32-3W5 is a 60 cm burrowed sandstone bed that thins laterally along strike to a 15 cm thick sandstone bed at 8-17-32-2W5. The E3 marker at 16-28-33-5W5 (D) is more substantial in thickness and is seen as 1.9 m of facies 5a. The lateral correlation of facies 5a at 16-28-33-5W5 to the core at 9-22-33-5W5 is problematic because some of the core (approx. 2 m) is missing at 9-22-33-5W5. Based on the core that is present, it appears that the sandstones associated with E3 at 16-28-33-5W5 amalgamate at 9-22-33-5W5 and become "muddier" along strike to the southeast.

6.2.4 Log Cross Section E-E′ and Core Cross Section E

Log cross section E-E′ is shown in figure 6.9 and the corresponding core cross section is shown in figure 6.10. It illustrates a similar allomember A-B southeastward thickening relationship to that observed in log cross section D-D′. The base of allomember A-B (BV) is also problematic in cross section E-E′ and the correlation shown is based primarily on the three wells (6-36-30-4W5, 8-12-30-3W5, 2-13-29-2W5) that tie into the dip oriented cross sections described earlier.

Correlation of the LM1 marker in allomember A-B is

Figure 6.9. Log cross section E-E'. Location of cross section is shown on accompanying map.

useful for showing the amount of erosion on the VE3 surface. This is shown in figure 6.9 as a lateral thinning of section between VE3 and LM1. The interval between LM1 and VE3 at 6-13-31-1W5 (E) is approximately 2.5 m thick and the interval thickens (approx. 15 m) to the southwest at 11-10-28-28W4 (E′). The VE3 surface in cross section E-E′ is relatively flat along strike, and roughly parallels LM2.

Two coarsening upwards units, designated D1 and D2 have been correlated in allomember D (Fig. 6.9) to facilitate a discussion of the lateral facies changes in this allomember southwest of Harmattan East. The correlation of these units may be questionable because the log character is often variable from well to well on the cross section. The base of D1 is shown in core cross section E-E′ (Fig. 6.10) at 6-36-30-4W5 and 2-13-29-2W5 where fine grained sandstones of facies 9 sharply overlie medium grained sandstones at the top of D2. Both cores show D1 as a sequence that coarsens upwards and is capped by non marine facies. The D2 sequence also coarsens upwards. Non marine facies in figure 6.10 are not correlated at 6-5-30-2W5 and 11-10-28-28W4. They were either not deposited at these locations, or more likely were deposited but were removed by erosion on the VE4 surface.

Figure 6.9 illustrates the lateral relationships of allomember E onlap markers in the southern areas of the study. The E3 marker (red) onlaps between 6-24-29-2W5 and 2-13-29-2W5 and amalgamates with the coarse sediment unit

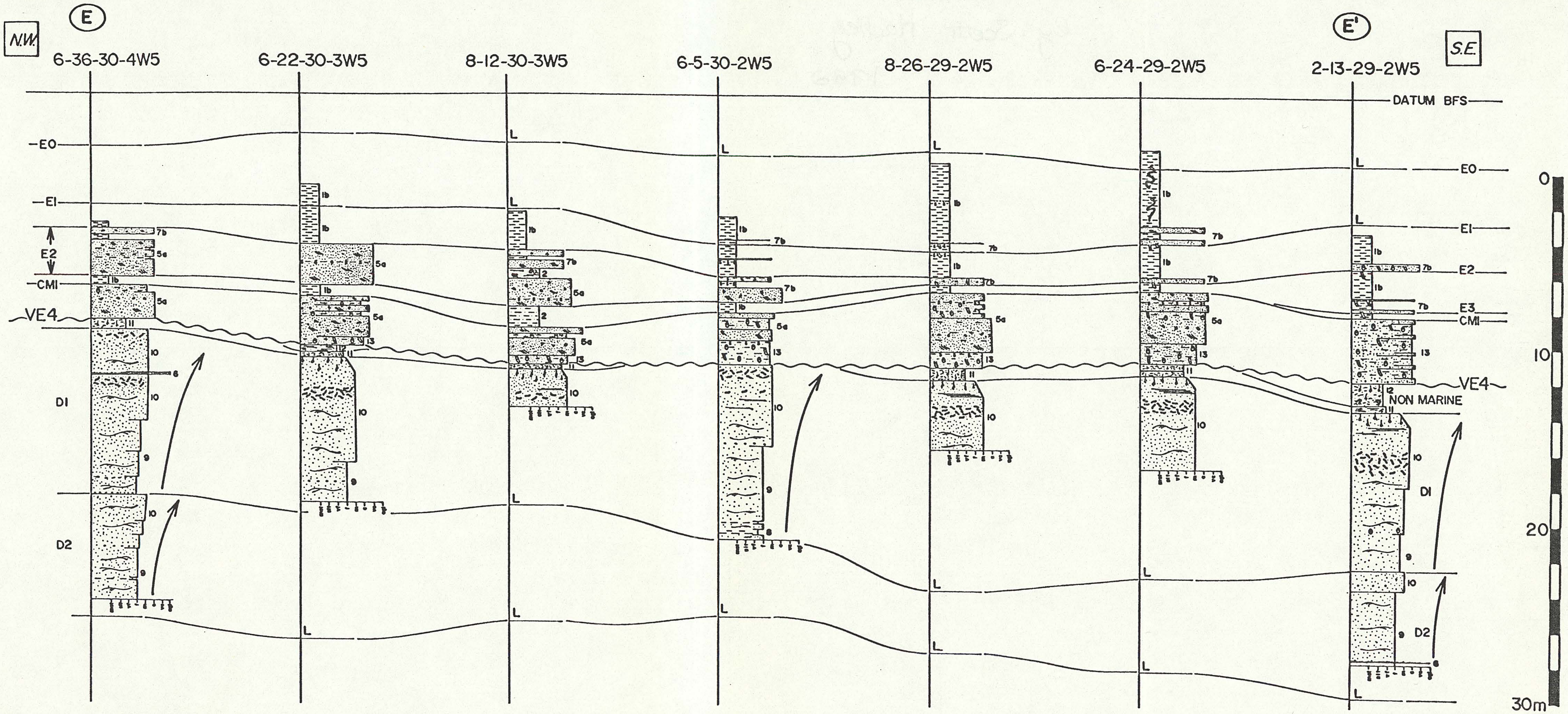

N.W.
E
6-36-30-4W5
6-22-30-3W5
8-12-30-3W5
6-5-30-2W5
8-26-29-2W5
6-24-29-2W5
2-13-29-2W5
E'
S.E.
DATUM BFS
EO
EI
E2
CMI
VE4
D1
D2
E3
NON MARINE
0
10
20
30m

(yellow). This marker also displays a similar thickness trend to that seen in log cross section D-D′ (ie. thins towards the southeast). The E2 marker (green) does not onlap in log cross section E-E′ but does show a substantial southeast thinning. Core cross section E-E′ shows the lateral thickness and facies changes of the E2 marker. At 6-36-30-4W5, the E2 marker is a 3 m structureless and cross bedded sandstone (facies 5a) that thins to the southeast at 2-13-29-2W5 where it is a 40 cm thick burrowed and bioturbated coarse grained sandstone (facies 7b).

6.3 <u>Summary</u>

The log and core cross sections show regional trends of the lateral distribution of Viking allomembers and facies, and illustrates the two dimensional geometry of VE bounding discontinuities either parallel or perpendicular to depositional strike of the Harmattan East field.

The following geometrical characteristics are consistently observed on the three dip log and core cross sections (oriented perpendicular to the strike of the field):

1) the BV pick (allostratigraphic base of Viking Formation) appears to overlie the Joli Fou Formation to the northeast of Harmattan East field and to the southwest, overlies a sandstone unit that is thought to represent a Basal Colorado sandstone or possibly a Joli Fou Formation equivalent sandstone. The correlation of the Joli Fou, Basal

Colorado sandstone, and BV are questionable because of the limited core control at these stratigraphic intervals,

2) the correlation of sandier upwards units between BV and VE3 are useful for illustrating the topography on the VE3 surface. The S/U units below VE3 depositionally thin, and appear to downlap towards LM2 in a northwestward direction,

3) the VE3 surface drops northeastward relative to the BFS datum. The most significant drops occur in two areas. The first is just southwest of Harmattan where up to 12 m of relief was recorded on cross section A-A′, and the second is northeast of Harmattan where 7 m of relief was recorded on cross section A-A′ and B-B′. The VE3 surface remains essentially flat at Harmattan relative to BFS and then drops again northeast of Harmattan,

4) allomember D thickens to the northeast and is dominated by fine grained hummocky and swaley cross-stratified sandstone at Harmattan East field, while medium grained cross-stratified sandstones, fine grained planar laminated sandstones, and nonmarine deposits dominate the upper part of allomember D southwest of Harmattan. Three S/U units were correlated on each cross section. These units plus the laterally correlative nonmarine deposits are useful for showing the apparent erosion on the VE4 surface. Each unit shows an undulating character with the other, with no systematic thickening or thinning trends. The first sandier

upwards unit (S/U 1) appears to downlap towards VE3 immediately northeast of 7-34-33-28W4 in C-C′. The nonmarine deposits thicken (maximum 7.5 m recorded on B-B′) southwest of Harmattan. Laterally equivalent nonmarine deposits are absent at Harmattan East field wells, and in northeasterly wells, presumably because of erosional downcutting on the VE4 surface,

5) the VE4 surface drops relative to BFS towards the northeast with the maximum relief recorded on cross sections being 13 m. This drop is produced by two subtle "steps" which seem to make up one gradual "step". The most pronounced "step" occurs northeast of Harmattan where the E4 marker appears to onlap with deposits on the VE4 surface (cross sections B-B′ and C-C′). The second step is defined by the onlap position of the E3 marker. This step occurs along the western margin of the Harmattan East field and can be seen on all three cross sections as relief up to 3 m,

6) the lowest stratigraphic deposits of allomember E, found between VE4 and CM1 (yellow-coarse sediment package) are thickest at Harmattan (up to 5m, cross section A-A′). The deposits progressively thin northeast of Harmattan from a thickness of less than 2 m to 10′s of cms (eg. well 10-30-33-1W5, A-A′). The deposits between VE4 and CM1 southwest of Harmattan remain at thicknesses between 2 and 3 m with several exceptions. The correlation of E markers above CM1 in wells southwest of Harmattan East show a thicker coarse

sediment package apparently produced by amalgamation of E marker sandstones with older deposits between CM1 and VE4. The coarse sediment package (CM1 to VE4) is dominated by cross bedded and structureless pebbly sandstone to the southwest. The thinner deposits to the northwest are predominantly bioturbated pebbly sandstone-mudstone,

7) the coloured markers designated E0 through E4 of allomember E represent the correlation of coarse grained sandstone beds and log markers above the CM1 surface. The lateral correlation of these markers shows that they sequentially onlap the CM1 surface in a southwest direction, with each "E" marker closely paralleling the BFS datum. E4 occurs at the lowest stratigraphic level and onlaps east of Harmattan in a line oriented roughly northwest-southeast. E4 does not appear on cross section A-A′ and is thought to onlap farther to the northeast outside the study area. E3 appears to onlap CM1 along the western margin of Harmattan in a northwest-southeast orientation. E2 onlaps the CM1 surface in the southwest portion of the study (cross sections A-A′ and B-B′). E2 appears to rest on VE4 and probably replaces the deposits between CM1 and VE4 to the northeast. E0 and E1 apparently do not onlap the CM1 surface in the study area. The BFS datum, E0 and E1 markers presumably merge or onlap with the VE4 and/or the CM1 surface further to the southwest outside the study area.

The E2 and E3 markers that onlap the CM1 surface southwest of Harmattan usually have cross bedded pebbly sandstone at their onlap positions. To the northeast this crossbedded sandstone changes laterally into thinner cross bedded sandstone beds that may contain mudstone and siderite rip up clasts. When traced further to the northeast in a basinal direction this laterally equivalent "E" marker may change into a thin (10's cm thick) coarse sandstone or bioturbated pebbly sandstone-mudstone with abundant Arenicolites burrows that eventually pass into a sideritized mudstone. This lateral facies change is usually achieved over distances of 10's of kms.

The two log and core cross sections oriented parallel to the strike of the Harmattan East field are useful for illustrating the lateral relationship between Caroline and Harmattan East, and also for showing the relationship between nonmarine and marine deposits southwest of these fields. The following characteristics were observed in cross section D-D' (Caroline to Harmattan East):

1) allomember A-B thickens towards the southeast from 12 m at Caroline to approximately 21 m southeast of Harmattan,

2) VE3 drops relative to BFS along strike towards the southeast. A gradual drop occurs at the southeast margin of Caroline where up to 8 m of relief was recorded on the VE3 surface between these two fields,

3) VE4 rises along the southeast margin of Caroline

and remains stratigraphically higher until it reaches Harmattan East where it abruptly drops about 5m, and continues to gradual drop to the southeast,

4) the coarse grained deposits between CM1 and VE4 remain a consistent thickness (approx. 4-5 m thick) at Caroline and Harmattan East but thin along strike southeast of Harmattan (approx. 1-2 m thick),

5) the "E" markers in allomember E exhibit lateral continuity from well to well. The E4 marker onlaps the CM1 surface southeast of Harmattan. The E3 marker onlaps CM1 at the northwest margin of Harmattan and southeast margin of Caroline. Presumably the E3 onlap position is influenced by the topographic rise on the VE4 surface between Caroline and Harmattan.

Cross section E-E′ is oriented parallel to the strike of Harmattan and is located southwest of section D-D′. The following characteristics are revealed on E-E′:

1) allomember A-B thickens towards the southeast in a similar manner to that observed on D-D′,

2) VE3 exhibits an undulating topography across the section with no recognizable pattern,

3) the nonmarine deposits in allomember D show lateral continuity in thickness across the section. The deposits are absent in two wells 6-5-30-2W5 and 11-10-28-28W4 presumably because of downcutting on the VE4 surface,

4) the coarse grained deposits between CM1 and VE4

remain a uniform thickness across the section,

5) the coarse grained beds in allomember E (E0 to E3) exhibit lateral continuity from well to well. The E2 marker is the thickest of these onlap markers. It is 1-2 m thick at wells located in the northwest portion of the study and thins to less than 1 m along strike to the southeast.

Chapter 7 Maps and two Dimensional Plots

7.1 Introduction

The purpose of this chapter is to examine in more detail the erosion surfaces that were described previously in chapter 6. Isopach maps were constructed to show changes in thickness between bounding surfaces, and to show topography on a particular surface. Specific emphasis was placed on mapping the morphology of both the VE3 and VE4 surfaces as these were the only documented erosion surfaces within the study area.

7.2 Construction of Isopach Maps

The first type of isopach made was used to illustrate the topography of both the VE3 and VE4 surfaces within the mapped area (T28 to T33, R28W4 to R4W5). This type of isopach map shows the interval from a lower datum (LD) 120 m below BFS. The use of a lower datum, parallel to BFS creates higher isopach values for topographic highs and lower values for topographic lows. If BFS (and hence LD) are assumed to be flat, then the isopach maps can be used to interpret topography on the VE3 and VE4 surface.

The second type of isopach map was constructed using subtracted values of an upper marker from the values of a lower marker. This subtraction produces a positive number which can be used to show actual differences in thickness between bounding discontinuities and/or log markers. Isopach maps of this type were constructed for the LM2 to VE3 interval, VE3 to VE4 interval, VE4 to CM1 interval, and the VE4 to BFS interval. Figure 7.1 shows the location of wells (data points) used in the construction of the maps.

The asterisks on each isopach map designate well locations at Harmattan East field. Asterisks representing wells in off-field locations have been left off the maps for the purpose of clarity. All data were recorded in Lotus 123 (raw numerical data is stored at McMaster University, Dept. of Geology). The conversion of CPA well numbers into an arbitrary x,y coordinate and the necessary subtractions were performed by Quick Basic programs. All isopach maps were constructed using the commercially available software package Surfer, published by Golden Software Inc. of Golden, Colorado.

7.3 VE3 Morphology: BFS-VE3 Topography Isopach and VE3 LM2 Thickness Isopach Map

The interval between LD (120 m below BFS) and VE3 was isopached (Fig. 7.2) to determine the morphology of the VE3 surface. Large numbers (relative to LD) suggest topographic "highs" along the surface. Figure 7.2 shows the rise in topography towards the southwest that was demonstrated on log

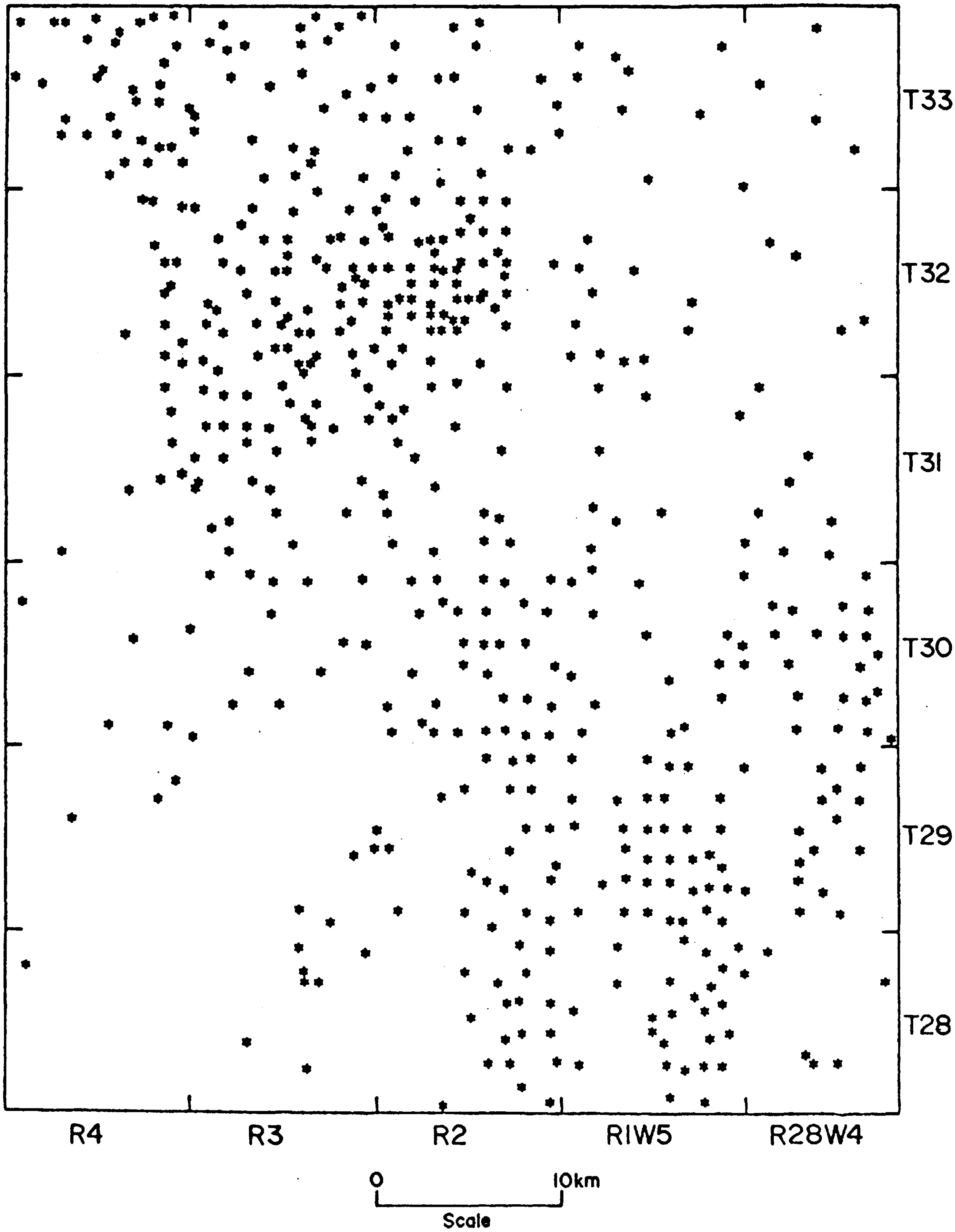

Figure 7.1. Location of data points used for the construction of isopach maps shown in this chapter. Asterisks mark the location of wells.

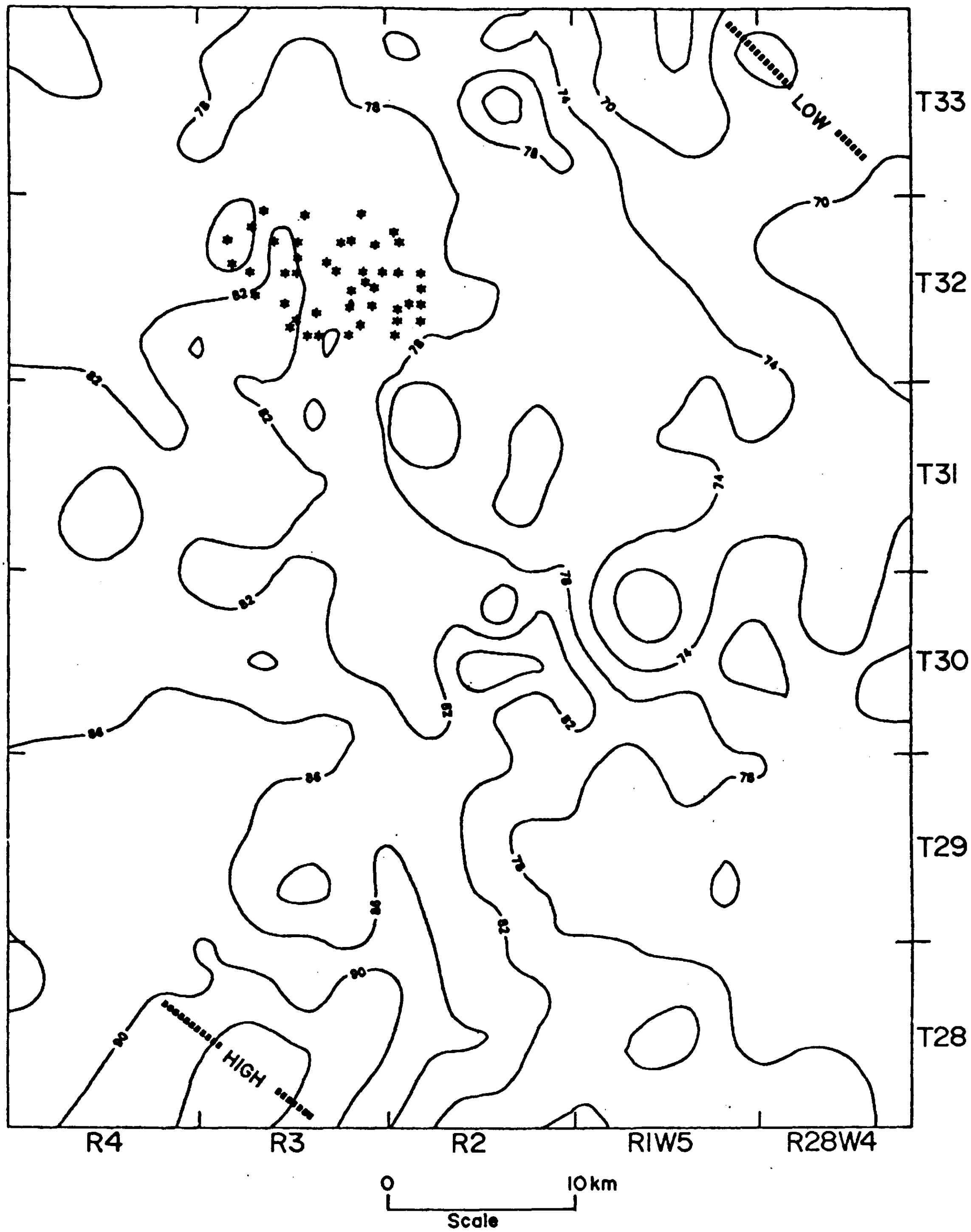

Figure 7.2. Isopach of 120 - (VE3 - BFS). This isopach is used to show topography on the VE3 surface. Small values represent lows and vice versa. Note the "low" in the northeast and "high" in the southwest.

cross sections A-A′ and B-B′ (Chapter 6). A pronounced high is located in the southwest quadrant on the map, and a low in the northeast quadrant. The dominant trend of the contour lines is northwest to southeast.

The total thickness isopach map of VE3 to LM2 (Fig. 7.3) is useful for showing the amount of erosion on the VE3 surface. Log cross sections discussed in chapter 6 showed LM2 as a relatively flat log marker parallel to the BFS datum. If, for the purpose of this discussion, we assume LM2 to be parallel to BFS, then thins on the map may represent areas of maximum erosion on the VE3 surface.

Overall, the total thickness of sediments between VE3 and LM2 are thinnest (approx 8 m thick) in the northwest portion of the map area, and thicken towards the south and east (up to 26 m).

7.4 <u>VE4 Morphology: BFS-VE4 Topography Isopach, VE4-VE3 Isopach, and BFS-VE4 Isopach</u>

The interval between VE4 and LD was also isopached to determine the morphology on the VE4 surface (Fig. 7.4). This map can be used to interpret the morphology of the VE4 surface assuming that LD and BFS are flat. The VE4 - LD isopach shows a pronounced northwest - southeast trend in the middle of the map that gradually shifts to a north - south orientation in the southwest. There is about 12 m of relief from the southwest portion of the map area to the northeast.

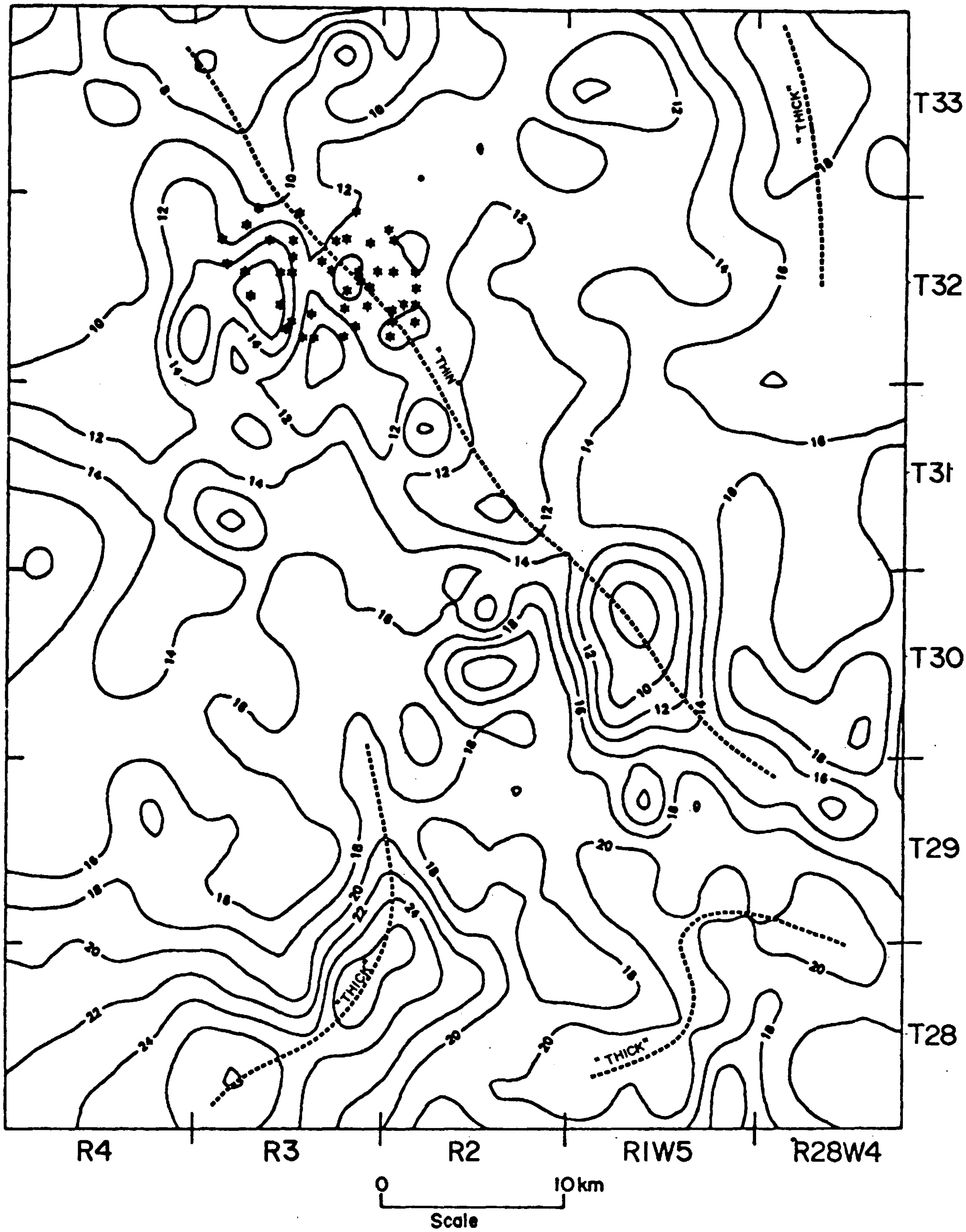

Figure 7.3. Isopach of VE3 to LM2. This isopach shows the total thickness of sediment between VE3 and LM2. Note the northwest-southeast trending "thin" across the middle of the map. Interpreted position of "thicks" are also shown.

A pronounced "step" trending northwest-southeast is situated throughout most of the middle portion of the map. The interpreted position of this "step" is shown on figure 7.4. The Harmattan East field appears to be situated on this "step" in a relative topographic "low", while a relative topographic "high" truncates the field boundary at the north towards Caroline. This step corresponds with the "Caroline step" of Davies (1990). For the purpose of this study, the "step" shown on figure 7.4 will also be referred to as the "Caroline step". It should also be pointed out at this time, that the "Garrington step" of Davies (1990) does not appear in the study area.

Figure 7.5 is a composite map that incorporates Davies (1990) VE4 topography map with the one created for this study. The map shows the position of the Caroline "step" and its relation to both the Caroline, Garrington, and Harmattan East fields. Davies lower datum was chosen 110 m below BFS, consequently the isopach values for his topography map are 10 m smaller than values presented on this studies figure 7.4, hence the contours do not match exactly. The map is still useful for showing the trend of the Caroline step and its relation to both Caroline and Harmattan East.

Three topographic profiles of the VE4 surface are shown on figure 7.6. The profiles labelled A through C are shown perpendicular to the strike of the Caroline "step". Each profile shows the gradual "step" like morphology of the

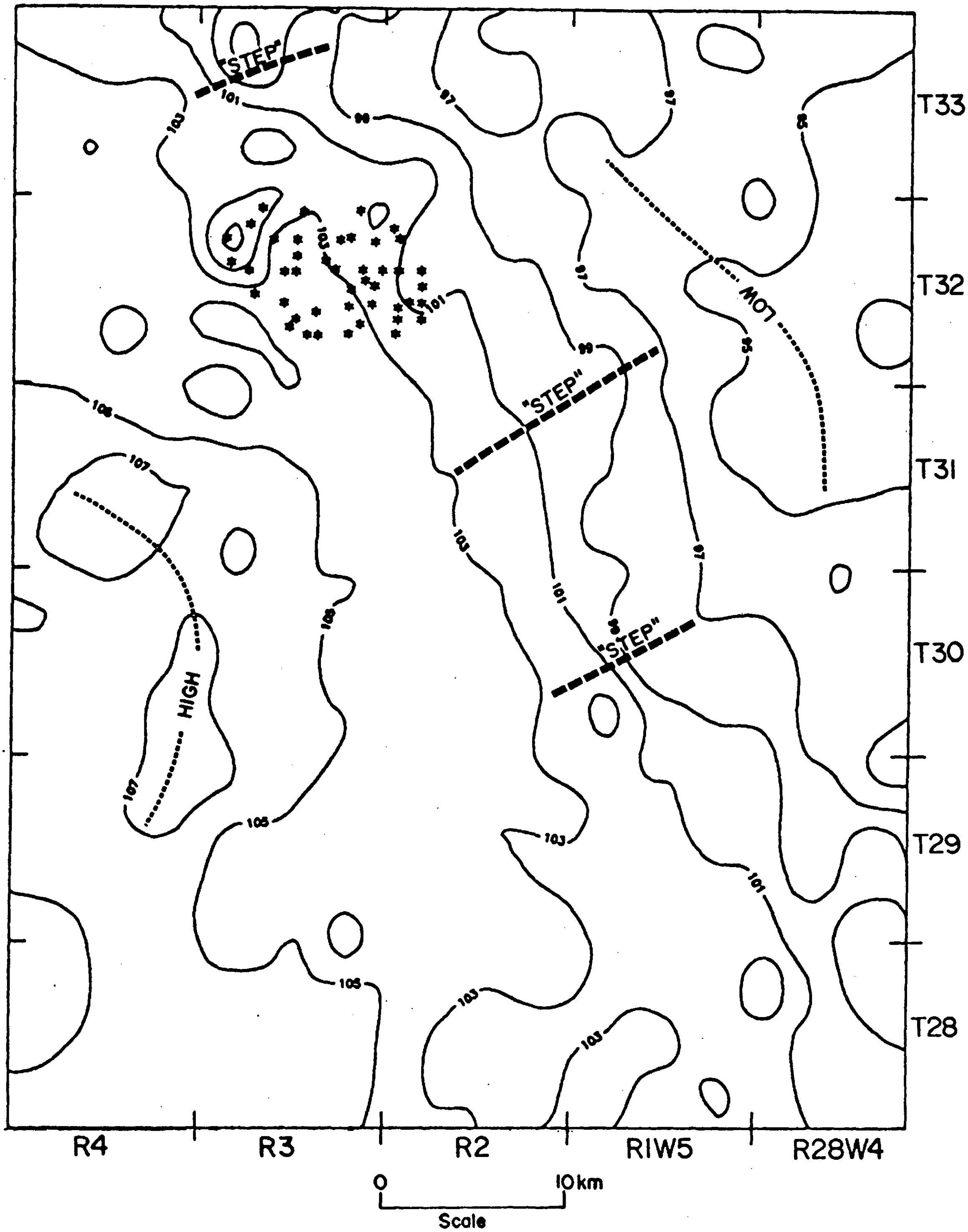

Figure 7.4. Isopach of 120 - (VE4 - BFS). This isopach is used to show topography on the VE4 surface. The numerical values are relative only. Note the "low" that occurs east of Harmattan and the "high" immediately to the southwest. Also note the interpreted position of a "step" on the VE4 surface.

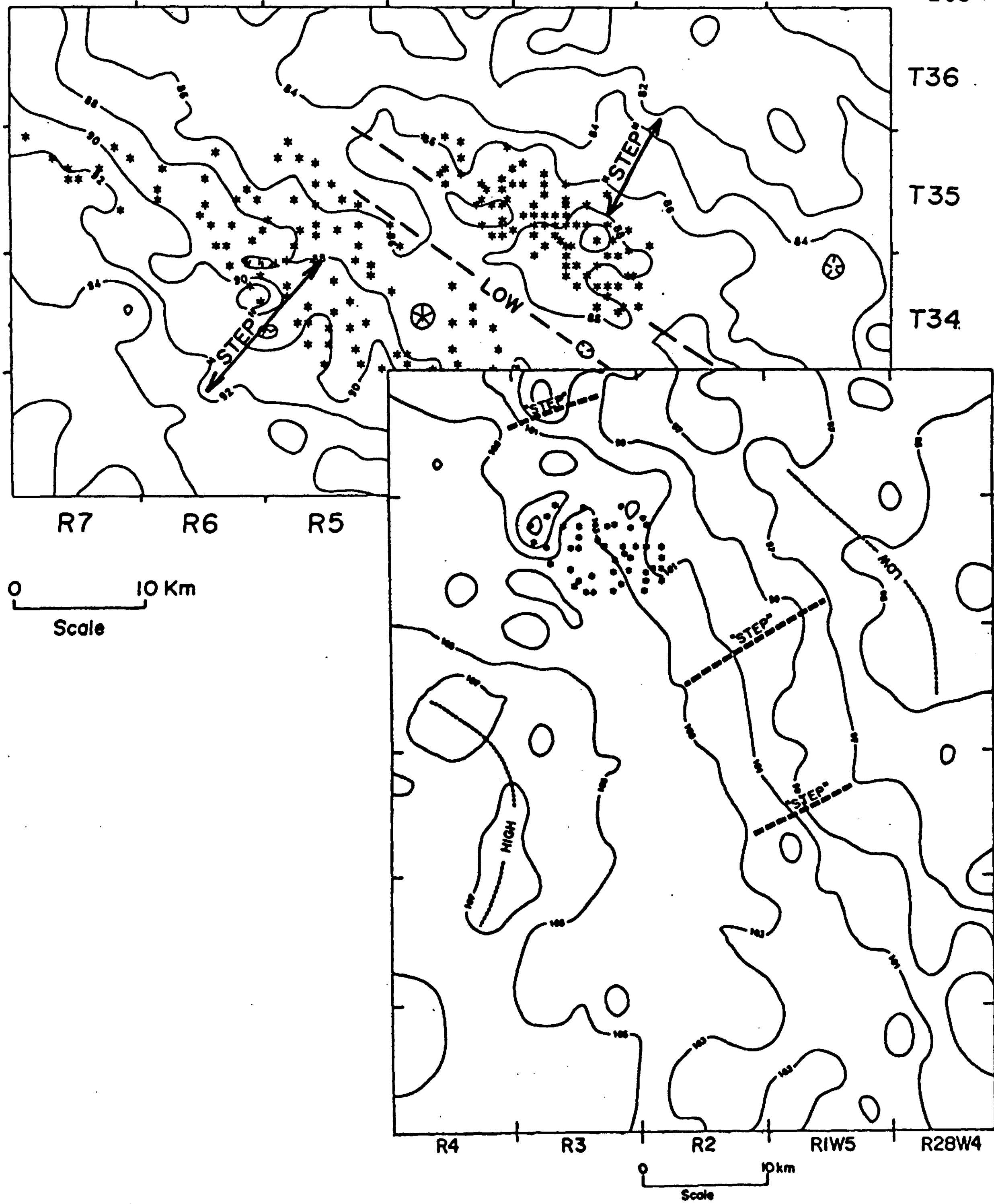

Figure 7.5. Composite map of two separate VE4 topography maps. This figure was combines Davies' (1990) VE4 topography map (his figure 6.3) which covers the Caroline and Garrington areas, and the VE4 topography map created for this study. Note the northwest-southeast "step" that coincides with the Caroline and Harmattan East fields. Also note the "low" that separates these two fields from the Garrington field.

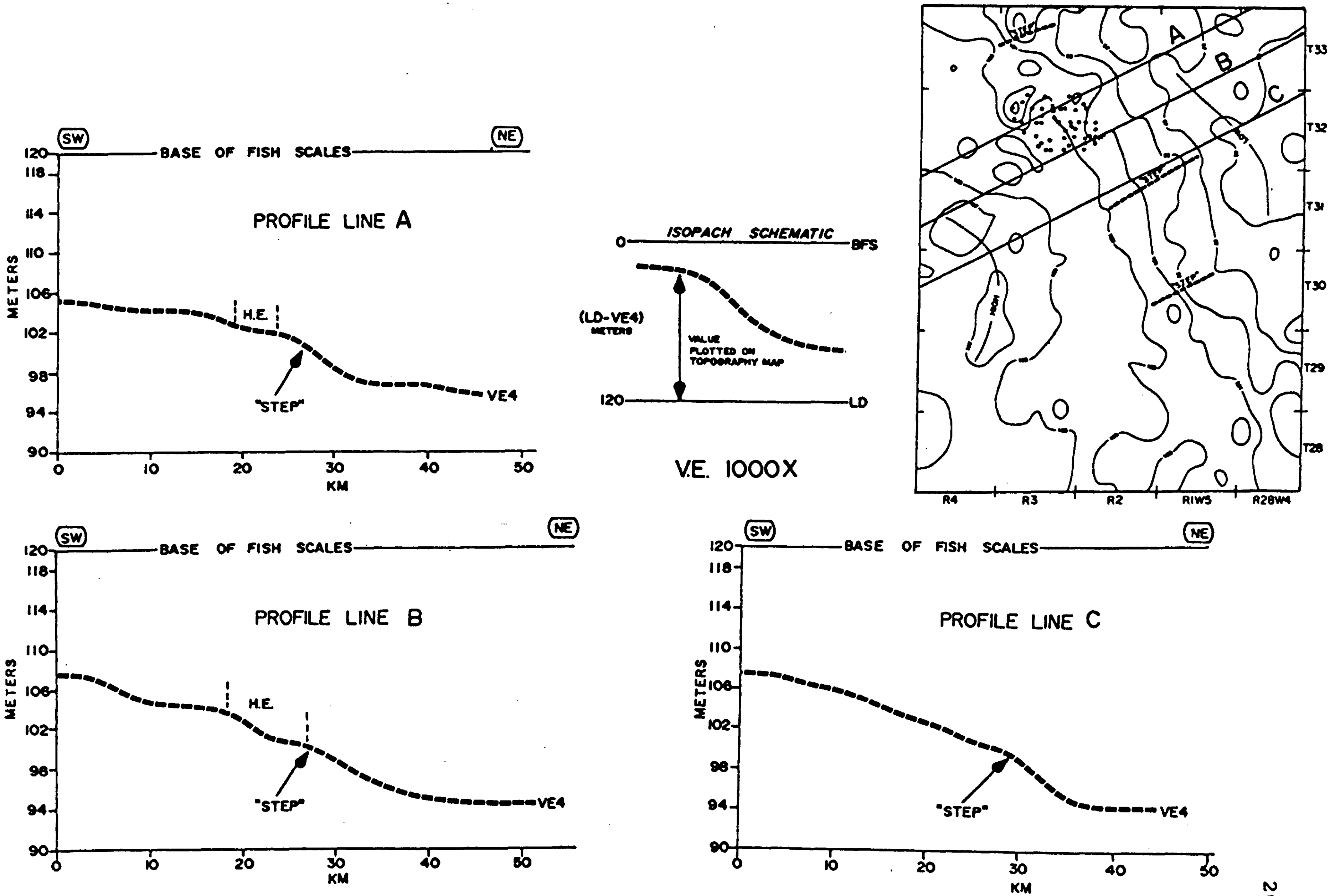

Figure 7.6. 2-D Plots. These plots were created using the isopach data of the VE4 topography map. The isopach schematic shows the subtraction and resultant value used to produce the isopach map. The inset map shows the location of profile lines A through C. The profile lines are discussed in text.

Caroline "step" rising to the southwest. The position of the Harmattan East field (H.E.) is shown on profile A and B. The field appears to be situated on a subtle depression or "notch" located in the upper part of the Caroline "step".

The BFS to VE4 isopach (total thickness of allomember E) is also useful for illustrating the morphology of the VE4 surface (Fig. 7.7). Assuming BFS is flat, then "thicks" represent topographic lows, and "thins" topographic highs. In general, a northwest-southeast trend is evident across the map area with the BFS to VE4 interval thinning (26 m to 12 m) towards the southwest in a similar trend that was observed on the LD - VE4 topography isopach. Alternatively, the map shows the rise in topography of the VE4 surface again assuming a flat BFS. This rise in topography is recorded by the progressive thinning of the interval towards the southwest. The VE4 surface appears to be getting closer to BFS in the southwest. Presumably the interval between VE4 and BFS becomes thinner and nonexistent further to the southwest as VE4 merges with BFS.

Facies were superimposed on the BFS to VE4 interval isopach to illustrate the erosional downcutting on the VE4 surface into underlying facies in allomember D. Figure 7.8 shows the BFS-VE4 isopach with location of various facies that occur directly below VE4 in allomember D. If the VE4 surface were flat, than one would expect similar facies to be preserved below VE4 across the map area. Figure 7.8 shows

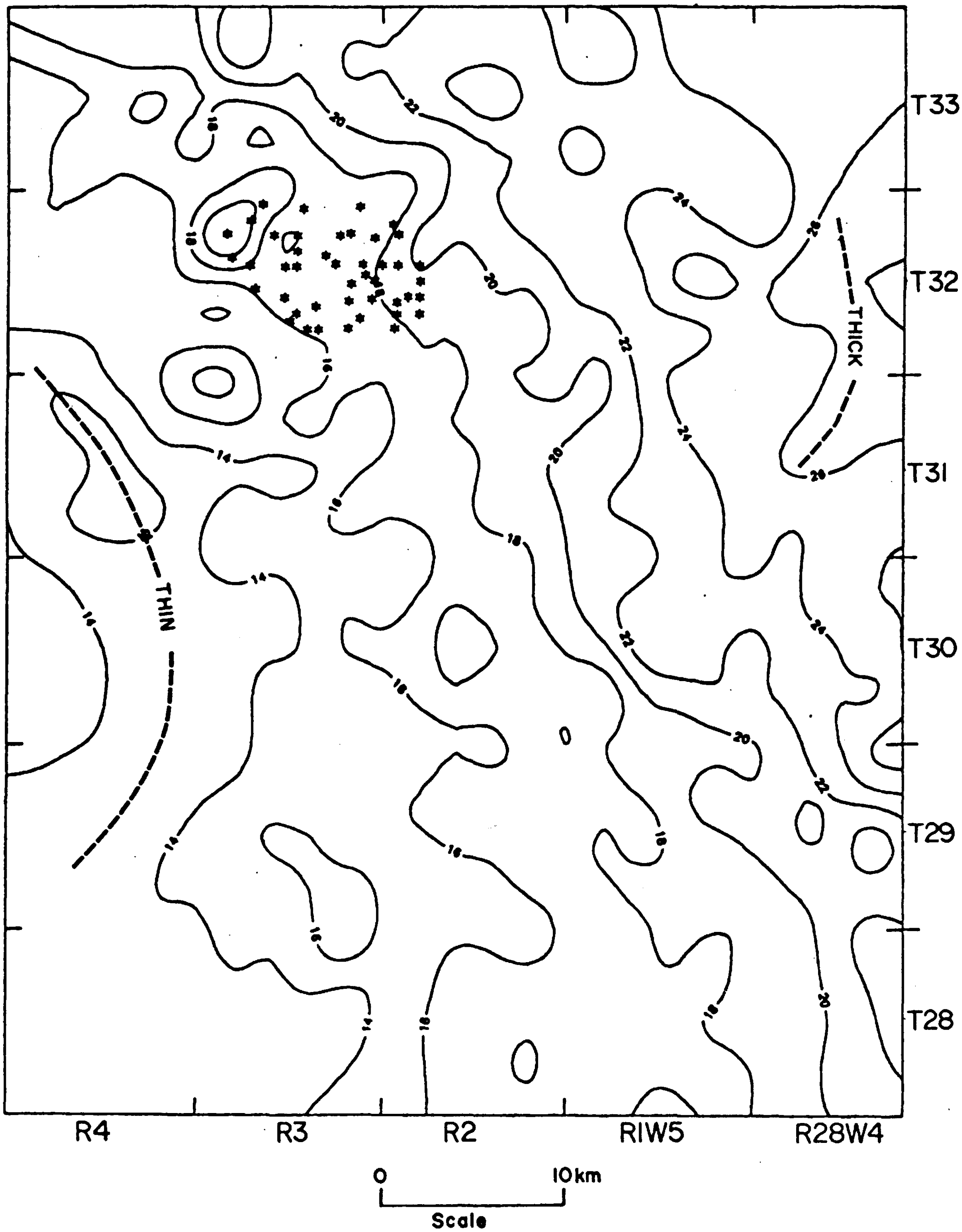

Figure 7.7. Isopach of BFS to VE4. This isopach shows the total thickness of sediment between BFS and VE4. Note the "thick" west of Harmattan East, and the "thin" immediately to the southwest.

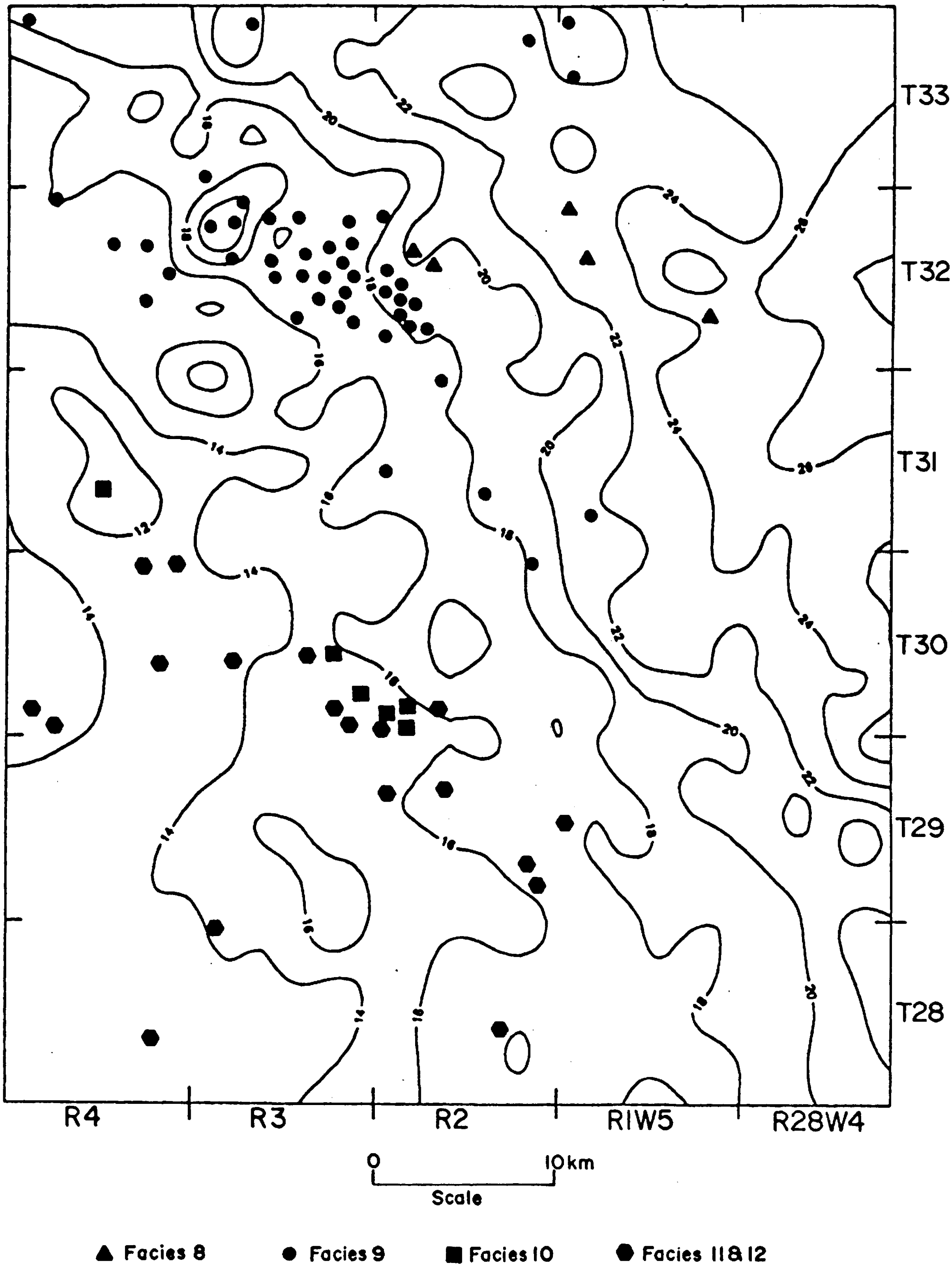

Figure 7.8. Facies distribution map of sediment directly below the VE4 surface, plotted on the BFS to VE4 isopach. Note the change in facies towards the southwest from facies 8 to facies 11 and 12.

that this is not the case. Four facies found directly below VE4 in the map area are: interbedded sandstone-mudstone (facies 8); thick bedded, nonbioturbated sandstone (facies 9); planar laminated and cross bedded sandstone (facies 10) and nonmarine facies 11 and 12 (grouped together for the purpose of this map). A lateral change in facies directly below VE4 is seen in a southwest direction towards areas of higher topography. Facies 8 occurs in areas northeast of Harmattan, facies 9 is concentrated at Harmattan and in areas northwest and southeast. Southwest of Harmattan, upper shoreface and nonmarine deposits (facies 10, 11, and 12) occur along a trend oriented northwest - southeast. Erosion on the VE4 surface appears to be greater in areas northeast of Harmattan where the surface cuts down into stratigraphically lower deposits in allomember D (mostly facies 8). Conversely, erosion on VE4 is of lesser magnitude southwest of Harmattan East where a continuous sequence from facies 8 through to facies 12 is preserved below VE4.

The relationship of the Harmattan East field to the total thickness isopach map of VE4 to VE3 is shown in figure 7.9. Harmattan East appears to be situated on a relative thin that is oriented west to east. The contours in figure 7.9 trend approximately northwest-southeast across the map area; however, in the vicinity of Harmattan East the contours shift to an east - west orientation. Overall, the thickness of sediments between VE4 and VE3 are thinnest (approx. 27 m)

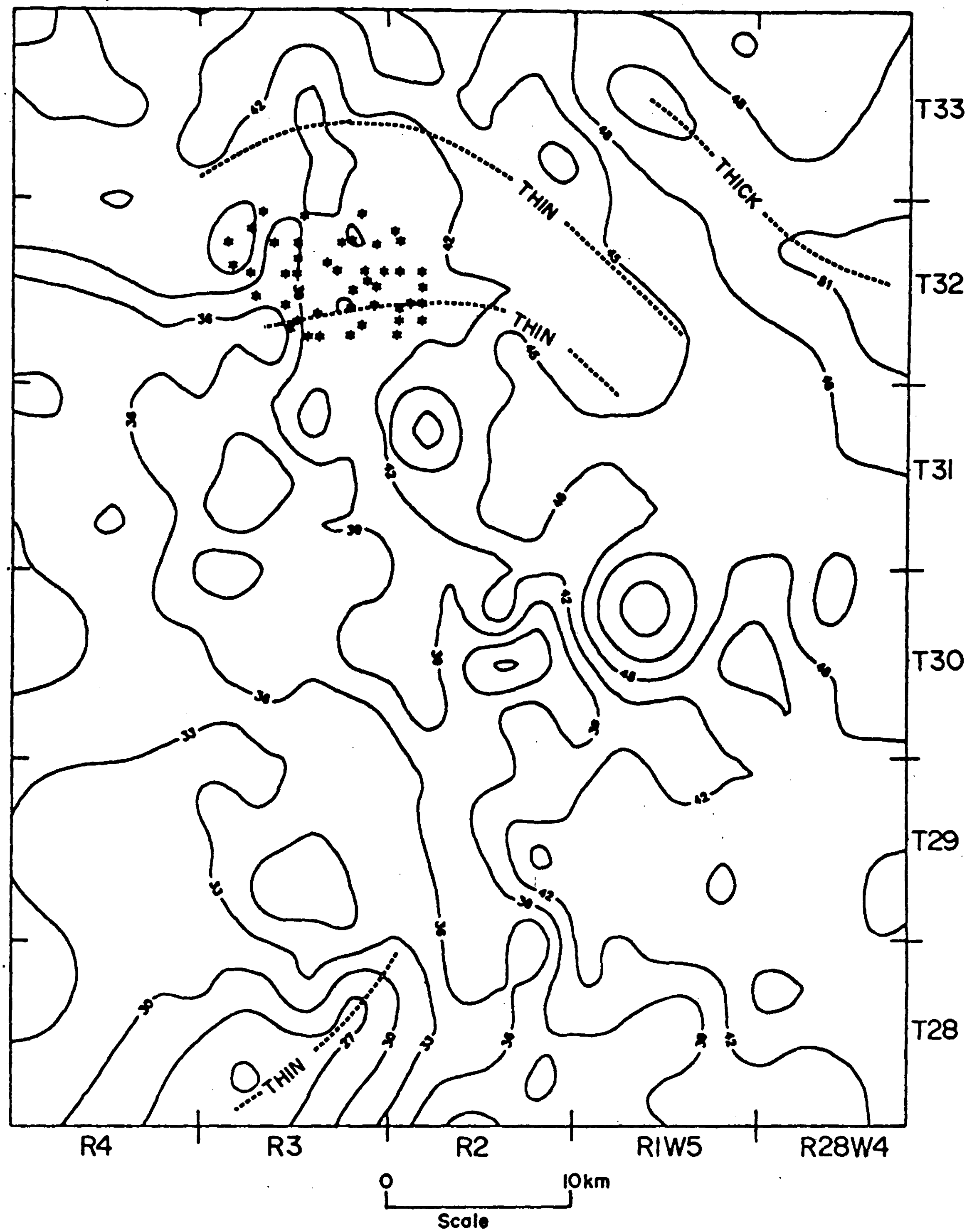

Figure 7.9. Isopach of VE4 to VE3. This isopach shows the total thickness of sediment between VE4 and VE3. The Harmattan East field appears to be situated on a relative "thin". Overall, the interval is thinnest in the southwest and thickens towards the northwest.

in the southwest portion of the map area, and thicken towards the northeast (up to 51 m thick). The variations in thickness between VE4 and VE3 may possibly be related to the surface morphology of the lower erosion surface (VE3). The VE3 surface was previously shown to be topographically high in the southwest (Fig. 7.2) portion of the map area. The VE4 to VE3 total thickness isopach shows a thin corresponding with a VE3 topographic "high" in the southwest portion of the map area, and a thick over a VE3 topographic "low" to the northeast. This may be interpreted in two ways. First, it suggests that erosion on the VE4 surface may have in part been influenced by the underlying topography on the VE3 surface. Secondly, potential "drape" on the VE3 surface may have created an irregular topography that was effected by erosion on the VE4 surface in different areas.

7.5 CM1 - VE4 Isopach Map

Figure 7.10 is an isopach map showing the thickness of the coarse grained sediment overlying the VE4 surface and bounded on the top by the CM1 surface. This interval represents the first deposits of allomember E deposited on the VE4 surface, and also comprises the reservoir interval at Harmattan East. Log and core cross sections in chapter 6 were used to show the lateral changes of the coarse sediment package and its relationship to coarse grained interbeds above. The correlations established a relationship

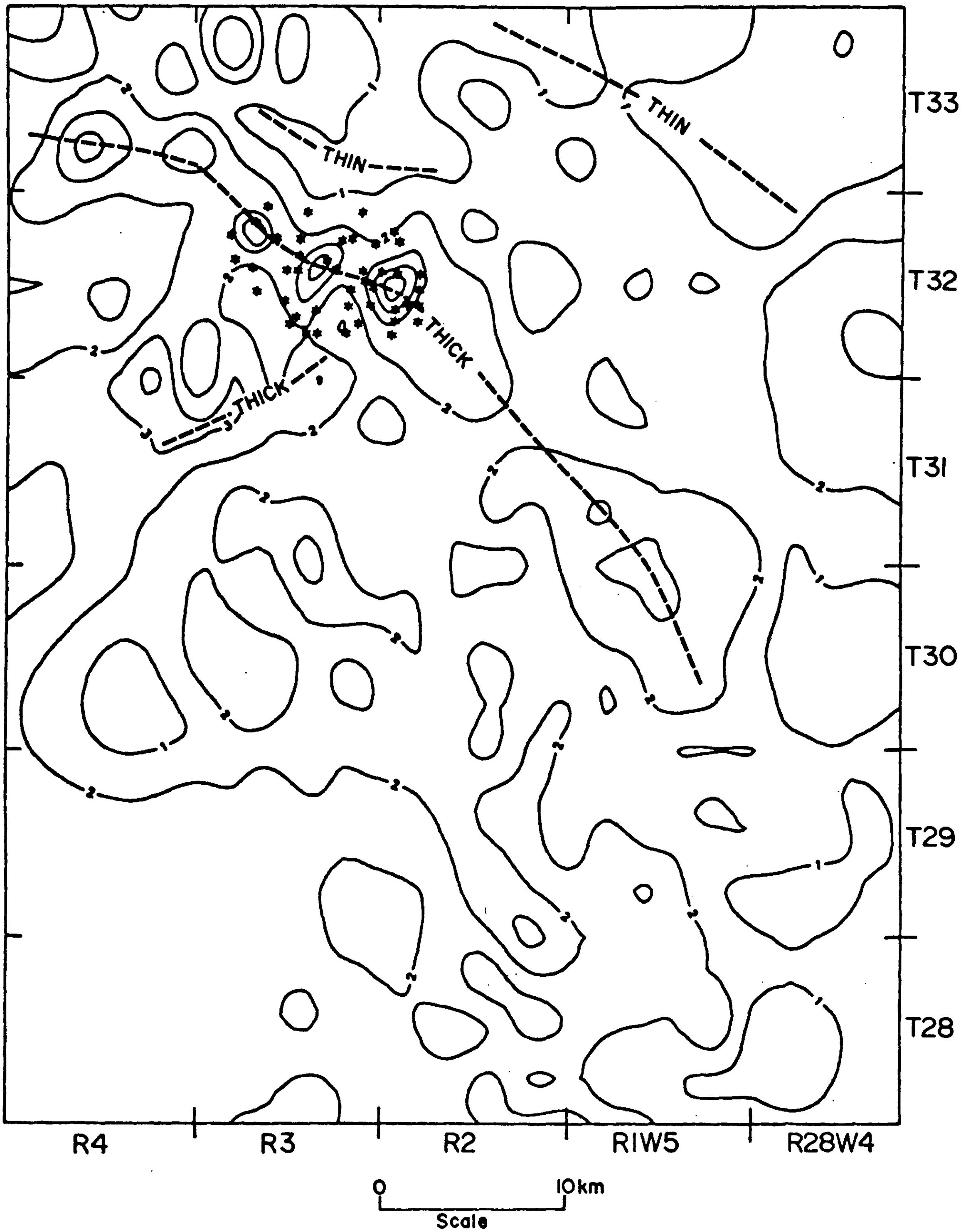

Figure 7.10. Isopach of the VE4 to CM1 interval. This map shows the thickness of the coarse grained sediment package which directly overlies the VE4 surface. Note the northwest-southeast trending "thick" at Harmattan East. Thinner deposits occur in off field areas to the northeast and in areas to the southwest.

between the "E" markers and their corresponding positions of onlap onto the CM1 surface. The CM1 to VE4 interval, therefore represents a combined thickness of primary coarse grained deposits (ie. initial sediments deposited on the VE4 surface), and secondary deposits which onlapped and amalgamated with the earlier deposited primary deposits.

The thickness of the CM1-VE4 interval averages 1-2 m across the map area. Closed isopach "thicks" appear to trend in a northwest-southeast orientation. The most obvious thickening of this interval occurs in the oil producing field areas located in the northwest quadrant of the map. Isolated "pod" like "thicks" form a northwest-southeast trend at the southeast limit of the Caroline field (3-4 m thick), and continues south and east through Harmattan East field where the deposits between CM1 and VE4 thicken up to 5 m. An additional "thick" occurs along the southwest margin of Harmattan East (up to 4 m thick) forming a ridge of coarse sediment oriented southwest - northeast. Also, the coarse sediment package appears to thin in a basinward direction northeast of Harmattan, and also along strike to the southeast of Harmattan. The geometry and stratigraphic relationship of the Caroline and Harmattan East fields, and their relationship to the CM1-VE4 interval are discussed in section 7.7 of this chapter.

Figure 7.11 is a composite map of Davies (1990) isopach of the coarse grained deposits on the VE4 surface

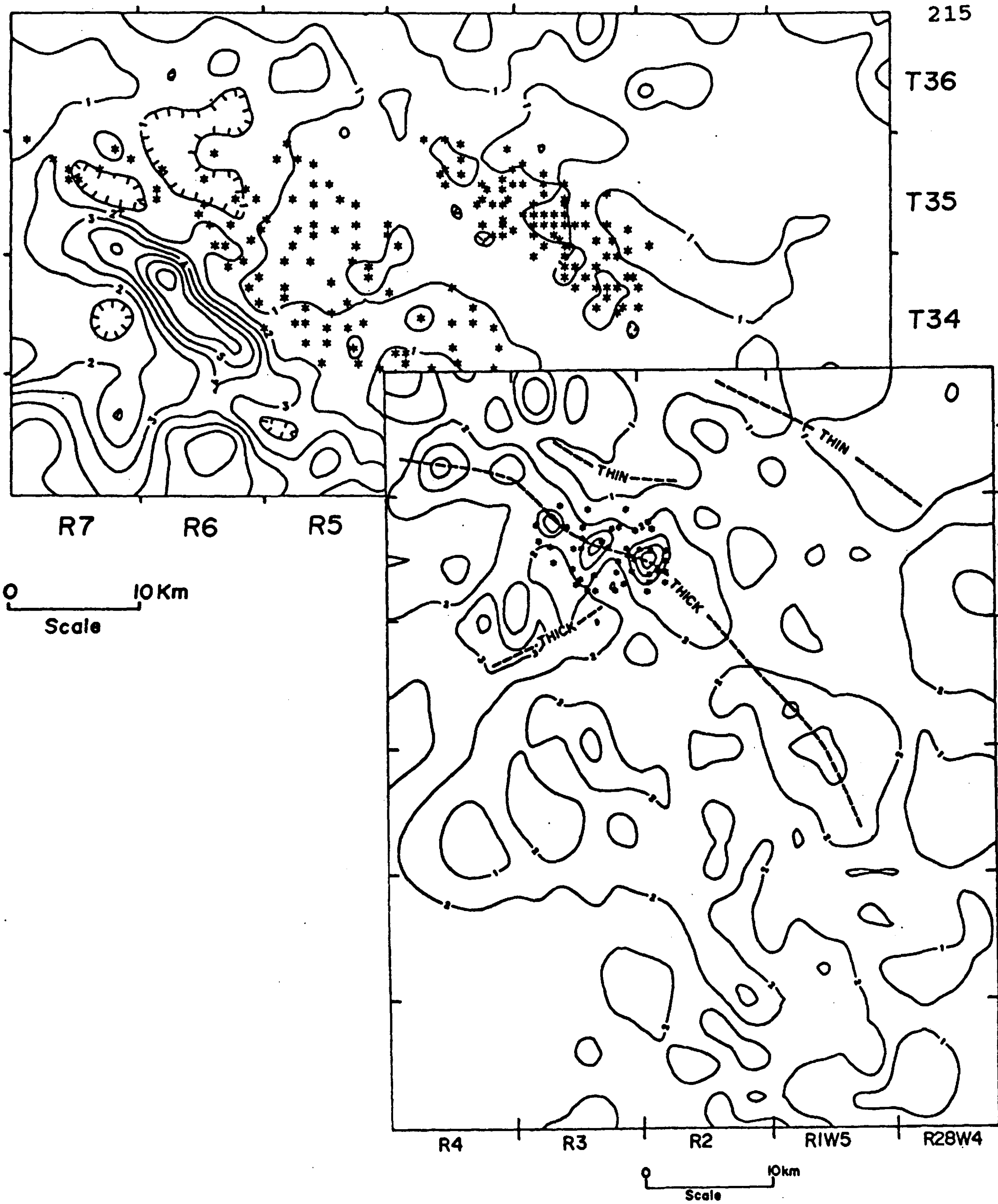

Figure 7.11. Composite map of two separate thickness maps of the coarse grained deposits directly overlying the VE4 surface. This figure combines Davies' (1990) VE4 to CM2 interval isopach (his figure 6.5), and the VE4 to CM1 isopach created for this study. Note the northwest-southeast thick that occurs at Caroline and extends along strike towards Harmattan East.

combined with the CM1-VE4 interval isopach of this study. The contours do not match exactly do to the limits of data at the boundaries of each map area, however, the map is useful for determining thickness trends of coarse grained deposits on VE4 and the relationship of these deposits to the various Viking oil fields.

The most dramatic feature apparent in figure 7.11 is the northwest-southeast linear ridge west of Caroline that extends along strike towards Harmattan East. This linear ridge of thickening is up to 8 m at Caroline and thins along strike towards Harmattan East where it is less than 2 m thick at the southeast margin of Harmattan East.

Three facies variations were superimposed on the CM1-VE4 interval (Fig. 7.12) in order to document lateral facies variation at this interval. The three facies variations plotted on the map are: facies 5a, facies 13, and interbedded facies 5a and 13. The facies of the coarse sediment package are primarily pebbly cross bedded and structureless sandstone (Facies 5a) with lesser amounts of pebbly bioturbated mudstone-sandstone (Facies 13). The CM1-VE4 interval may also be composed of an interbedded facies 5a and 13. The map is somewhat limited in data because most cores occur within the Harmattan East field, with only sporadic core control in off field areas.

Figure 7.12 shows that facies 5a occurs more frequently at Harmattan East where it is thickest. Facies

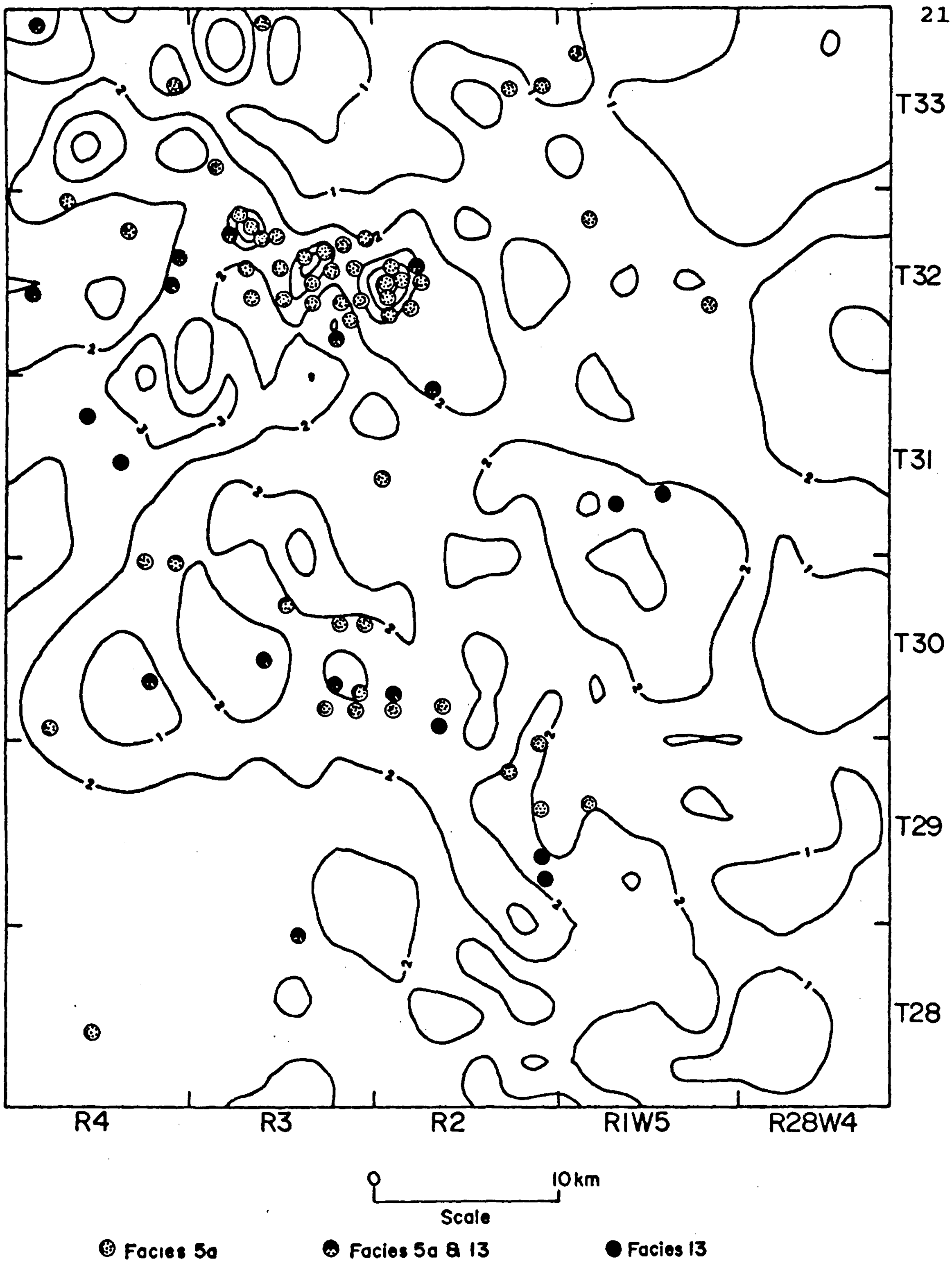

Figure 7.12. Facies distribution map of the VE4 to CM1 interval. This is the same map as figure 7.10 with the facies determined from core superimposed. Facies 5a occurs more frequently at Harmattan East where it is thickest. In off-field areas, facies 5a is thinner and occurs as an interbedded facies 5a and 13. Facies 13 occurs in areas southeast of Harmattan.

5a also occurs in off field areas, but is thinner and occurs as an interbedded facies 5a and facies 13. Southeast of Harmattan the CM1-VE4 interval documents a lateral change in facies along depositional strike. Facies 5a occurs within the field boundary. Interbedded facies 5a and 13 occurs along the southeast margin of the field and eventually passes into a CM1-VE4 interval composed of facies 13. In summary, "thicker" pebbly cross bedded sandstones are concentrated at Harmattan East and thin in off field wells with no apparent pattern. Lateral facies variations along strike appear to document a change from "cleaner" pebbly cross bedded sandstones within the field boundary to "muddier" pebbly bioturbated mudstone-sandstone equivalents in off field positions.

7.6 E0-E4 Onlap Position Maps

Onlap positions of "E" markers within allomember E were discussed previously in chapter 6. Well log cross sections A-A- to E-E′ showed a series of onlapping markers, E0 - E4 that sequentially onlap the CM1 surface in a southwesterly direction. The position of onlap is defined at the point where the base of each bed amalgamates with the CM1 surface, and the separating shale (facies 1b) pinchout. Location maps where each marker occurs are shown on figure 7.13. An interpreted line is drawn on each map which approximates each respective position of onlap. The E0 and

Figure 7.13.

(next 2 pages): Location maps of the E0 to E4 markers in allomember E.

a) well locations (as indicated by asterisks) where the E0 marker is recognized on well logs. E0 is present over the entire map area and presumably onlaps towards the southwest outside the study area.

b) well locations where the E1 marker is recognized on well logs. E1 does not onlap CM1 in the study area.

c) well locations where the E2 marker is recognized on well logs. E2 onlaps the CM1 surface in the extreme southwest portion of the map area.

d) well locations where the E3 marker is recognized on well logs. E3 onlaps the CM1 surface along the southwest margin of Harmattan East.

e) well locations where the E4 marker is recognized on well logs. E4 onlaps west of Harmattan and close to the E3 onlap line towards Caroline.

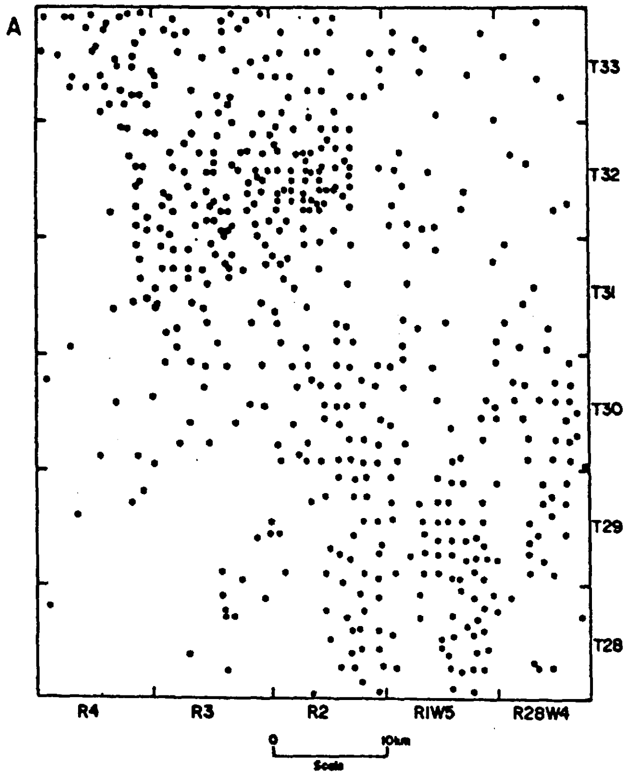
A
T33
T32
T31
T30
T29
T28
R4
R3
R2
R1W5
R28W4
0
10km
Scale

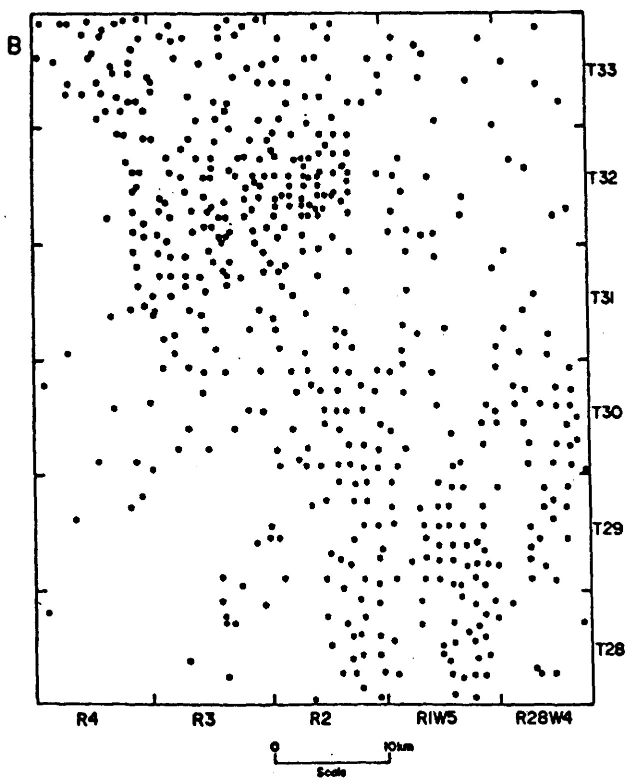
B
T33
T32
T31
T30
T29
T28
R4
R3
R2
R1W5
R28W4
0
10km
Scale

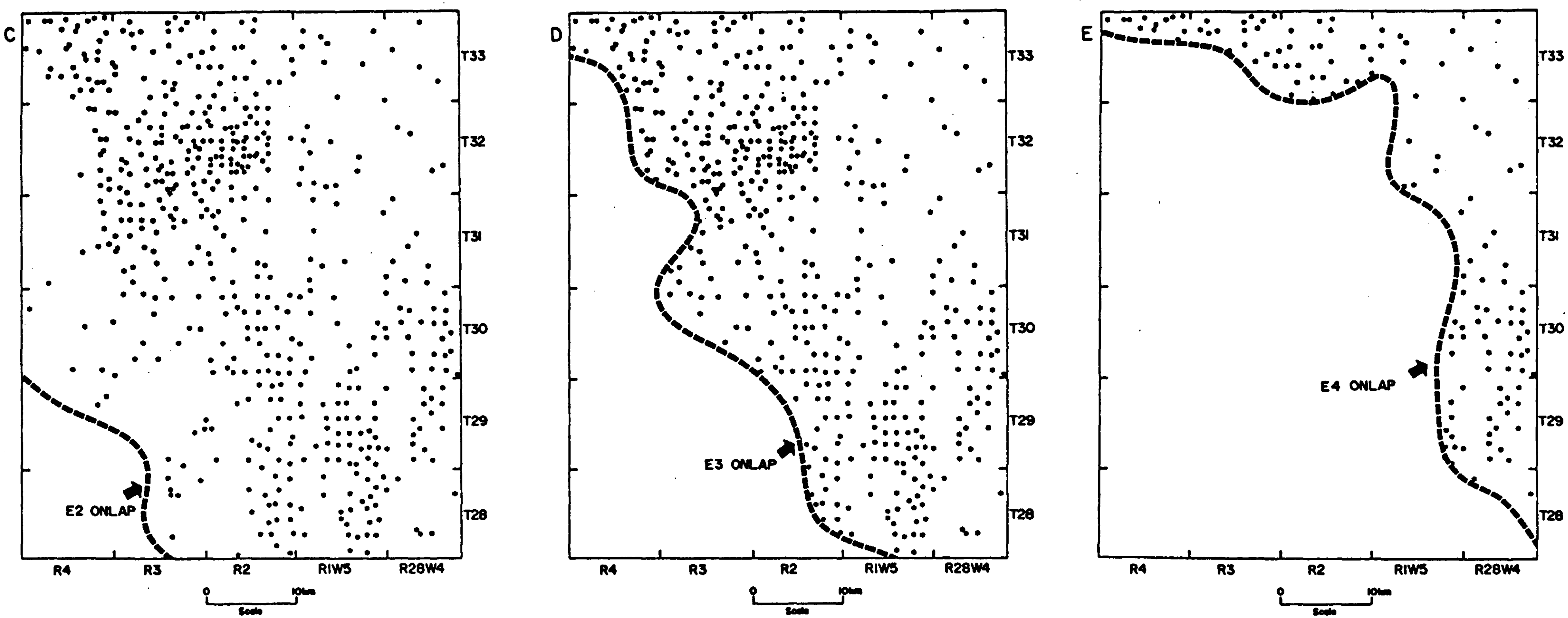
C
T33
T32
T31
T30
T29
T28
E2 ONLAP
R4
R3
R2
R1W5
R28W4
0
10km
Scale
D
T33
T32
T31
T30
T29
T28
E3 ONLAP
R4
R3
R2
R1W5
R28W4
0
10km
Scale
E
T33
T32
T31
T30
T29
T28
E4 ONLAP
R4
R3
R2
R1W5
R28W4
0
10km
Scale

E1 markers do not onlap within the map area (Fig. 7.13). Both of these markers are situated stratigraphically higher in allomember E and presumably onlap further to the southwest.

Figure 7.13 shows that E4 onlaps the CM1 surface just east of the Harmattan East field, while E3 and E2 onlap south and west of Harmattan East. The onlap edges trend roughly southwest - northeast. Crenulations along these edges may be caused by insufficient well control or alternatively may be related to topography on the underlying VE4 surface.

Two additional maps were constructed in order to ascertain if relationships exist between onlap positions of "E" markers, the thickness of the CM1-VE4 interval, and the topography of the VE4 surface. Figures 7.14 and 7.15 show the interpreted position of the onlap markers superimposed on the CM1-VE4 isopach map and the VE4 topography map respectively.

In order to further verify the relationship of subsurface morphology of erosion surface VE4 to position of onlap ("E" markers); two dimensional plots were constructed using data from the isopach maps and a series of profile lines (Fig. 7.16). The plots were constructed by transferring each contour line - profile intersection value to an x-y grid. The VE4 and CM1 surfaces were obtained using this method with each horizon hung relative to the BFS datum. The "E" marker onlap positions were also transferred to the

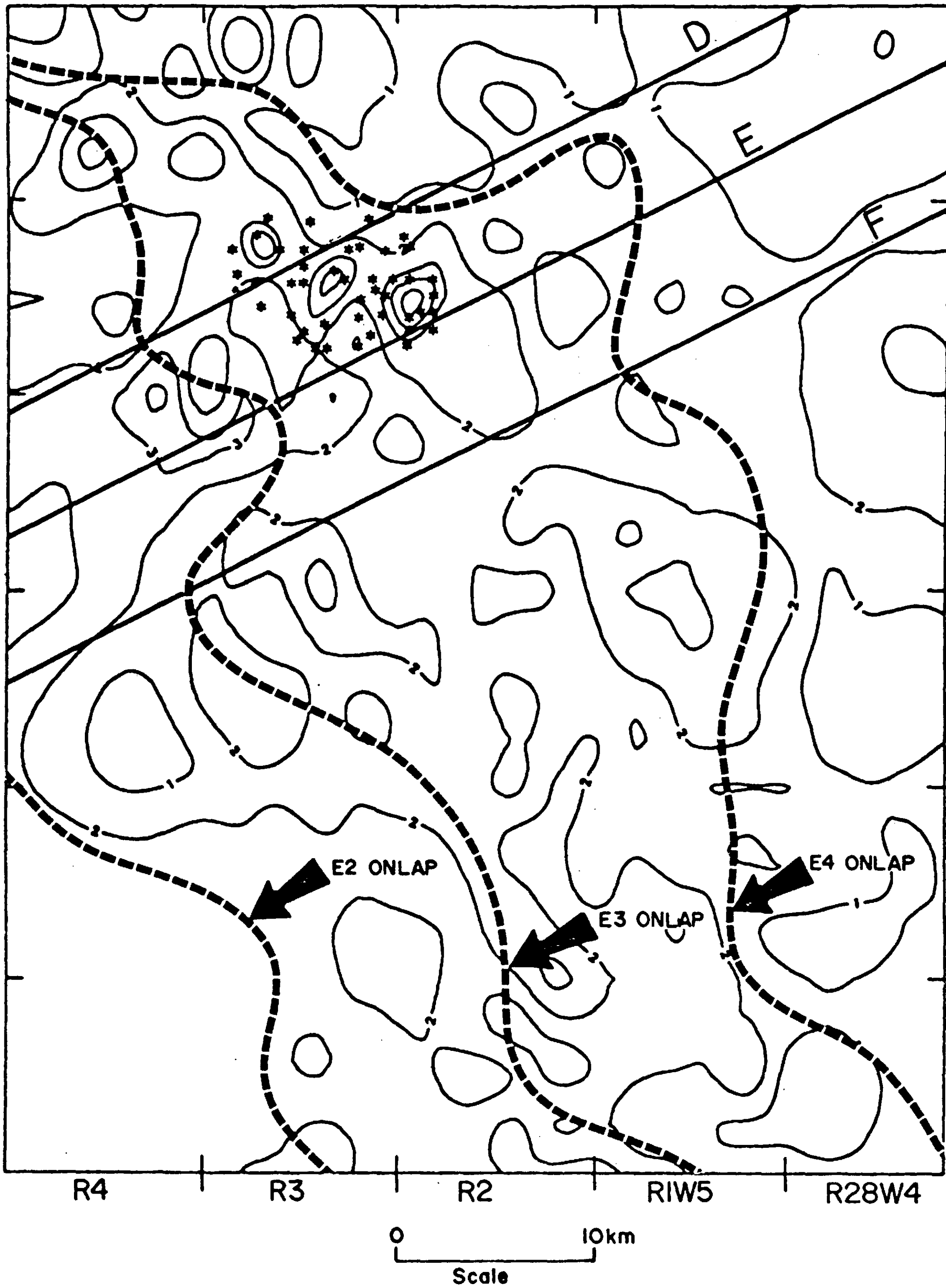

Figure 7.14. Relationship of the onlap markers with respect to the VE4-CM1 interval. The E marker onlap positions have been superimposed on the VE4-CM1 isopach. Note that the E2 and E3 markers onlap CM1 southwest of Harmattan East. The E4 marker onlaps south and west along the thick identified previously in figure 7.10. Profile lines D through F are used for the construction of 2-D profiles in figure 7.16.

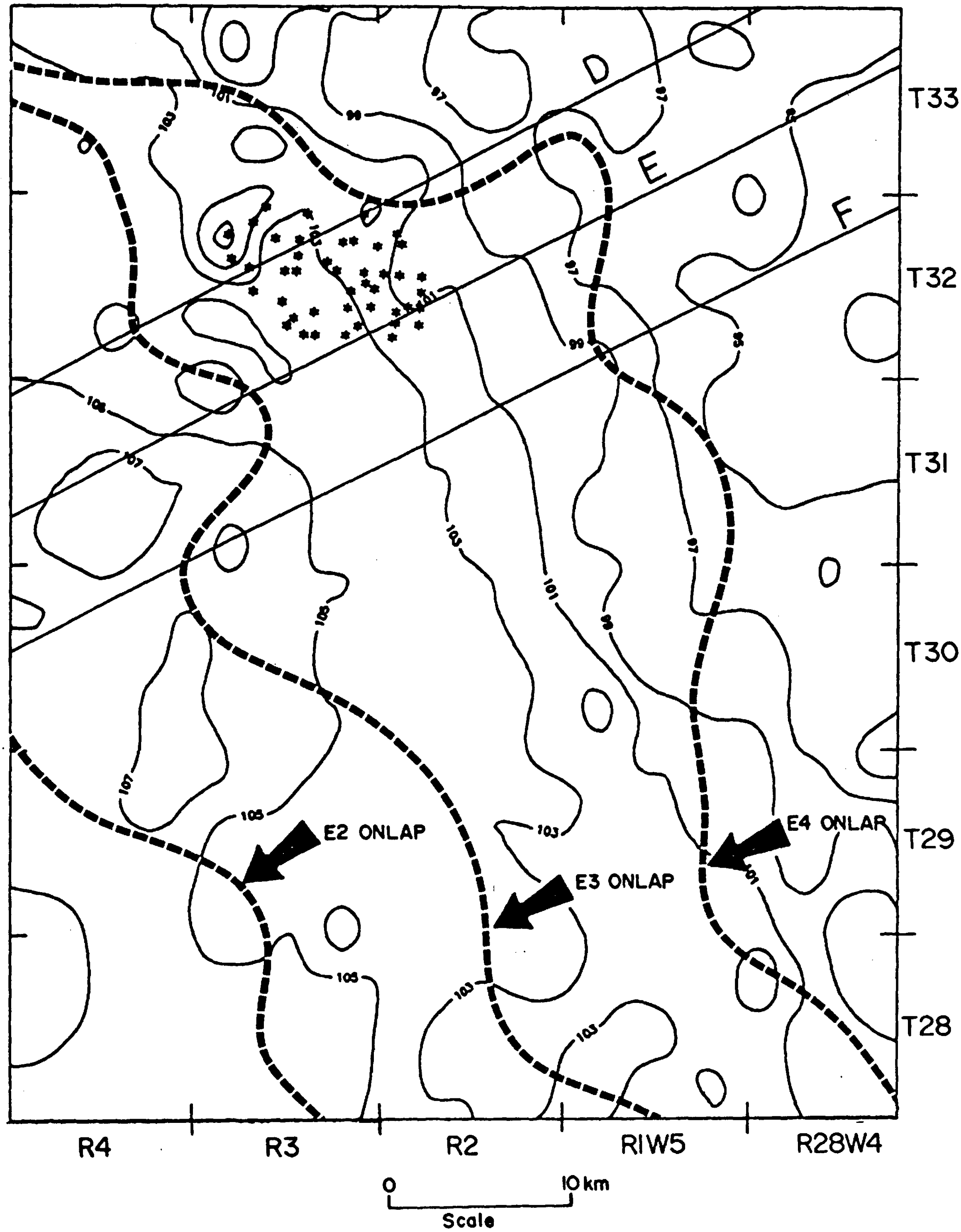

Figure 7.15. Relationship of onlap markers with respect to the VE4 topography isopach map. The E marker onlap positions have been superimposed on the VE4 topography map. Profile lines D through F are used for the construction of 2-D profiles in figure 7.16.

Figure 7.16.

2-D Plots. These plots were constructed using the VE4-CM1 thickness isopach (Fig. 7.14) as well as, the VE4 topography iospach map (Fig. 7.15). The VE4 surface is hung relative to the BFS datum and therefore shows the topographical relationship of the surface. The CM1 interval thickness was superimposed on the VE4 surface. Each plot was constructed approximately perpendicular to the strike of VE4 topography. The location of lines D through F are shown on figures 7.14 and 7.15. Profiles are discussed more fully in text.

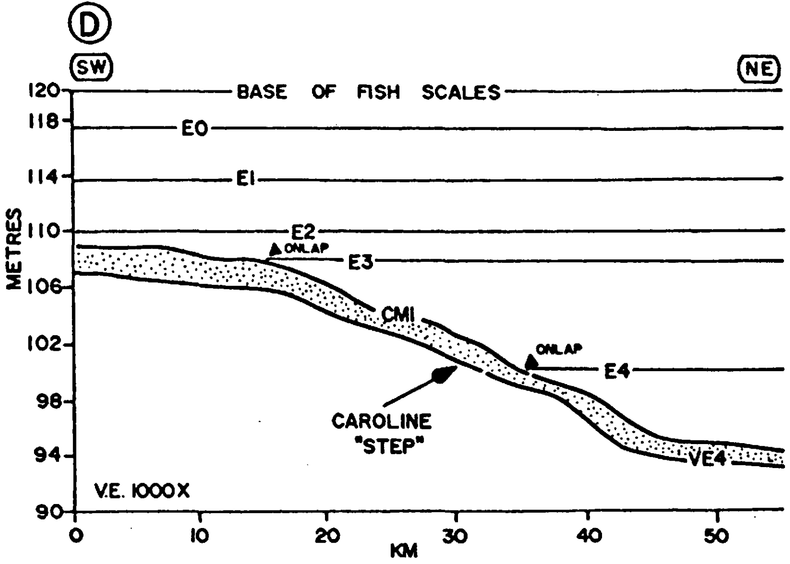
D
SW
NE
BASE OF FISH SCALES
E0
E1
E2
ONLAP
E3
CM1
ONLAP
E4
CAROLINE
"STEP"
VE4
V.E. 1000X
METRES
KM

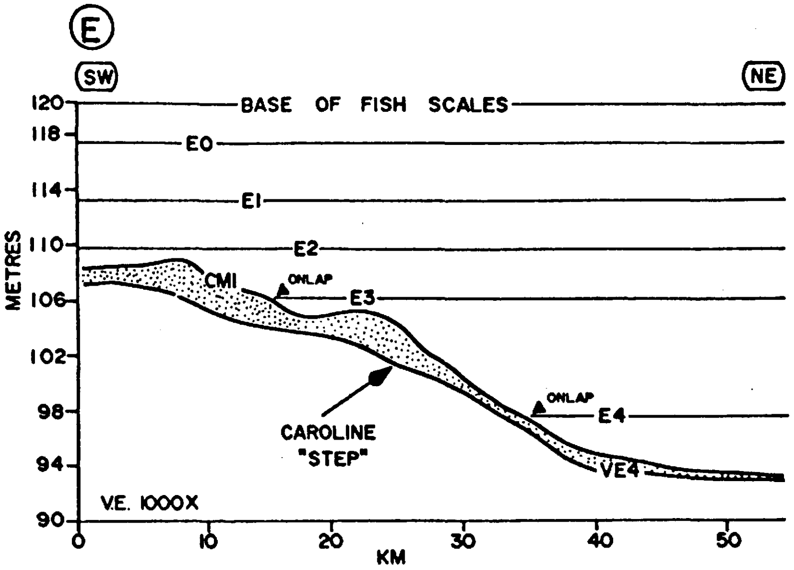
E
SW
NE
BASE OF FISH SCALES
E0
E1
E2
CM1
ONLAP
E3
ONLAP
E4
CAROLINE
"STEP"
VE4
V.E. 1000X
METRES
KM

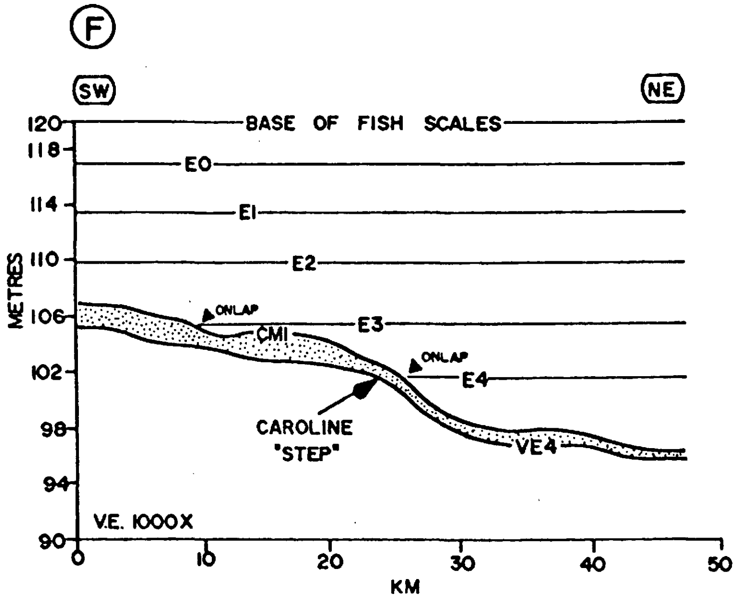
F
SW
NE
BASE OF FISH SCALES
E0
E1
E2
ONLAP
E3
CM1
ONLAP
E4
CAROLINE
"STEP"
VE4
V.E. 1000X
METRES
KM

plots based on their intersection with each profile line. Each "E" marker was then drawn as a planar unit relative to the BFS datum.

The three plots illustrated in figure 7.16 confirm many of the previously made observations. These include:

1) each profile line shows one dramatic "step" in the VE4 topography that has been termed the Caroline "step". Topographical relief on the three lines appears to increase from northwest to southeast; Line D has about 6.7 m of relief on the VE4 surface, Line E has about 10.2 m o f relief, while Line F has about 14m. The average slope for the Caroline "step", based on the three plots is 0.040°.

2) two "E" markers onlap onto the CM1 surface. The E4 marker onlaps approximately in the middle of the Caroline "step" along the eastern margin of the Harmattan East field. The E3 marker onlaps at or near the top of the Caroline step along the western margin of the Harmattan East field.

7.7 Geometry and Stratigraphic Relationship of the Caroline, Garrington and Harmattan East Oil Fields

Recognition of bounding discontinuities and allomembers in the study area has provided a stratigraphic framework which can be used to interpret the spatial and stratigraphic relationship of the Harmattan East oil field to the proximal Caroline and Garrington oil fields. The three fields are in close proximity to one another, with the

Caroline field situated north~~east~~west of Harmattan along a similar line of depositional strike. The unitized boundaries of Caroline and Harmattan are approximately 8 km apart, and the Garrington field is situated 16 km directly north of the Harmattan East field boundary (Fig. 7.17).

The spatial geometries of each field, as revealed in plan view is "pod like" with a northwest - southeast linearity (Fig. 7.17). Caroline, the largest of the three fields, appears to be the most linear. Its shape resembles some of the Cardium fields which are often long and linear (eg. Caroline and Lochend Cardium fields, Pattison, 1988).

The Viking reservoir at Harmattan East ("E pool"; ERCB, 1990) consists of porous rocks (up to 12% porosity and 20-70 md permeability; Grant, 1985) confined to the CM1-VE4 interval in allomember E. This contrasts with the Viking "A pool" at Caroline field which was interpreted by Davies (1990) to be producing from the E3 coarse grained interbed. Figure 7.18 is a structural schematic showing the relationship of the Caroline reservoir unit to the Harmattan East reservoir interval. The E3 interbed onlaps and amalgamates with the CM1 surface along the southwest margin of Harmattan East and is separated from the top of the CM1 surface at Harmattan by an intervening dark mudstone. This dark mudstone may act as the top and lateral seal for the reservoir unit at Harmattan East. The bottom seal at this field may be a function of the low permeability fine grained

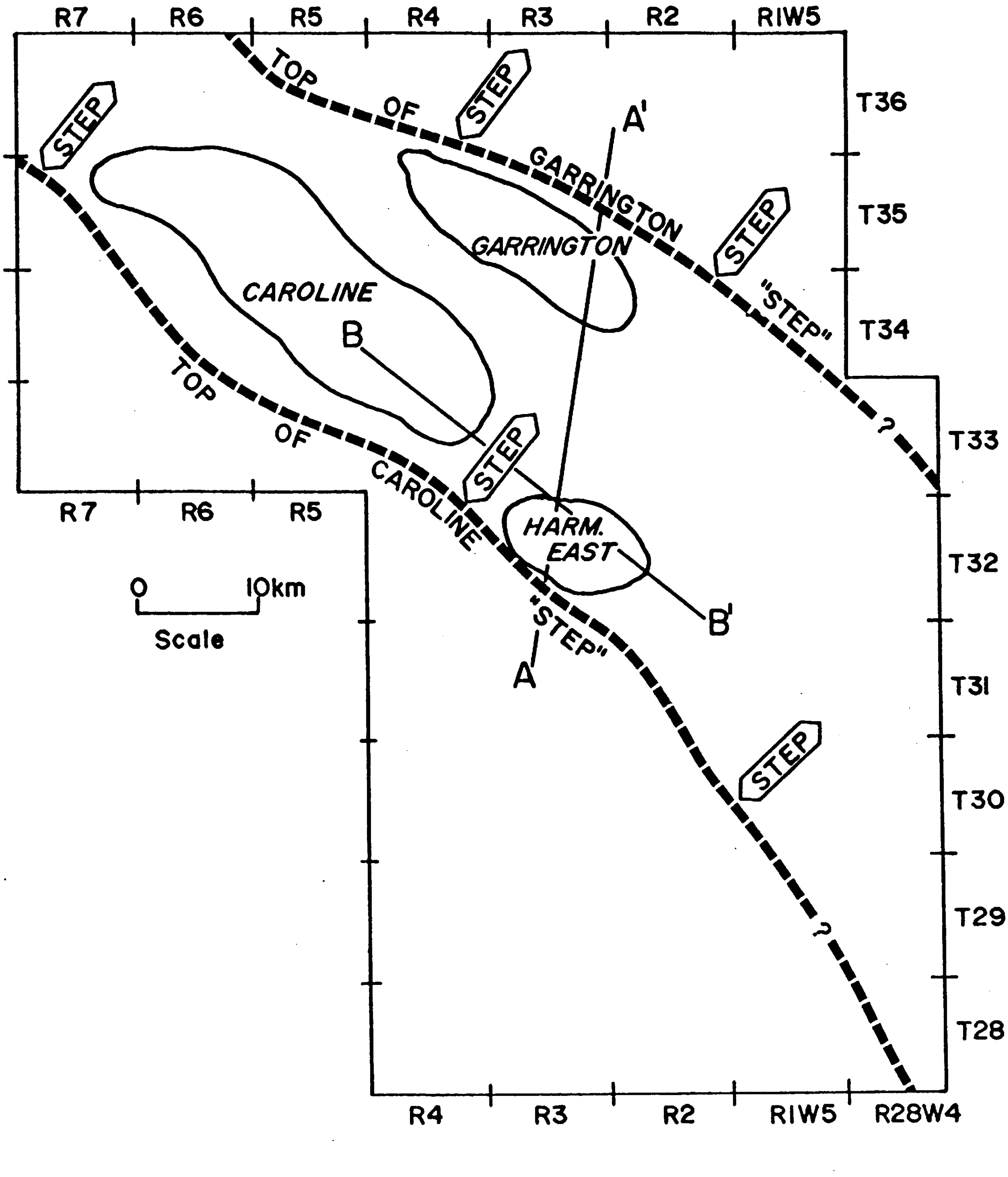

Figure 7.17. Location of Harmattan East, Caroline and Garrington oil fields, and their relationship to the VE4 Caroline and Garrington "steps". Profile lines A-A′ and B-B′ show the location of structural schematic cross sections shown in figures 7.18 and 7.19.

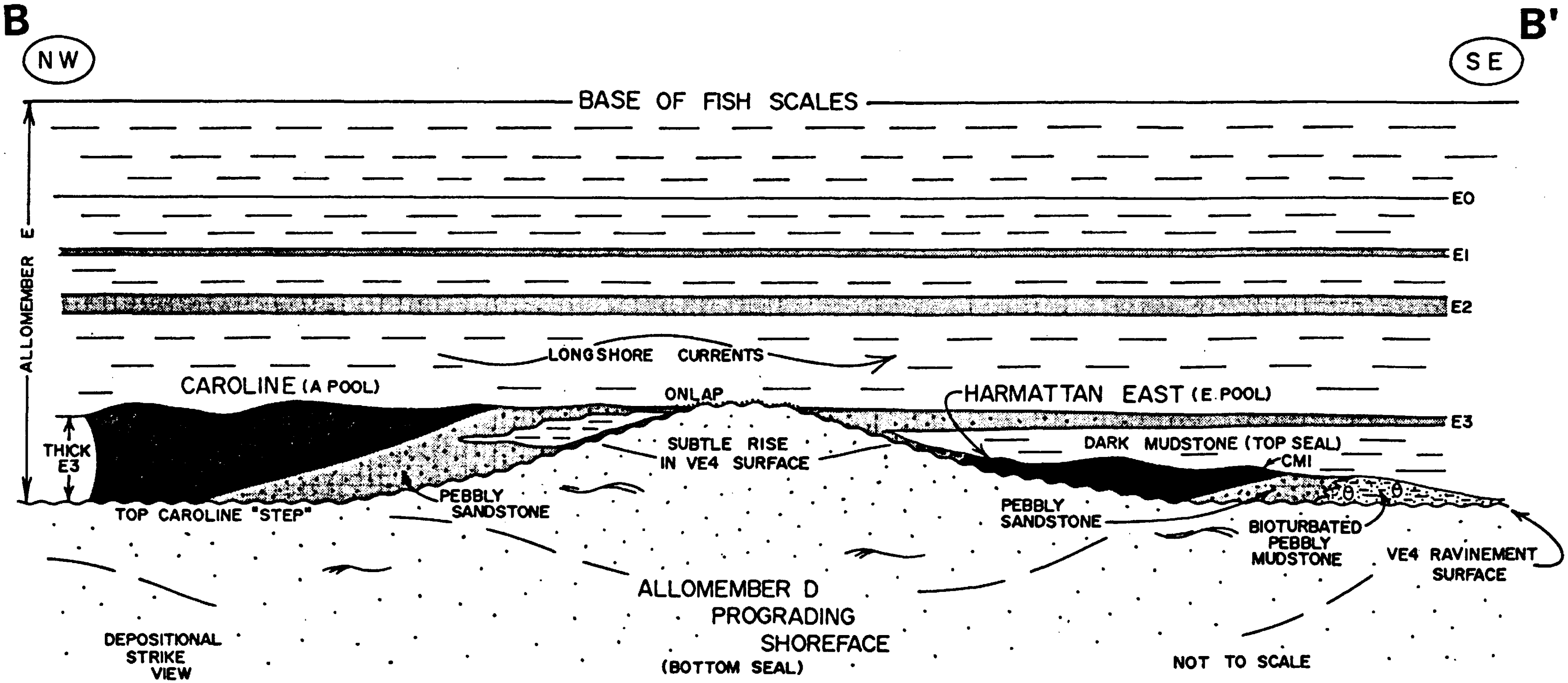

Figure 7.18. Schematic cross section B-B′ showing the stratigraphic relationship of the Caroline "A-pool" to the Harmattan East "E-pool". The oil-water contact is shown as a tilted contact to illustrate the separation between the two pools. The cross section is a view along depositional strike. No scale is implied.

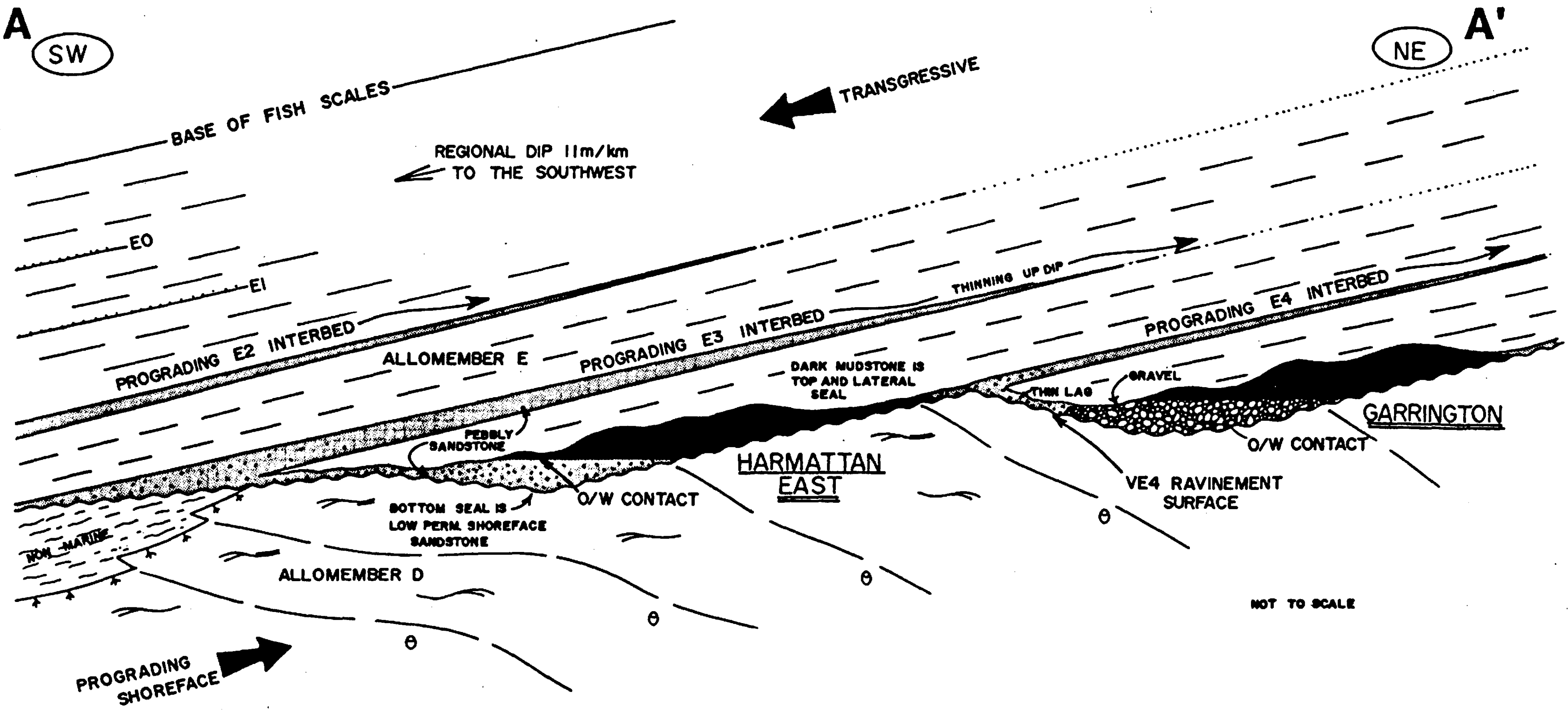

Figure 7.19. Schematic structural cross section showing the stratigraphic relationship of the Harmattan East oil field to the Garrington oil field. Regional dip is to the southwest at approximately 11 m per km. Note the thin pebbly sandstone lag separating the two fields. The top and lateral seals to both fields are dark mudstones. The bottom seal to both fields are low permeabilty sandstones of allomember D. No scale is implied.

shoreface sandstones of allomember D below (Grant, 1985) (Fig. 7.18).

The E3 interbed may not be productive at Harmattan East for several reasons. First, the interbed thins and becomes muddier to the southwest, and may lack sufficient reservoir quality porosity and permeability to trap hydrocarbons. Secondly, the oil water contact lies near the western boundary of the Harmattan East field (Grant, 1985). Since the E3 interbed is separated from the reservoir sandstones (CM1-VE4 interval) by mudstone, and onlaps southwest (downdip) of the oil water contact; it is probably not in communication with the oil filled reservoir (Fig. 7.18). This scenario is analogous to the Caroline field where Davies (1990) indicated the oil-water contact closely paralled the western boundary of the field. Thicker sediments in the CM2-VE4 (E3 interbed) interval (Davies, 1990) west of Caroline, although laterally equivalent to the oil producing interval, are non-productive because they occur downdip of the oil water contact. The eastern boundary of the Caroline field was attributed by Davies (1990) to be the result of the E3 interbed becoming thinner and muddier basinward, eventually pinching out into mudstones near Garrington.

The along strike separation of Caroline from Harmattan East may be related to the subtle "high" on the VE4 surface between these two fields (Fig. 7.18) Log cross section D-D′ (Chapter 6) showed a subtle rise in the CM1-VE4 interval between the southeast boundary of Caroline and the northeast boundary of Harmattan. The producing E3 interbed at Caroline onlaps this rise in topography amalgamating with the CM1 surface, thus separating it from Harmattan East. Further work is needed to ascertain the structural position of each oil-water contact relative to this high in order to confirm a structural control for physical separation of these two pools.

The stratigraphic relationship of the Garrington field to Harmattan East is shown in the structural schematic depicted in figure 7.19. The relationship of the reservoir intervals of these two fields can also be explained in terms of allostratigraphic relationships of allomembers and internal facies. Davies (1990) indicated Viking oil at Garrington field is being produced from the CM2-VE4 interval and not the E3 interbed as at Caroline. Preliminary work by Davies indicated the western boundary of Garrington is controlled by the oil-water contact, and the eastern boundary by thinning and muddying of the CM2-VE4 interval basinward.

Previous discussions in this chapter have indicated that the coarse grained deposits at Garrington are found at stratigraphically lower positions in allomember E on the VE4 ravinement surface near a stillstand "step" position termed Garrington (Davies, 1990) In contrast, the Caroline and Harmattan East fields occur in the vicinity of a younger "step" termed Caroline (Fig. 7.17). The Harmattan East Viking reservoir is separated from the Garrington field for several reasons. First, the coarse grained deposits at Harmattan East and Caroline are younger and coincide at or near the top of the younger Caroline "step" (Fig. 7.19) Secondly, the Garrington coarse sediment package was blanketed by dark mudstones laid down below the E3 interbed. These mudstones likely seal the updip boundaries of the Harmattan East and Caroline fields from the downdip (western) boundary of Garrington (Fig. 7.19). Thirdly, the CM1-VE4 interval at Harmattan thins basinwards (towards Garrington) becoming a thin (< 20 cm thick) veneer of pebbly sandstone that does not appear to be in communication with reservoir rocks at Garrington (Fig. 7.19).

In summary, the factors controlling the boundaries of the three fields appear to be both stratigraphic and structural (post depositional). The stratigraphic controls responsible for separation of these fields are:

1) depositional thinning of the coarse grained reservoir package along strike and up dip,

2) lateral facies changes along strike and up dip from pebbly crossbedded sandstone (reservoir) to bioturbated pebbly mudstones (non-reservoir),

3) reservoir rocks at Caroline and Harmattan East are stratigraphically younger than reservoir rocks at Garrington,

4) dark mudstones of allomember E form the top and lateral

seal, while fine grained low permeability sandstones of allomember D form the bottom seal to the coarse grained reservoir units.

Structural controls which influenced field boundaries include:

1) regional dip of reservoirs toward the southwest influences the downdip limit of the oil-water contact and essentially delineates the western margin of the fields,

2) topography on the VE4 surface expressed as a high between Caroline and Harmattan broke the along strike continuity of the E3 reservoir interbed at Caroline, and prevented it from merging with the reservoir unit at Harmattan East.

7.8 Summary of Observations

Isopach maps and 2-D plots in this chapter have documented a VE3 erosion surface with two "steps" and a VE4 erosion surface with one general "step". The "steps" on both of these surfaces are linear and mainly trend northwest - southeast. The Caroline "step" (VE4 surface) exhibits and undulatory topography that dips to the northeast at 0.040%.

Erosion of underlying facies directly below VE4 is documented by the preservation of nonmarine deposits in the southwest and marine deposits to the northeast. Nonmarine deposits may have occurred as far northeast as Garrington or Harmattan East but were likely removed by erosional downcutting on the VE4 surface. The VE3 surface appears to be more undulatory than VE4 however, both surfaces show a similar rise to the southwest.

The coarse sediment package between CM1 and VE4 is thickest at Harmattan East and areas to the southwest and northwest. The interval thins to the northeast along the lower portion of the Caroline "step". With respect to the VE4 surface, the thicker deposits are found near the top and along the Caroline "step", and immediately west of "E" marker onlap positions. The coarse sediment package at Harmattan East is characterized by pebbly cross bedded sandstone. In off field positions it is predominantly interbedded facies 5a and 13, while in areas along strike of Harmattan East to the southeast, it is mostly pebbly bioturbated mudstone-sandstone (facies 13).

The "E" markers within allomember E have been shown to sequentially onlap the CM1 surface in a southwesterly direction. E4 onlaps the CM1 surface in the middle of the Caroline "step". The E3 marker onlaps the CM1 surface at the western margin of Harmattan East and along the top of the Caroline "step". E2 onlaps at the "high" in the southwest corner of the map. The E0 and E1 markers do not onlap in the map area and presumably onlap the CM1 surface southwest of the study area.

The Harmattan East oil field is producing from the coarse grained CM1-VE4 interval in allomember E. The western boundary of the field is determined by the downdip limit of the oil-water contact. The field is separated from Caroline by a rise in the VE4 surface. The E3 producing interbed of Caroline onlaps this VE4 rise and is separated from the Harmattan reservoir rocks by dark mudstones in allomember E. The eastern boundary of Harmattan is controlled by the thinning of the CM1-VE4 interval basinwards in the vicinity of Garrington. Oil is produced at Garrington from stratigraphically lower coarse grained deposits found on the VE4 surface.

Chapter 8 Interpretations

8.1 Introduction

Previous chapters established a stratigraphic framework for the Viking Formation at Harmattan East and Crossfield. The purpose of this chapter is to interpret the facies, their facies associations, and the relationship of these associations with respect to separating bounding discontinuities. The erosion surfaces, correlative conformities and allomembers are discussed in ascending order. Finally, a summary of the sequence of events responsible for the internal stratigraphy of the Viking Formation is presented at the end of this chapter.

8.2 BV (Correlative Conformity - Base Viking)

BV is interpreted as a correlative conformity in the study area, and it represents the allostratigraphic base of the Viking alloformation. The correlation of BV as a log marker was shown in previous chapters to either rest on mudstones of the Joli Fou or on Basal Colorado sandstones in the southwest part of the study. This correlation is very difficult to establish with any certainty because of the limited core control over this interval in the study area.

8.3 Allomember A-B

Allomember A-B lies directly on BV and is sharply truncated at the top by the VE3 erosion surface. As discussed previously this allomember is rarely cored, therefore its stratigraphic position within the regional Viking allostratigraphy is less certain. The reference locality core (6-24-32-3W5) shows the entire allomember to be a single sandier and coarsening upwards sequence as follows: dark mudstones overlie BV and gradationally pass upwards into muddy siltstones and sandy siltstones which in turn pass upward into pale sandstones that are extensively burrowed by Ophiomorpha. This facies succession is thicker and more complicated in areas to the southwest where the pale sandstone is overlain by fine grained, burrowed laminated sandstone-mudstone (facies 7a) and interbedded sandstone-mudstone (facies 8).

In the Caroline and Garrington area, Davies (1990), designated the deposits between VE3 and BV as allomember B/C. Boreen and Walker (1991) and Pattison (1990) designated the channel-estuarine deposits at Willesden Green and Crystal as allomember C. These workers showed a major erosion surface termed VE2 that occurs at the base of incised valleys at Willesden Green and Crystal. These incised valleys cut down into the regional shelf deposits of allomembers A and B, and are overlain by valley-fill deposits (allomember C). Channel-estuarine deposits of allomember C and the VE2 erosion surface are not present in the Harmattan East and Crossfield area. Therefore, allomember A-B in this study area is interpreted to be part of the regional Viking sandier upwards successions of Boreen and Walker (1991).

Boreen and Walker (1991) interpreted a north to northeast sediment source for allomember A and B which was thought to have switched to a southwest dominant source during the later part of allomember A and B deposition. The sandier upwards units of allomember A-B southwest of Harmattan East may represent the progradational deposits of an as yet undiscovered rooted shoreface further to southwest. Additional mapping southwest of this study may verify this.

Evidence within allomember A-B when viewed in conjunction to similar Viking deposits in other areas of the basin, indicates a vertical transition upwards in depositional environments from a deep, quiet water setting at the base to a shallow water - moderate energy setting at the top. The high diversity of trace fauna seen in the upper deposits of allomember A-B is compatible with the Cruziana ichnofacies and implies relatively uniform rates of sedimentation, bottom water conditions, and minimal turbidity all characteristic of a lower shoreface environment of deposition (Moslow and Pemberton, 1988). Hummocky cross-stratification and wave ripples in the upper parts of allomember A-B suggest deposition in the lower shoreface of a wave dominated shoreline (Leckie, 1986a).

8.4 Erosion Surface VE3

This surface cuts into allomember A-B, and has a relative relief of up to 14 metres at Harmattan East - Crossfield. In general, the surface displays an undulating "step like" topography that rises to the southwest. This surface has been correlated as far north as Crystal (Pattison, 1990).

The VE3 contact is consistently overlain by a conglomeratic lag in most areas where it has been correlated in the basin. At Harmattan East the surface is characterized by a sharp facies change from pale sandstones below to either conglomerate or fine grained, burrowed and laminated sandstone-mudstone above. The conglomerate lag that rests on VE3 normally occurs as thin beds interbedded with facies 7a, and is usually found within the first metre above the erosional contact. The top of this interbedded facies may represent a maximum flooding surface associated with the major transgression responsible for the VE3 surface (see Fig. 5.1, chapter 5). The greatest thickness of conglomerate lag on the VE3 surface measured in core of this study was 45 cm.

Erosion on the VE3 surface was demonstrated previously in figure 6.1 where the VE3 surface truncated underlying log markers in allomember A-B. Other evidence for erosion on the VE3 surface is given by Davies (1990) for the Caroline - Garrington areas. Davies noted up to 22 m of relief on a thin burrowed and gravel veneered VE3 surface.

Boreen and Walker (1991) observed a thin gravel-veneer on the VE3 surface that erosively overlies the transgressively filled estuarine deposits of allomember C at Willesden Green, and that the VE3 surface in this area is often penetrated by sand filled <u>Arenicolites</u> and <u>Skolithos</u> burrows.

Davies (1990) discussed three environments in which the VE3 surface could have formed. These are; fully subaerial, fully submarine, or initially subaerial and modified by subsequent transgression. Discussions relating to each of these mechanisms has been made for similar surfaces in the Viking (Downing and Walker, 1988; Boreen and Walker 1991) and also for the Cardium Formation (Bergman and Walker, 1987,1988; Eyles and Walker, 1988; Pattison, 1988; Wadsworth and Walker, 1991).

A complete subaerial mechanism for the creation of the VE3 surface in the study area is rejected because no evidence of nonmarine and/or incised channel deposits were found anywhere along the surface. A fully marine mechanism such as localized bottom scour is also not favoured for the creation of the VE3 surface. The substantial relief (14 m) and "step" like morphology of this surface would seem unlikely to be produced in a deeper water environment (ie. kms from a paleoshoreline) where bottom currents would be of lesser magnitude than at shallow water shoreline areas.

The most probable mechanism for creating the topographic relief and "step" like geometry on the VE3 surface is initial subaerial erosion (ie channeling and valley production by rivers) during a sea level lowering followed by a basinward transgressive event that removed shallow marine and nonmarine deposits from the sedimentary record. The VE3 morphology discussed in Chapter 7 can be explained by different rates of transgression during a sea level rise. An increase in the rate of transgression followed by periodic stillstands would allow the shoreface environment to translate landward and vertically, thus producing a "step" like morphology. The erosion surface produced by such a process is termed a ravinement surface (Nummendal and Swift, 1987). The fact that the VE3 surface separates underlying progradational deposits of allomember A-B from overlying progradational shoreface deposits of allomember D, and is covered by a conglomeratic lag indicates it must represent a major transgressive ravinement surface. The conglomeratic lag on VE3 represents the winnowed toe of shoreface deposit produced during erosional shoreface retreat to the southwest. The VE3 surface is the sedimentary expression of a major sea level rise that terminated a Viking progradational event likely sourced from the southwest. A maximum flooding surface is thought to separate the basal portion of allomember D (approximately first metre of sediment overlying VE3) from the thicker overlying regressive deposits of middle and upper allomember D. Initiation of a second progradational event (allomember D) blanketed the transgressive deposits on the VE3 surface with shoreface and nonmarine deposits at Harmattan East - Crossfield.

8.5 Allomember D

This allomember occurs between VE3 and VE4 and represents the deposits produced by another regional sea level lowering in the Viking. The most common vertical facies succession of allomember D at Harmattan East field consists of sandier upwards successions where fine grained, burrowed and laminated mudstone-sandstone (facies 7a) is gradationally overlain by interbedded sandstone-mudstone (facies 8) which in turn is overlain by thick bedded non-bioturbated sandstone (facies 9). In southern parts of the study, the sediments of allomember D form a coarsening upwards succession that contains a similar vertical sequence to that described above. In these areas, facies 9 is often overlain by parallel laminated and cross-bedded sandstone (facies 10) which in turn is overlain by nonmarine facies 11 and 12.

Similar vertical facies successions (mostly facies 7a,8,9) have been documented at Caroline and Garrington (Davies, 1990). Isolated, thin occurrences (<1m) of lower allomember D sediments occur as far north as the Crystal field (Pattison, 1990), and as far east as Joffre (Downing and Walker, 1988). Deposits of allomember D are stratigraphically equivalent to the "Viking regressive facies" of Leckie (1986a) and the "fine grained sandstone association" of Hein et al (1986). Allomember D sediments also comprise part of Leckie and Reinson's (in press) "prograding cycle 2".

Preliminary interpretations discussed in Chapter 4 suggested facies 6 through 10 were deposited in a storm dominated marine environment while facies 11 and 12 were deposited in nonmarine settings such as coastal plains and shallow lagoons. The vertical facies succession in allomember D in this study suggests deposition in progressively shallower water depths towards the southwest.

The lowermost part of this sequence (facies 7a) consists of alternations of thinly bedded mudstone and wave rippled sandstone beds. This part of the sequence is interpreted to have been deposited in a lower shoreface environment. Waning storm events or smaller storms may have formed the wave ripples that are indicative of a shallow, wave agitated environment (Dott and Bourgeois, 1982; Plint and Walker, 1987). The presence of trace fossils Skolithos and Arenicolites are compatible with a "storm related ichnofacies" (Frey and Howard, 1985).

Facies 8, above, is interpreted to represent deposition in an offshore transition zone to lower shoreface environment in shallower water depths than facies 7a. The abundant low angle lamination in the sandstones of this facies may represent hummocky cross-stratification (HCS).

Wave ripples are often found at the top of these beds and likely represent reworking of HCS bed tops as large storms waned or possibly by later storm reworking. The Skolithos ichnofauna found in the upper part of this facies are indicative of a soft-bottomed, high energy shallow marine environment.

Facies 9 commonly overlies facies 8 and in general is thicker bedded with minimal disruption of the sandstone beds by burrowing organisms. The abundant low angle inclined stratification is interpreted as swaley cross-stratification (SCS) formed in a storm dominated shelf to shoreline setting at or just above fair weather wave base. SCS has previously been interpreted as a storm related structure and may represent amalgamated HCS sandstone beds (Leckie and Walker, 1982; McCrory and Walker, 1986; Plint and Walker, 1987; Rosenthal and Walker, 1987). The overall absence of mudstone in this facies suggests a shallower shoreface environment than proposed for facies 8. Another common aspect of facies 9 are the abundant gravel stringers. Several of these stringers can be correlated locally within the study area, where core control is closely spaced. Their presence in facies 9 suggests that gravel was being supplied to this shallow water environment periodically. Pebbles and cobbles were likely transported by rivers to the beach and were subsequently transported offshore during intense storms, forming coarse middle to lower shelf deposits. Similar gravel stringers have been reported in other storm-dominated prograding shorefaces (Bourgeois, 1980; Howard and Rieneck, 1981; Rosenthal and Walker, 1987; Davies, 1990).

Facies 10 is the final or capping facies of this storm dominated marine succession. The SCS sandstones of facies 9 below pass upwards into fine and medium grained parallel laminated and cross-bedded sandstones of facies 10. This facies is interpreted to represent deposition in an upper shoreface and beach environment. The monospecific assemblage <u>Macaronichnus</u> found near the top of this facies suggests an extreme high energy upper shoreface to foreshore setting (G. Pemberton, pers. comm., 1988). The overlying planar laminated sandstones that directly overlie the <u>Macaronichnus</u> burrowed sandstones were likely deposited in the swash zone of a beach environment. This high energy marine facies is often overlain by a rooted horizon and successively thicker nonmarine deposits further to the southwest. The rooted interval of this facies is a direct indicator of subaerial exposure during deposition of allomember D.

The Viking nonmarine deposits in allomember D are only preserved in areas southwest of Harmattan East and in one location (T33 R6W5) southwest of Caroline field (Davies, 1990). The nonmarine deposits in the study area are characterized by two facies. The first, facies 11 (rooted brown mudstone-siltstone) often gradationally overlies facies

10 and resembles the paleosols described by Retallack (1981), Leckie (1986b), and Plint and Walker (1987). This facies has two variations which may been produced in two different although mutually coexisting environments (refer to Chapter 4.2.12). The grey green type may represent well drained soils where organics were destroyed by subaerial oxidation. Conversely, the brown type may represent deposition of sediment in a poorly drained, and poorly aerated location of the coastal plain. Interbedded coals in this facies likely represent vegetated environments in backshore environments or along margins of shallow ponds or lakes (Plint and Walker, 1987). Destruction of the original sedimentary structures in this facies may have resulted from bioturbation by roots and/or soil forming processes (Leckie, 1986b).

Rooted laminated mudstone-sandstone (facies 12) is the second nonmarine facies found overlying the storm dominated marine sequence in allomember D. This facies is often found overlying facies 11. The presence of roots, post depositional sedimentary structures (convolution and syneresis cracks) suggest a depositional environment comparable to brackish lagoons, large ponds or shallow lakes. The absence of body fossils (eg. bivalves, gastropods, and fish remains) in this facies indicate harsh ecological conditions within the environment of deposition that were not suitable for sustaining animal life. The proposed environment of deposition is thought to have been similar to the backshore environment that exists along the present day Georgia coast. The water in lagoons and ponds proximal to the Georgia coast is often acidic, discoloured, and transmits minimal light, and is generally not suitable for animal life; however, these waters do contain abundant rooted (floating) plants (Frey and Pemberton, 1987). Similar plants may have been responsible for the bioturbation and root traces observed in this facies. Syneresis cracks in this facies suggest that salinity changes occurred during deposition of this sediment (Plummer and Gostin, 1981; Plint and Walker, 1987).

Primary sedimentary structures in facies 12 (previously discussed in Chapter 4) were attributed to sand being supplied to the depositional environment as washover fans, dunes, and small rivers and creeks in the backshore environment. Wave action in the lagoons and small lakes could have concentrated and redistributed sand in the shallower portions of these water bodies while muds may have accumulated in the deeper quieter water. Convolution structures may have formed in muddier sediments during the release of methane gas. Interstitial waters of many modern sediments are often saturated with methane derived from the oxidation of organic matter. Increasing amounts of methane may have elevated pore pressure in the sediment, and as localized pressure was reduced, a loss of sediment stability occured creating convolution structures (Monroe, 1969; Plint and Walker, 1987).

The storm dominated prograding shoreface deposits and overlying nonmarine units at Harmattan East suggest a major southwesterly sediment source for allomember D. This is supported by the presence of nonmarine and beach deposits southwest of Harmattan (a paleoshoreline), and the progressive thinning and loss of sand to the north and northeast. The thinning of allomember D is thought to be related to depositional thinning to the northeast during progradation and erosional removal of upper allomember D deposits by transgressive erosion during formation of the VE4 surface. The major cause of the shoreline progradation may have been a regional drop in sea level, or a high rate of sediment into the basin during a tectonically influenced stillstand (Leckie, 1986a).

Other evidence for progradation of allomember D and subsequent subaerial erosion is related to the minor occurrences of fluvial deposits (facies 5b). The sandstones of facies 5b were previously shown in Chapters 4 and 5 to be: 1) petrographically different from the uppershoreface sandstones (facies 10 in allomember D) and the overlying transgressive lag sandstones (facies 5a in allomember E), and 2) the deposits of facies 5b are erosively based and incise down into thick HCS and SCS sandstones of the prograding shoreface succession.

The sandstones of facies 5b are interpreted to be deposits of unidirectional flows in fluvially dominated channels. These deposits are consistent with the interpretation of shoreface progradation during a relative lowering of sea level. The allomember D shoreline presumably advanced during shoreface progradation allowing for both fluvial incision and subaerial exposure. Fluvial and nonmarine deposits similar to those identified at Harmattan may have existed as far northeast as Joffre, but were removed from allomember D by subsequent transgressive erosion on the VE4 surface. The fluvial deposits, although not widespread in the Harmattan East area, should be expected as this is the area closest to a paleoshoreline, and is also an area where VE4 erosion was minimal. Further drilling in this area could locate other undiscovered fluvial systems that cut down into allomember D.

8.6 Erosion Surface VE4

The storm dominated prograding shoreface deposits of allomember D are erosively truncated by the regionally extensive VE4 surface which in turn is overlain by the coarse grained deposits and mudstones of allomember E. The VE4 surface can be correlated into the Caroline and Garrington areas adjacent to this study area (Davies, 1990), and as far north as the Crystal field (Pattison, 1990). In the Willesden Green area, VE4 truncates allomembers D and C and in places erosionally overlies allomember B (Boreen and

Walker, 1991). Downing and Walker (1988, p.1216) recognized 16 m of erosion on the VE4 surface at Joffre (their E3) and Leckie and Reinson (in press) documented a "step" like topography at the top of their "prograding cycle 2" which is stratigraphically equivalent to the VE4 surface of this study.

The following observations have been made about the VE4 surface in the Harmattan East - Crossfield area:

1) the surface shows an undulating topography that gently climbs to the southwest resulting in approximately 14 m of relief,

2) one step termed Caroline is present on the VE4 topography and is correlatable along strike with the VE4 Caroline step of Davies (1990),

3) the VE4 surface sharply truncates facies 9, 10, 11, and 12 across the study area. It mainly rests on upper shoreface deposits at Harmattan East field, and on nonmarine deposits in the southwest part of the study,

4) coarse grained pebbly crossbedded sandstones overlie the VE4 surface across most of the study area. These sandstones are thickest at Harmattan East and are discussed in the following section (8.8).

The mechanism responsible for the formation of the VE4 surface is thought to be similar to that previously discussed for the VE3 surface. Like VE3, the VE4 surface is interpreted to have formed by shoreface incision during a basinwide transgression. This transgression was responsible for creating a second major ravinement surface that is correlatable over most parts of the Viking basin.

Isolated occurrences of shallowly incised fluvial deposits into the progradational shoreface sediments of allomember D are evidence of relative sea level lowering and subaerial erosion in a northeast direction. The coarse grained pebbly sandstones and dark mudstones overlying the VE4 surface indicate older subaerial erosion was modified during a subsequent marine transgression in the form of erosional shoreface retreat.

The model of shoreface retreat and corresponding erosion assumes that as sea level rises, the shoreface profile moves upwards and landward, and the ravinement surface cut by this process will also climb landwards. The sediment is eroded from the shoreface profile by storm and/or tidal currents and redeposited above the ravinement surface in a basinward direction (Walker, 1985; Nummedal and Swift, 1987).

Variations in the rate of sea level rise could be used to explain the undulating and southwestward-climbing steplike geometry on the VE4 surface that was observed in the study area. Chapter 7 has shown that a "step" (termed Caroline) occurs along the southwest margin of the Harmattan East field and is correlatable along strike to the northwest with the Caroline "step" identified by Davies (1990). The "step" may represent a significant stillstand position or a period of slow transgression. The thicker coarse grained deposits on the VE4 surface at Harmattan East field may be related to this stillstand event, as fluvial systems supplied sediment to the newly created shoreline. Rapid transgression resulting from an increase in sea level would shut most of the sediment supply off at the shoreface and would flood the coarse sediment package on the ravinement surface. Continued transgression would blanket the offshore environment with mudstones and preserve the previous stillstand shoreface as one sided scour dipping into the basin.

The erosional shoreface model has been used to explain the geometry of the VE4 erosion surface in other areas of the Viking basin (Boreen and Walker, 1991; Davies, 1990; Downing and Walker, 1988; and Pattison, 1990) and has also been used to explain similar stepped erosion surfaces in the Cardium (eg. E4 through E7), (Bergman and Walker, 1987, 1988; Eyles and Walker, 1988; Legitt et al., 1990; McLean, 1987; Pattison, 1988; Wadsworth and Walker, 1991).

The application of this model is also useful for explaining the one sided scour of the steps, as well as, the concave upwards, gently dipping geometry observed on the VE4 surface at Harmattan East. Modern shoreface environments occur between the beach and offshore transition zone, which is typically at about 5 to 15 m (fair weather wave base). Modern shorefaces typically are one sided scours, and exhibit

8.7 Allomember E and the Base of Fish Scales

Allomember E lies directly upon the VE4 erosion surface and is bounded at the top by the Base of Fish Scales condensed horizon. The facies association of allomember E is dramatically different from that of the storm dominated prograding shoreface deposits of allomember D. The shallowing and coarsening upwards HCS and SCS sandstones, beach deposits and nonmarine sediments found below VE4 contrast to the complex succession of pebbly crossbedded sandstones, bioturbated pebbly mudstones and dark mudstones found above VE4.

The predominant vertical facies association in allomember E at Harmattan East is characterized by a thick 5-6 m coarse sediment package mostly made up of crossbedded and structureless pebbly sandstone, with lesser amounts of bioturbated pebbly mudstones. The thicker coarse sediment package (CM1-VE4) is in turn overlain by thinner coarse grained burrowed and laminated mudstone-sandstone units, which pass sharply upwards into dark mudstones. An upper condensed section of fish skeletal remains called the Base of Fish Scales informally marks the allostratigraphic top of the Viking alloformation. In off field areas the coarse sediment package immediately overlying VE4 is in general thinner, muddier and more bioturbated (mostly facies 13).

The most complicated stratigraphic style of deposition in allomember E is exhibited by the coarse grained sandstones (E0-E5 markers) that are found interbedded with dark mudstones. The cross sections in chapter 6 have shown that mudstone encased coarse grained sandstone units (termed E0 -E5 in this study) sequentially onlap the CM1 surface in a southwesterly direction. The following features characterize these coarse grained units in the study area:

1) the interbeds are thickest (2-3 m) at their point of onlap and thin (10's of cms) in a basinward direction,

2) the interbeds onlap and amalgamate with the CM1 surface at or near the upper portions of the Caroline "step",

3) the E2 and E3 units onlap and replace the deposits between the CM1 to VE4 interval southwest of Harmattan East approximately at a "tread" position,

4) the E2 unit is a crossbedded pebbly sandstone at the point of onlap southwest of Harmattan East field. Basinward (northeastward), this same unit passes into thinner crossbedded sandstone with sideritized, mudstone ripup clasts at Harmattan East field. Northeast of Harmattan, the laterally equivalent E2 unit is a thin (<10 cm thick) coarse sandstone bed that is burrowed with <u>Arenicolites</u>,

5) the positions of onlap define northwest - southeast paleoshorelines each closely paralleling the Caroline "step".

The above mentioned features can be explained by the model of erosional shoreface retreat proposed for creation of the VE4 erosion surface. The lowermost crossbedded and structureless pebbly sandstones and bioturbated pebbly mudstones (CM1-VE4 interval) represent transgressive lag deposited as marine processes reworked the older subaerially exposed VE4 surface. Rivers supplied coarse sediment to stillstand "step" locations that formed as a result of wave and/or tidal scour.

Direct evidence of lowstand river deposits was previously discussed in section 8.6. Another source of sediment may have been produced by erosion of older allomembers. The reworked sediment may have been derived from the coarse estuarine channel fill of allomember C (Boreen and Walker, 1991; Pattison, 1990) or the coarsening upwards shoreface sediments of allomember D. Davies (1991, p.161) recognized a dominantly conglomeratic deposit directly on VE4 at Garrington field that changed to cross stratified sandstones in the vicinity of Caroline. The source of the gravel on VE4 at Garrington may have been reworked gravel stringers found in the uppershoreface deposits of allomember D at Harmattan East. These gravel stringers may have been the dominant sediment source for the Garrington shoreface. The channels and rooted beach deposits southwest of Harmattan East are not conglomeratic. Conglomerate filled channels may still exist and have not been discovered, or they supplied gravel to the Garrington shoreline but were later removed during subsequent transgressive erosion on VE4.

The coarse sediment overlying VE4 may have been transported and redistributed in the shoreface environment by storm-influenced tidal currents, and also transported along strike (southeastward) by longshore drift. Reworking of the sediment on top of the VE4 ravinement surface during transgressive stillstands likely produced the sedimentary structures that dominate the sedimentary record between the CM1-VE4 interval, and in the coarse grained interbeds (E markers).

The random interbedding of crossbedded pebbly sandstones and bioturbated pebbly mudstones in the lower part of allomember E is difficult to interpret. Many features associated with these coarse grained deposits are indicative of rapidly changing flow conditions which might be attributed to tides. Although not diagnostic, the presence of interbedded shale and pebbly sandstones, armoured mud balls, rip up clasts, possible clay lined drapes (14-8-31-1W5, sect. 4.2.15), and sharp interbedding of the facies are all suggestive of a regularly fluctuating flow regime. Similar structures have been recognized at this stratigraphic interval at Caroline and Garrington field areas (Davies, 1990), and Willesden Green area (Boreen and Walker, 1991). Compound cross stratification in the Viking at Caroline was also interpreted as tidal by Leckie (1986a).

Similar sedimentary structures exist in modern tidal shelves for example sand ridges and sand waves in the North Sea (Houbouldt, 1968; McCave, 1971; Terwindt,1971). Most modern tidal shelves or shelves of a mixed tide-storm influence do not show simple patterns of sedimentation (Anderton,1976). The tidal bedforms usually exhibit a patchy distribution on the sea floor and often show a range in types of bedforms and resultant stratification (Levell,1980, Johnson and Baldwin.1986).

The more diagnostic characteristics of tidal conditions (eg. compound crossbedding, clay lined drapes) are relatively rare in this study area and appear to be more abundant at Caroline field (Leckie 1986a, Davies 1990) and Willesden Green area (Boreen and Walker, 1990). A mixed storm-tidal shoreface environment is therefore likely for deposition of the coarse grained deposits on top of the VE4 surface at Harmattan East.

Another variation of the coarse sediment package on the VE4 surface is the bioturbated pebbly mudstone facies. The facies distribution map of the VE4-CM1 interval (chapter 7) showed facies 13 occurring mostly in areas southeast of Harmattan East field. The facies was shown to change laterally along strike and shoreward from pebbly crossbedded sandstone to mostly bioturbated pebbly mudstone. The sandier intervals of facies 13 may represent partially preserved bedding. The coarser material (pebbles) may have been brought into an offshore environment by storms. Possible clay lined drapes in one core of this facies southeast of Harmattan (14-8-31-1W5) suggests tidal currents may also have contributed to sediment dispersal. During fair weather periods, mud may have been incorporated into the sediment by organisms.

The stratigraphic relationship of the coarse grained interbeds and dark mudstones, and the onlapping relationship with the CM1-VE4 interval can also be explained in terms of rates of transgression in this mixed storm and tidally influenced seaway. As mentioned early, during a rapid transgression the offshore area is starved of sediment supply and dark mudstones slowly accumulate. During slow transgression or stillstand an incised shoreface developed (eg. at Garrington field), and sediment was supplied to the newly created shoreline by rivers or by erosion of older coarse sediment. A minor sea level fall allowed coarse grained sediment to prograde basinwards overtop of mud that had been deposited below fair weather wave base. Processes likely responsible for moving sediment offshore may have included storm modified tidal currents, and possibly storm rip currents (Boreen and Walker, 1991). This basinward transport would account for the northeast thinning and muddying of each E marker interbed. The cross sections in Chapter 6 show the E markers thickening shoreward where they amalgamate with the CM1-VE4 interval. Therefore, the distal equivalents of these E markers can be thought of as an extension of the CM1-VE4 interval basinwards. The E markers are essentially time lines that record periods of still stand and minor sea level falls during the overall sea level rise and transgression.

Another aspect of the coarse grained interbeds (E markers) is that they are often burrowed by Skolithos and Arenicolites. The vertical burrows are interpreted to have formed during periods of nondeposition (fairweather periods), and later filled with sand. Sideritized mudstones (rarely more than 10cm thick) frequently occur directly below these beds and are also penetrated by Arenicolites and rarely Skolithos. The sideritized intervals may represent condensed sections where slow sedimentation rates during a rapid sea level rise resulted in authigenic mineral precipitation (siderite), and a semi lithified burrowed bed (Loutit et al., 1988). Similar sideritic and bioturbated sandier horizons were observed by Wadsworth and Walker (1991) above the E7 surface in the Cardium.

The fact that burrowed sideritized mudstones directly underlie the coarse grained interbeds in the study area implies that immediately following a rapid sea level rise, a stillstand, or minor sea level fall must have occurred allowing coarse sediment to be shed basinward. Renewed transgression terminated sediment supply and allowed organisms to colonize the top of the newly deposited "E" unit. The top the coarse grained interbed was burrowed and bioturbated and then overlain by transgressive mudstones (facies 1b). These mudstones are thought to have been deposited in an offshore environment where storm and tidal currents could not deliver coarse sediment. During each stage of sea level rise, areas of the basin that were formerly above fair weather wave base were shifted into deeper environments. An increase in the rate of transgression would shutoff or substantially reduce the sediment supply to the new shoreline thus allowing dark mudstones to blanket the older coarse grained deposits below.

Continued transgression further to the southwest, outside the study area, would logically favour a similar style of deposition for the remainder of the allomember. Cross sections presented in Chapter 6 showed the VE4 surface climbing towards the southwest approaching the Base of Fish Scales datum. Presumably the E0 and E1 markers and the remaining Lower Colorado shales would onlap the CM1 surface southwest of the study area. The Base of Fish Scales condensed section by analogy may also onlap CM1; alternatively, the horizon represents a maximum flooding surface that buries but does not onlap CM1.

8.9 Summary: Sedimentology and Depositional History

The chronological order of events responsible for the deposition of the Viking allomembers at Harmattan East - Crossfield are summarized as follows:

1) deposition of basinal and offshore transitional mudstones, siltstones and fine grained sandstones of allomember A-B on top of Joli Fou shales and Basal Colorado sandstones (Fig.

8.1A). The thickening and sandier upwards trend of the upper part of allomember A-B suggests a sediment source and progradation from the southwest was responsible for deposition of this allomember,

2) a major drop in relative sea level allowed valleys to incise into previously deposited progradational sediments of allomember A-B (Fig. 8.1B) This drop probably coincides with Weimer's (1984, p.17) "basinwide incisement of drainage" 97 million years ago. The VE2 surface records this erosion at Willesden Green (Boreen and Walker, 1991), and Crystal field (Pattison, 1990),

3) nonmarine sediments and uppershoreface deposits of allomember C were eroded at Harmattan East and other areas of the basin to the northeast during the ensuing transgression that produced the VE3 ravinement surface (Fig. 8.1C). Incised shorefaces were cut at least as far northeast as Joffre (Downing and Walker, 1988). Continued southward transgression produced shorefaces at Gilby, as well as estuarine back filling at Willesden Green and Crystal (Boreen and Walker, 1991; Pattison, 1990). A minor shoreface "step" was created at Garrington (Davies, 1990) and two minor "steps" were created on the VE3 surface in the area of this study, presumably during minor stillstands or slower rates of transgression,

4) an increase in sediment supply from the southwest, a relative sea level lowering, and possibly increased

Figure 8.1. (Next 3 pages)

Summary diagram of depositional history of the Viking alloformation within the study area and just north of Garrington field. Diagrams A through H are discussed in section 8.9. No vertical of horizontal scale is implied (Modified after Davies, 1990).

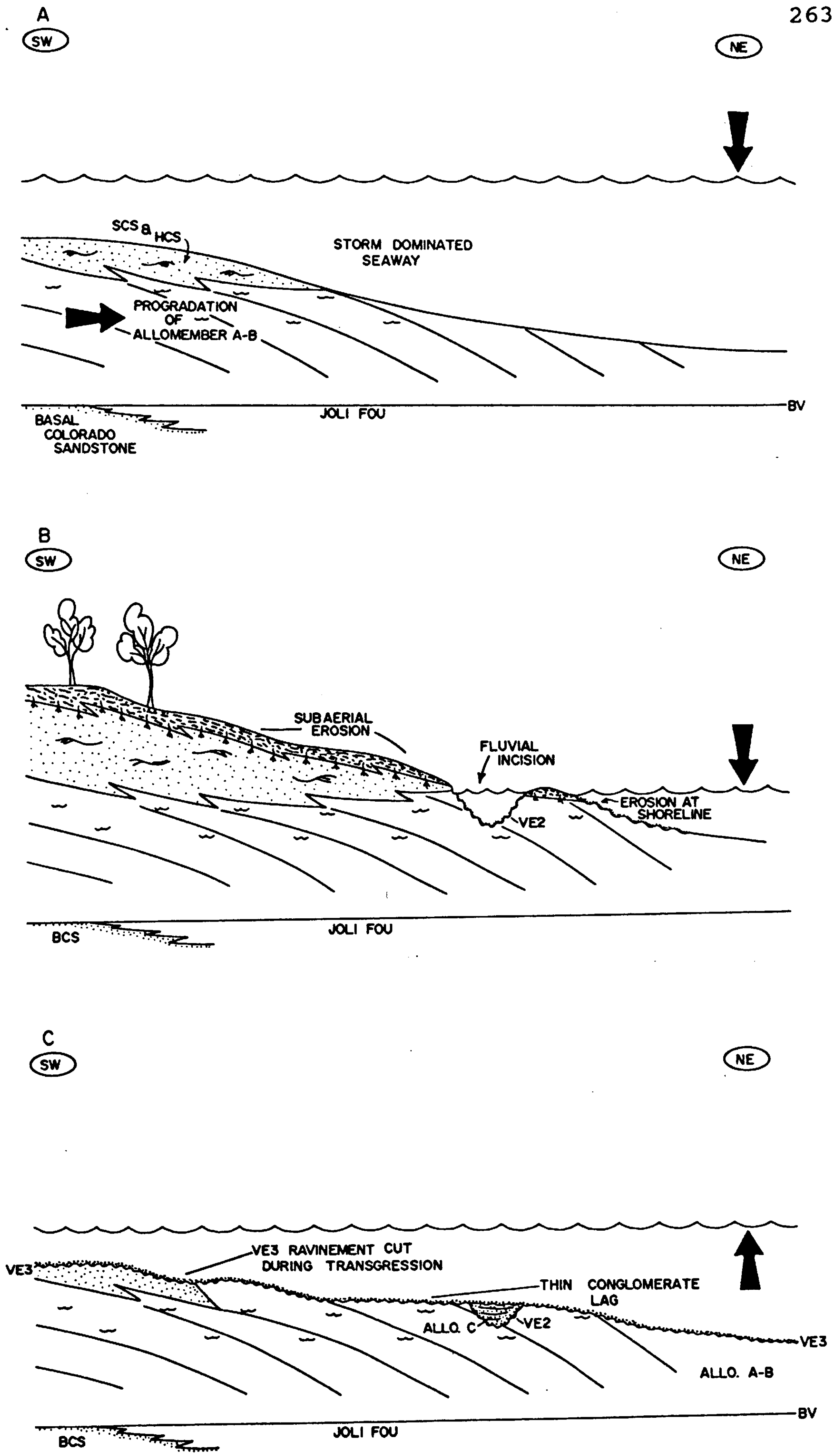
A
SW
NE
SCS & HCS
STORM DOMINATED
SEAWAY
PROGRADATION
OF
ALLOMEMBER A-B
BV
JOLI FOU
BASAL
COLORADO
SANDSTONE
B
SW
NE
SUBAERIAL
EROSION
FLUVIAL
INCISION
EROSION AT
SHORELINE
VE2
JOLI FOU
BCS
C
SW
NE
VE3
VE3 RAVINEMENT CUT
DURING TRANSGRESSION
THIN CONGLOMERATE
LAG
ALLO. C
VE2
VE3
ALLO. A-B
BV
JOLI FOU
BCS

D.

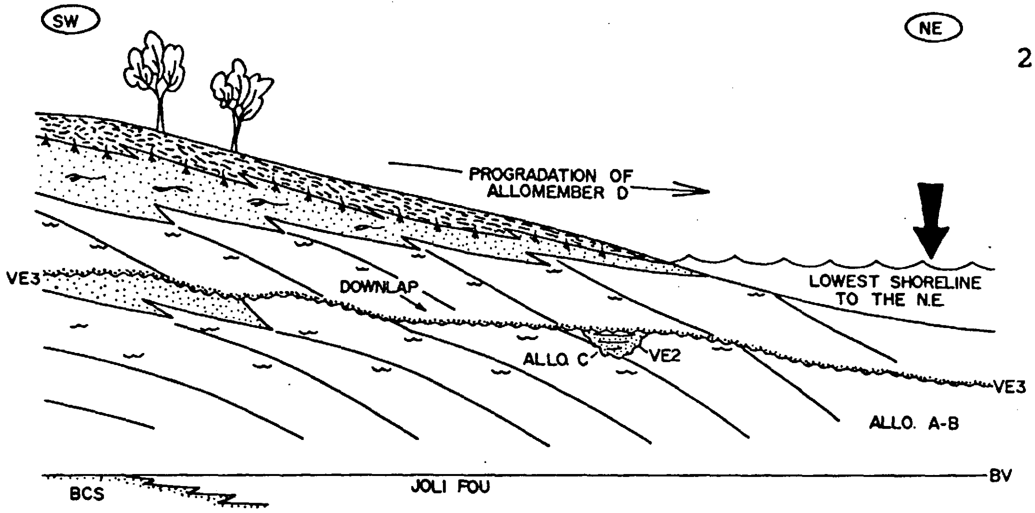
SW
NE
PROGRADATION OF ALLOMEMBER D
LOWEST SHORELINE TO THE N.E.
VE3
DOWNLAP
ALLO. C
VE2
VE3
ALLO. A-B
BV
BCS
JOLI FOU

E

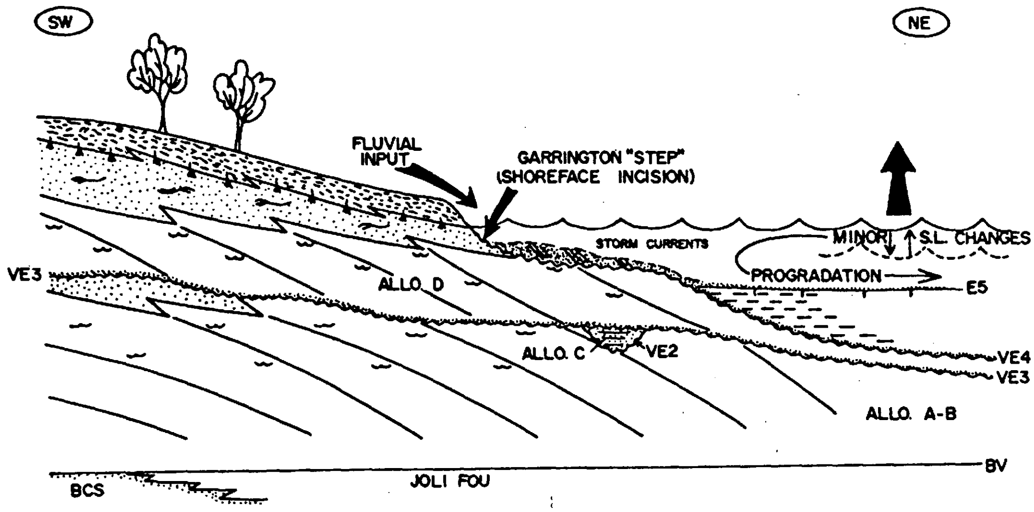
SW
NE
FLUVIAL INPUT
GARRINGTON "STEP" (SHOREFACE INCISION)
STORM CURRENTS
MINOR S.L. CHANGES
PROGRADATION
E5
VE3
ALLO. D
ALLO. C
VE2
VE4
VE3
ALLO. A-B
BV
BCS
JOLI FOU

F

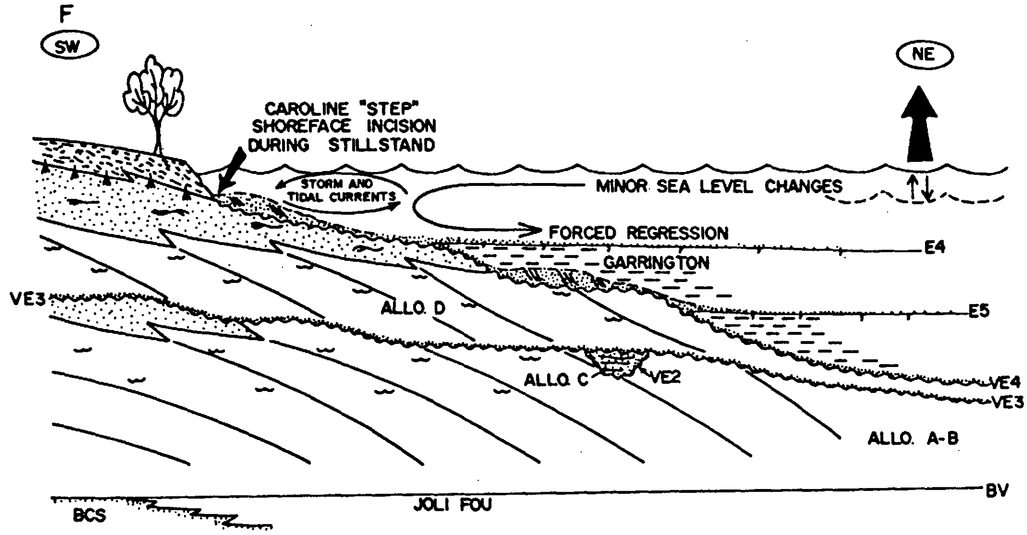
SW
NE
CAROLINE "STEP" SHOREFACE INCISION DURING STILLSTAND
STORM AND TIDAL CURRENTS
MINOR SEA LEVEL CHANGES
FORCED REGRESSION
E4
GARRINGTON
VE3
ALLO. D
E5
ALLO. C
VE2
VE4
VE3
ALLO. A-B
BV
BCS
JOLI FOU

G

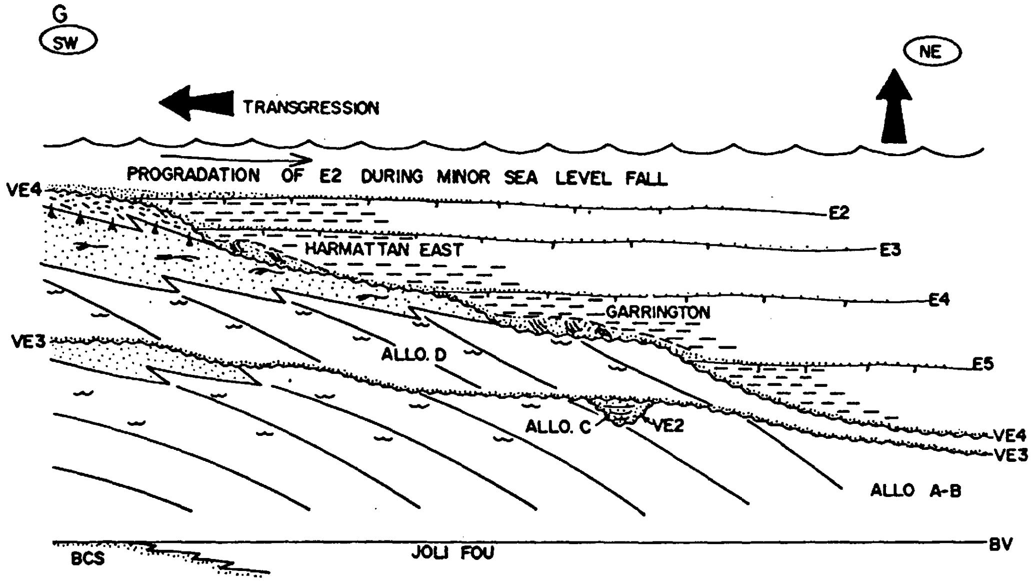
SW
NE
TRANSGRESSION
PROGRADATION OF E2 DURING MINOR SEA LEVEL FALL
VE4
E2
HARMATTAN EAST
E3
E4
GARRINGTON
VE3
ALLO. D
E5
ALLO. C
VE2
VE4
VE3
ALLO A-B
BCS
JOLI FOU
BV

H

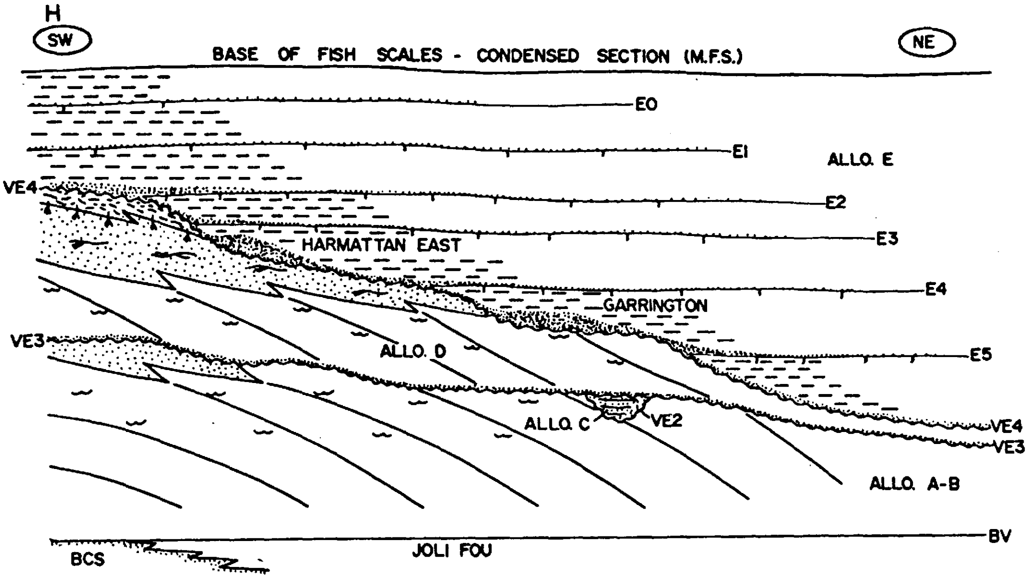
SW
NE
BASE OF FISH SCALES - CONDENSED SECTION (M.F.S.)
EO
EI
ALLO. E
VE4
E2
HARMATTAN EAST
E3
E4
GARRINGTON
VE3
ALLO. D
E5
ALLO. C
VE2
VE4
VE3
ALLO. A-B
BCS
JOLI FOU
BV

subsidence resulted in renewed progradation of the shoreface deposits of allomember D towards the northeast (Fig. 8.1D). The basin was predominantly storm dominated at this time as shown by the HCS and SCS shoreface deposits. Progradation may have proceeded as far northeast as Joffre. Older shelf areas were subaerially exposed and incised by fluvial systems. Terrestrial sedimentation occurred on the alluvial plain where coals, paleosols, shallow lake and fluvial deposits were laid down. The fluvial channel fill deposits identified southwest of Harmattan East and Caroline are thought to have supplied coarse sediment to the transgressive shorelines.

5) allomember E represents deposits of a basinwide transgression near the end of Viking deposition (Fig. 8.1E) The resulting transgression produced the VE4 ravinement surface that can be traced as far north as the Willesden Green area (Boreen and Walker, 1991). North of Willesden Green, VE4 is either a correlative conformity or is coplanar with the VE3 surface (Pattison, 1990). Multiple stillstands or slow rates of transgression are thought to have produced the "steplike", southwestward climbing morphology on the VE4 surface. Fluvial systems are thought to have supplied the coarse sediment to shoreface incisions. During minor sea level falls, storm and tidal currents reworked sediment at these shorefaces and transported sediment basinward as sheet sands over older "stepped" shorefaces (eg. Garrington) (Fig.

8.1E, F) forming onlapping markers E4 and E5. The E3 and E4 onlap markers are coincidental with stillstands responsible for the Caroline "step" (Fig. 8.1F). The E2 marker onlaps southwest of the Caroline "step" (Fig. 8.1G), while the E1 and E0 markers likely onlap at younger stillstand positions at paleoshorelines southwest of the study (Fig. 8.2H).

6) continued transgression blanketed the coarser interbeds with predominantly offshore dark mudstones (Colorado shales). A major pause in basin deposition led to the formation of a regionally extensive condensed section (Base of Fish Scales) (Fig. 8.2H). This horizon may represent a maximum flooding surface associated with the VE4 transgression. The overlying Base of Fish Scales sandstone may represent a distal component of a BFS shoreline further to the southwest.

Chapter 9 Conclusions

1) Bounding discontinuities in the Harmattan East - Crossfield area have allowed the recognition of several allomembers which comprise the Viking alloformation. Each of the allomembers contain different vertical and lateral facies associations.

2) Two bounding discontinuities, VE3 and VE4 have been interpreted as erosional surfaces and correlated in the study area. These surfaces are regionally extensive ravinement surfaces and are correlatable into the adjacent Caroline and Garrington fields, as far north as Crystal, and as far northeast as Joffre.

3) Subdivision of the Viking Formation into allomembers and erosion surfaces provides a framework for relating sand bodies in this study to other sandbodies in the Viking Basin.

4) Deposition of the Viking alloformation was controlled by major and minor sea level changes. Two major progradational events are recorded by the deposits of allomember A-B and D. Two basinwide transgressive events are recorded by the VE3 and VE4 ravinement surfaces.

5) Coarse grained deposits on the VE4 surface comprise the reservoir rocks at Harmattan East, Caroline, and Garrington oil fields. The coarse grained deposits at Harmattan East

are not tidal sand ridges, but instead represent mixed storm-tidal current deposits formed in a shoreface environment.

6) The Harmattan East oil field is producing from the coarse grained CM1-VE4 interval in allomember E. The western boundary of the field is determined by the downdip limit of the oil-water contact. The field is separated from Caroline by a rise in the VE4 surface. The E3 producing interbed of Caroline onlaps this VE4 rise and is separated from the Harmattan reservoir rocks by dark mudstones in allomember E. The eastern boundary of Harmattan is controlled by the thinning of the CM1-VE4 interval basinwards in the vicinity of Garrington. Garrington field produces from stratigraphically lower coarse grained deposits found on the VE4 surface.

REFERENCES

Amajor, L.C., 1980. Chronostratigraphy, depositional patterns and environmental analysis of sub-surface Lower Cretaceous (Albian) Viking reservoir sandstones in central Alberta and part of southwestern Saskatchewan. Unpublished Ph.D Thesis, University of Alberta, Edmonton, 596 p.

____________, and Lerbekmo, J.F., 1980. Subsurface Correlation of Bentonite Beds in the Lower Cretaceous Viking Formation of South-Central Alberta. Bulletin of Canadian Petroleum Geologists, v. 28, no. 2, p. 149-172.

____________, 1984. Lower Cretaceous Viking barrier island, southwestern Alberta, Canada. American Association of Petroleum Geologists Bulletin, v. 68, p. 448 (abs).

____________, 1986. Patterns of hydrocarbon occurrences in the Viking Formation, Alberta, Canada. Journal of Petroleum Geology, v. 9, no. 1,p. 53-70.

Banerjee, I, 1989. Tidal sand sheet origin of the transgressive Basal Colorado Sandstone (Albian): a subsurface study of the Cessford Field, Southern Alberta. Bulletin of Canadian Petroleum Geology, v.37, p. 1-17.

Basu, A., Young, S.W., Suttner, L.J., James, W.C., and Mack, G.H., 1975. Re-evaluation fo the use of undulatory extinction and polycrystallinity in detrital quartz for provenance interpretation. Journal of Sedimentary Petrology, v.45, p. 873-882.

Beach, F.K., 1956. Reply to De Weil on turbidity current deposits. Bulletin of the Alberta Society of Petroleum Geologists, v. 4, no. 8, p. 175-177.

Beaumont, E.A., 1984. Retrogradational shelf sedimentation: Lower Cretaceous Viking Formation, central Alberta. In Tillman, R.W. and C.T. Siemers, (eds.), Siliciclastic Shelf Sediments; Society of Economic Paleontologists and Mineralogists, Tulsa, Oklahoma, Special Publication no. 34, p. 163-177.

Bergman, K.M., and Walker, R.G., 1987. The importance of sea level fluctuations in the formation of linear conglomerate bodies: Carrot Creek Member, Cretaceous Western Interior Seaway, Alberta, Canada. Journal of Sedimentary Petrology, v. 57, p.651-665.

________________________________, 1988. Formation of Cardium erosion surface E5 and associated deposition of conglomerate: Carrot Creek Field, Cretaceous Western Interior Seaway, Alberta. In James, D.P. and Leckie, D.A. (eds.), Sequence Stratigraphy, Sedimentology: Surface and Subsurface: Canadian Society of Petroleum Geologists Memoir 15, p. 15-24.

Boethling, F.C., 1977a. Increase in gas prices rekindles Viking-Sandstone interest. Oil and Gas Journal, v. 75, p . 196-200.

______________, 1977b. Typical Viking Sequence: A marine sand enclosed with marine shales. Oil and Gas Journal, v. 75, p. 172-176.

Boreen, T.D., 1989. Sedimentology, Stratigraphy and Depositional History of the Lower Cretaceous Viking Formation at Willesden Green, Alberta. Unpublished M.Sc. Thesis, McMaster University, Hamilton, 190 p.

___________, and Walker, R.G., 1991. Definition of allomembers and their facies assemblages in the Viking Formation, Willesden Green area, Alberta. Bulletin of Canadian Petroleum Geology, v. 39, p. 123-144.

Boyles, J.M., and Scott, A.D., 1982. A model for migrating shelf-bar sandstones in the Upper Mancos Shale (Campanian), northwestern Colorado. American Association of Petroleum Geologists Bulletin, v. 66, p. 491-508.

Caldwell, W.G.E., North, B.R., Stelck, C.R. and Wall, J.H., 1978. A Foraminiferal Zonal Scheme for the Cretaceous System. In Stelck, C.R., ed., Western and Arctic Canadian Biostratigraphy; Geological Association of Canada, Sp. Paper 18, p. 496-575.

Cant, D.J. and Hein, F.J., 1986. Depositional sequences in ancient shelf sediments: Some contrasts in style. In: Knight, R.J. and McLean, J.R. (eds.), Shelf Sands and Sandstones; Canadian Society of Petroleum Geologists, Memoir 11, p. 303-312.

_________, and O'Connell, S. 1988. The Peace River Arch: its structure and origin. In: James, D.P. and Leckie, A.D. (eds.), Sequences, Stratigraphy, Sedimentology: Surface and Subsurface. Canadian Society of Petroleum Geologists, Memoir 15, p. 537-542.

Davies, S.D, 1990. The Sedimentology, Stratigraphy and Depositional Environments of the Lower Cretaceous Viking Formation at Caroline and Garrington, Alberta, Canada. Unpublished M.Sc. Thesis, McMaster University, Hamilton, 207 p.

De Raaf, J.F.M., Boersma, J.R. and Van Gelder, A., 1977. Wave-generated structures and sequences from a shallow marine succession, Lower Carboniferous, County Cork, Ireland. Sedimentology, v. 24, p. 451-483.

De Wiel, J.E., 1956. Viking and Cardium not turbidity current deposits. Bulletin of the Alberta Society of Petroleum Geologists, v. 4, p. 173-174.

Downing, K.P., 1986. The Depositional History of the Lower Cretaceous Viking Formation at Joffre, Alberta, Canada. Unpublished M.Sc. Thesis, McMaster University, Hamilton, 138 p.

_____________, and Walker, R.G., 1988. Viking Formation, Joffre Field, Alberta: shoreface origin of long, narrow sand body encased in marine mudstones. American Association of Petroleum Geologists Bulletin, v. 72, no.1, p. 1212-1228.

Dott, R.H., and Bourgeois, J., 1982. Hummocky stratification: significance of its variable bedding sequences. Bulletin Geological Society of America, v. 93, p. 663-680.

Evans, W.E., 1970. Imbricate linear sandstone bodies of Viking Formation in the Dodsland-Hoosier area of south - western Saskatchewan, Canada. Bulletin of the American Association of Petroleum Geologists, Bulletin, v. 54, p. 469-486.

Eyles, C.H., and Walker, R.G., 1988. "Geometry" and facies characteristics of stacked shallow marine sandier-upward sequences in the Cardium Formation at Willesden Green, Alberta. In: James, D.P. and Leckie,A.D. (eds.), Sequences, Stratigraphy, Sedimentology: Surface and Subsurface. Canadian Society of Petroleum Geologists, Memoir 15, p. 85-96

Energy Resources Conservation Board. Alberta's Reservesof Crude Oil, Oil Sands, Gas, Natural Gas Liquids, and Sulfur at December, 1990. ERCB Report 91-25.

Folk, R.L., 1974. Petrology of Sedimentary Rocks, Hemphill's, Austin, Texas, 170 p.

Frey, R.W., and Pemberton, S.G., 1985. Biogenic structures in outcrops and cores. 1. Approaches to ichnology. Bulletin of Canadian Petroleum Geology, v.33, p. 72-115.

________________________________, 1987. The Psilonichnus ichnocoenose and its relationship to adjacent marine and nonmarine ichnocoenoses along the Georgia Coast. Bulletin of Canadian Petroleum Geology, v. 35, p. 333-354.

Gammel, H.G., 1955. The Viking Member in central Alberta. Bulletin of the Alberta Society of Petroleum Geologists,v.3, p. 63-69.

Glaister, R.P., 1959. Lower Cretaceous of southern Alberta and adjoining areas. Bulletin of the American Association of Petroleum Geologists, v. 43, p. 590-640.

Grant, S.K., 1985. Sedimentology and reservoir geology, Viking Formation, Harmattan East Field, south-central Alberta. Unpublished M.Sc. Thesis, University of Alberta, 216p.

__________, Hein, F.J. and Longstaffe, F.J. 1984. Geology of the Harmattan oil field, Viking Formation, south-central Alberta. Geological Association of Canada, Annual meeting, Program with Abstracts, v. 9, p. 68.

Hein, F.J., Dean, M.E., DeIure, A.M., Grant, S.K., Robb, G.A., and Longstaffe, F.J., 1986. The Viking Formation in the Caroline, Garrington, and Harmattan East Fields, western south-central Alberta: Sedimentology and Paleogeography. Bulletin of Canadian Petroleum Geology. v. 34, p. 91-110.

__________, Robb, G.A., Wolberg, A.C. and Longstaffe, F.J., 1991. Facies descriptions and associations in ancient reworked (?transgressive) shelf sandstones: Cambrian and Cretaceous examples. Sedimentology. v. 38, p. 405-431.

Helmold, K.P., 1985. Provenance of feldspathic sandstones - the effect of diagenesis on provenance interpretations: a review. In Zuffa, G.G. ed., Provenance of Arenites: Boston, D. Reidel Publishing Company, p. 139-163.

Houghton, H.F., 1980. Refined techniques for staining plagioclase and alkali feldspars in thin section. Journal of Sedimentary Petrology, v. 50, p. 629-631.

Howard, J.D., and Reineck, H.E., 1981. Depositional facies of high energy beach-to-offshore sequence, comparison with low-energy sequence. American Association of Petroleum Geologists Bulletin, v. 65, p. 807-830.

Hunt,W.C., 1954. The Joseph Lake-Armena-Camrose Producing Trend, Alberta. In: Clark, L.M. (ed.) Western Canada Sedimentary Basin. p. 452-463.

Johnson, H.D., and Baldwin, C.T., 1986. Shallow siliciclastic seas. In: Reading, H.G., ed., Sedimentary Environments and Facies: Blackwell Scientific Publications, Oxford, p. 229-282.

Jones, H.L., 1961. Viking deposition in southwestern Saskatchewan with a note on the source of the sediments. Bulletin of the Alberta Society of Petroleum Geologists, v. 9, p. 231-234.

Kastner, M., and Siever, R., 1979. Low temperature feldspars in sedimentary rocks. American Journal of Science, v. 279, p.435-479.

Koke, K.R., and Stelck, C.R., 1985. Foraminifera of a Joli Fou shale equivalent in the Lower Cretaceous (Albian) Hasler Formation, northeastern British Columbia. Canadian Journal of Earth Sciences, v. 22, p. 1299-1313.

Koldijk, W.S., 1976. Gilby Viking B: a storm deposit. In: Lerand M.M. (ed.), The sedimentology of selected clastic oil and gas reservoirs in Alberta. Canadian Society of Petroleum Geologists, p. 62-67.

Krinsley, D.H., 1978. The present state and future prospects of environmental discrimination by scanning electron microscopy. In Whalley, W.B., ed., Scanning electron microscopy in the study of sediments, Norwich, England, Geological Abstracts, p. 169-179.

______________, and Doornkamp, J.C., 1973. Atlas of quartz sand surface textures. Cambridge University Press, 91 p.

______________, and Marshall, J.R., 1987. Sand grain textural analysis: an assessment. In Marshall, J.R., ed., Clastic Particles, Scanning Electron Microscopy and Shape Analysis of Sedimentary and Volcanic Clasts. New York, Von Nostrand Reinhold Company, p. 2-7.

______________, and Trusty, P., 1985. Environmental interpretation of quartz grain surface textures. In Zuffa, G.G. (ed.), Provenance of Arenites: Boston, D. Reidel Publishing Company, p. 213-229.

Leckie, D.A., 1986a. Tidally influenced, transgressive shelf sediments in the Viking Formation, Caroline, Alberta. Bulletin of Canadian Petroleum Geology, v. 34, p. 111- 125.

____________, 1986b. Rates, controls and sandbody geometries of transgressive-regressive cycles: Cretaceous Moosebar-Gates formations, British Columbia. American Association of Petroleum Geologists Bulletin, v. 70, p. 516-535.

____________, and Foscolos, A.E., 1986. Paleosols and Late Albian sea level fluctuations: preliminary observations from the northeastern British Columbia foothills. In: Current Research, Part B, Geological Survey of Canada, Paper 86-1B, P. 429-441.

____________, and Potocki, D.J., 1988. Sandstone dikes and an estimate of their depth of injection in the Colorado Shales (Cretaceous), Alberta. In: James, D.P. and Leckie, A.D. (eds.), Sequences, Stratigraphy, Sedimentology: Surface and Subsurface. Canadian Society of Petroleum Geologists, Memoir 15, p. 325-330.

____________, and Reinson, G.E., in press, Effects of Middle to Late Albian sea level fluctuations in the Cretaceous interior seaway, western Canada. In Caldwell, W.G.E. and Kaufmann, E., (eds.), Geological Association of Canada Special Paper: Evolution of Western Interior Basin

____________, and Walker, R.G., 1982. Storm and tide dominated shorelines in the Cretaceous Moosebar-Lower Gates interval-outcrop equivalents of deep basin gas trap in Western Canada. American Association of Petroleum Geologists Bulletin, v. 66, p. 138-157.

Leithold, E.L., and Bourgeois, J., 1984. Characteristics of coarse-grained sequences deposited in nearshore, wave-dominated environments--examples from the Miocene of southwest Oregon. Sedimentology, v. 31, p. 749-775.

Lerand, M.M., and Thompson, D.K., 1976. Provost field-Hamilton Lake pool. In: Clack, W.J.F., and Huff, G. (eds.), Joint Convention on Enhanced Oil Recovery, Core Conference. Calgary, Canadian Society of Petroleum Geologists-Petroleum Society of Canadian Institute of Mining, p. B1-B34.

Levell, B.K., 1980. Evidence for currents associated with waves in Late PreCambrian shelf deposits from Finnmark, North Norway. Sedimentology, v. 27, p. 153-166.

Longstaffe, F.J. and Ayalon, A., 1987. Oxygen-isotope studies of clastic diagenesis in the Lower Cretaceous Viking Formation, Alberta: implications for the role of meteoric water. In Marshall, J.D., ed., Diagenesis of Sedimentary Sequences, Geological Society Special Publication No. 36, p. 277-296.

Loutit, T.S., Harbendol, J., Vail, P.R., and Baum, G.R., 1983. Condensed sections: the key to age dating and correlation of continental margin sequences. In: Wilgus, C.K., Posamentier, H., Van Wagoner, J., Ross, C.A., and Kendall, C.G.St., C., (eds.), Sea-Level Changes: An Integrated Approach: Society of Economic Paleontologists and Mineralogists Special Publication 42, p. 183-216.

Marshall, D.J., 1988. Cathodoluminescence of geological materials. Boston, Published by the Academic Division of Unwin Hyman Ltd., 146 p.

Matter, A. and Ramseyer, K., 1985. Cathodoluminescence microscopy as a tool for provenance studies of sandstones. In Zuffa, G.G., ed., Provenance of Arenites: Boston, D. Reidel Publishing Company, p. 191-211.

McBride, E.F., 1987. Diagenesis of the Maxon sandstone (Early Cretaceous), Marathon region, Texas: a diagenetic quartzarenite. Journal of Sedimentary Petrology, v. 57, p. 98-107.

McCrory, V.L., and Walker, R.G., 1986. A storm and tidally-influenced prograding shoreline--Upper Cretaceous Milk River Formation of Southern Alberta, Canada. Sedimentology, v. 33, p. 47-60.

McLean, D.J., 1987. Geometry of Facies Packages and E5 Erosion Surfaces in the Cardium Formation, Ferrier Field, Alberta. Unpublished M.Sc. thesis, McMaster University, Hamilton, Canada, 144 p.

Molenaar, N., 1986. The interrelation between clay infiltration, quartz cementation, and compaction in lower Givetian terrestrial sandstones, Northern Ardennes, Belgian. Journal of Sedimentary Petrology, v. 56, p. 359-369.

Moslow, T.F., and Pemberton, S.G., 1988. An integrated approach to the sedimentological analysis of some Lower Cretaceous shoreface and delta front sandstone sequences. In: James, D.P. and Leckie,A.D. (eds.), Sequences, Stratigraphy, Sedimentology: Surface and Subsurface. Canadian Society of Petroleum Geologists, Memoir 15, p. 373-386.

Niedoroda, A.W., Swift, D.J.P., and Hopkins, T.S., 1978. The shoreface. In R.A. Davis Jr. ed., Coastal Sedimentary Environments: Springer-Verlag, New York, p. 533-624.

North American Commission on Stratigraphic Nomenclature, 1983. North American Stratigraphic Code. American Association of Petroleum Geologists Bulletin, v. 67, p. 841-875.

Nummedal, D. and Swift, D.J.P., 1987. Transgressive stratigraphy at sequence-bounding unconformities: some principles derived from Holocene and Cretaceous examples. In: Nummedal, D., Pilkey, O.H., and Howard, J.D., (eds.), Sea Level Fluctuations and Coastal Evolution: Society of Economic Paleontologists and Mineralogists, Special Publication 41, p. 241-260.

Oliver, T.A., 1960. The Viking-Cadotte relationship. Journal of the Alberta Society of Petroleum Geologists. v. 8, p. 247-253.

Pattison, S.A.J., 1988. Transgressive, incised shoreface deposits of the Burnstick Member (Cardium "B" Sandstone) at Caroline, Crossfield, Garrington, and Lochend; Cretaceous Western Interior Seaway, Alberta,Canada. In: James, D.P. and Leckie, A.D. (eds.), Sequences, Stratigraphy, Sedimentology: Surface and Subsurface. Canadian Society of Petroleum Geologists, Memoir 15, p. 155-165

________________, 1990. Valley fill sediments at Crystal and Viking Formation allostratigraphy. McMaster University Geology Department, Technical Report90-1, 72 p.

________________, 1991. Sedimentology and allostratigraphy of regional valley fill, shoreface and transgressive deposits of the Viking Formation (Lower Cretaceous), Central Alberta. Unpublished PhD. Thesis, McMaster University, Hamilton, 380 p.

Pemberton, S.G. and Frey, R.W., 1983. Biogenic structures in Upper Cretaceous outcrops and cores. Canadian Society of Petroleum Geologists, Conference on the Mesozoic of Middle North America, Field Trip Guidebook 8, 161 p.

Plint, A.G., and Walker, R.G., 1987. Cardium Formation 8. Facies and environments of the Cardium shoreline and coastal plain in the Kakwa Field and adjacent areas, northwestern Alberta. Bulletin of Canadian Petroleum Geology, v. 35, p. 48-64.

___________, Walker, R.G., and Bergman, K.M., 1986. Cardium Formation 6. Stratigraphic framework of the Cardium in subsurface. Bulletin of Canadian Petroleum Geology, v. 34, p. 213-225.

Plummer, P.S., and Gostin, V.A., 1981. Shrinkage cracks: Desiccation or syneresis? Journal of Sedimentary Petrology, v.51. p.1147-1156.

Power, B.A., 1987. Depositional environments of the lower Cretaceous (Albian) Viking Formation at Joarcam Field, Alberta, Canada. Unpublished M.Sc. Thesis, McMaster University, Hamilton, 165p.

____________, 1988. Coarsening-upward shoreface and shelf sequences: examples from the lower Cretaceous Viking Formation at Joarcam, Alberta, Canada; In: James, D.P. and Leckie,A.D. (eds.), Sequences, Stratigraphy, Sedimentology: Surface and Subsurface. Canadian Society of Petroleum Geologists, Memoir 15, p. 185-194.

Powers, M.C., 1953. A new roundness scale for sedimentary particles: Journal of Sedimentary Petrology, v. 23, p.117-119.

Pozzobon, J.G., and Walker, R.G., 1990. Viking Formation (Albian) at Eureka, Saskatchewan: a transgressed and degraded shelf sand ridge. American Association of Petroleum Geologist Bulletin, v. 74, p. 1212-1227.

Raddysh, H., 1986. Sedimentology of the Viking Formation at Gilby "A" and "B" Fields, Alberta. Unpublished B.Sc. Thesis, McMaster University, Hamilton, 241 p.

____________, 1988. Sedimentology and "geometry" of the Lower Cretaceous Viking Formation, Gilby A and B fields, Alberta. In: James, D.P. and Leckie, A.D. (eds.), Sequences, Stratigraphy, Sedimentology: Surface and Subsurface. Canadian Society of Petroleum Geologists, Memoir 15, p. 417-430.

Raychaudhuri, I., 1989. Sedimentology and Stratigraphy of the Lower Cretaceous Viking Formation, Chigwell Field, Alberta, Canada. Unpublished B.Sc. thesis, McMaster University, Hamilton, Ontario, 70 p.

Reinson, G.E., Clark, J.E., and Foscolos, A.E., 1988. Reservoir geology of Crystal Viking field, Lower Cretaceous estuarine tidal channel-bay complex, south central Alberta. American Association of Petroleum Geologists Bulletin, v. 72, p. 1270-1294.

______________, and Foscolos, A.E., 1986. Trends in sandstone diagenesis with depth of burial, Viking Formation, southern Alberta. Bulletin of Canadian Petroleum Geology, v.34, p. 126-152.

______________, Foscolos, A.E., and Powell, T.G., 1983. Comparison of Viking sandstone sequences, Joffre and Caroline Fields. In: McLean, J.R. and Reinson, G.E. (eds), Sedimentology of selected Mesozoic clastic sequences. Canadian Society of Petroleum Geologists, p. 101-117.

Ribault, L.L., 1978. The exoscopy of quartz sand grains. In Whalley, W.B., ed., Scanning electron microscopy in the study of sediments, Norwich, England, Geological Abstracts, p.319-328.

Robb, G.A., 1985. Sedimentology and Diagenesis of the Viking Formation, Garrington. Unpublished M.Sc. Thesis, University of Edmonton, 181 p.

Roessingh, H.K., 1959. Viking deposition in the southern Alberta Plains. Alberta Society of Petroleum Geologists, 9th Annual Field Conference, p.130-137.

Rosenthal, R.P., and Walker, R.G., 1987. Lateral and vertical facies sequences in the Upper Cretaceous Chungo Member, Wapiabi Formation, southern Alberta. Canadian Journal of Earth Science, v. 24, p. 771-783.

Rudkin, R.A., 1964. Chapter II: Lower Cretaceous. In McCrossan, R.G., and Glasiter, R.P., (eds.), Geological History of Western Canada, Canadian Society of Petroleum Geologists, Calgary, Alberta, p. 65-76.

Ryer, T.A., 1987. Stratigraphy, sedimentology, and paleoenvironments of the Viking Formation, southern Alberta. (abs.). Canadian Society of Petroleum Geologists Reservoir, v. 14, No. 6, p. 1-2.

Scholle, P.A., 1979. Memoir 28-A Colour Illustrated Guide to Constituents, Textures, Cements, and Porosities of Sandstones and Associated Rocks. American Association of Petroleum Geologists, Tulsa.

Scott, A.C. and Collinson, M.E., 1978. Organic sedimentary particles: results from scanning electron microscope studies of fragmentary plant material. In Whalley, W.B., ed., Scanning electron microscopy in the study of sediments, Norwich, England, Geological Abstracts, p. 137-138.

Shelton, J.W., 1973. Models of sand and sandstone deposits: a methodology for determining sand genesis and trend: Viking Sandstone, Cretaceous, Joffre Field, Alberta. Bulletin of the Oklahoma Geological Survey, v. 118, p. 91-94.

Sibley, D.F. and H. Blatt, 1976. Intergranular pressure solution and cementation of the Tuscarora orthoquartzite. Journal of Sedimentary Petrology, v. 46, p. 881-896.

Simpson, F., 1975. Marine Lithofacies and Biofacies of the Colorado Group (Middle Albian to Santonian) in Saskatchewan. In: Caldwell, W.G.E. (ed.), The Cretaceous system in the Western Interior of North America, Geological Association of Canada, Special Paper No. 13, p. 553-587.

Sippel, R,F., 1968. Sandstone petrology, evidence from luminescence petrography. Journal of Sedimentary Petrology, v. 38, p. 530-554.

Slatt, R.M., 1984. Continental shelf topography: key to understanding distribution of shelf sand-ridge deposits from Cretaceous Western Interior Seaway. Bulletin of the American Association of Petroleum Geologists, v. 68, p. 1107-1120.

Slipper, S.E., 1918. Viking Gas Field, Structure of Area. Geological Survey Summary Department, 1917, Part C, p. 8c.

Smith, J.V. and R.C. Stenstrom, 1965. Electron-excited luminescence as a petrologic tool. Journal of Geology, v. 73, p. 627-635.

Stelck, C.R., 1958. "Stratigraphic Position of the Viking Sand". Journal Alberta Society Petroleum Geologists, v. 6, No. 1, p. 2-7.

____________, 1975. The Upper Albian Miliammina manitobensis zone in northeastern British Columbia. In: Caldwell, W.G.E., (eds.), The Cretaceous system in the Western Interior of North America: Geological Association of Canada, Special Paper No. 13, p. 253-275.

____________, and Koke, K.R., 1987. Foraminiferal zonation of the Viking interval in the Hasler Shale (Albian), northeastern British Columbia. Canadian Journal of Earth Science, v. 24, p. 2254-2278.

Swift, D.J.P., and Rice, D.D., 1984. Sandbodies on muddy shelves: a model for sedimentation in the Western Interior Seaway, North America. In: Tillman, R.W. and Siemers, C.T. (eds.), Siliciclastic shelf sediments, Society of Economic Paleontologists and Mineralogists, Special Publication 34, p. 43-62.

Thomas, M.B., 1977. Depth-porosity relationships in the Viking and Cardium Formations in Central Alberta. Unpublished M.Sc. Thesis, University of Calgary, 147 p.

Tillman, R.W., and Martinsen, R.S., 1984. The Shannon Sandstone complex, Salt Creek Anticline area, PowderRiver Basin, Wyoming. In: Tillman, R.W., and Siemers, C.T., (eds.), Siliciclastic Shelf Sediments: Society of Economic Paleontologists and Mineralogists Spec. Publ. 34, p. 85-142.

Tizzard, P.G., and Lerbekmo, J.G., 1975. Depositional history of the Viking formation, Suffield ares, Alberta, Canada. Bulletin of the Canadian Society of Petroleum Geologists, v. 23, p. 715-752.

Wadsworth, J.A. and Walker, R.G., 1991. Morphology and origin of erosion surfaces in the Cardium Formation (Upper Cretaceous, Western Interior Seaway, Alberta) and their implications for rapid sea level fluctuations. Canadian Journal of Earth Science, v. 28, p. 1507-1520.

Walker, R.G., 1983a. Cardium Formation 2. Sound body geometry and stratigraphy in the Garrington-Caroline-Ricinus area, Alberta-the "ragged blanket" model. Bulletin of Canadian Petroleum Geology, v.31, p. 14-26.

____________, **1983b.** Cardium Formation 3. Sedimentology and stratigraphy in the Garrington-Caroline area, Alberta. Bulletin of Canadian Petroleum Geology, v. 31, p. 213-230.

____________, **1984.** Shelf and shallow marine sands. In: Walker, R.G., (ed.), Facies Models (second edition), Geoscience Canada reprint series 1, p. 141-170.

____________, 1985. Geological evidence for storm transportation and deposition on ancient shelves. In: Tillman, R.W., Swift, D.G.P., and Walker, R.G., (eds.), Shelf Sands and Sandstone Reservoirs. Society of Economic Paleontologists and Mineralogists Short Course Notes No. 13, p. 243-303.

Weimer, R.J., 1984. Relation of unconformities, tectonics and sea-level changes, Cretaceous of Western Interior, U.S.A. In: Inter-regional unconformities and hydrocarbon accumulations, J.S. Schlee (ed.). American Association of Petroleum Geologists, Memoir 36, p. 7-35.

Welton, J.E., 1984. SEM petrology atlas: Methods in Exploration Series, Published by The American Association of Petroleum Geologists, Tulsa, Oklahoma, 237 p.

Wickenden, R.T.D., 1949. Some Cretaceous sections along Athabasca River from the mouth of Calling River to below Grand Rapids, Alberta. Geological Survey of Canada, Paper 49-15, 31 p.

Williams, G.D., and Stelck, C.R., 1975. Speculations on the Cretaceous Paleogeography of North America. In: Caldwell, W.G.E., ed., The Cretaceous System in the Western Interior of North America; Geological Association of Canada, Special Paper, No. 13, p. 2-7.

Wilson, J.C. and McBride, E.F., 1988. Compaction and porosity evolution of Pliocene sandstones, Ventura Basin, California. American Association of Petroleum Geologists Bulletin, v. 72, p. 664-681.

Wilson, P., 1978. A scanning electron microscope examination of quartz grain surface textures from the weathered Millstone Grit (Carboniferous) of the southern Pennines, England: a preliminary report. In Whalley, W.B. ed., Scanning electron microscopy in the study of sediments, Norwich, England, Geological Abstracts, p. 319-328.

Zinkernagel, U., 1978. Cathodoluminescence of quartz and its application to sandstone petrology. Contributions to Sedimentology, No. 8. Stuttgart: E. Schweizerbart'sche Verlagsbuchhandlung.

APPENDIX 1

MEASURED CORE - HARMATTAN EAST AREA

WELL NUMBER	CORED INTERVAL	SURFACES
14-30-31-28W4	1865.8-1878.0 m	None
08-29-32-28W4	1826.0-1836.0 m.	None
09-11-28-02W5	7149.0-7154.6" 7194.0-7214.0	Roots
06-15V-28-02W5	2282.0-2314.8 m.	Roots, VE4
11-24-28-02W5	2205.5-2220.8 m.	VE3?
06-31-28-03W5	2494.0-2511.3 2512.0-2530.0m.	Roots,VE4,VE3
05-14-28-04W5	2620.0-2638.0 2638.8-2656.6m.	Roots,VE4,BFS
06-19-29-01W5	2111.0-2141.0 m.	Roots, VE4
11-12-29-02W5	7179.0-7237.0 7238.0-7262.0′	Roots, VE4
02-13-29-02W5	7125.0-7205.0′	Roots, VE4
06-24-29-02W5	2175.3-2193.4 m.	Roots, VE4
08-26-29-02W5	2163.5-2179.0 m.	Roots, VE4
16-36-29-03W5	2220.0-2237.2 m.	Roots, VE4
06-05-30-02W5	2092.0-2110.3 m.	Macro, VE4
06-06-30-02W5	2220.0-2228.0 m.	VE4
14-05-30-02W5	2190.0-2198.4 2199.0-2217.4m.	VE4
06-07-30-02W5	2212.0-2230.0 m.	VE4
06-31-30-02W5	2236.6-2246.5 m.	None
06-36-30-02W5	2077.0-2119.0 m.	VE4, VE3
06-01-30-03W5	2245.0-2258.0 m.	None
14-01.30-03W5	2241.6-2246.0 m.	VE4?
06-02-30-03W5	2237.0-2249.0 m.	Roots, VE4
06-11-30-03W5	2238.0-2248.0 m.	Roots, VE4
08-12-30-03W5	2249.0-2260.6 m.	Roots, VE4
06-17-30-03W5	2336.0-2369.0 m.	Roots, VE4
06-22-30-03W5	2256.0-2274.0 m.	Roots, VE4
14-23-30-03W5	2227.0-2241.4 m.	VE4
09-26-30-03W5	7246.0-7319.0′	VE4
08-05-30-04W5	2585.0-2603.0 m.	Roots, VE4
09-06-30-04W5	2649,6-2661.0 m.	Roots
06-14-30-04W5	2498.0-2506.2 m.	Roots, VE4
11-35-30-04W5	8065.0-8130.0′	Roots, VE4
06-36-30-04W5	2436.0-2441.0 2441.1-2457.2m.	VE4
06-24-30-05W5	2648.0-2663.0 m.	Roots, VE4
05-05-31-01W5	2045.0-2063.0 m.	None
14-08-31-01W5	2032.0-2050.2 m.	VE4
10-09-31-02W5	7110.0-7132.0′	None
06-10-31-02W5	2150.5-2165.0m.	VE4
06-18-31-02W5	2175.0-2211.2 m.	VE4
14-32-31-02W5	2124.0-2153.8 m.	VE4, BFS
11-16-31-04W5	2452.0-2470.2 m.	VE4
07-28-31-04W5	7808.0-7812.0 7814.0-7864.0′	VE4,
06-12-32-01W5	1898.0-1916.0 m.	VE4,
04-20-32-01W5	2015.0-2030.0 m.	None

WELL LOCATION	CORED INTERVAL	SURFACES
16-29-32-01W5	2002.0-2026.0 m.	VE4
06-07-32-02W5	2169.0-2191.5 m.	VE4
14-07-32-02W5	2177.0-2195.0 m.	VE4
16-07-32-02W5	2147.25-2165.25 m.	VE4
06-08-32-02W5	2136.0-2138.5 m.	VE4
14-08-32-02W5	2131.0-2150.0 m.	VE4
06-17-32-02W5	2133.2-2149.6 m.	VE4
08-17-32-02W5	2105.0-2123.0 m.	VE4
06-18-32-02W5	2171.0-2193.2 m.	VE4
08-18-32-02W5	2148.0-2164.2 m.	VE4
14-18-32-02W5	2170.0-2188.0 m.	VE4
16-18-32-02W5	2147.0-2165.0 m.	VE4
06-19-32-02W5	2161.0-2186.0 m.	VE4
08-19-32-02W5	2142.0-2159.5 m.	VE4
16-19-32-02W5	2150.0-2166.0 m.	VE4
06-20-32-02W5	2122.0-2158.2 m.	VE4,VE3
06-30-32-02W5	2169.2-2173.0 2173.2-2185.4m.	VE4
16-10-32-03W5	2215.0-2231.2 m.	VE4
06-11-32-03W5	2230.6-2249.2 m.	VE4
14-11-32-03W5	2220.3-2229.0 m.	VE4
16-11-32-03W5	2217.0-2231.4 m.	VE4
08-12-32-03W5	2190.0-2208.0 m.	VE4
14-12-32-03W5	2207.0-2225.0 m.	VE4
16-12-32-03W5	2194.1-2201.0 m.	None
08-13-32-03W5	2179.0-2197.0 m.	VE4
14-13-32-03W5	2217.0-2236.4 m.	VE3
16-13-32-03W5	2182.0-2200.2 m.	VE4
08-14-32-03W5	2203.25-2211.5 m.	VE4
14-14-32-03W5	2209.0-2224.25 m.	VE4
16-14-32-03W5	2206.0-2224.0 m.	VE4
16-15-32-03W5	2214.0-2232.0 m.	VE4
06-16-32-03W5	2204.0-2222.25 m.	VE4
14-16-32-03W5	2198.0-2208.0 m.	None
08-20-32-03W5	2225.0-2234.0 m.	VE4
08-21-32-03W5	2202.0-2212.5 m.	VE4
16-21-32-03W5	2210.0-2229.0 m.	VE4
06-22-32-03W5	2228.0-2246.25 m.	VE4
14-22-32-03W5	2222.4-2234.0 m.	VE4
16-22-32-03W5	2210.0-2228.0 m.	VE4
06-23-32-03W5	2203.0-2221.0 m.	VE4
08-23-32-03W5	2203.0-2221.0 m.	VE4
14-23-32-03W5	2215.0-2232.8 m.	VE4
16-23-32-03W5	2202.0-2220.0 m.	VE4
06-24-32-03W5	2210.0-2251.2 m.	VE3 to BV
08-24-32-03W5	2182.0-2199.75 m.	VE4
14-24-32-03W5	2186.0-2200.0 m.	VE4
06-25-32-03W5	2175.7-2193.0 m.	VE4
08-25-32-03W5	2169.0-2180.0 m.	VE4
06-27-32-03W5	2194.0-2211.6 m.	VE4
08-27-32-03W5	2193.0-2205.6 m.	VE4
14-27-32-03W5	2192.0-2210.0 m.	VE4

WELL LOCATION	CORED INTERVAL	SURFACES
16-27-32-03W5	2208.0-2226.0 m.	VE4
08-28-32-3W5	2206.0-2223.4 m.	VE4
14-28-32-03W5	2184.02205.25 m.	VE4
16-28-32-03W5	2192.8-2206.2 m.	VE4
06-29-32-03W5	2226.5-2232.3 m.	VE4
08-29-32-03W5	2201.0-2215.0 m.	VE4
16-29-32-03W5	2195.0-2213.5 m.	VE4
08-34-32-03W5	2189.4-2202.0 m.	None
15-14V-32-04W5	2343.0-2371.6 m.	VE4
11-18-32-04W5	8144.0-8164.0′	VE4
07-24V-32-04W5	2288.0-2304.0 m.	VE4
13-26-32-04W5	2363.0-2381.0 m.	None
05-27-32-04W5	2372.0-2385.75 m.	VE4
07-32-32-04W5	2412.0-2430.0 m.	VE4
10-19-33-01W5	6555.0-6607.0′	VE4
10-30-33-01W5	1991.6-2005.4 m.	VE4
10-23-33-02W5	2008.6-2022.3	VE4
04-25-33-02W5	1993.4-2008.6 m.	VE4
06-33-33-02W5	2070.0-2086.2 m.	None
06-06-33-03W5	2270.0-2282.9 m.	VE4
06-12-33-03W5	2178.0-2196.0 m.	VE4
06-33-33-03W5	2215.0-2233.0 m.	VE4
07-19-33-04W5	7938.0-7979.0′	CM1
11-31-33-04W5	2387.1-2405.8 m.	VE4
06-02-33-05W5	2491.75-2508.5 m.	VE4
14-09-33-05W5	2586.0-2602.4 m.	VE4
14-10-33-05W5	2483.2-2491.4	VE4
10-11-33-05W5	2492.0-2499.7 m.	VE4
15-13-33-05W5	2453.0-2471.5 m.	VE4
02-14-33-05W5	8122.0-8222.0′	VE4
11-19-33-05W5	2640.0-2651.25 m.	CM1
09-22-33-05W5	2429.7-2443.8 m.	VE4
07-24-33-05W5	2453.0-2464.7 m.	VE4
16-28-33-05W5	2514.0-2532.0 m.	VE4
06-34-33-05W5	2460.0-2469.0 2469.9-2478.8m.	VE4

Appendix 2 Regional Stratigraphy: Colorado Group

2.1 Introduction: Colorado Group

In central Alberta the base of the Colorado Group is taken at the top of the Mannville Group (Aptian-Albian), and at the top is taken at the base of the Lea Park Formation (Santonian-Campanian) (Simpson, 1975). The Viking Formation belongs to the Lower Colorado Group. The regional stratigraphy of the Lower Colorado Group is discussed by Roessingh (1959); Glaister (1959); Rudkin (1964); Tizzard and Lerbekmo (1975); Simpson (1975); and Leckie and Reinson (in press).

The Lower Colorado Group in central Alberta includes in ascending order: the Joli Fou Formation, the Viking Formation, and an upper unnamed shale all considered to be primarily marine deposits. The stratigraphy of the Lower Colorado Group is discussed below (2.2)

2.2. Lower Colorado Group Stratigraphy - Alberta

2.2.1 Joli Fou Formation

In central Alberta dark grey to black bentonitic marine shales of the Joli Fou Formation (Wickenden, 1949; Gammell, 1953; Stelck, 1958) occur at the base of the Colorado Group.

The Joli Fou is 18 to 36 m thick, and thins rapidly towards the west until the overlying Viking Formation merges with the Mannville Group. Simpson (1975, p.559) reports the Joli Fou Formation displays a northerly and northeasterly increase in sand.

In southern areas of Alberta the Lower Colorado includes the "Basal Colorado Sandstone" (Banerjee, 1989), the Bow Island Formation, and the overlying shale interval. The Joli Fou is indistinguishable from the Viking in this area because of its increased silt and sand content. Both the Joli Fou and Viking grade laterally into the Bow Island Formation (Gammell, 1955). In the northwestern United States the Joli Fou is equivalent to Thermoplis and Skull Creek Shales. (Gammell, 1955; Glaister, 1959; Tizzard and Lerbekmo, 1975; Leckie and Reinson, in press) (Chapter 2 - Fig. 2.2).

2.2.2 Viking Formation

The Viking Formation overlies the Joli Fou Formation and consists of multiple sandstone and conglomerate units enclosed by marine shales. Cant and Hein (1986, p. 308) describe the Viking Formation as containing "stratigraphically isolated patchy sandstones".

The Viking Formation ranges from 18 to 36 m thick over most of central Alberta (Beaumont, 1984) and attains a thickness of 45 to 50 m in southern Alberta where it merges with part of the Bow Island Formation (Leckie and Reinson, in press). The Viking Formation becomes progressively thinner to the northeast in the vicinity of St. Paul (T58 R9W4) (Gammell, 1955).

The stratigraphic correlation of the Viking Sandstone (Slipper, 1918) of Alberta to units in British Columbia and northwestern areas of the United States has been subject to controversy for many years (Stelck and Koke, 1987; Leckie and Reinson, in press). According to Leckie and Reinson (in press, p. 7), "the primary dispute involves the Peace River Formation in northwestern Alberta and how its members (Cadotte and Paddy) correlate with Viking and Joli Fou Formations in the subsurface of the central Alberta plains". Stelck and Koke (1987) provide the most recent published correlations between the Viking Formation and Peace River Formation. Foraminiferal evidence in their work suggests the Cadotte member of the Peace River Formation is of Middle Albian age whereas the Viking Formation in central Alberta is Late Albian in age.

Viking Formation equivalents in Alberta include; the Paddy Member of the Peace River Formation in the northwest (Rudkin, 1964; Stelck and Koke, 1987); the Pelican Formation in the northeast, the Bow Island in the south (Boethling, 1977a), and the Mill Creek Formation in the southern Alberta foothills (Leckie, 1986a). Viking Formation equivalents in the northwestern United States include the Muddy, J, and Newcastle sandstones (Simpson, 1975; Beaumont, 1984; Weimer, 1984).

2.2.3 Upper Shale Above Viking

Gammell (1955) describes the upper shale which overlies the sandstones and conglomerates of the Viking Formation as dark grey in colour with sparse silt portions and thin black chert pebble beds. In the Caroline area of Alberta, conglomerates and conglomeratic sandstones have been observed within these upper shales (Hein et al., 1986; Leckie 1986a; Leckie and Reinson, in press).

The upper shale unit averages 45 m under the central plains area of Alberta and becomes progressively thinner southwest towards the Foothills Belt as a 3 m to 6 m shale between the Base of Fish Scales Marker and the top of the Viking Formation.

The upper shales overlying the Viking are left unnamed in previous work on the Viking by Glaister and Oliver (1960). In central Alberta, these shales are referred to as the Lloydminister Shale by Tizzard and Lerbekmo (1975) and Amajor and Lerbekmo (1980). Other authors have referred to these same shales in central Alberta as the Colorado Formation (Boethling, 1977b; Beaumont, 1984). In the recently published work of Stelck and Koke (1987) this same interval is referred to as Post Viking Shales. The Lower Colorado shales are equivalent to the Mowry Formation in Montana and Wyoming (Stelck and Koke, 1987) The term Lower Colorado Shales is used in this study following the work of

Leckie and Potocki (1988) and Leckie and Reinson (in press).

2.3 Biostratigraphy and Age Correlation

The most recent published work on Albian stratigraphy of Western Canada is based primarily on biostratigraphic zonation, supplemented by lithological correlations and radiometric dating of bentonites (Stelck and Koke, 1987; Leckie and Reinson, in press).

Stelck and Koke (1987, p.2225) indicate that foraminifera occur within the Viking sequence in the subsurface in Alberta but the total numbers recovered have never been great, while Bulluck (1950 in Stelck, 1975) found no evidence for a faunal break between the Joli Fou Formation and the Viking Sandstone. Dating of the Viking has therefore been accomplished by constraining the formation between shales with reliable fossil zones.

The Joli Fou Formation in west-central Alberta belongs to the Haplophragmoides gigas Zone (Caldwell et al., 1978). Other microfauna which have been identified include a dinoflagellate Spinidinium vestium which occurs at the base of the Joli Fou Formation in central Alberta (7-29-55-21 W4M) (Leckie and Reinson, in press, p. 10).

The shales directly overlying the sandstones and conglomerates of the Viking Formation belong to the Miliammina manitobensis zone. These same shales in west-central Alberta contain foraminiferal assemblages of the

Verneuilina canadensis and Haplophragmoides postis goodrichi Subzones of the late Albian Miliammina manitobensis Zone. Colorado shales between the conglomerate beds described by Hein et al. (1986) and Leckie (1986a) at Caroline contain a "dwarf" assemblage of low species diversity consisting of Ammodiscus, Miliammina, Haplophragmoides collyra, and rare Verneuilinoides. Leckie and Reinson (in press, p. 24) suggest the small size of the individuals and low species diversity may indicate a stressed, brackish or marginal marine depositional setting. In contrast, shales overlying these conglomerates yielded "normal" agglutinated assemblages which Leckie and Reinson suggest represent neritic conditions of 25-100 m water depth.

Based on biostratigraphic and lithostratigraphic correlations, Leckie and Reinson (in press) suggest the Cadotte Member of the Peace River Formation [thought previously to be correlative to the Viking Formation] is significantly older. Stelck and Koke (1987) indicate a major erosional gap exists between the Cadotte and Viking and the time represented by the unconformity would have to be added to the age separation between the two sandstones. This gap in time is yet to be resolved. The Paddy Member of the Peace River Formation of north-east British Columbia is interpreted to be correlative with the Viking Formation to the south in western Alberta (Stelck and Koke, 1987; Leckie and Reinson, in press).

Chronological dating using Potassium-Argon absolute ages obtained from biotite crystals in bentonite horizons within the Viking give an age of 100 +/- 2 Ma (Tizzard and Lerbekmo, 1975). Weimer (1984), using Potassium-Argon absolute ages dated the Viking Formation at 97 Ma (Robb, 1985).

2.4 Stratigraphy: Mannville-BFS Interval

The stratigraphic base of the Viking Formation is placed at the base of the sandstone or sandy shale overlying the Joli Fou shales (Tizzard and Lerbekmo, 1975, p. 719). Amajor and Lerbekmo (1980, p. 155) suggest the stratigraphic base of the Viking in south-central Alberta occurs at the base of a 30 to 60 cm bentonite bed which overlies shales of the Joli Fou. The Joli Fou - Viking contact has been interpreted as a slight disconformity, a regional disconformity, and an angular unconformity (Evans, 1970; Beaumont, 1984; Hein et al., 1986).

The stratigraphic top of the Viking is conformable with the overlying Lower Colorado Shales, and is commonly placed at the top of a black, chert pebble stringer or chert rich sandstone (Tizzard and Lerbekmo, 1975, p. 719). The definition for top of Viking is problematic in southern areas of Alberta. Hein et al. (1986, p. 94) observed chert pebble conglomerates and pebbly sandstones (termed Viking "A" grits) in the Caroline, Garrington and Harmattan areas of Alberta.

These grit beds are enclosed in Lower Colorado shales and were interpreted by Hein et al. as equivalents to the main reservoir sands, and therefore included as part of the Viking Formation.